Evaluating donor variability of ovine adult stem cells - implications for orthopaedic animal models

Eatelaf Muhammad Hassan

Thesis Submitted to Keele University/Institute for Science and Technology in Medicine

for the Degree of Doctor of Philosophy in Cell biology and Tissue Engineering

March 2019

To my beloved husband

Abed

Whom this thesis has never been exist without his help and

support

Abstract

Articular cartilage is a specialised tissue which covers the articulating surfaces at the end of the mammalian bone. This thin layer performs essential functions such as load bearing and shock absorption in joints. However, it lacks the ability to satisfactorily self-repair. This characteristic of the cartilage tissue makes this tissue of interest to tissue engineering and regenerative medicine therapies.

Within sheep populations, there is a significant individual variation in the characteristics of the ovine bone marrow-derived mesenchymal stem cells (oMSCs). These variations are demonstrated in the differentiation responses of oMSCs to multiple inducing factors such as nutrients and biomechanics. These differences may impact on the choices of treatment strategies that are used within regenerative medicine.

This study aims to investigate the variation in characteristics of oMSCs and to design in vitro growth protocols for oMSCs in 3D culture. These 3D growth conditions will be compared for static and dynamic culture. For comparison, native articular cartilage and engineered cartilage structures were also characterised through the measurement of mechanical and biochemical properties in addition to histological and immunohistological assessment.

Mechanical conditioning of the cells and 3D constructs was carried out using the Magnetic Ion Channel Activation (MICA) technology developed previously. The pioneering bio-magnetic technology offers a novel way to stimulate mechanically sensitive membrane channels using remotely controlled magnetic nanoparticles (MNPs) which lead to the differentiation of bone marrow-derived stromal stem cells in vitro.

This thesis has effectively demonstrated that there is a clear individual variation between the sheep donors in regard to oMSCs characterisation and tri-lineage differentiation potential. The effect of this variation on dynamic and static culture has been identified. The study has also demonstrated that mechanical stimulation of the transient receptor potential cation channel subfamily V member 4 (TRPV-4) enhances chondrogenic differentiation of oMSCs.

Mechanical stimulation of oMSCs for their differentiation towards chondrogenesis in 3D hydrogels using the MICA technology, firstly Twik-related potassium channel 1 (TREK-1) ion canal was targeted. However, no consistent response in all the ovine donors was observed. The total amounts of sGAG, total collagen and total protein produced by the cells during culture was enhanced in mechanically stimulated gels for potentially only three out of the five donors. However, mechanical testing revealed significant increase in Young's Modulus for the dynamically cultured gels compared to static gels.

Whereas, mechanical stimulation oMSCs targeting the Transient receptor potential cation channel subfamily V member 4 (TRPV4) resulted in increased cellular responses as shown by mechanical testing, biochemical analysis, histological and immunobiological analysis compared to TREK-1 targeted samples.

In summary, this thesis sets out to systematically explore the ovine mesenchymal stem cell population derived from multiple donors. With this information, we can ultimately start to address the issues of personalised approaches to regenerative therapies.

Keywords: ovine MSCs, MNPs, MICA technology, articular cartilage, chondrogenesis, cell therapy, regenerative medicine, bone marrow derived mesenchymal stem cell.

Contents

Contents

Publications and presentations

Published articles

Hareklea Markides, Jane S. McLaren, Neil D. Telling, Noura Alom, **E 'atelaf A. Al-Mutheffer,** Richard O. C. Oreffo, Andrew Zannettino, Brigitte E. Scammell, Lisa J. White and Alicia J. El Haj 2018. Translation of remote-control regenerative technologies for bone repair. *NPJ Regenerative medicine*, 3**,** 9.

Published conference abstracts

Eatelaf Mutheffer, Yvonne Reinwald, Katie Bardsley, Alicia El Haj (2017). Donor variability of ovine mesenchymal stem cell differentiation potential -clinical implications for cell therapies. European Cells and Materials Vol. 33 Suppl. 2, (P268).

E A Al-Mutheffer, Y Reinwald, K Bardsley, A J El Haj (2017). Evaluating donor variability of ovine mesenchymal stem cell differentiation potential – clinical implications for cell therapies.

E A Al-Mutheffer, Y Reinwald, A J El Haj (2018). Evaluating donor variability of ovine adult stem cells oMSCs - implications for orthopaedic animal models. eCM Online Periodical, 2018, Collection 4, TCES Conference Abstracts (page 081).

Poster presentations

The Tissue and Cell Engineering Society (TCES) 2017

E A Al-Mutheffer, Y Reinwald, K Bardsley, A J El Haj. Evaluating donor variability of ovine mesenchymal stem cell differentiation potential – clinical implications for cell therapies.

Tissue Engineering and Regenerative Medicine International Society (TERMIS) 2017.

Eatelaf Mutheffer, Yvonne Reinwald, Katie Bardsley, Alicia El Haj Donor variability of ovine mesenchymal stem cell differentiation potential -clinical implications for cell therapies

The Tissue and Cell Engineering Society (TCES) 2018

E A Al-Mutheffer, Y Reinwald, A J El Haj. Evaluating donor variability of ovine adult stem cells oMSCs - implications for orthopaedic animal models.

Acknowledgements

I would like to thank sincerely my lead supervisor Professor Alicia El-haj and my second supervisor Dr. Yvonne Reinwald who have guided me constantly throughout my PhD, for their patience, motivation and immense knowledge. They have not only contributed scientific guidance towards my work but have also helped me in the development of my career as a researcher. Besides my supervisors, I would also like to thank my fellow members of Alicia's group. They are really such a diverse and interesting group of people. With special thanks to those who helped me with my PhD work; Dr. Katie Bardsley, Dr. Michael Rotherham. I would particularly like to thank Dr. Hareklea Markides, who has provided me with invaluable advice in cell isolation and characterisation.

I am also thankful to all the staff members and students at ISTM for their kindness and support in my studies. In particular Dr. Abigail Rutter and her cheerful smile, Dr. Hamza Abu Owida and all my colleagues the Iraqi students.

I would like to thank my country Iraq and then my sponsor (Ministry of Higher Education and Scientific Research, Republic of Iraq) for offering me the opportunity for this study. I thank the College of Veterinary medicine Bagdad University.

Last but not the least, I would like to thank my husband Abed, my daughters Zainab and Shahzenan, my son Muhammed, my brothers and my sisters for supporting me spiritually throughout my study.

Funding

I extend my gratitude towards the funding body, the Iraqi Ministry of Higher Education & Scientific Research, which generously supported and fully funded this work.

Abbreviations

µL	Microliters
3D	three-dimensional
AC	articular cartilage
ACI	Autologous chondrocyte implantation
Ad M	adipogenic media
ALP	alkaline phosphatase
APTES	3-Aminopropyltriethoxysilane
BM-MNCs	bone marrow-derived mononuclear cells
BM-MSCs	bone marrow-derived mesenchymal stem cells
BM-oMSCs	bone marrow derived ovine mesenchymal stem cells
BMPs	bone morphogenic proteins
BGP	beta -glycerol-phosphate
BSA	bovine serum albumin
Ca^{+2}	calcium ion
CC	confined compression
CD	cluster of differentiation
CD 29	cluster of differentiation 29 Integrin beta-1
CD 31	cluster of differentiation 31 Platelet endothelial cell adhesion molecule (PECAM-1)
CD 44	cluster of differentiation 44 homing cell adhesion molecule (HCAM)
CD 45	cluster of differentiation 45 leukocyte common antigen (LCA)
Ch M	chondrogenic media
CLSM	confocal laser scanning microscope
CPC	cetylpyridium chloride monohydrate
DAPI	4',6-diamidino-2-phenylindole
ddH2O	double distilled water
Dex	Dexamethasone
dH_2O	distilled water
DMMB	dimethylmethylene blue
DMSO	dimethyl sulfoxide
DOTAP	1,2-Dioleoyloxy-3-(trimethylammonium)propane
EDAC	N-(3-Dimethylaminopropyl)-N′-ethylcarbodiimide hydrochloride
EDTA	ethylenediaminetetraacetic acid
FBS	foetal bovine serum
FITC	fluorescein isothiocyanate
g	Gram
g	Earth's gravitation force
GAG	Glycosaminoglycan
H&E	haematoxylin and eosin
H_2O_2	hydrogen peroxide
HCl	hydrochloric acid

HEPES buffer	4-(2-Hydroxyethyl) piperazine-1-ethanesulfonic acid
hMSCs	human mesenchymal stem cells
HSP-90beta	heat shock protein-90 beta
IBMX	3-isobutyl-1methylxanthine
IGF1	like insulin like growth factor 1
IMS	industrial methylated spirit 99%
M	normality or equivalent concentration
m T	millitesla
MACS	magnetic cell sorting
MAPCs	multipotent adult progenitor cells
MES buffer	2-(4-morpholino) ethane sulphonic acid buffer
MICA	Magnetic Ion Channel Activation
MNPs	magnetic nanoparticles
MRI	magnetic resonance imaging
MSCs	mesenchymal Stem Cells
N	normality or equivalent concentration
$NaHCO_3$	sodium hydrogen carbonate
Nd FeB	neodymium Iron Boron
NHS	N-hydroxy succinimide
OA	osteoarthritis
oB M-MSCs	ovine bone marrow derived mesenchymal stem cells
OCD	osteochondritis dissecans
oMSCs	ovine mesenchymal stem cells
Os M	osteogenic media
P	passage
P	p-value (statistics)
P^{-3}	phosphorus ion
P/S	penicillin and streptomycin
pAb	primary antibodies
PBS	phosphate buffered saline.
PGs	Proteoglycans
PPAR-Ɣ	peroxisome proliferator-activated receptor-Gama
R T	room temperature
RBCs	red blood cells
Rpm	revolution / minute
SCD	stearoyl- CoA desaturase
SCs	stem cells
SFM	serum free media
Sol	solution
sGAG	sulphated glycosaminoglycan
SPIONs	superparamagnetic iron oxide nanoparticles
STRO-4	a monoclonal antibody (designated STRO-4) which specifically binds human and ovine HSP-90beta.
STZ	the superficial (tangential) zone of articular cartilage

SZP	superficial zone protein
TGF-β	transforming growth factor-beta
TREK-1	TWIK-related potassium channel-1
Triton™	4-(1,1,3,3-Tetramethylbutyl) phenyl-polyethylene glycol
TRP	Transient receptor potential cation channel
TRPV4	Transient receptor potential cation channel subfamily V member 4
UCC	unconfined compression

List of figures

List of tables

CHAPTER 1

Introduction and literature review

Overview

The bony skeleton is a specific organ, which serves several functions. It provides mobility, support, and protection. In addition, it acts as a reservoir for essential minerals involved in homeostasis through the Ca^{+2} and P^{-3} ion storage and has hematopoietic function during blood cells production. Human and other vertebrates' bodies are supported by the skeletal system that acts as a system of levers which enable movement along with the muscles and essential connective tendons and ligaments (Saladin, 2010). The bones join each other forming joints or articulations, which can be classified according to their anatomy and physiology into three types: Synarthroses (Fibrous joints), which is immovable and connected by fibrous connective tissue, Amphiarthroses (Cartilaginous joints), which is slightly movable and connected by fibrocartilage, and lastly Diarthroses (Synovial joints), which is a movable and complex joint structure that determines the extent of movement (Van De Graaff, 2001). Joints enable the hard and rigid skeleton to move at different locations (Pazhoumand-Dar *et al.*, 2015).

Unlike bone tissue injuries, which are able to heal easily with a restoration of the original tissue in most cases, cartilage tissue is considered to have limited capacity for self-repair (Buckwalter, 1992).

Therapeutic approaches in musculoskeletal regenerative medicine, which use adult bone marrow-derived mesenchymal stem cells (BM-MSCs) are promising. Various approaches for the repair of articular cartilage have been investigated including stem cell-based engineered tissues, with properties closely mimicking those of native cartilage (Johnson *et al.*, 2012; Wang *et al.*, 2006).

Within the field of regenerative medicine and tissue engineering, magnetic nanoparticles (MNPs) have specific multifunctional roles as they can tag, track and activate the stem cells inside the body (Markides *et al.*, 2012)

To translate current experimental treatment strategies into the clinic, different animal-based studies must be performed before their successful translation into human practice to ensure

a successful and secure healing of the tissue defect. Sheep are the most representative animal model for human orthopaedics, because they are similar in bone structure, biochemical and mineral compositions as well as weight, physiology and immunology. Finally, sheep mimic humans in embryonic development and ageing (Andersen *et al.,* 2018).

1.1 Articular cartilage / structure and biology

Articular surfaces of long bones are protected by a low-friction, wear-resistant tissue, the articular cartilage, which is designed to bear and distribute loads. Articular cartilage is an avascular hyaline cartilage, which enables movement by providing a low friction surface for articulation. Despite the unparalleled mechanical behaviour cartilage has poor regenerative capacities and low metabolic activity due to the scarcity of endogenous stem cells, the lack of nutrient supply, vascular and neural network as well as lymphatic tissue (Diekman and Guilak, 2013).

Articular cartilage is composed of one type of cells called chondrocytes and a dense extracellular matrix (ECM). Chondrocytes constitute about 5% of the net weight of the articular cartilage (Alford and Cole, 2005). However, chondrocytes' metabolism is responsible for the extracellular matrix maintenance and making it stable and copious (Lu *et al.,* 2011).

1.1.1 Articular cartilage zones

Structurally, articular cartilage can be divided into four zones: the superficial tangential zone (STZ), the middle or transitional zone, the deep radial zone, and the zone of calcified cartilage (Figure 1.1).

These zones have different components and functions. For example, the superficial zone, which forms approximately 10% to 20% of articular cartilage thickness, represents the articulating surface, a smooth sliding surface which resists shearing. It has the highest

collagen content of the four zones and collagen fibrils are packed densely with a highly ordered arrangement parallel to the articular surface (Mow *et al.*, 1989).

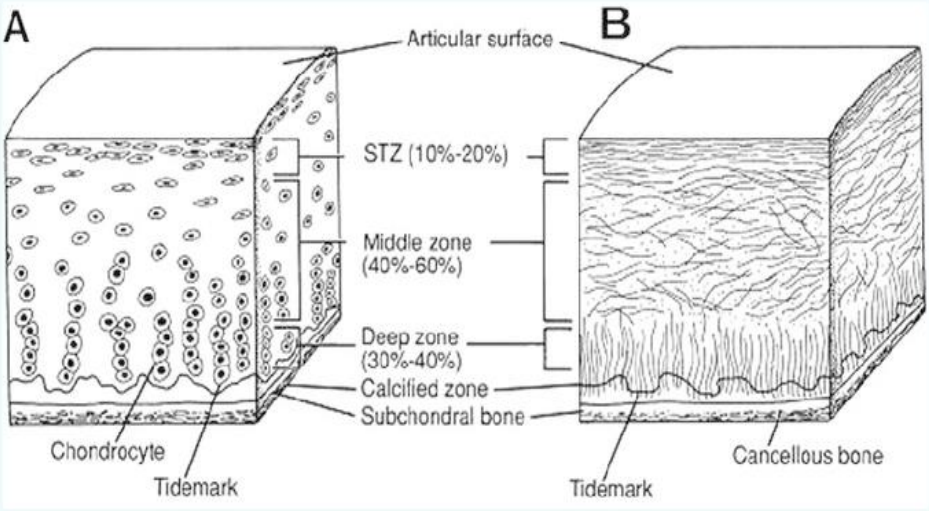

Figure 1. 1: Cross-sectional diagram of healthy articular cartilage. *A) cellular organization in the zones of articular cartilage and B) collagen fibre architecture is shown (Sophia Fox et al., 2009).*

This layer comparatively has a high number of chondrocytes, which are flat in shape. The health and integrity of the superficial layer is essential for protecting the other deeper layers. In addition, this layer is responsible for the characteristic compressive of the cartilage nature, because it is in direct contact with the synovial fluid and that enables it to resist shearing, tensile and compressive force that shed within the joint (Sophia Fox *et al.*, 2009).

The middle zone forms about 40% to 60% of the articular cartilage volume and has a higher compressive modulus than the superficial zone. Collagen fibers are thicker and less organised. Fibrils are packed loosely and aligned obliquely to the surface. This layer has a different layout of the collagen fibre which is mostly oblique or un-organised. Furthermore, the middle zone contains spherical shaped chondrocytes at a low density. The transitional layer's function is to resist the compression force (Bhosale and Richardson, 2008).

The deep zone makes up for 30% of the cartilage. Its main characteristic is the presence of large diameter collagen fibrils, which are oriented perpendicularly to the articular surface. The deep zone provides the greatest resistance to compressive forces. Finally, the last zone, is the calcified cartilage tidemark, which separates the deep zone from the calcified cartilage. It rests directly on the subchondral bone. It is there that the chondrocytes get

characteristically arranged in columnar orientation, parallel to the collagen fibres and vertical to the joint line. (Pearle *et al.,* 2005).

1.1.2 Chondrocytes

Chondrocytes are the cartilage cells, they originate from undifferentiated mesenchymal stem cells when they lose their pluripotency, then proliferate and congregate together in a dense aggregate of chondrogenic cells in the chondrification site. These chondrogenic cells differentiate into so-called chondroblasts, which then synthesise the cartilage ECM. The chondroblast is now a mature chondrocyte that is usually inactive but can still secrete and degrade the matrix, depending on conditions (Somoza *et al.,* 2014).The morphology and function of the chondrocytes depend on their location in the zones of the articular cartilage. The superficial zone chondrocytes have an elongated appearance and express proteins, that have lubricative and protective functions, and secrete relatively little proteoglycan (Wong *et al.,* 1996). One of the important proteins involved in surface lubrication is a superficial zone protein (SZP). This protein is identified as a functionally important molecule, which is used to distinguish the chondrocytes phenotype of the superficial zone from those in deeper layers, because only cells in the superficial zone are able to biosynthesize SZP (Schumacher *et al.,* 1999; Wang *et al.,* 2006). Otherwise, chondrocytes of the middle zone are more rounded than the cells in the superficial layer. Chondrocytes of the deep zone are typically arranged in a columnar fashion. On the other hand, the chondrocytes of the calcified cartilage zone, are small and are embedded in a chondroid matrix speckled with apatite salts (Wang and Kandel, 2004).

Articular cartilage homeostasis is very important. It occurs through the interaction between chondrocytes and the dense extracellular matrix which balance the anabolism and the catabolism of the matrix (Pearle *et al.,* 2005). In this circumstance, cells form a specific microenvironment which is responsible for the turnover of the ECM in its immediate vicinity. This microenvironment acts to confine the chondrocyte within its own matrix, and accordingly, prohibit and avoids any passage to adjacent areas of cartilage. Chondrocytes

interaction within the matrix is rare due to their widespread distribution and sparsity in number. However, these cells respond to numerous stimuli from their environment such as growth factors, mechanical loads, piezoelectric forces, and hydrostatic pressure. Chondrocyte viability depends the vigorous chemical and mechanical environment (Buckwalter, 1991).

1.1.3 Extracellular Matrix

Biochemically, the extracellular matrix (ECM) of the articular cartilage is composed of water which forms about 65%-80% of the healthy cartilage tissue and some dry components which are primarily composed of type II collagen, and proteoglycans as large aggregation. Other various minor collagens and non-collagenous proteins, lipids, phospholipids, and glycoproteins are making up the minor, poorly defined classes of cartilage molecules (Kiyotake *et al.,* 2016; Schwarz *et al.,* 2012). Cartilage ECM contains crucial bioactive signals is considered a promising chondroinductive material.

1.1.4 Water

Water is the major component of the articular cartilage, one third of this water is accompanying the collagen's intrafibrillar space. Small quantities of water are found as intracellular space. However, a considerable amount of water fills the pore space of the matrix (Maroudas *et al.,* 1991; Torzilli, 1985). Articular cartilage water is a dissolvent for different elements like inorganic ions (Na^+, Ca^{2+} , Cl^- and K^+, Mg^{2+}) (Lai *et al.,* 1991).

The water content is different in concentration according to the zone from about 80% at the superficial zone to 65% in the deep zone (Buckwalter and Mankin, 1998b). The fluid exchange through articular cartilage zones, and surface helps chondrocytes to receive alimentary elements and provide lubrication for the cartilage. The flow of water through the cartilage zones and across the articular surface helps chondrocytes to receive alimentary elements and provide lubrication for the cartilage. The mixture of fluid and matrix provides, the viscoelastic and mechanical properties of the hyaline cartilage. In biomechanical terms, viscoelastic materials composed of two main phases, the solid organic phase and a movable

interstitial fluid phase. This allows the cartilage to offer efficient load distribution (Lu and Mow, 2008; Williams *et al.*, 2007).

1.1.5 Collagen

The major structure of the ECM is collagen which forms about 60% of the dry weight of cartilage. Collagen type II represents the vast majority of this component. It is comprised of collagen fibrils and fibre and forms a network in the ECM incorporating proteoglycan aggregates. It also provides the tensile strength that is required to give articular cartilage its resistance to loading (Kiyotake *et al.*, 2016). Other types of collagen, such as collagen type I, III, VI, IX X and XI are present as minor contributors to the articular cartilage matrix (Jansen *et al.*, 2010). The minor collagen types aid to produce and stabilise the type II collagen fibril network (Maroudas *et al.*, 1991). Different types of collagen and their functions were mentioned in Table 1.1 (Bhosale and Richardson, 2008).

Table 1. 1: Different types of cartilage collagen and their functions.

Collagen type	***Morphological location***	***Function***
I	It is the primary collagenous component of bone tissue and fibrocartilage.	Expressed by cells in freshly isolated non-calcified cartilage tissue
II	Principal component of microfibril (90–95%)	Tensile strength
III	Also found in other connective tissues	In cartilage forms a mesh crosslinked with other type III fibres and type II fibres
VI	Pericellular matrix	Helps chondrocytes to attach to the matrix
IX	Cross-linked to surface of microfibril	Tensile properties and facilitates fibril interaction with proteoglycans
X	Closely related to the hypertrophied cells in calcified cartilage layer	Structural support and aids in cartilage mineralization
XI	Within or on microfibrils	Regulates collagen fibril size

1.1.6 Proteoglycans

Proteoglycans (PGs) are a family of molecules composed of a core protein linked by covalent bonds with one or more linear glycosaminoglycan chains. The proteoglycans are the second-largest group of macromolecules in the ECM. There are several kinds of proteoglycans included in the ECM, which are essential for normal cartilage function. They can be divided into two classes, the large proteoglycans, such as aggrecan and small proteoglycans, such as decorin, biglycan, fibromodulin, lumican, and mimican. The most abundant and the largest PG is aggrecan. This molecule reacts with hyaluronan to form large proteoglycan aggregates through protein links (Smith and Goodship, 2008). Aggrecan has numerous highly sulphated glycosaminoglycan side-chains, which hold water and therefore give the cartilage its mechanical properties. The small proteoglycans are mostly related with collagen fibrils formation and modelling. Deficiency of the decorin gene in mice resulted in large, irregular-sized collagen fibrils, which is believed to be caused by unregulated lateral fusion and this was associated with weak and fragile skin (Danielson *et al.,* 1997).

1.1.7 Chemical and physical cues promoting cartilage formation

During cartilage formation each zone is preserved by a unique combination of cellular, biomolecular, mechanical, and physical factors. Zonal arrangement of articular cartilage during development is formed by controlling the secretion and locative distribution of transforming growth factor-β (TGF-β), bone morphogenetic protein (BMP), and insulin growth factor (IGF) family (Dy *et al.,* 2010). The exterior superficial zone is maintained by TGF-β1 and BMP-7 signalling (Moeinzadeh *et al.,* 2016). Chondrocytes in the superficial zone express pre-chondrogenic marker Sox-9 and superficial zone protein (SZP) (Andrades *et al.,* 2012; Las Heras *et al.,* 2012). The middle zone is maintained by TGF-β1 and IGF-1 signalling. Pre-hypertrophic chondrocytes in the middle zone highly express aggrecan, glycosaminoglycans, and collagen type II (Klein *et al.,* 2009; Nguyen *et al.,* 2011). Hypertrophic chondrocytes in the calcified zone are maintained by TGF-β1 signalling.

Chondrocytes in the calcified zone express hypertrophic markers alkaline phosphatase (ALP) and collagen type X (Nguyen *et al.,* 2011).

1.1.7.1 Biochemical cues

In order to keep tissue homeostasis and regeneration of the cartilage, some molecules are involved in the expansion and differentiation of mesenchymal stem cells MSCs (see sections 1.4.1.1-1.4.1.5) for example, Wnt protein, transforming growth factor-beta (TGF-β) superfamily, bone morphogenic proteins (BMPs) and cytokines (Cruz *et al.,* 2017). Wnt is a family of proteins that are reported to control bone mass *in vivo* and act directly on MSCs (Liu *et al.,* 2009; Takada *et al.,* 2009). These proteins also have influence on cartilage differentiation. The TGF-β superfamily includes many growth factors, which regulate the developmental skeletogenesis and postnatal skeletal homeostasis (Piek *et al.,* 1999). TGF-β has distinctive importance and was used for years to produce and assess cartilage (Albro *et al.,* 2013). BMPs are important morphogens, which regulate chondrogenesis and skeletogenesis during normal embryonic development (Hogan, 1996). Studies confirmed that MSCs cultured in the presence of BMP-2 increased osteoblastic indicators like alkaline phosphatase activity and expression of osteocalcin. This effect increases in the presence of dexamethasone (Rickard *et al.,* 1994).

Other factors which influence the differentiation of the MSCs interact, at different levels, with the Wnt and/or TGF-β /BMP pathways. These factors include fibroblast growth factor (FGF), platelet-derived growth factor (PDGF) and many transcription factors (TFs). FGF-2 aids the cell proliferation and maintenance of the undifferentiated MSCs phenotype over time (Martin *et al.,* 1997). PDGF was shown to inhibit osteogenic differentiation although, they are very important for the growth and essential in the differentiation of MSCs (Gruber *et al.,* 2004; Kratchmarova *et al.,* 2005).

1.1.7.2 Physical cues

Tissues and cells in the human body are influenced by a range of different external forces, which affect the cells development and maintenance. MSCs have been shown to be highly

mechanosensitive. Hence, physical stimulations can be considered a possible method for controlling of MSCs differentiation *in vitro* (Delaine-Smith and Reilly, 2012). Cells sense the physical environment through receptors by converting mechanical forces into biochemical signals. These processes involve changes in intracellular calcium concentration or the activation of diverse signalling pathways. These signals can adjust the cellular and extracellular structure through mechanosensitive feedback and can modulate diverse cellular functions as migration, communication, contraction, secretion, proliferation, differentiation and apoptosis, which are all crucial for organ development and homeostasis (Jaalouk and Lammerding, 2009).

Interactions between biochemical and mechanical signals to stimulate differentiation pathways have been reported and it is becoming clear that mechanical forces can critically direct stem cell behaviour (Estes *et al.,* 2004). There are several mechanical forces which affect the bone marrow environment, like tension, compression and fluid- induced shear (Gurkan and Akkus, 2008). Accordingly, various ways were developed to stimulate cells mechanically *in vitro*. These include tensile stress through stretching (tensile stress) (Brown, 2000), hydrostatic pressure (Angele *et al.,* 2003) platen abutment (compressive stress) (Goligorsky, 1988), shear stress through fluid flow (El Haj and Cartmell, 2010; Reinwald *et al.,* 2016), ultrasound (Iwashina *et al.,* 2006; Kobayashi *et al.,* 2009), high frequency, low magnitude displacement (vibration) (Edwards and Reilly, 2011; Go *et al.,* 1983; Lau *et al.,* 2010; Roundy *et al.,* 2003) and direct cell magnetic stimuli (Crawford *et al.,* 2006; Harrison *et al.,* 2017; Leung *et al.,* 2009).

Recently, cells can be instructed to change their function or undergo differentiation *in vitro* through the influence of the combination of appropriate chemical, physical and/or signals by different bioreactors, will mentioned in detail in this chapter (Section 1.5).

1.2 Cartilage disorder and pathology

Articular cartilage defects may result from injury, joint and cartilage infections or osteochondral pathology, such as osteonecrosis and osteochondritis dissecans.

Osteochondritis dissecans (OCD) is a disorder that affect joints, most frequently in children and teenagers. This illness occurs when a small segment of bone begins to separate from its surrounding region due to a lack of blood supply (Berndt and Harty, 1959). In adults, cartilage defects have bad prognosis for regeneration, which could lead to the development of degenerative arthritis (Zhang *et al.,* 2016). Cartilage lacks blood and lymphatic vessels so that, the cells infiltration in the normal inflammation process after the injury rarely occurs and the injury recovery is delayed or injuries do not heal (Zhang *et al.,* 2009). Adding to injuries and other pathological cartilage disorders, the construction of cartilage is not stable during the lifetime of an individual. Thus, following tissue maturation there is continuous chondrocytes activity to preserve the structure of the cartilage.

In a study, authors concluded that articular cartilage lesions were most frequently seen in patients during their forties, with full thickness lesions common in young adults in their third decade, following acute traumatic injuries, monotonous minor trauma and major evident injuries which all can lead to osteoarthritis (Mankin, 1982). A study of 72 knee injury patients, concluded that 95% of patients experienced with pain, 76% with swelling and 18% with ossify joint , with history of trauma in 68% of the patients (Johnson-Nurse and Dandy, 1985).

1.2.1 Cartilage ageing process

The cartilage aging process is not fully understood. Researchers hypothesized that aging occurs due to reduced responsiveness of chondrocytes to anabolic growth factors such as insulin like growth factor 1 (IGF1) (Loeser *et al.,* 2000), which along with a reduction in cellularity leads to a decrease in the chondroitin sulphate and aggrecan components of the cartilage and associated reduction in the water content (Jerosch, 2011). In addition, changes in the GAG structures including the extent and position of sulphation group have been reported (Hickery *et al.,* 2003). Furthermore, the collagen within the ECM becomes increasingly cross-linked resulting in increased cartilage stiffness (Grogan and D D'lima, 2010). Consequently, cartilage loses its ability to resist the forces placed upon it and this is

reflected in a gradual degeneration of the cartilage structure. These changes to the ECM reduce the ability of the cartilage and that usually progresses to degenerative disease state osteoarthritis (Zhang *et al.,* 2009). United States-based estimates suggest that symptomatic osteoarthritis affects 12% of individuals over the age of 24 increasing to 33% for those over 60 (Lawrence *et al.,* 2008).

1.2.2 Osteoarthritis

Osteoarthritis (OA) is the progressive erosion of articular cartilage and is characterised by severe pain, rigidity in the di-arthroidal joints and the subsequences limit joint mobility and function (Toai *et al.,* 2010). Most joints can be affected to develop OA, but knees, hips and small hand joints are the most frequently affected sites (Gupta and Gupta, 2005). The exact pathophysiology of OA is still unclear, but a fundamental characteristic of OA is the thinning or diminishing of articular cartilage and that is associated with pain, inflammation, and radiologically observable histopathologic lesion such as sclerosis and osteophytes. In addition to the synovial irritation, inflammation and bone remodelling processes lead to further roughness to the superficial layer which could cause accelerate joint damage. OA is not only a cartilage disease, but it is considered as a dynamic pathological condition that affects the whole joint tissues including the synovium and subchondral bone (Lee and Wang, 2017).

1.3 Cartilage damage repair - traditional and novel approaches

The treatments of the articular cartilage injury represent a great therapeutic challenge due to the tissue repair deficiency and its mal-regenerative ability. Numerous attempts have been made to regenerate articular cartilage (Marks, 2017). The treatment depends on the condition of the patient and their degree of cartilage damage. However, in a case of complete cartilage degeneration, total joint replacement is the only option (Benders *et al.,* 2013; Brittberg *et al.,* 1994).

The first attempts in regenerative medicine were surgical options such as microfracture, which is a simple arthroscopic procedure and by far is the most common method used as a first-line treatment for symptomatic chondral defects (Zhang *et al.,* 2016).

Autograft and less common allograft and xenograft transplantations are another surgical treatment have adopted to repair the cartilage defects. In this technique, a full depth plug of tissue is collected from a non-weight bearing area in the joint of the patient (Autograft) or from another Human (allografts) or animal (xenografts) (Wang *et al.,* 2015), followed by an implantation process into damage region of joint in order to obtain healthy tissue graft (Clair *et al.,* 2009). Each method has its own advantages and disadvantages. In spite of the excellent medical outcomes using the autografting method, there are some shortcomings which include inadequate donor tissues both in terms of capacity and quality, donor area morbidity (Laurencin *et al.,* 1999). Also, stability of the graft tissue at high weight-bearing region over time as a result of the graft tissue being extracted from a non-weight bearing area (Malloy and Hilibrand, 2002).

When other methods fail to repair the cartilage damage or when the articular cartilage has severe damage and advanced joint disease, then either total or partial joint replacement are employed. This method is done to restore typical function by removing the injured joint and implanting artificial shell (such as alloys and titanium), a polymer surface (such as polyethylene) as well as a metal stem. However, it comes with its own limitations including loosening of the artificial implant, wearing off and short life-span of implant (maximum of 15 years) and increasing pain of the patient (Zhang *et al.,* 2009).

The other surgical attempt is autologous chondrocyte implantation (ACI) (Gupta *et al.,* 2006). This method is suitable for partial cartilage lesions. ACI has been used clinically to repair both craniofacial and articular cartilage defects since 1987 (Marlovits *et al.,* 2006). The procedure was considered as the first application of cartilage regenerative medicine when a small cartilage piece is harvested from a low-weight-bearing area of the knee joint. The chondrocytes are enzymatically isolated from the biopsy and the cells are then grown *in*

vitro under the most optimal conditions to expand active chondrocytes. After 2–3 weeks, a suspension of these cells then is implanted surgically into the cartilage defect site under a periosteum flap to produce new cartilage tissue. This original technique was first described by Brittberg and colleagues and called cell-based therapy. This technique has been developed to involve scaffolds and growth factors and subsequently, considered as tissue-engineering techniques (Brittberg *et al.*, 1994). In spite of the favourable outcomes described elsewhere (Corpus *et al.*, 2012), this technique has a number of limitations such as the possibility of producing fibrocartilage, which has a different mechanical property from hyaline cartilage and requires multiple invasive surgeries (Zhang *et al.*, 2009).

1.4 Regenerative Medicine- a novel approach for cartilage defect repair

Principally, regenerative medicine involves a multidisciplinary effort to replace or repair diseased tissue and the fundamental components of regenerative medicine are cell therapy and tissue engineering (Terzic and Nelson, 2013). These two foundations are linked by the same aim, which is to design a safe, effective and consistent therapies for maintenance, regeneration or replacement of malfunctioning organs. This is done by seeding the appropriate cells into a three-dimensional (3D) scaffold, then culturing the resulting construct in a bioreactor under mechanical conditions to promote cell and tissue growth (Figure 1.2) (Borenstein *et al.*, 2007).

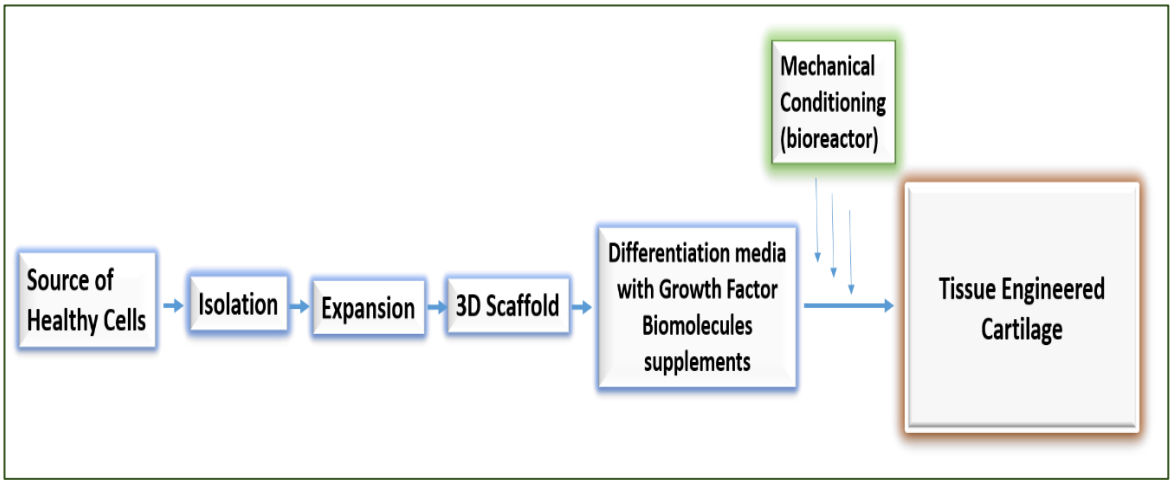

Figure 1. 2: A scheme displaying the fundamental pillars of the regenerative medicine for cartilage repair.

As a part of regenerative medicine, tissue engineering approaches are emerging as a reliable way to restore cartilage. The treatment of joint surface lesions aims to restore pain-free joint function by helping the formation of new tissue that has the structure and strength of natural articular cartilage (Chen *et al.,* 1997; Li *et al.,* 2013; Steadman *et al.,* 2003).

1.4.1 Cell therapy for cartilage tissue engineering

Within the advancement of tissue engineering, new techniques, cell sources, and biomaterials are being used to overcome the limitations of the traditional cartilage repair techniques. The goal in cartilage regeneration is to find an ideal cell source that can be easily isolated, is capable of expansion, and can be cultured to express and synthesize cartilage-specific molecules such as type II collagen and aggrecan (Chung and Burdick, 2008).

Foremost, chondrocytes have been widely studied to evaluate their role in producing, maintaining, and remodelling the cartilage ECM. However, there are some limitations using this cell source (Ikada, 2006; Liu *et al.,* 2017). Some of these challenges include limited availability of autologous chondrocytes and the invasiveness of the chondrocytes harvest process as well as the fact that it causes donor-site morbidity (Kock *et al.,* 2012). The monolayer culture methods that are used to expand chondorcytes cause them to dedifferentiate towards the fibroblastic phenotype with different properties for articular cartilage (Bonaventure *et al.,* 1994; Goessler *et al.,* 2004).

De-differentiation decreases the expression of collagen II, aggrecan and other proteins related with articular cartilage as well as an increased expression of collagen I, (Bonaventure *et al.,* 1994; Goessler *et al.,* 2004; Stewart *et al.,* 2000). Alternative cell types have been used including fibroblasts which are easily obtained in high numbers and can be directed toward a chondrogenic phenotype (Nicoll *et al.,* 2001).

In this context, stem cells which have a remarkable potential to develop into many different cell types in the body during early life and growth have been introduced as a possible cell source for orthopaedic tissue engineering since the eighties(Bruder and Fox, 1999; Tuan *et*

al., 2002). Additionally, these cells can be modified genetically to induce or enhance chondrogenesis (Gurusinghe and Strappe, 2014).

1.4.1.1 Stem cells

Stem cells are undifferentiated cells that can differentiate into specialised cells and they are found in multicellular organisms. In mammals, there are two main types of stem cells, embryonic stem cells and adult stem cells such as mesenchymal stem cells. Stem cells have two crucial properties; one of them is the ability to self-renew and creating new stem cells by symmetric division. Self-renewability is the process that permits to obtain two daughter cells which have the exact same characters of the mother cell. The other property is the ability to differentiate into multiple different types of daughter cells by asymmetric division (Barry and Murphy, 2004; Lodi *et al.,* 2011).

Stem cells have been introduced as a possible cell source for orthopedic tissue engineering (Bruder and Fox, 1999; Tuan *et al.,* 2002). Accordingly, investigations on cellular therapies focus on progenitor cell populations such as bone marrow derived mesenchymal stem cells (BM-MSCs), which also have the ability to differentiate into cartilage cells (Pittenger *et al.,* 1999). Clinically, autologous BMSCs have been used to repair articular cartilage defects by surgical transplantation of collagen-embedded BMSC constructs (Nejadnik *et al.,* 2010; Wakitani *et al.,* 2004; Wakitani *et al.,* 2007) and by direct intra-articular injections of BM-MSCs (Orozco *et al.,* 2013).

1.4.1.2 Mesenchymal stem cells

Due to their unique biological properties, mesenchymal stem cells (MSCs) have generated a great amount of interest in the field of regenerative medicine. These cells were discovered by Alexander Friedenstein and his coworker in 1968 as an adherent fibroblast-like population in the bone marrow (Friedenstein *et al.,* 1968). Subsequently, MSCs were isolated from various tissues such as adipose tissue (Zuk *et al.,* 2002), peripheral blood, umbilical cord and placenta (Kern *et al.,* 2006), liver and other adult and embryonic tissues (Fiegel *et al.,* 2006).

For better characterization of MSCs, the International Society of Cellular Therapy has defined MSCs by the following three characteristics. First, they must be adherent to plastic under standard tissue culture conditions. Second, they must express certain cell surface markers such as cluster of differentiation (CD) CD 73, CD 90, and CD 105, and lack expression of other markers including CD 45, CD 34, CD 14, or CD 11b, CD 79 alpha or CD 19 and human leukocyte antigen HLA-DR surface molecules. Finally, MSCs must have the capacity to differentiate (Niwa, 2013).

Although five stem cell sources are in current use, umbilical cord blood, amniotic fluid, bone marrow, mobilised peripheral blood, and adipose tissue stem cells, yet clinical applications were mainly limited to bone marrow and peripheral blood, which can be harvested easily and safely. In contrast, the use of other MSC sources are limited due to complicated and uneasy harvesting as well as unsafely expanding sufficient quantities (Burt *et al.,* 2008).

1.4.1.3 Multi-lineage differentiation potential of bone marrow derived MSCs

Bone marrow derived MSCs (BM-MSCs) are multipotent stem cells. Studies demonstrated that populations of BM-MSCs from human and other species have the capacity to develop into terminally differentiated mesenchymal phenotypes both *in vitro* and *in vivo,* including bone (Bruder *et al.,* 1998; Kadiyala *et al.,* 1997), cartilage (Kadiyala *et al.,* 1997), tendon (Awad *et al.,* 1999; Young *et al.,* 1998), muscle (Ferrari *et al.,* 1998), adipose tissue (Wong, 2004) and hematopoietic-supporting stroma (Weiss and Sakai, 1984). This capacity to differentiate into a diversity of connective tissue cell types has made them an interesting cell source for clinical tissue regeneration strategies, especially for bone (Ma, 2013; Orciani *et al.,* 2017), cartilage (Lee and Wang, 2017) and tendon (Lui, 2015; Sigal *et al.,* 2016; Yang *et al.,* 2013).

1.4.1.4 Tri-lineage differentiation of BM -MSCs

In order to stimulate adult MSCs to differentiate into different tissue types, specific differentiation media must be used. For instance, osteogenic differentiation occurs when MSCs are cultured in a monolayer with the presence of b-glycerol-phosphate, ascorbic acid-

2-phosphate, dexamethasone and foetal bovine serum in the culture media. The assessment of the osteogenic differentiation is obtained from the alteration in morphology, increasing regulation of alkaline phosphatase activity, and the complexity of a mineralised extracellular matrix (Toai *et al.,* 2010).

Whereas, the ideal culture environment for the induction chondrogenesis of MSCs must consists of a three-dimensional culture format, in the absence of bovine serum (serum-free medium), with involvement of a member of the transforming growth factor-beta (TGF-b). Hence, cells show a rapid morphological change and several cartilage-specific extracellular matrix components begin to appear. This is accompanied by an accumulation of glycosaminoglycan. TGF-β1, β2, and β3 have the ability to induce this chondrogenic response (Barry *et al.,* 2001). To induce adipogenic differentiation, MSCs should be seeded in a monolayer with the presence of isobutylmethylxanthine (IBMX) to produce large lipid-filled vacuoles. This process is induced by the nuclear receptor and transcription factor, peroxisome proliferator-activated receptor-Gama (PPAR-Ɣ), as well as fatty acids synthetase and is suppressed by both interleukin-1 and tumour necrosis factor-alpha (Sarugaser *et al.,* 2005).

With a view to utilise the regenerative medicine in cartilage repair, understanding the chondrogenesis inside the body is essential. Hence, it is known that during fracture healing and microfracture treatment of cartilage defects, the site of the injuries is invaded by MSCs from the bone marrow, synovial fluid and other surrounding soft tissues. These invaded cells are proposed to proliferate extensively and differentiate along a cartilaginous or an osteogenic lineage in response to local environmental cues such as growth factors and cytokines (Fortier *et al.,* 2011). MSCs may be able to directly sense their mechanical environment within a regenerating tissue and differentiate based on the local magnitude of shear strain, hydrostatic pressure, tensile strain, compressive strain and/or fluid flow they experience. Physical, chemical and mechanical cues are known to regulate the mechanisms of repairing following the injuries (Delaine-Smith and Reilly, 2012).

1.4.1.5 STRO-4 positive bone marrow derived stem cells

Cells isolated with STRO-4, a monoclonal antibody (mAb), have reactivity against commonly associated cell surface molecule markers like CD 29, CD 44, and CD 166. In addition, STRO-4 selected cells are able to identify the beta isoform of heat shock protein-90 (Hsp90β). It was reported that these STRO-4 positive MSCs (STRO-4^{+} MSCs) exhibited multilineage differentiation potential and were capable of forming a mineralized matrix, lipid-filled adipocytes, and chondrocytes capable of forming a glycosaminoglycan-rich matrix. (Gronthos *et al.,* 2009).

STRO-4 was found to selectively isolate ovine and human marrow-derived progenitor cells MPCs that exhibit high proliferative potential and multilineage differentiation capacity, the antibodies to Hsp90β were used as an effective single marker that identifies a highly conserved epitope expressed by MSCs from both ovine and human tissues (Gronthos *et al.,* 2009).

1.4.2 Scaffolds used for cartilage tissue engineering

Scaffolds fabricated from biomaterials were used to reduce the disadvantages related to cell-based therapy, such as insufficient incorporation into host tissues, imprecise cell distribution, and degeneration of healthy cartilage. A scaffold-based approach is based on cells proliferating in a 3D environment. This approach has been developed to improve the repair of cartilage lesions with autologous chondrocytes or *in vitro* differentiated MSCs (Hubbell, 1995; Yang *et al.,* 2001).

Scaffolds to be used for musculoskeletal tissue engineering should have properties similar to the native tissue. Scaffolds intended for musculoskeletal tissue engineering applications should be biodegradable, biocompatible and bioresorbable. They should not elicit any adverse host-immune reaction. Scaffolds should possess appropriate surface area and architecture for cell adhesion and proliferation. Scaffolds should also be mechanically stable to withstand the load, possess good handling properties allowing the scaffolds to be customised in accordance to the defect size (Arzi *et al.,* 2015). Use of polymeric materials /

biomaterials is the most effective alternative. Scaffolds intended for musculoskeletal tissue engineering applications should meet certain criteria such as: biodegradable, biocompatible and bioresorbable. They should not elicit any adverse host-immune reaction. With a feature of appropriate surface and architecture for cell adhesion and proliferation is an important characteristic of the scaffold. The scaffold also should be mechanically stable to resist the load. Also, possess good handling properties, that gives a possibility to be customised in accordance to the defect size (Getgood *et al.*, 2009).

Early scaffolds fabricated from simple synthetic materials like polyethylene meshes, carbon implants or carbon-polylactic acid polymers were used for skeletal tissue regeneration (Aragona *et al.*, 1981). The attention is now shifting towards the use of natural polymers like proteins and carbohydrates for the tissue engineering and a few of them are commercially available (Babu *et al.*, 2013; Sell *et al.*, 2010).

Many materials have been used as a scaffold for cell delivery in cartilage regeneration. The primary focus was on polymeric materials, in forms of hydrogels, sponges, and fibrous.

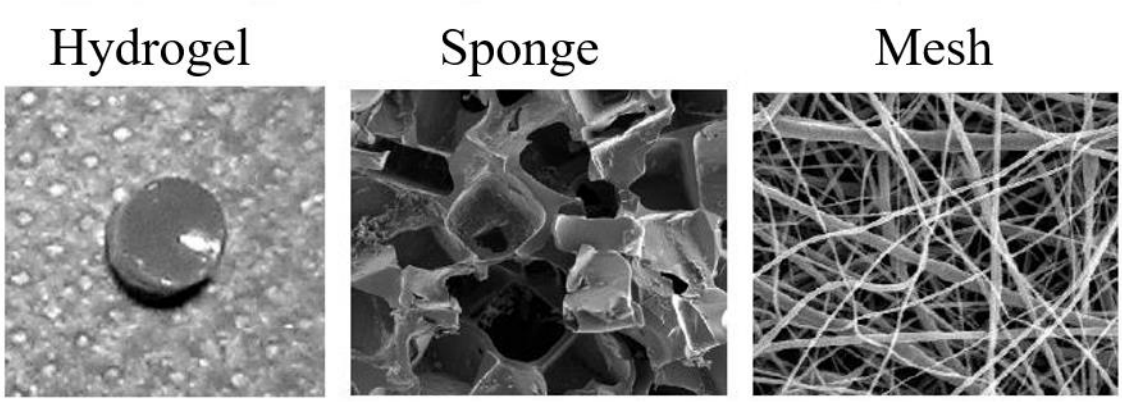

Figure 1. 3: Polymeric scaffold types.

The main function of the scaffold is providing a 3D environment that is required for the new cartilaginous tissue. Ideal scaffolds for cartilage regeneration should have specific characteristics like directed controlled degradation, they should encourage cell expansion, differentiation, and ECM production. In addition, they should be permeable and enable the exchanging of the nutrition and the waste products with the surrounding tissue. Furthermore,

scaffolds should be capable to adhere and integrate into the surrounding native cartilage tissue.

Various materials have been investigated for their suitability as a cartilage scaffold. The following sections summarise the commonly used materials in cartilage tissue engineering.

1.4.2.1 Synthetic scaffolds

Poly-α-hydroxy esters polymers such as poly (lactic acid) (PLA) and poly (lactic-coglycolic acid) (PLGA) are synthetic polymers used for cartilage tissue engineering scaffolds (Woodruff and Hutmacher, 2010). They are biodegradable synthetic polymers which can be fabricated into 3D matrices (Zhang *et al.,* 2009) and have suitable surface structure for cell attachment, proliferation, and differentiation (Hutmacher, 2006). Their structure, degradation features, and mechanical properties can be adjusted (Nuernberger *et al.,* 2011). Despite that there is a shortage associated with using synthetic polymers in cartilage engineering applications like lack signalling molecules for cell attachment and their degradation products may cause an increase in host response including inflammation which might lead to failure of the implant *in vivo* (Zhang *et al.,* 2009).

1.4.2.2 Natural scaffolds

Several natural biomaterials have been used for cartilage repair and regeneration due to their biocompatibility for cell attachment and differentiation (Hubbell, 1995). Hyaluronic acid (Burdick and Prestwich, 2011), agarose (Rahfoth *et al.,* 1998) and alginate (Fragonas *et al.,* 2000) and protein-based collagen (Nehrer *et al.,* 1998) are examples.

Hyaluronic acid scaffolds have bioactive properties with the ability to unite with chondrocytes. Hyaluronan based matrices enhance the production of collagen type II and GAG by the chondrocytes *in vitro* and *in vivo*. However, their mechanical properties cannot satisfy the cartilage tissue (Solchaga *et al.,* 2002). Hyaluronic acid was used in developing an injectable in situ forming type II collagen/hyaluronic acid hydrogel (Kontturi *et al.,* 2014). This hydrogel is able to maintain chondrocyte viability and characteristics, this potential injectable scaffold for cartilage tissue engineering helped to overcome the shortage of using

hyaluronan-based matrices (Solchaga *et al.,* 2001). On the other hand, Yu and his colleagues have fabricated an injectable hyaluronic acid/ polyethylene glycol hydrogel with excellent mechanical properties for cartilage tissue engineering (Yu *et al.,* 2013).

1.4.2.3 Protein-based collagen

One of the most popular natural biomaterials are collagens which represent essential protein content in ECM of the articular cartilage and they play an important role in cell adhesion, proliferation and differentiation. Therefore, it is regarded as one of the promising materials for constructing cartilage tissue engineering scaffolds.

Collagen type I usually utilises integral or after proteolytic removal of the small particles (like small nonhelical telopeptides), which reduces possible antigenicity. Native collagen is presented in two formulas as swollen hydrogels or as sparse fibers in a lattice-like organisation. The chondrocytes embedded in the hydrogel maintain their natural morphology and secrete cartilage specific ECM (Yuan *et al.,* 2014). Favourable hyaline cartilage regeneration with good chondrocyte morphology was observed after 24 weeks imbedded chondrocytes in the collagen-based hydrogel and injected it into the damaged rabbit cartilage without a periosteal graft (Funayama *et al.,* 2008).

Collagen type I and III is being commercially utilised for matrix associated chondrocytes implantation. Scaffolds fabricated from collagen are cultured with chondrocytes ex vivo followed by their implantation at the articular cartilage defect area (Bartlett *et al.,* 2005).

1.5 Bioreactors provide mechanical stimulation for cartilage repair

Bioreactor technology is pivotal for tissue engineering. Bioreactors are devices that provide mechanical stimulus *in vitro* to provide a tissue growth environment mimicking *in vivo* conditions. Bioreactors have the potential to improve the efficiency of the overall tissue engineering concept (Hansmann *et al.,* 2013). Till now, different bioreactor systems for tissue-specific applications have been developed, some of them are already commercially available (Cartmell *et al.,* 2002; El Haj and Cartmell, 2010; Fayol *et al.,* 2013; Meinert *et*

al., 2017; Reinwald *et al.*, 2016; Reinwald and El Haj, 2018). However, these have not resulted in clinically successful tissue-engineered implants. (Hansmann *et al.*, 2013).

To achieve the goal of generating biological substitutes that recapitulate the morphological, biochemical, as well as mechanical properties of native articular cartilage (Buckwalter and Mankin, 1998a; Solheim *et al.*, 2016), combination of cells and biomaterials, as well as external stimulation through biological and/or mechanical factors is used (Atala *et al.*, 2012). This has inspired the design of various bioreactor systems (Schulz and Bader, 2007) which aim to provide mechanical stimuli to support tissue maturation under a strictly controlled and closely monitored loading conditions. The working principles of such systems involve, for example, the application of hydrostatic pressure (Angele *et al.*, 2003; Elder and Athanasiou, 2009), compressive (Demarteau *et al.*, 2003; Tran *et al.*, 2011) or shear loading (Jin *et al.*, 2001; Waldman *et al.*, 2003).

A commercially available oscillating magnetic bioreactor was used to mechanically stimulate different receptors remotely after treatment with MNPs and this was enhanced after mechano-stimulation using the magnetic array. (Henstock *et al.*, 2014; Markides *et al.*, 2018; Rotherham and El Haj, 2015). This magnetic force bioreactor provided by MICA Biosystems (Figure 1.4) consists of arrays of permanent magnets.

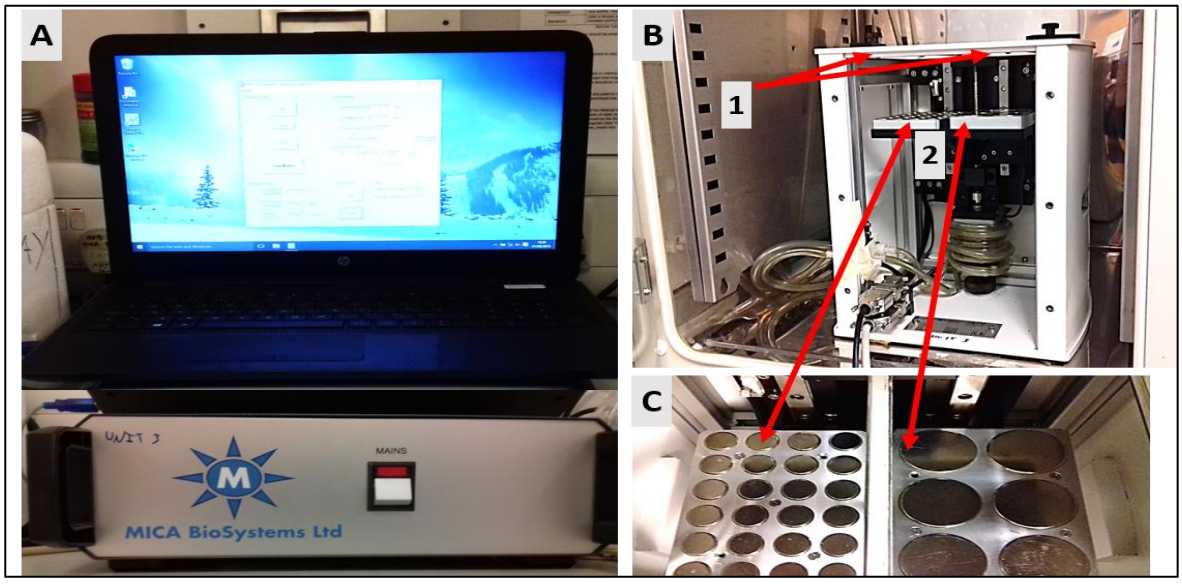

Figure 1. 4: Oscillating magnetic bioreactor (MICA Biosystem). *(A) Bioreactor control system, (B) the system inside the standard cell culture incubator 1) cell culture holder. 2) a moving magnetic array situated beneath the culture plates delivering a vertically oscillating external magnetic field, C) different types of magnetic array (24 and 6 well).*

The magnets can be remotely positioned to move the arrays toward and away from culture plates in a vertical plane to impart magnetic field gradient, the system can be housed inside a standard tissue culture incubator maintained at standard conditions. The apparatus is controlled by software which regulates parameters such as the speed, frequency and number of loops of the arrays.

The principle of the action of this system depends on the fact that the MNPs can be controlled using the external magnetic field (Marcos-Campos *et al.*, 2011) and stimulate mechanotransduction process of the cells by targeting the mechanosensitive channel with MNPs.

1.7 Mechanotransduction

Mechanotransduction is the process by which the physical force is converted into a biological signal, this vital process occurs through so called mechano-sensitive proteins like Integrins, ion channels and growth factor receptors. Mechanotransduction revolve when applied forces induce conformational changes in these mechano-sensitive receptors. This leads to changes in their activation state, subsequently signalling to downstream intracellular signalling pathways (Farge, 2003; Ingber, 2006; Kiyotake *et al.*, 2016). Various cell types express mechano-sensitive receptors including cartilage cells. Activation of mechanosensors leads to downstream, ultimately leading to transcription of mechano-sensitive genes and changes in gene expression that alter cell proliferation, migration, differentiation and the production of signalling molecules such as cytokines (Mammoto *et al.*, 2012). The detection of the mechanical forces by the cell will occur through mechanosensitive molecules. Many molecules are involved in mechanotransduction like primary cilium, cadherins surface receptor, integrin, ion channels and some other molecule (Ingber, 2006).

During mechanotransduction that mediated through stretched activated ion channels, there is a mechanical disruption of the cell membrane which causes conformational changes in ion channels and consequently controlling ion flow across the cell membrane by the opening and closing of the ion channels. This results in ion instability across the cell which results

in changes to cell activity (Ingber, 2006). Targeting specific mechano-sensitive ion channels on the cell membrane of MSCs with functionalised, biocompatible, magnetic nanoparticles (MNPs), ion channel can be controlled with an oscillating external magnetic field. The movement of the particle creates a pico-newton force that is transferred to the ion channel to which the MNPs have attached, spreading the mechanical stimulus via mechanotransduction pathways inside the cells. Examples for Mechano-sensitive ion channels are Twik-related potassium channel (TREK-1) and Transient receptor potential cation channel subfamily V member 4 (TRPV4).

1.7.1 Twik-related potassium channel 1 (TREK-1)

TREK-1 is expressed in most tissues and is particularly presented in tissues of the nervous system, lung, heart and smooth muscle (Aimond *et al.,* 2000; Fink *et al.,* 1996; Koh *et al.,* 2001; Medhurst *et al.,* 2001). This ion channel regulates the resting membrane potential of the cell (Fink *et al.,* 1996; Lesage and Lazdunski, 2000; Patel and Honoré, 2001). It is sensitive to a number of stimuli like heat, lipids and pH. TREK-1 channels are also known to be mechanoresponsive to the forces such as stretch leading to the opening and closing of the channels. This results in movement of potassium ions across the cell membrane that leads polarisation of the cell (Hughes *et al.,* 2007; Patel *et al.,* 1998).

1.7.2 Transient receptor potential cation channel subfamily V member 4 (TRPV4)

TRPV4 is the fourth member of the vanilloid subfamily in the transient receptor potential (TRP) superfamily of ion channels. The TRPV4 gene, initially named "vanilloid-receptor related osmotically activated channel" (VR-OAC) and TRPV4. It is a calcium permeable cation channel that is detectable in both sensory and non-sensory cells. It is widely expressed and located on the plasma membrane of numerous human and animal cell types, in addition to some fungi. TRVP4 is expressed in different types of tissues including kidneys, lungs, hearts, brains, endothelial cells and trigeminal sensory ganglia. The channel has several different modes of activity or occurrence and is involved in a wide range of functions from

osmoregulation to thermosensing. TRPV4 was originally identified as an osmotically activated channel (Nilius *et al.,* 2003). However, this channel can be stimulated by diverse stimuli like hypo-osmotic swelling (O'Neil and Heller, 2005), shear stress (Sidhaye *et al.,* 2008), non-noxious temperatures (Story, 2006) and acidity (Cao *et al.,* 2018).

1.8 Nanomagnetic technology

Nanomagnetic technology is a novel tool for activating the cells physically. Magnetic nanoparticle (MNPs) are three-dimensional Nano scaled magnetic particles made from materials like nickel, cobalt and iron. Iron magnetic nanoparticle particles are safer for biomedical purpose because it has been reported that cobalt and nickel are toxic to biological Objects (Berry, 2005; Hofmann-Amtenbrink *et al.,* 2010).

Researchers began to investigate whether a variation on the magnetic twisting technique could be used to activate mechanosensitive ion channels (Barry *et al.,* 2001; Barry and Murphy, 2004; Glogauer and Ferrier, 1997; Glogauer *et al.,* 1995; Pommerenke *et al.,* 1996).

Nanomagnetic actuation was applied to numerous areas of biology and biomedical science for example to study mechanical properties (Septiadi *et al.,* 2018), mechanosensitive ion channel signalling pathways (Hughes *et al.,* 2005) targeted activation of specific ion channels (Hughes *et al.,* 2008) and the construction of 'biochips' and mechanical conditioning of cells for regenerative medicine applications (Wang *et al.,* 2008). Studies have shown that manipulation of integrin attached to magnetic particles leads to changes in intracellular calcium signalling within osteoblasts (Chen *et al.,* 2016; Hughes *et al.,* 2007; Pommerenke *et al.,* 1996; Scott *et al.,* 2008). Thus, magnetic particles offer a tool for applying controlled mechanical stimuli to osteoblasts and can be used to stimulate intracellular calcium signalling over prolonged periods of time (Chen *et al.,* 2016). The mechanism of the mechanical stimuli using magnetic nanoparticles is showed in Figure 1.5.

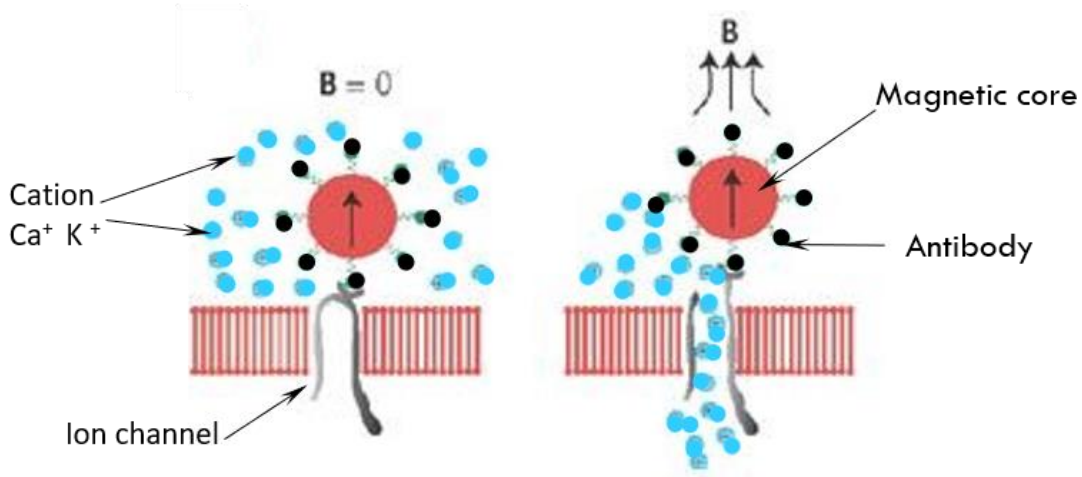

Figure 1. 5: Targeted ion-channel activation. *Magnetic nanoparticles (100 nm–2.7 µm) are attached to an ion channel via an antibody (left), upon activation of a high-gradient magnetic field source (right), the ion channel is forced open. B = magnetic field vector (Dobson, 2008).*

It is not necessary for the particles to be magnetically blocked. Instead they may be superparamagnetic. By applying a strong magnetic field with a high gradient, the particles experience a translational force that can pull the particles and hence activate nearby mechanosensitive ion channels (Pankhurst *et al.*, 2003).

Adding to MRI (Magnetic resonance imaging), researchers have investigated MNPs for cell-based therapy for other fields, like enhance transfection (Pickard *et al.*, 2011), induce hyperthermia (Kobayashi, 2011), force *in vitro* aggregation (Fayol *et al.*, 2013), enable regenerative therapies (El Haj *et al.*, 2015) and activate cell receptor signalling on the cell membrane (Henstock *et al.*, 2014). The characteristics of small size and magnetic properties of the MNPs , in addition to versatile surface coatings (Gupta and Gupta, 2005), lead to enhance existing and future regenerative cell therapies.

1.9 *in vivo* animal models for orthopaedics

Animal model is a commonly used method for testing medical substances or tissue engineering approach (Cibelli *et al.*, 2013). At present, there is no animal model can give representative comparison for all research questions for orthopaedic regeneration of humans. In fact, each animal model was selected to treat a specific research question. For instance, the investigations of bone biology and response to growth factor combinations could be assessed within small animals such as mice or rats. Chondrogenesis has been extensively

studied in murine models by subcutaneous (Amiel *et al.,* 2001; Puelacher *et al.,* 1994), intramuscular (Haisch *et al.,* 2000) and intraarticular implantations (Lammi *et al.,* 2001; Matsumoto *et al.,* 2008; Oshima *et al.,* 2005; Pagnotto *et al.,* 2007). However, small animal models like rodent and rabbit are related with natural spontaneous healing of cartilage not seen in larger animals and humans (Dawson, 1925). Thin articular cartilage and the small size of the articular joints are the main reasons for limited treatments. In addition, there are difficulties to follow up post-operative in this animal models like bandaging, restricted weight-bearing and physical therapy. Additionally, the movement pattern are much different from that of humans, leading to differences in cartilage loading patterns (Cook *et al.,* 2014). Due to cost related issues, basic cartilage tissue engineering studies are undertaken *in vitro* and the transition to *in vivo* animal models depended on the need. Generally, costs per animal increase with animal size (Chu *et al.,* 2010). Initially small animal models was used, including mice, rats and rabbits (Chu *et al.,* 2010; Cook *et al.,* 2014). Especially Immune-compromised mice which are useful in testing ectopically implanted xenogeneic cartilage-like tissues derived from human cells. However, the microenvironment of ectopic sites differs from joints. From other points and even though joints in rats and rabbits are sufficiently large for surgical manipulation and these animals are commonly used to study cartilage repair. But, the cartilage is thinner than that of humans, cartilage defects in these animals may spontaneously heal, and joint biomechanics and loading differ from humans (Cook *et al.,* 2014).

All these disadvantages have led to necessity and motivate to placement large animal models of cartilage repair.

Most utilized large animals in cartilage repair are swine, caprine, equine and ovine (Bornes *et al.,* 2014; Kuyinu *et al.,* 2016). These large animals gives a pre-clinical stifle joint model that have applicable and similar in size and anatomy to a human knee joint than a small animal (Cook *et al.,* 2014). In a review study Music and his colleagues did, they summarised

cartilage repair studies that used these four large animals between 1993 and November 2017, (Figure 1.6).

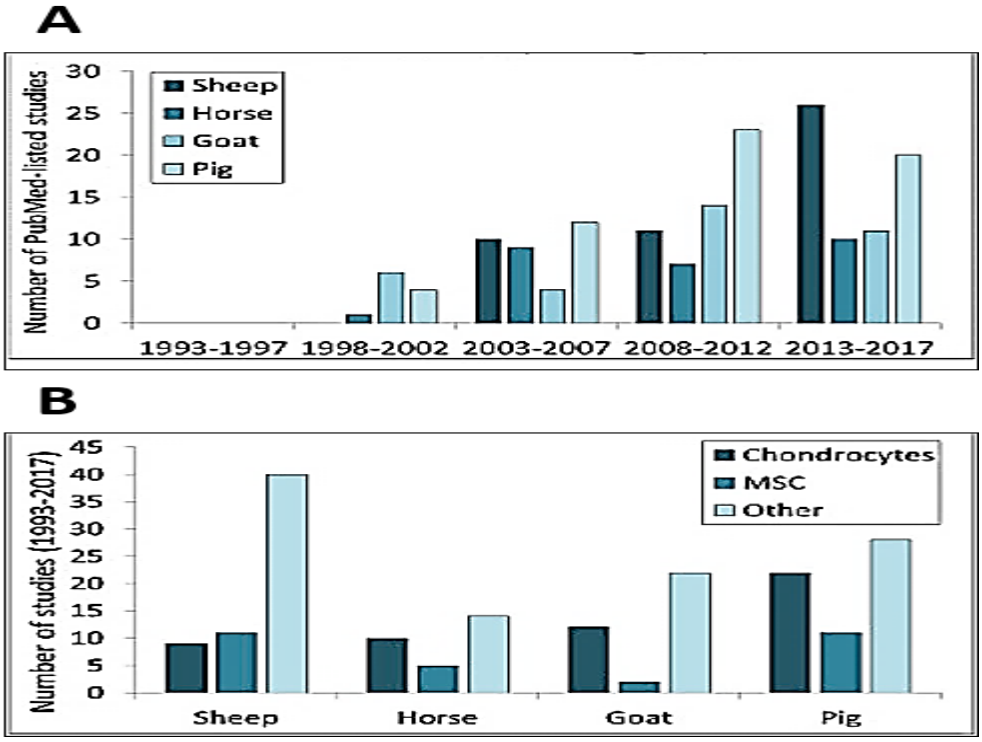

Figure 1. 6: The large animals used in cartilage defect repair. *A) number of publications that used the indicated large animal model to study cartilage repair. B) Number of chondrocytes or MSC-based cartilage repair studies reported from 1993- 2017(Music et al., 2018).*

The two most common animal models were sheep and pig, with sheep being the most commonly used large animal between 2013 and November 2017 (Music *et al.*, 2018). Although there are some limitations and disadvantages of using sheep as animal model for orthopaedic studies, like high cost, ethical consideration and quadrupedal gait, this animal model is the best representative option for better clinical translation to the human practice. Sheep are docile and have similar large bone structure, biochemical, and mineral composition of humans. In addition, the size and basic anatomy of the sheep skeleton are generally comparable with the humans (Wilke *et al.*, 1997). Hence, orthopaedic implants including engineered cartilage tissue are commonly tested in sheep model (Egermann *et al.*, 2008; Hoemann *et al.*, 2011; Music *et al.*, 2018; Potes *et al.*, 2008; Yoshiya and Dhawan, 2015). Numerous studies have performed utilised sheep in orthopaedic and cartilage engineering. Examples of sheep trials that have been performed for cartilage repair and MSCs studies are shown in Tables 1.2 and 1.3.

Table 1. 2: Summarised the studies that investigated ovine MSCs, (N/A= not available).

References	Kind of Study	Bread of sheep used	Sex	Age (year)	Sites of isolation	The output of the study
(Rentsch et al., 2010)	Isolation and expansion oBM-MSCs and their osteogenic differentiation potential	Merino sheep	N/A	N/A	Iliac crest bone marrow aspirates	The isolated oMSC are able to proliferate and maintain the ability to differentiate into multiple mesenchymal cell types CS as part of the artificial matrix could induce the osteogenic differentiation of oMSC
(Czernik et al., 2013)	Differentiation Potential and green fluorescent protein (GFP) Labeling oBM-MSCs	Sarda breed	Female	6–7	Iliac crest bone marrow aspirates	oBM- MSCs exhibit morphological and transdifferentiation potential parallel to hMSCs. plus, development of a sheep preclinical model for MCS transplantation in an isogenic context.
(Mccarty, Gronthos, et al., 2009)	Characterisation and developmental potential of oBM-MSCs	N/A	N/A	1-4	Iliac crest bone marrow aspirates	oMSCs were effectively harvested from bone marrow aspirates and exhibit morphological, immunophenotypical and multipotential *in vitro* and *in vivo*.
(Lyahyai et al., 2012)	Isolation oMSC from Peripheral blood	Rasa Aragonesa breed		1.5-6	Peripheral blood	First attempted to isolate oMSC peripheral blood. these cells can transdifferentiate into neuron-like cells and express PRNP.
(Jäger et al., 2006)	Multipotent Mesenchymal Progenitor Cells from Ovine Cord Blood	Moorschnucken sheep	Neonatal lamb	After natural birth	Blood from the umbilical cord	First attempted to isolate cord blood-derived MSCs from sheep and osteo-, chondro- and adipogenic differentiation. The mesenchymal population of ovine cord blood should be the target for future investigations.
(Heidari et al., 2013)	oMSCs derived from Bone Marrow, Liver, and Adipose Tissue	N/A	N/A	30-35day foetus	From bone marrow liver and adipos tissue (foetus was obtained from the slaughterhouse)	The three sources of foetal sheep MSCs had the same multilineage differentiation potential. Among the three sources of MSCs the bone marrow and adipose tissue derived MSCs had the highest and the lowest proliferative potential, respectively. In all the three sources of MSCs, there was a negative relationship between cell seeding density at culture initiation and proliferative. The liver derived MSCs are good alternative for bone marrow derived MSCs.
(Fadel et al., 2011)	Protocols for obtainment and isolation of two mesenchymal stem cell sources in sheep	Santa Ines	N/A	Female	Umbilical cord blood and adipose tissue	Umbilical blood collection and gather adipose tissue samples from kidney area was very well succeeded was innocuous to the foetus and pregnant sheep

Table 1. 3:Summarised the literatures that use sheep model in cartilage defect, repair and regenerative medicine, (N/A= not available).

References	Kind of Study	Bread of sheep used	Sex	Age	Sites of oMSC and/or chondrocytes isolation	Site of defect	The output of the study
(Al Faqeh et al., 2012)	Cell therapy for osteoarthritis by chondrogenic-induced oBM-MSCs	Siamese long tail sheep	N/A	12 months	Iliac crest bone marrow aspirates	Surgically induced osteoarthritis knee joints	Intra-articular injection into OA knee joints of sheep with autologous bone marrow stem cells cultured in chondrogenic medium has the possibility of retarding the progression of OA
(Guo et al., 2004)	Repair of large articular cartilage defects with implants of autologous mesenchymal stem cells seeded into tricalcium phosphate in a sheep model	N/A	male or female	6-12 months	Iliac crest bone marrow aspirates	Non-weight bearing area of the medial femoral condyle	This is the first report of repairing large, full-thickness articular cartilage or osteochondral defects of the weight-bearing area on the medial condyle of the femur by implants of MSCs
(Hao et al., 2010)	Sheep articular cartilage defects repair *in vivo* by chitosan hydrogels	N/A	male or female,	8–12 months	The articular cartilage tissue was cut off from the non-weight-bearing areas to isolate chondrocytes	Non-weightbearing area of the medial femoral condyle	Tissue-engineered cartilage via combining a novel, natural scaffold technology with autologous chondrocytes proved to have great potential for regenerating damaged knee cartilage in the animal model *in vivo*.
(Kandel et al., 2006)	Repair of osteochondral defects with biphasic cartilage-calcium polyphosphate constructs in a sheep model	N/A	N/A	N/A	Chondrocytes were isolated form cartilage harvested from trochlear ridge	The defect was made in distal aspect of the trochlear groove of the femur using a specially designed	This study suggests that biphasic constructs may be a suitable approach for osteochondral defect repair as the implants were maintained up to 9 months in sheep
(Burger et al., 2007)	The purpose of this study was to analyse cartilage changes after traumatic meniscal lesions	blackhead Merino sheep (Schwarzkopf)	female	16–20 months	No cell therapy	A radial tear in the medial meniscus	Ovine knee serves as a good model for cartilage changes in knee alterations such as injuries of collateral and cruciate ligaments, joint capsule and knee-involving tendons.
(Aagaard et al., 2003)	Assess the effect of immediate and delayed transplantation on articular cartilage.	Icelandic sheep	female	n/m	No cell therapy	Surgery on the medial menisci in both knees.	Immediate meniscal allograft transplantation reduced, but did not prevent, articular cartilage degeneration during short observation periods, and that immediate transplantation was superior to delayed transplantation

To avoid rejection of heterologous or xenogeneic cells, autologous cells are used preferably, but ovine MSCs (oMSCs) are unlike human MSCs (hMSCs). Ovine MSCs are not well studied regarding isolation, expansion, and characterisation. For that reason, some studies investigated growth characteristics, differentiation, and surface antigen expressions of oMSCs (Adamzyk *et al.,* 2013). As in humans, there are individual variations between different donors in animals, but despite large donor-dependent variations, standard protocols and media for hMSCs differentiation were established by Pittenger in 1999 (Pittenger *et al.*, 1999). In contrast, oMSCs differentiation and characterization protocols are still not standardised.

1.10 Thesis Aims and Objectives

The main hypothesis underpinning this work is studying the effect of dynamic conditioning on the chondrogenic differentiation of oMSCs. This will be precedent by the characterisation of oMSCs and native sheep cartilage. Firstly, the native sheep cartilage will be characterised biochemically and mechanically for the comparison with the engineered cartilage to be produced in this PhD study with studying the variation of these characteristics between different donors.

In addition, another precedent study will be focusing on the study of oMSCs characteristics to enrich the information about *in vitro* oMSCs differentiation and characterisation protocols that are still not standardised because using sheep as a preclinical model for orthopaedics research will need excessive and advanced *in vitro* studies. Furthermore, determining variations in characterisation and chondrogenic differentiation may allow studying the potential influence of donor variations on clinical outcomes in regenerative medicine and tissue engineering for cartilage repair.

1.10.1 Aims

The aim of this thesis is to use the pioneering MICA technology to enhance the chondrogenic differentiation of oMSCs to form cartilage and to explore the effect of mechanical stimulation on the oMSCs by remotely activating mechano-sensitive cation channels on the oMSCs membrane by directed mechanical stimuli.

In addition, this thesis aims to determine variations between oMSCs donors and native sheep cartilage by characterisation and chondrogenic differentiation of the oMSCs. This allows to study the potential influence of donor variations on clinical outcomes in regenerative medicine and tissue engineering for cartilage repair.

1.10.2. Objectives

The objectives of this thesis are

- Isolation and biochemical as well as mechanical characterisation of oMSCs to determine donor variability between 13 donors
- To study the donor variation of the oMSCs characterisation for tri-lineage differentiation and CD markers expression.
- Isolation, biochemical and mechanical characterisation of native sheep cartilage to determine donor variation.
- To study the effect of mechanical stimulation using MICA technology on the chondrogenic potential of the isolated oMSCs.
- To compare static culture conditions with mechanical culture conditions by targeting the TREK-1 mechano-sensitive potassium ion channel and investigate the donor variability in this response.
- To compare TREK-1 and TRPV4 mechanosensitive channel activation using MICA technology after targeting them with magnetic nanoparticles (MNPs) to study donor variation and to compare dynamic and the static growth condition.

CHAPTER 2

Materials and Methods

2.1 Materials

Materials which have been used in this thesis were sourced from the manufacturer or their distributors within the United Kingdom, except for those which were referred to in the text (Table 2.1).

Table 2. 1: List of reagents and their manufacturers

Reagents and materials	Companies and catalog numbers
3-Aminopropyltriethoxysilane (APTES)	Sigma – Aldrich, UK, Cat# 440140-100ML
3-isobutyl-1methylxanthine (IBMX)	Sigma – Aldrich, UK, Cat# I5879
Alamar blue	INVITROGEN Cat# DAL 1100
Alcian Blue	Sigma- Aldrich, UK. Cat# A3157-25G
Alexa Fluor ® 555 goat anti-rabbit – IgG	ThermoFisher Scientific Cat# A21428
Alizarin Red S	Sigma- Aldrich, UK. Cat# A5533-25G
Alpha minimum essential medium without l-glutamin (α MEM)	LONZA Cat# BE12-169F
Ammonium acetate ≥98.0%,	AnalaR NORMAPUR ® prod.no. 100134T
Anti-K_{2p}2.1 (TREK 1) 0.2ml	Alamon labs Cat# APC-047
Anti-Mouse IgG MicroBeads secondary antibodies	Miltenyi Biotec 130-048-401
Ascorbic Acid	AnalaR®, BDH, UK Cat# 103033E
Beta –Glycerophosphate (BGP)	(Sigma – Aldrich, UK, Cat# G5422)
Bovine serum albumin (BSA)	Sigma- Aldrich, UK. Cat# A9418
calcium chloride	Sigma- Aldrich, UK Cat# C-5080
CD marker Anti-bovine CD 29	KINGFISHER BIOTEC.INC. Cat# WS0577B-100
CD marker Anti-bovine CD 44	KINGFISHER BIOTEC.INC. Cat# WS0521B-100
CD marker Anti-bovine CD 45 R	KINGFISHER BIOTEC.INC. Cat# WS05284B-100
CD marker Mouse anti ovine CD31	BIO-RAD Cat# MCA1097GA
Cetylpyridinum chloride (CPC)	Sigma- Aldrich, UK Cat# C0732-100G
Collagen type I rat tail	Corning Cat# 354236 - 100 mg (3.55mg/ml)
DAPI	Sigma – Aldrich, UK, Cat# D9542- 50 mg
Dexamethasone	Sigma – Aldrich, UK, Cat# D2915
Dimethyl sulfoxide (DMSO)	Sigma – Aldrich, UK, Cat# D2650
Dimethylmethylene blue (DMMB)	Sigma – Aldrich, UK, Cat# 341088_1G
Direct Red 80 (Sirius red)	Sigma- Aldrich, UK. Cat# 365548-25G
DOTAP	Sigma- Aldrich, UK. Cat# D6182
Douglas MEM high glucose (DMEM) 4.5mg/ml	Lonza Biowhittaker, UK Cat# BE12-614F
Douglas MEM low glucose (DMEM) (1mg/ml)	Lonza Biowhittaker, UK Cat# BE12-707F

DPX Mountant for	Sigma – Aldrich, UK, Cat# 06522-100ML
Eosin	Sigma – Aldrich, UK, Cat# HT110116-500ML
Ethanol	Fisher Scientific Code: E/0650/17
Ethylenediaminetetraacetic acid disodium salt dihydrate (EDTA)	Sigma- Aldrich, UK. Cat# E5134
Fetal bovine serum (FBS)	Biosera Cat# FB-1001G/500
Glycine	Sigma – Aldrich, UK, Cat# G 8898-1kg
Goat pAb to Rb IgG 1mg/ml Secondary antibody	Abcam Cat# ab 97196
HCl	Sigma – Aldrich, UK, Cat# 258148- 2.5L
Hematoxylin Gill No.3	Sigma – Aldrich, UK, Cat# GHS3-500ML
Heparin Sodium	WORKHARDT, UK 5,000 I U /ml
HEPES buffer	Sigma – Aldrich, UK, Cat# H0887
Histological Clearing agent (Histo-Clear)	National diagnostics order no. HS-200
Histology slide mounting medium DPX mountant	Sigma- Aldrich, UK. Cat# 06522-100ml
Hydrogen peroxide H_2O_2	Sigma – Aldrich, UK, Cat# H0887
ImmPACT ™ DAB Peroxidase Substrate Kit	VECTOR LABORATORIES Cat# SK-4105
ImmunoCruz™ rabbit ABCA staining system	SANTA CRUZ BIOTECHNOLOGY, INCsc-2018
Indomethacin	Sigma – Aldrich, UK, Cat# I7378
Industrial methylated spirit 99% (IMS)	GENTA MEDICAL Cat# GM707
Insulin	Sigma-Aldrich, UK Cat# I 9728
Isopropanol (2-propanol)	Fluka® Cat# 34965-2.5L
ITS (insulin, transferrin, sodium selenite. (Liquid Media Supplement)	Sigma- Aldrich, UK. Cat# 13146-5ml
L- Ascorbic acid	Sigma- Aldrich, UK. Cat# A4544-25G
L-Glutamine	Sigma-Aldrich, UK Cat# G7513
L-proline	Sigma- Aldrich, UK. Cat# P5607
Methanol	Fisher Scientific Code: M/3950/21
NaCl	Sigma – Aldrich, UK, Cat# 5925-1Kg
Nanomag -silica Nanoparticles	Micromod Partikel technologie GmbH Cat# 09-02-252
Neutral buffered formalin solution 10%	Sigma- Aldrich, UK. Cat# HT501320-9 5L
N-hydroxysuccinimide (NHS)	Sigma- Aldrich, UK. Cat# 130672-25 g
Non-essential Amino Acid Solution NEAA	Sigma- Aldrich, UK. Cat# M7145-100ml
Normal goat serum	VECTOR LABORATORIES Cat# S-1000
Oil Red O	Sigma- Aldrich, UK. Cat# O0625-25G
Penicillin-Streptomycin P/S	Sigma-Aldrich, UK. C Cat# at# P4333
Phosphate buffered saline (PBS)	LONZA Cat# BE17.516F and /or Sigma – Aldrich, UK. Cat# H3393
Pierce™ BCA Protein Assay Kit	Thermo Fisher Scientific: reagent A Product No. 23227, reagent A Product No. 23224
Proteinase K	Sigma – Aldrich, UK, Cat# P 2308

Quant-iT™ PicoGreen™ dsDNA Assay Kit	Thermo Fisher Scientific Cat# P11496
Rat anti mouse IgG1 microbeads	Miltenyi Biotec Cat# 130-047-101
Red blood cells lysing buffer	Sigma- Aldrich, UK. Cat# R7757
Rosiglitazone	Sigma-Aldrich, UK. Cat# R2408-10MG
Sodium bicarbonate	Sigma- Aldrich, UK. Cat# S5761-500g
Sodium chloride	Fisher Scientific Code: S/3120/53
Sodium hydroxide	Sigma- Aldrich, UK. Cat# S8045 -1KG
Sodium Pyruvate	Sigma- Aldrich, UK. Cat# S8636
STRO-4 hybridoma primary antibody	Kindly offered by Dr Markides, These antibodies were prepared by Australian team, and freezed in a 20µL aliquots ready to make working concentration solution by adding 980 µL of PBS.
Transforming growth factor-beta1 (TGF-β1)	Peprotech, UK. Cat# 100-21
Transforming growth factor-beta2 (TGF-β3)	Peprotech, UK. Cat# 120-14E
Triton™ X-100	Sigma- Aldrich, UK. Cat# T8787
Trypan blue	Biosera 0.5% sol. Cat# L 0990-100ml

2.2 General Methods

All general methods like general cell culture, histological methods, mechanical and biochemical analysis are explained in detail in this chapter and will be referred to by their sections whenever they are mentioned in this thesis.

2.2.1 Bone marrow aspiration

Thirteen adult female English Mule sheep, non-pregnant, skeletally mature (age 2 - 4 years, weight 64.5 - 89.5 kg) were used in this study. The sheep were housed at the Sutton Bonnington Animal Facility at Nottingham University. All surgical procedures, including anesthesia, were observed.

2.2.1.1 Animal preparation for surgery

Animals were prepared for surgery by firstly, starving the sheep for 24 hours pre-general anesthesia. Also, by restricting access to water from the time that premedication was administered.

2.2.1.2 Analgesia

Appropriately sized Fentanyl patches (Durogesic® Janssen-Cilag Ltd cat # N02A B03) were applied 12 to 24 hours prior to the surgery, to provide a total dose of 2 μg/kg/hr (Ahern *et al.,* 2009). All wool on the antebrachium area was carefully sheared circumferentially from the elbow joint to the carpus joint, avoiding traumatizing the skin. Next, the lateral aspect was scraped with chlorhexidine for 30 seconds, defatted with isopropyl alcohol wipes for a further 30 seconds. Then, allowed to air dry for 2 minutes. A required piece of patch was applied to the skin on the lateral aspect of the sheared area and was held in place for 30 seconds. The patch was then covered with a self-adhesive bandage and an adhesive tape was applied over the entire area to secure the bandage to the skin. Care was taken to avoid heating up the patch-skin interface to avoid variable fentanyl absorption. The patches were bandaged over at all times to make sure that they were remaining in place and the animal could not ingest them.

2.2.1.3 Anaesthesia

Xylazine 2% in a dose of 0.1 mg /kg body weight was administered as premedication drug by deep intramuscular injection. The animals were left in a quiet place and a calm atmosphere for 10 to 15 minutes post-administration. Next, they were injected with combination of Ketamine (2mg/kg body weight) and Midazolam (0.25-0.3 mg/kg body weight) intravenously as induction anaesthetic agents. The animals were prepared for maintenance general anesthesia, and were supplied with oxygen, and an intravenous catheter was applied in the cephalic vein. After that, the larynx was sprayed with a lignocaine spray, to facilitate the insertion of the endotracheal tube, which was formerly lubricated with local anaesthetic gel. Anaesthesia was then, provided by low levels of isoflurane using appropriate flow rates in oxygen. A stomach tube was placed once the animal was anaesthetised to prevent inhalation of ingests and was removed at the end of the procedure.

2.2.1.4 Surgery

Bone marrow was surgically aspirated from the sternum bone of the animals. Surgery was performed under general anaesthesia, as explained above. The surgical area was prepared by shearing the wool from the sternum region and was then thoroughly cleaned with warm soapy water followed by antiseptic swabs. The surgeon proceeded to puncture the sternum using sterile Jamshidi needle. The needle was connected to 50-ml syringe which was coated with 1% heparin sodium (5ml of heparin “5000 IU/ml” in 500 ml phosphate buffered saline). The bone marrow was pumped vigorously to take out the aspirate. The aspirate was then transferred to 50 ml falcon tubes containing collecting media (Table 2.2).

Table 2. 2: Media composition. *Media used for the bone marrow collection, oMSC isolation, expansion and proliferation and as basic control media for all experiments in this thesis.*

Media types	Compositions
10% FBS proliferation media (basic media, B M)	alpha minimum essential medium (αMEM) without L-glutamine supplemented with:10% fetal bovine serum (FBS).1% L-glutamine. 1% Penicillin/streptomycin (P/S) (Penicillin - 50 I.U. /ml and Streptomycin- 50 µg/ ml).
20% FBS basic media (B M)	Same composition of Basic media, except using 20% FBS instead 10% FBS.
Collecting media	Same Basic media compositions supplemented with 1% heparin.
Serum free media (SFM)	Same Basic media compositions but, without FBS.

The aspiration process was repeated 10 times for each donor, to fill a total of three to four 50 ml tubes depending on the aspirate volume. Tubes were kept on ice and transported back to the cell culture laboratory at Keele University to proceed with the oMSCs isolation process.

2.2.2 BM-oMSCs isolation, expansion, differentiation and cell culture

2.2.2.1 Isolation and stro-4 selection by magnetic cell sorting (MACS)

All stocks and working solutions were previously prepared for the bone marrow-derived ovine mesenchymal stem cells (B M-oMSC) isolation and the stro-4 selection process (Table 2.3).

Table 2. 3: Materials and stocks' compositions and preparations that used in BM-oMSCs isolation and stro-4 selection process.

Materials and solutions	Compositions and preparation
Blocking Buffer	17 ml αMEM, 2 ml rat serum, 0.2 g BSA and 1 ml FBS All contents were mixed together and filter steriled
MACS Buffer	1 L PBS, 5 g BSA and 0.74448 g EDTA disodium salt (2 Mm). All contents were mixed and dissolved overnight then filter steriled.
STRO-4 antibody	Kindly offered by Dr Markides. This antibody was prepared by our Australian team collaborators, aliquoted into a 20 µL in 1.5 ml centrifuge tubes and were left to freeze at -20ºC. This aliquot was ready to make 1:50 working concentration solution by adding 980 µL of PBS.
1:5 MACS secondary antibodies	200 µL MACS rat anti mouse IgG1 microbeads were added to 800 µL MACS buffer

Fresh bone marrow was filtered with a cell strainer (100 µm, Falcon USA Cat. #352360) to remove bone fragments and clots. The volume was topped up to 50 ml with a serum free media (SFM) (Table 2.2) and then centrifuged at 220 *g* for 30 minutes (Heraeus Megafuge 8 centrifuge / Thermo Fisher Scientific) choosing soft deceleration. After centrifugation, the supernatant was carefully removed leaving a small amount to avoid disturbing the cell aggregate. Then, 3 ml of red blood cells lysing buffer were added for 3 minutes until red blood cells (RBCs) were lysed and changed the colour. After that, up to 50 ml of ice-cold PBS were added.

This step was repeated until all red blood cells were virtually lysed. The tubes were centrifuged again at 220 *g* for 30 min at soft deceleration. Centrifugation was repeated until a creamy white pellet of bone marrow-derived mononuclear cells (BM-MNCs) was formed. The supernatant was removed. After that 3ml of sterile blocking buffer were added to resuspend the pellet. About 100 µL of this cell suspension was directly seeded in a T25 cell culture containing about 3 ml of 20% FBS basic media, labelled with the donor number, unsorted cells and date and subsequently incubated in a standard condition (Section 2.2.2.2). The remaining cell suspension was left in the refrigerator for 30 minutes for MACS STRO-4 selection process. Thereafter, 25 ml of cold MACS buffer (Table 2.3) was added to the cell

suspension, which was then centrifuged at 220 *g* for 5 minutes and the supernatant was removed. Subsequently, 1 ml of STRO-4 hybridoma primary antibody working solution was added and incubated at 4^{o}C for 30 minutes. Then the tube was topped up with MACS buffer to a final volume of 20 ml. This was followed by centrifugation and washing twice with 5 ml of MACS buffer. Subsequently, the cells were resuspended in 1 ml of 1:5 diluted secondary antibodies in MACS buffer, mixed carefully and incubated at 4^{o}C for 30 minutes. Then the tube was topped up with 10 ml chilled MACS buffer then centrifuged and gently washed three times with 5 ml chilled MACS buffer to remove excess antibody. Finally, cells were resuspended in 3 ml MACS buffer preparing them for MACS separation steps.

The MACS separation was carried out as follows. Firstly, two sterile 20 ml tubes were labelled with negative and positive. Then, a LS MACS cell separation column (LS MACS® Cell Separation Columns Miltenyi Biotec Ltd.Cat # 130-042-401) was placed in a magnetic manual cell separation (Figure 2.1), and the negative labelled tube was placed under it. Then, 3 ml of MACS buffer was added to the column. After the buffer had flown through the column (wetting the column), the cell suspension was added for separation.

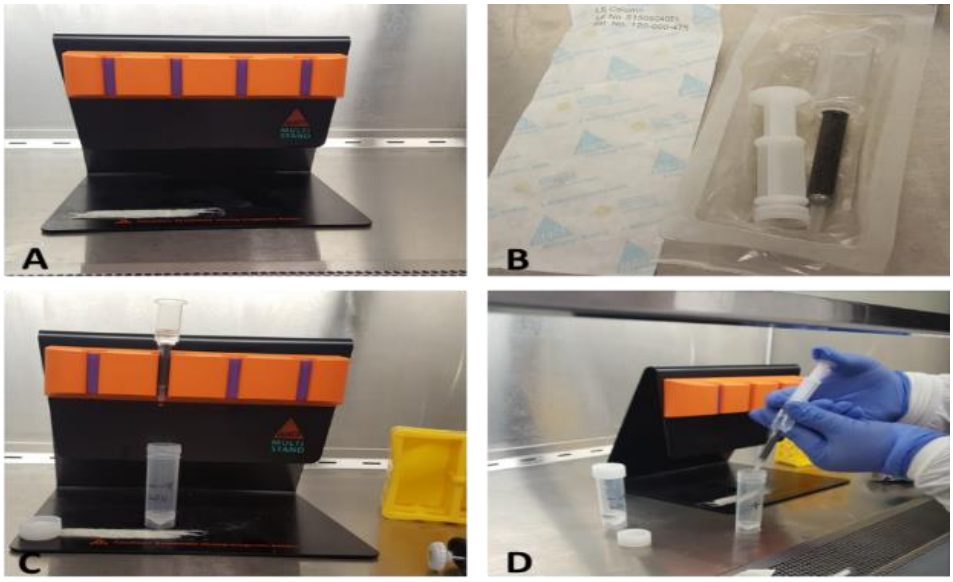

Figure 2. 1: MACS separation of STRO-4 positive BM-oMSCs. *A) manual cell separator, B) LS MACS Cell separation columns and plunger, C) LS MACS Cell separation columns placed in cell separator and contain negative cells which flown through the LS column towards the ne negative labelled tube, D) the positive cells pressed down firmly towards the positive labelled tube by the plunger provided.*

Cells were then washed with 1 ml MACS buffer and added again to the column. Subsequently, the column was washed three times to wash out all STRO-4 negative cells, while STRO-4 positive cells remained attached to the magnetic column. Then, the column was removed away from the magnetic holder and 5 ml of MACS buffer was added to the column and the plunger was placed on top of the tube and pressed down to push the positive cells out toward the positive tube. The tube was then washed twice with alpha MEM serum free media. Both the positive and negative tubes were centrifuged at 1200 rpm for 5 minutes. Lastly, cells were resuspended with known amount of 20 % FBS basic medium (Table 2.2), counted and seeded into T25 monolayer cell culture flask (Corning® cell culture flasks surface area 25 cm^2, angled neck, Sigma – Aldrich, UK product # CLS431080), containing 3ml of 20 % FBS basic medium. Cells were incubated in a standard incubator, for 72 hours. After 3 days, non-adherent cells were removed and fresh 20 % FBS proliferation basic media was added. Upon reaching 80-90% confluence, cells were passaged in monolayer culture using cell proliferation and storage protocols (Sections 2.2.2.2 - 2.2.2.5). The isolated BM-oMSCs of all thirteen donors were used for the experiments performed in this PhD thesis. Cells were used at passage 3 for all experiments unless otherwise stated.

2.2.2.2 Expansion of BM-oMSCs

BM-oMSCs were cultured and expanded under standard cell culture conditions with cells receiving total media changes every 2-3 days and passaged when they reach 80 - 90 % confluence. Standard incubation conditions were at 37^o C with 5% CO_2 incubator. All activities took place within a class II Biological Safety Cabinet under sterile conditions. The composition of the proliferation media which was used in all experiments as control basic media is mentioned in Table 2.2.

2.2.2.3 Cell passaging

Enzymatic sub-culture with 1x Trypsin /EDTA (Ethylenediaminetetraacetic acid) in calcium and magnesium free PBS was used for cell passaging and cell banking when cells reached about 80 - 90 % confluency. Trypsination was carried out by aspirating the media

and washing the cell monolayer with PBS. Adherent cells were then incubated with pre-warmed 1x trypsin/EDTA until cells began to round up and detach. Cells were encouraged to detach from the culture surface through gentle tapping of the culture vessel. Next, an equal volume of 10% FBS basic media was added to neutralize the trypsin activity. The resultant cell suspension was transferred to centrifuge tubes and was centrifuged at 1200 rpm for 5 minutes. After that, the supernatant was aspirated carefully, and the cell pellet was re-suspended in a small known quantity of basic media to produce a single cell suspension. Cells were counted using a haemocytometer and cell density was determined as described in section 2.2.3. Subsequently, cells were re-seeded in basic media in T175 flasks (Corning® cell culture flasks surface area 175 cm^2, angled neck, Sigma – Aldrich, UK product # CLS431079) at a cell density at about $5X10^5$ cells /flasks (60-100 cells /cm^2).

2.2.2.4 Cell counting and trypan blue exclusion test of cell viability

After trypisination approximately 10 µL of the resultant single cell suspension were transmitted to a hemocytometer (KOVA Glasstic ® Slide 10 HBI – 87157) and counted under a light microscope. The number of cells per millilitre was calculated by equation 2.1.

$$No.of\ cells\frac{No\ of cell}{ml} = \frac{cells\ counted}{No\ of\ large\ square}\ X\ 10^4 \qquad \text{Equation 2.1}$$

The total cell number in the cell suspension was determined by multiplying the number (No.) of cells/ ml by the total volume of media used to prepare the cell suspension, equation 2.2.

$$Total\ cell\ No = \frac{No\ of cell}{ml}\ X\ Total\ volume\ (ml) \qquad \text{Equation 2.2}$$

When cell viability was determined using trypan blue, a small aliquot of 50 µL of the suspension was mixed 1:1 with trypan blue, this 1:1 dilution was considered as a dilution factor in the total cell account. Briefly, after trypsinisation, the cell pellet was resuspended in a 3 ml basic media and a small aliquot of 50 µL of cell suspension was used and added to

an equal amount of trypan blue (dilution factor =2). About 10 µL of this suspension were used for cell counting using a haemocytometer. Trypan blue stains the dead cells dark blue whereas living cells will remain unstained as their cell membrane is intact. Both live and dead cells were counted under a light microscope as previously explained in section 2.2.3. This process was repeated 4 times (4 large squares). Total cell number was calculated by the equation 2.3.

$$No.\frac{of cells}{ml} = \frac{Cells\ counted}{No.of\ large\ square}\ \text{X}\ dilution\ factor\ \text{X}10^4 \qquad \text{Equation 2.3}$$

The above equation was used separately to count number of both dead and life cells. Lastly, the viability percentage was estimated by the equation 2.4.

$$Viability(\%) = \left[1 - \left(\frac{total\ dead\ cells}{total\ cells}\right)\right]\text{X}100 \qquad \text{Equation 2.4}$$

2.2.2.5. Cell storage and banking

According to good cell culture practice, regular banking of cells was carried out during passaging. Pelleted cells were re-suspended in a small known volume of freezing medium, consisting of 10% dimethyl sulfoxide (DMSO) in FBS. About 1 ml of the suspended cells was transmitted to labelled freezing vials (about 1 X 10^6 cells / ml) and transferred to a freezing container (NALGENE Cat#5100-0001) filled with isopropanol, to achieve a -1 ^oC/ minute rate of cooling and then placed directly in a -80 ^oC freezer overnight. After that, the vials were transferred to liquid nitrogen storage until needed.

2.2.2.6 Preparation of basic media and differentiation media

Supplements required to prepare the adipogenic media (Ad M), osteogenic media (Os M) chondrogenic media (Ch M) and other media used in this study were prepared as stock solutions, aliquoted and frozen at -20^oC. These stocks were ready to use in a calculated ratio to prepare fresh media each time. The differentiation media supplements were mentioned in each relevant section according to each experiment in this study.

2.2.2.7 Cells Seeding in monolayer 2D cell culture

Monolayer cell culture was used to differentiate potentials of the BM-oMSCs. The cells were seeded at passage three (P3) in 24 well plates at a density of 5x10^3 cell/well. Cells were

seeded in triplicate for each condition and each time point. The cells were cultured using basic media until they reached 80-90% confluence. Then, cells were incubated with either differentiation media (treated) or basic media (control). Media was changed every 2-3 days during the experiment. Experimental plates were examined regularly under the light microscope (OLYPUSU. CMAD3 Olympus Optical Co., Tokyo, Japan) to investigate the first appearance of the differentiated cells, at specific time points, which will be mentioned in each experiment. The 2D tissue cultures were fixed to their plates (fixation protocol related to each lineage), as will be mentioned below and stored in PBS at 4^{o} C until histology was performed.

In case of adipogenesis and chondrogenesis, cells were fixed with by 10% neutral buffered formalin for 15 minutes. Osteogenic differentiated cells were fixed with 95% methanol for 15-20 minutes.

2.2.2.8 Three-dimensional pellet cell culture for chondrogenesis of BM-oMSCs

To compare the chondrogenic potential of the BM-oMSCs, 3D pellet cell culture was used, as described by (Jackson *et al.,* 2007). For this purpose, cells at P3 were trypsinised and counted, the total cell suspension was divided into two equal parts and centrifuged with 1200 rpm for 5 minutes. After that, the trypsin/media supernatant was removed. One part of the cells was resuspended with basic media (B M) (control group) and the other part was resuspended with chondrogenic media (Ch M) (treated group) at a density of $5X10^{5}$ cells/ ml. Then 1 ml of each cell suspension was transmitted to 1.5 ml centrifuge vials. Cell suspensions were centrifuged at 300 *g* for 5 minutes to form a cell aggregate. The vials were then incubated in a standard incubator overnight to form cell spheroids. Cell pellets at day 1 were collected and stored at -20°C for DMMB and PicoGreen analysis. Whereas, day 1 histology cell pellets were fixed using 10% neutral buffered formalin solution overnight and then washed with PBS. Pellets were stored at 4°C until histology was performed. Cell pellets for day 10 and day 20 were continued to receive media changes every 2-3 days with the

appropriate medium type B M or Ch M and were frozen or fixed as described above for day 1 pellets at the appropriate time points.

2.2.2.9 Three-dimensional hydrogels for chondrogenesis of BM-oMSCs

Three dimensional (3D) hydrogels were prepared to study chondrogenesis of BM-oMSCs under mechanical conditioning (Nöth *et al.*, 2007). Briefly, cells at P3 were trypsinised and counted, then appropriate number of cells was labelled with activated nanoparticles (Section 2.5.2). Cells were resuspended in 20% 4-(2-hydroxyethyl)-1-piperazineethanesulfonic acid (HEPES) buffer in basic media to prepare HEPES-cell suspension containing about $2X10^5$ in each 100 µL. Meanwhile, about 200 µL of collagen I rat tail (stock concentration 3.55mg/ml) was added to each well of a non-treated flat bottom 48 well culture plate (CytoOne cat# CC7672-7584). Thereafter, 100 µL of the HEPES-cell suspension was added to each 200 µL collagen and mixed carefully with the tip of the pipette.

The 48 well plates were then incubated at 37ºC in a cell culture incubator for 30 minutes to allow the collagen to solidify at the bottom of the wells. Then 1 ml of B M or Ch M were added. Plates were left overnight in the incubator. Lastly, day 1 gels were harvested after 24 hours and fixed for histology or frozen at -20ºC for biochemical analysis. While the remaining gels continued to receive a daily mechanical stimulation (Section 2.5.3) and a total media change every 2-3 days until day 20.

2.2.2.10 Assessment of metabolic activity by Alamar blue assay

AlamarBlue® reagent was used to assess cell viability in two experiments. In oMSCs isolation and characterisation, the test was performed on 2D cell culture the donor 13 oMSCs passages P1, P2 and P3. While for hydrogel experiment, alamer blue was performed during the experimental time at day 1, day10 and day 20 in 3D hydrogel cell culture.

In both cases, the assay was performed in same way as following: changing the media to 10% reagent in media (either Ch M or B M as 10% of the sample volume) followed by 3 hours incubation at 37ºC. During this period, the blue resazurin (alamar blue reagent) is reduced to resorufin, which is a red colourimetric indicator. After 3 hours, while working in

the dark, about 100 µL (n=8) of the resultant colourimetric media from each well was transferred to a 96 well plate. Acellular control samples (10% alamar blue in basic media) was used as a blank. The absorbance was read by a plate reader then read the absorbance of alamarBlue® at 570 nm, using 600 nm as a reference wavelength (normalized to the 600 nm value). Plotted as a bar chart of the absorbance intensity in Excel.

2.3 Surface marker characterisation of BM-oMSCs by flow cytometry

Cells at P3 and 80% confluence were subjected to flow cytometry to specify characteristic clusters of differentiation (CD) surface epitopes using anti CD 29, CD 44, CD 45 and CD 31 antibodies. Therefore, cells were trypsinised, counted and resuspended to achieve a concentration of about $5X10^6$ cell/ml in ice-cold blocking buffer (Barker and Seedhom), which was prepared by dissolving 0.732 g Ethylenediaminetetraacetic acid (EDTA) and 2.5 g bovine serum albumin (BSA) in 500 ml PBS. Then, the cell suspension was incubated at 4^o C for 1 hour. Thereafter, 1 ml aliquots for the cell suspension containing approximately $5X10^5$ cells were prepared and added to 1.5 ml Eppendorf tubes. The tubes were centrifuged at 300 *g* in 4^o C for 10 minutes. The supernatant was discarded. The final primary antibody concentration was 1:1000 in 100 µL of cell suspension containing $5X10^6$ cell/ml. The tubes were incubated for 15 minutes at 4^o C. After 15 minutes, the cells were washed with 1 ml BB to remove excess antibodies, centrifuged at 300 *g* for 10 minutes and then the supernatant were discarded. Next, Fluorescein isothiocyanate FITC conjugated secondary antibodies were added to the cells in a final concentration of 1:100 followed by incubation in the dark at 4^oC for 15 minutes. Subsequently, cells were washed with 1 ml BB, centrifuged at 300 *g* for 10 minutes and finally resuspend with 150 µL BB or PBS. In case of conjugated primary antibodies FITC conjugated CD 31, IgG1 and IgG2α control isotypes.

The cell labelling with antibodies was minimised into three steps, after resuspended with 100 µL of cold BB, cells were mixed with 10 µL of relevant FITC conjugated primary

antibodies, final concentration 1:10 dilution, and left in dark at 4^{o}C for 10 minutes. Secondly, cells were washed with 1 ml cold BB and centrifuged at 300 *g* for 10 minutes. Finally, cells were resuspended with 150 µL BB or PBS.

For analysis, a flow cytometer (Cytomics FC 500, Beckman Coulter), with at least 50000 events counts was used. The acquired data were analysed using Flowing Software (version 2.5.1). IgG1 was the isotype control for CD 29, CD 44 and CD 45. While, IgG2α was the isotype control for CD 31, FL1 channel was used for analysis. Percentage positive events were determined using gates to exclude 99% of the appropriate isotype control events.

2.4 Histology

2.4.1 Histochemical staining of oMSCs cultured in monolayer to assess stem cell differentiation

2.4.1.1 Alcian blue staining to assess chondrogenesis

Detection of chondrogenic differentiation in the fixed monolayers was accomplished by investigating the presence of glycosaminoglycans (GAG) by alcian blue stain. Therefore, 1g of the dye was dissolved in 100 ml 3% glacial acetic acid to prepare a working solution of 1% (w/v) alcian blue. The staining solution was filtered using a 0.2µm syringe filter (Sarstedt 83.1826.001) into a storage reagent bottle and stored at room temperature (RT). The solution was filtered again, and the pH was adjusted to 2.5 before use each time.

To stain the cells, well plates were removed from the fridge, PBS was removed, and cells were washed with dH_2O before enough amount of dye was added to cover the cells completely. Plates were incubated overnight at RT. Afterwards; the dye was removed, and the monolayers were rinsed gently with water until the water became clear. After that, a small amount of dH_2O was added to the stained monolayers and cells were images were captured immediately through light microscope (OLYMPUS, CKX41Tokyo Japan) and camera (MicroPuplisher SN: Q29364, Canada) at 4x, 10x, and 20x magnification.

2.4.1.2 Alizarin red S staining to assess osteogenesis

Detection of osteogenic differentiation in the fixed monolayers was accomplished by alizarin red S staining of the mineralised calcium deposits. Alizarin red S aqueous solution 1% (w/v) was prepared in dH_2O and left overnight to dissolve completely. The solution was then filtered with a 0.2 μm syringe filter and the pH was adjusted to 4.0 using 0.1 M HCl.

To stain the samples, PBS was removed, and cells were washed with dH_2O. Subsequently, alizarin red S stain solution was added to fully cover the monolayer and left to incubate for 20 minutes at RT. After that, the dye was removed, and the monolayers were washed with water gently to not remove the superficial mineral layer. Then, a small amount of dH_2O was added to the stained monolayers and samples were imaged under a light microscope.

Semi-quantitative analysis was performed to assess osteogenesis by eluting the alizarin red stain using 5 ml of 10% Cetylpyridinum chloride (CPC) for each well. Samples were incubated overnight at RT following which absorbance was read in a plate reader at 562 nm.

2.4.1.3 Oil Red O staining to assess adipogenesis

Adipogenesis of the monolayers was assessed by Oil Red O stain of intracellular lipid droplets. A stock solution of concentrated dye was prepared first by dissolving of 0.35 g Oil Red O powder in 100% isopropanol. The solution was mixed well and left at least overnight before being used to ensure maximum saturation of the solution. Then, the stock solution was filtered with a 0.2μm syringe filter and kept in RT until use. A 60% (v/v) working solution was prepared fresh immediately prior to staining by mixing 6 ml stock solution with 4 ml of doubled distilled water (ddH_2O). The working solution was allowed to sit at RT 20 minutes followed by filtration.

Fixed cells culture was washed twice with distilled water after PBS was removed. Then, 500 μL of Oil Red O working solution were added to each well and left for 10 minutes at RT Later the dye was removed, and cells were washed four times with ddH_2O. A small amount of distilled water was left in each well for imaging. Images were captured directly by a light microscope.

Adipogenic differentiation was assessed semi- quantitatively by de-staining the Oil Red O with 200µL of 100% isopropanol for each well. Samples were incubated for 10 minutes at RT while plates were shaken gently. The absorbance of the eluted dye was measured by plate reader at 492 nm using 100% isopropanol as control.

2.4.2 Histology and immunohistochemistry of native tissue and 3D samples

Formalin fixed native sheep cartilage tissue, 3D cell pellets and 3D hydrogel samples were prepared for histology and immunohistochemistry by the following procedures.

2.4.2.1 3-Aminopropyltriethoxysilane (APTES) slides coating

In order to increase the adherence capacity of the slides' surface and improve section adhesion, 3-Aminopropyltriethoxysilane (APTES) was used for coating standard microscope slides (SuperFrost® glass Microscope Slides AA00008032E), prior to using them for histology and immunohistology. For this purpose, clean slides were arranged within the slide holder and soaked in acetone for 2 minutes to remove any microscopic dirt. Slides were then air dried by allowing the acetone to evaporate. Dry slides were then soaked in freshly prepared 2% (v/v) APES in acetone for another 2 minutes and then washed twice with dH_2O for 2 minutes. After that, the slides were placed at 60 °C overnight before being stored airtight until use.

2.4.2.2 Paraffin embedding of samples

Because of their small size, cell pellets were manually processed for histology in their Eppendorf tubes. Therefore, storage PBS was removed and about 1 ml of 70% IMS was added and left overnight. Then, pellets were dehydrated gradually by incubation for one hour each at 70%, 90%, 100% and 100% isopropanol. Then, the samples were placed in the centre of Tissue Embedding Chambers (MILES Scientific Tissue Embedding Centre) with labelled plastic caskets. Then, freshly melted paraffin wax was added to fill the caskets completely. Samples were left in melted wax at 60 °C overnight to allow the paraffin to embed the samples throughout. Thereafter, the melted wax was replaced by fresh wax and samples were

placed on a cooling plate to allow fast cooling of the samples. The resulting paraffin blocks were stored at RT until samples were sectioned.

Native sheep cartilage and hydrogel samples were dehydrated, and wax embedded using an atomized tissue processor (KD-TS6B Vacuum Tissue Processor). Briefly, samples were loaded in labeled tissue cassette (Shandon™ Tissue-Processing/Embedding Cassettes II cat # 1001060) and then placed in the tissue possessor basket. Samples were dehydrated gradually in varying alcohol concentrations and incubated in melted wax at 60 °Cover night. A day later, the samples were taken out from the basket. Each sample was placed in an aluminum plate, which was subsequently filled with fresh paraffin. Samples were covered with labelled cassette lids and then allowed to cool rapidly on a cooling plate. All blocks were stored at RT until use.

2.4.2.3 Sample sectioning and de-paraffinisation

Prior to sectioning, paraffin blocks were trimmed to facilitate the sectioning process. Blocks were then located in the rotary microtome and about 2-3 consecutive 7 μm sections were obtained using a microtome (Thermo Shandon Manual Microtome AS 325) and transmitted carefully to a tissue float distilled water bath at 40 ^{o}C. Sections were then mounted on APTES coated slides. Slides were left overnight at 60 ^{o}C to let them dry and firmly adhered to the slides following which slides were stored until histology and immunohistochemistry staining was performed. Shortly before sections were subjected to the desired stain, they were deparaffinized in three changes of histological Histo-Clear and rehydrated by using decreasing concentrations of industrial methylated spirit (IMS) (100% ,100%, 90%, 70% and 50%) for 3 minutes each and, then two changes of dH_2O for 5 minutes each. Slides were then directly subjected to histology or immunohistochemistry stains.

2.4.3 Histological staining of the paraffin sections

2.4.3.1 Haematoxylin and Eosin staining

Haematoxylin and Eosin (H&E) stain was performed by immersing the slides in the haematoxylin Gill No.3 dye for 5 minutes, followed by gentle washing with tap water. After

that, the slides were immersed in an alcoholic Eosin dye for 30 second followed by gentle washing with tap water. The sections were dehydrated after staining by dipping the stained slides in different ascending IMS concentration, namely 70%, 90%, 100% and 100% for 3 minutes each, followed by two changes of Histo-Clear for 5 minutes each. Subsequently, slides were mounted with DPX mounting medium and covered with coverslips. Finally, slides were visualized using the EVOS microscope (AMG, Advanced Microscopy Group) at 4 x, 10 x, 40 x, and 80 x magnification. Images were taken across the different areas of the section.

2.4.3.2 Alcian blue staining

Deparaffinised and rehydrated sections were incubated overnight with 1% alcian blue (pH 2.5). The dye was prepared as explained in Section 2.4.1.1. Slides were kept in a wet environment to prevent the dye from drying during the staining time. After that the dye was washed off the slides with tap water, and the sections were subjected to the dehydration, clearing, DPX mounting and imaged, as mentioned in Section 2.4.3.1.

2.4.3.3 Toluidine blue staining

Deparaffinised and rehydrated sections were incubated for 10 min with 1% toluidine blue staining solution which was prepared by dissolving 1 g toluidine blue dye in 1% (w/v) sodium borate. The solution was stirred until the dye was dissolved completely. The solution was filtered prior to use. After staining, the slides were washed with dH_2O several rinses and rehydrated with two changes of 96% ethanol and absolute ethanol each for 1 minute. Then slides were passed from absolute alcohol to the next steps of clearing and DPX mounting as mentioned in Section 2.4.3.1.

2.4.3.4 Sirius red staining

To prepare the Sirius Red stain (direct red), 0.5 g of Sirius red powder was dissolved in 45 ml of distilled water. After that, 50 ml of absolute ethanol was added followed by 1.0 ml of 1% sodium hydroxide. The solution was mixed vigorously before 4.0 ml of 20% sodium chloride was added. Then the solution was left to stand overnight before filtration. The

staining protocol was briefly, the deparaffinised and rehydrated sections were stained with sirius red stain for 1 hour and then washed with tap water. Next, slides were dehydrated, cleared, DPX mounted and imaged, as mentioned in section 2.4.3.1.

2.4.3.5 Picro-sirius red staining

Picro-sirius red stain kit was used to stain paraffin sections after deparaffinisation and rehydration. Therefore, adequate picro-sirius red solution was added to completely cover the sections and incubated for 1 hour. The slides were then quickly rinsed in two changes of 0.5% acetic acid solution provided with the kit. Then, samples were rinsed with absolute alcohol, and dehydrated with two changes of absolute alcohol for 2 minutes each. Slides were then cleared, mounted and imaged as mentioned in section 2.4.3.1.

2.4.4 Immunohistochemistry staining of paraffin sections

2.4.4.1 Enzymatic antigen retrieval

Antigen retrieval is important to break the protein cross-link formed by formalin and thereby uncovered hidden antigenic sites. Enzymatic antigen retrieval was used for this purpose. Briefly, the deparaffinised and rehydrated sections were isolated with a hydrophobic pen (Vector Laboratories ImmEDGE™ Hydrophobic Barrier Pen Mfr # H-4000 – Item # OU-93951-68) and placed in a flat position in a humidified chamber to prevent samples' dryness. Each sample was covered directly with a drop of freshly prepared 0.1% trypsin working solution (Table 2.4) and the humidification chamber was transferred to 37 °C incubator for 15 minutes. Slides were then washed three times for 5 minutes each with PBS.

Table 2. 4: Trypsin working solution preparation for enzymatic antigen retrieval.

	Materials and solutions	***Compositions and preparation***
solution ***1***	***0.5%Trypsin stock solution***	1ml Trypsin/EDTA 10x in 4 ml dH_2O mixed well, aliquots and stored at -20 ^oC
solution***2***	***1% calcium chloride stock solution***	0.1 g in 10 ml dH_2O mixed well and stored at 4 ^oC
working solution	***0.1%Trypsin***	1 ml (stock solution 1) + 1 ml (stock solution 2) + 8 ml dH_2O. Mixed and adjust pH to 7.8 with 1N NaOH

2.4.4.2 Quench endogenous peroxidase activity

After enzymatic antigen retrieval, tissue section slides were incubated for 10 minutes in 3% hydrogen peroxide H_2O_2 diluted in PBS to quench endogenous peroxidase activity. Then samples were washed twice in PBS for 5 minutes each. After that, excess PBS was blotted and blocking serum consisting of 1.5% normal goat serum was added to the sections. Sections were incubated at RT for 1 hour to reduce non-specific staining. Thereafter, the blocking serum was carefully blotted. Before using specific antibodies to detect antigens by immunohistochemistry (IHC), all potential nonspecific binding sites in the tissue sample must be blocked to prevent nonspecific antibody binding, this normal goat serum is intended for use as a blocking solution when a second antibody of goat origin is applied in an immunohistochemical staining procedure.

2.4.4.3 Primary antibody staining

According to the instruction of the ABC Kit, the tissue sections were labelled with the primary antibodies to be examined (collagen II, collagen X or aggrecan). In brief, after the blocking step, the sections were incubated overnight at 4^{o} C with the primary antibody at a final concentration of 1.5 µg/ml in 1.5% blocking serum in a humidification chamber. Subsequently, slides were washed twice with PBS. Then sections were incubated with biotinylated secondary antibodies (final concentration: 1µg/ml diluted in 1.5% blocking serum) for 30 minutes at RT. Sections were washed twice with PBS for 5 minutes each.

Then, the sections were incubated with few drops of AB enzyme reagent (avidin and biotinylated horseradish peroxidase) for 30 minutes at RT, washed with three changes PBS for 5 minutes each. After that, sections were incubated with 1-3 drops of peroxidase substrate for 30 seconds to10 minutes (or until desired stain intensity developed). The staining was checked by rinsing with dH_2O and then, viewed under light microscope. If necessary additional peroxidase substrate was added and samples were incubated for longer time. Finally, sections were washed with dH_2O for 5 minutes.

Sections were optionally stained with counterstain, (Gill's # 2 hematoxilin) for 5-10 second, then slides were immediately washed with three changes dH_2O and were dehydrated in 95 % ethanol and two changes of absolute ethanol for 10 seconds each.

2.5 Magnetic Nanoparticle preparation and mechanical conditioning

2.5.1 Magnetic nanoparticles activation and antibody coating

Under sterile conditions, the nanoparticles were activated covalently coated with TREK1 and /or TRPV4 antibodies in order to prepare them to be used for labelling the BM-oMSCs. Materials and solutions preparation for MNPs antibody coating were mentioned in Table 2.5.

Table 2. 5: Materials and stocks' compositions and preparation essentials for nanoparticles' antibody coating

	Materials and Solutions	***Compositions and Preparation***
1	***Nanoparticles suspension***	Nanomag -silica Stock, 250 nm diameter, COOH surface 10 mg/ml
2	***2 M $NaHCO_3$***	Dissolve 3.36 g in 20 ml dH_2O
3	***0.5 M $NaHCO_3$***	Dissolve 0.8401 g in 20 ml dH_2O
4	***0.1 M MES buffer 2-(4-morpholino) ethane sulphonic acid buffer***	Dissolve 0.390 g of MES salt in about 15 ml of dH_2O then adjust to pH 6.3 with 2M and 0.5 M $NaHCO_3$, Sterile filtered with (0.2 µm syringe filter)
5	***0.5 M MES buffer***	Dissolve 1.95 g of MES salt in about 15 ml of dH2O then adjust to pH 6.3 with 2 M and 0.5 M $NaHCO_3$, then complete to final volume 20 ml, Sterile filtered with (0.2µm syringe filter)
6	***6.3 pH EDAC/NHS solution***	Weigh 12 mg of N-(3-Dimethylaminopropyl)-N′-ethylcarbodiimide hydrochloride (EDAC) in a Stasted tissue culture dish (TC Dish 60, Standard Order number: 83.3901), then add 24 mg N-hydroxysuccinimide (NHS), the mixture was dissolved in 2 ml of filter sterile 0.5 M MES-buffer, pH 6.3, then Sterile filtered with (0.2µm syringe filter). The pH must be adjusted as long as concentration stays same.
7	***Secondary antibody goat pAb to Rb IgG 1 mg/ml***	Minimum 20 µg secondary antibody used for each 0.1 ml of 10 mg/ml nanoparticle suspension (1 mg/ ml stock was aliquots of 20 µL and freeze in -20 ^oC)
8	***Primary antibodies TREK1 pAb TRPV4 pAb***	Minimum 12 µg pAb used for each 0.1 ml of 10 mg/ml nanoparticle suspension (1mg/ml stock was aliquots of 12 µL and freeze in -20 ^oC)
9	***Glycine 25 mM***	Dissolve 7.5067 mg in dH2O Sterile filtered with (0.2 µm syringe filter) Use minimum 10 µL

The activation of the MNPs by following procedure was carried out just before labelling the cells with the antibody coated MNPs. The stock solution of the MNPs was vortex before use and 0.1 ml was transmitted to a sterile 1.5 ml centrifuge tubes (= final concentration of 1 mg of MNPs of 10 mg /ml) for each antibody. Then 20µL of EDAC/NHS solution was added (the activation take place when the carboxyl group of the MNPs react with EDAC/NHS solution to produce Amine group which enable the MNPs to be labelled with the biological secondary antibody).

The tubes were incubated for 60 minutes at RT with continuous mixing. Then, the particles were washed with 0.2 ml of 0.1 M MES buffer using a permanent magnet array and resuspended with 0.1 ml of 0.1 M MES buffer (Figure 2.2).

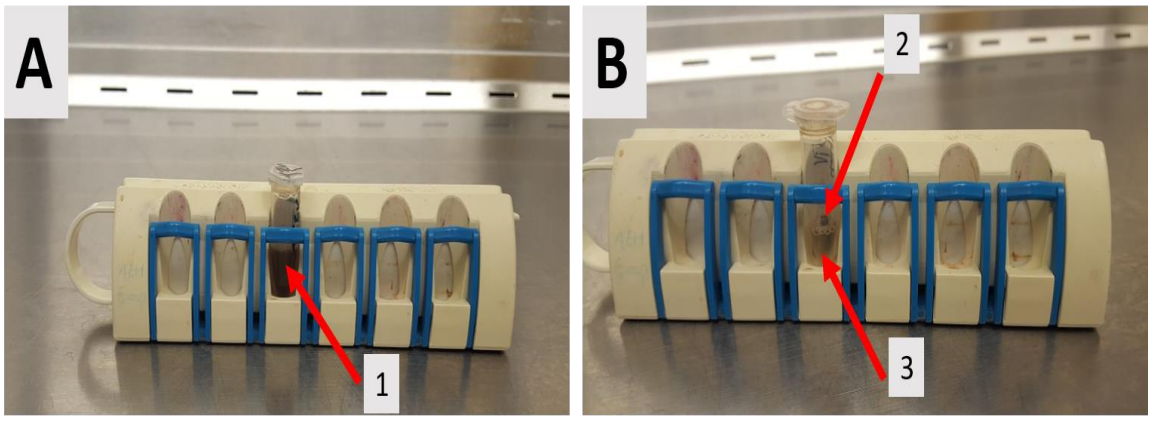

Figure 2. 2: Washing steps of MNPs with MES in a permanent magnet array. *A) 1.5 ml vials with MNPs (1) the suspension inside the magnet array. B) Same vial with suspension after 2-3 minutes (2) the MNPs were adhered to the vial's wall according to the magnetic forces (3) the clear washing fluid can easily discard by pipette.*

For the antibody labelling of the NPs, 20 µL of 1mg/ml stock secondary antibody was added to the activated MNPs, which were then incubated under continuous mixing for 3 hours at RT or overnight at 4 ^{o}C. MNPs were then washed and resuspended with 0.1 ml of 0.1 M MES buffer containing 12 µg primary antibody. MNPs were blocked with 10 µL of 25 mM glycine buffer in PBS and incubated under continuous mixing for 30 minutes at RT. Lastly, MNPs were washed with 0.1 ml of 0.1% BSA in PBS and resuspended with 1ml of 0.1% BSA in PBS (1mg/ml activated antibody coated MNPs solution) and subsequently stored sterile at 4 ^{o}C.

In order to test the coating efficiency of MNPs, samples of the antibodies coated MNPs were tested for sizing, zeta potential and oscillating movement and data were compared with uncoated MNPs.

2.5.1.1 MNPs sizing and zeta potential

The activated and coated MNPs were analysed for surface charge and size by dynamic light scatting (DLS). DLS measurements were performed using a zetasizer (Malvern zetasizer model 3000 HAS. Briefly, 50µL of particle stock solution was diluted in 3 ml of dH_2O. This solution was used to fill the cuvette of the instrument. The cuvette was placed in the zetasizer and scanned. After that, the same diluted solution was injected to the chamber Ad-hoc for zeta potential measurement in the zetasizer.

The measurements were performed at RT. The data was analysed by excel and graphs were plotted to compare the size and surface charge of the coated and uncoated MNPs.

2.5.1.2 Oscillating movement using alternate current susceptometer (ACS)

Alternate current susceptometer (ACS) was used to measure the oscillating movement of the MNPs before and after labelling with the antibodies (TREK-1 and TRPV-4 antibodies.).

After that, 200µl of MNPs sample (uncoated or coated MNPs suspension) was filled in a 1 ml Shell vial, (starburst septa, flat bottom SuPELCO catalogue number, 33321-U), firmly closed with the lid then put inside the ACS and was scanned by pressing the scan bottom.

2.5.2.3 Fluorescent immunohistostaining for the detection of TREK1 and TRPV4 antibodies

Prior to using TREK1 and TRPV4 antibodies in MNPs antibody coating, the two antibodies were tested for cross-reactivity with sheep BM-oMSC and native sheep chondrocytes. For this purpose, BM-oMSC P3 and sheep chondrocytes (P1, isolated from fresh hyaline articular cartilage from knee joint) were used. Sheep chondrocytes were kindly provided by Miss Nicola Foster at the Guy Hilton research centre. Both cell types were cultured with B M in a 24 well plate. When cells reached 70% confluence, the media was aspirated. Cells were washed with PBS and fixed using 10% neutral buffered formalin for 20 minutes at RT.

Subsequently, cells were washed with 1% (w/v) BSA in PBS to remove the formalin. Cells were permeabilised and blocked by adding 0.5 ml of permeabilisation-blocking solution (PBS containing 0.3% TitronX-100, 1% BSA and 10% normal goat serum) for 45 minutes at RT. Afterwards, the monolayer was incubated overnight at 4^{o} C with 300µL/well of diluted primary antibodies (10 µg/ml in permeabilisation-blocking solution). A negative control was prepared by incubating the cells with the permeabilisation-blocking solution in the absence of a primary antibody. After that, the monolayer was washed three times with 1% BSA in PBS for 5 minutes each. Cells were further incubated with 300 µL /well of diluted secondary antibody Alexa Fluor $^{®}$ 555 goat anti-rabbit – IgG in a dark for 2 hours at RT (dilution 1:400 in 1% BSA in PBS). Samples were then washed with PBS twice and counter stained with DAPI for 2 minutes. To remove excess dye, samples were washed with PBS twice and were immediately imaged using a confocal microscope (Confocal laser scanning microscope (CLSM, Olympus Fluoview FV 1200 with Fluoview software (4.1 version).

2.5.2 Cell labelling with antibody-coated MNPs

BM-oMSC were labelled with the antibody-coated MNPs prior to seeding them in 3D hydrogel (Section 2.2.2.9).

Shortly, after trypsination and cell counting, cells were resuspended at a cell density of 1x 10^{6} cells/ml in serum-free medium (SFM) to avoid interaction between MNPs and FBS. The cell suspension was aliquoted to 1 ml into 1.5 ml Eppendorf tubes. At the same time 4 µL of 1,2-Dioleoyloxy-3-(trimethylammonium) propane (DOTAP) was added to 100 µL MNPs. The MNP was shaken carefully and incubated for 15 minutes at RT. Subsequently, 25 µL of DOTAP- MNPs suspension was added to each 10^{6} cells/ml and allowed to incubate at 37^{o} C in a cell culture incubator for 3 hours. The resultant MNPs labelled cell suspensions were washed with PBS to remove unbound MNPs before resuspending cells in 20% HEPES-buffer for incorporation into 3D hydrogels as previously explained in section 2.2.2.9.

2.5.3 Magnetic stimulation of MNPs-labelled BM-oMSCs seeded hydrogels

Cell-seeded hydrogels were divided into two groups, magnetically stimulated group (treated) and non-magnetically stimulated group (control). The MNPs labelled cells of the treated groups were subjected to mechanical stimulation by a vertically oscillating magnetic force bioreactor (MICA Biosystems). Magnetic field stimulation was performed for 1 hour a day for 5 days per week over the course of 20 days.

The tissue culture plates of the treated group were placed on a holder over the permanent magnetic arrays of the bioreactor, which was situated inside an incubator at 37^{o}C and 5% CO_2. Meanwhile, the control group was kept in identical culture condition without being subjected to a magnetic field.

Magnetically stimulated groups were exposed to a magnetic field of approximately 1.4 - 75 Millitesla (m T) (according to the distance of the array toward the tissue culture plate) from a six well array of permanent magnetic (Neodymium Iron Boron (Nd FeB)) situated beneath the culture plates at a 1 Hz frequency.

2.7 Compression test and Young's Modulus

Native sheep cartilage and hydrogel samples were tested for mechanical properties by compression test using Bose ElectroForce 3200 system. The mechanical tester was fitted with 22N load cell. Load was applied at a rate of 0.0025mm/sec to a final displacement of 0.2 mm. The test was performed at RT. Prior to mechanical testing initial sample height and diameter were measured using digital calliper (DRAPER® Digital calliper 0-150 mm, stock no. 52427). The procedure for the mechanical testing is shown in Figure 2.3. Full details on the testing machine have been previously given (Patel *et al.*, 2008).

The samples were laid on the sample holder plate of the apparatus, which was connected to the actuator of the testing machine. The collected data was analysed using Excel to plot force-displacement curve, stress-strain curve and estimate Young's modulus. Force-displacement curve was plotted for each sample by firstly collecting data from the mechanical tester. Then the load averages were calculated for each 0.0125 mm displacement

(proximally 10 points from 0 - 0.5 mm), and finally, the force-displacement curve was plotted.

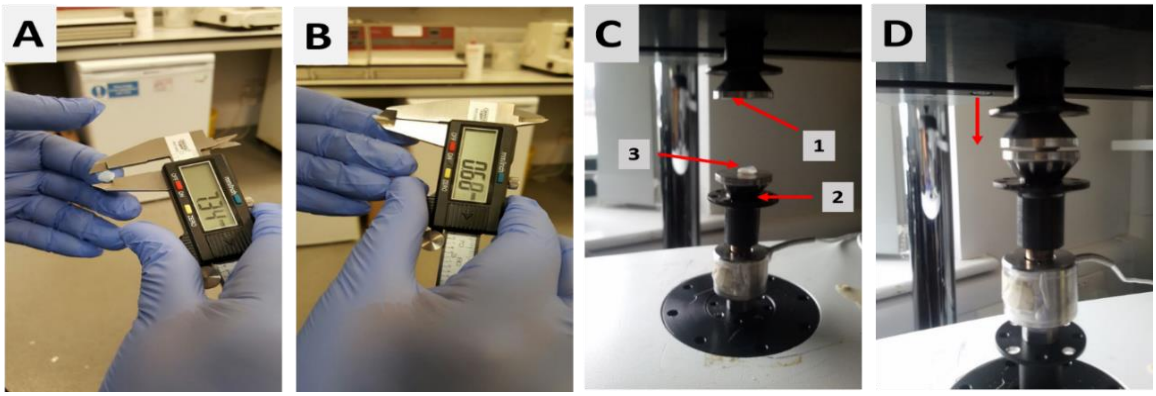

Figure 2. 3: Mechanical Testing of samples. *Samples area and height were measured using digital calliper (A, B). The Bose machine actuator (C), the compression plate connected to the load cell (1). A sample (3) was loaded on the sample holder base of the apparatus (2) and 22 N maximum load was applied. The compression was performed by the compression plates in a vertical direction towards the samples surface (the arrow). (D).*

Stress and strain were calculated for each sample using equation 2.5 and 2.6 and graphs were plotted. Young's modulus was determined as the slope of the curve from the linear range using equation 2.7.

$$stress\ (б) = \frac{F}{A} \qquad \text{Equation 2.5}$$

$$strain\ (\varepsilon) = \frac{\triangle L}{L0} \qquad \text{Equation 2.6}$$

$$E = \frac{\triangle б}{\triangle \varepsilon} \qquad \text{Equation 2.7}$$

F = Force, Load [N]

L0 = sample length before compression, [m]

A = sample area, [m^2]

ΔL = length by which sample is displaced, [m]

E = Young's modulus [N/m^2 or Pa].

$\triangle б = б_2 - б_1$ the differences between two stress values on the linear area of a stress strain curve [N/m^2 or Pa].

$\triangle \varepsilon = \varepsilon_2 - \varepsilon_1$ the differences between two strains values on the linear area of a stress strain curve [no unit].

2.6 Assessment of biochemical composition of native cartilage and 3D cultures

Samples allocated for biochemical assays in each experiment (native sheep cartilage, 3D cell pellet and 3D hydrogel samples) were digested in a known volume of a proteinase K solution. The digest solution was prepared by dissolving 50 μg/ml proteinase K in 100 mM ammonium acetate. The digested samples were divided into aliquots according to the required amount of each assay and frozen at -20 ^{o}C until use.

2.6.1 Quantification of DNA content using PicoGreen assay

Quant-iT PicoGreen double stranded DNA assay Kit was used to determine the DNA content of the samples. The assay was performed following the manufacture's protocol. Briefly, dsDNA standards were prepared at concentrations of 20, 10, 5, 2.5 and 1.25 μg/mL in 100 mM ammonium acetate, 10 μL of standard and samples' aliquots (the experimental and the native sheep samples which were prepared according to (Section 1.6) in Duplicate were diluted 1 in 10 in x1 TE buffer, provided by the kit and pipetted into a 96 well microplate. Woking in the dark, PicoGreen working solution (1:200 diluted in x1 TE buffer) was prepared immediately before use. To each sample and standard, 100 μL of the working solution was added and incubated in the dark for two minutes before being spectrophotometrically read using a Synergy 2 plate reader at excitation of 480 nm and emission of 520 nm. Concentrations were determined using a calibration curve with linear regression. The values obtained were subtracted from blank values (using 10 mM ammonium acetate in TE buffer).

2.6.2 Quantification of sulphated Glycosaminoglycan (sGAG) by DMMB assay

DMMB assay was carried out to quantify sulphated GAG (Farndale *et al.,* 1986). Working DMMB solution and Chondroitin 4 sulphate stock solution was prepared (Table 2.6).

Table 2. 6: Materials and stocks' compositions and preparation for DMMB assay

	Materials and solutions	*Compositions and preparation*
1	***Solution 1 dissolvent***	5ml 37% HCl in 500 dH_2O +1.16gNaCl + 1.5g Glycine
2	***DMMB solution***	16 g of DMMB is dissolved in solution 1, light sensitive stored in dark at R T
3	***Chondroitin 4 sulphate***	Standard solution of 500µg/ml in 100 mM ammonium acetate aliquoted and freezed in -20 ^oC. This concentration was diluted 1:10 to use it as a first concentration to make a fresh serial dilution of 50, 25, 12.5, 6.25, 3.125, 1.6 and 0.78 µg/ml

50 µL of each sample and Chondroitin 4 sulphate standard serial dilution were transmitted in duplicate to a 96 well microplate, plates were then transferred to a Synergy 2 plate reader. An automated dispense unit was used to dispense 200 µL of DMMB solution into each well meanwhile the absorption was read at 530 nm. Each well was read individually to increase reproducibility and decrease the potential for precipitation of the DMMB-GAG complex. The data collected was then analysed by Excel to determine the concentration in µg/ml using a calibration curve with linear regression. sGAG concentrations were calculated from the standard curve in µg/ml and 100 mM ammonium acetate was subtracted as a blank.

2.6.3 Total protein assay

Pierce™ BCA Protein Assay Kit was used to determine the total protein amount in the samples. Protein standards were prepared according to the manufacturer's protocol using BSA stock of 2 mg/ml by preparing serial dilutions A to I (Table 2.7).

Table 2. 7: Preparation of diluted bovine serum albumin (BSA) standard.

Vial	Dilution Vol(µL)	BSA Vol (µL)	Final BSA concentration (µg/ml)
A	0	300 of stock	2000
B	125	375 of stock	1500
C	325	325 of stock	1000
D	175	175 of vial B dilution	750
E	325	325 of vial C dilution	500
F	325	325 of vial E dilution	250
G	325	325 of vial F dilution	125
H	400	100 of vial G dilution	25
I	400	0	0 = blank

The working reagent (WR) was prepared by mixing 50 parts of BCA Reagent A with 1 part of BCA Reagent B (50:1, Reagent A: B). Then, 25µL of each standard and samples were pipetted in a 3 replicate into 96 well microplate. After that 200 µL of WR was added to each well. Plates were mixed on a plate shaker for 30 seconds. Thereafter, plates were incubated at 37°C for 30 minutes. Plates were then left to cool before the absorbance was measured at 562nm.

2.6.4 Total collagen assay

Chondrex Sirius Red Collagen Detection Kit was used to determine the total collagen amount in each sample. The assay was performed following the manufacturer's instructions. Ultra-purified distilled water was used to prepare sufficient amounts of 0.05 M acetic acid solution and standard solutions as serial dilutions of 500, 250, 125, 63, 31.5, 16, 8, and, 4 µg/ml. Following each, 50 µL of blank, diluted standard and the samples were added to 1.5 ml centrifuge tubes. Then, 250 µL of Sirius Red Solution was added to each tube. Tubes were vortexed and incubated for 20 minutes at RT. Samples were then centrifuged at 10 000 rpm for 3 minutes and the supernatant was discarded carefully by pipette without disturbing the pellet. Thereafter, 250 µL of washing solution was added to each tube. The tubes were vortexed again and centrifuged at 10 000 rpm for 3 minutes before resuspending again in washing solution. After another centrifugation the supernatant was discarded carefully and 250 µL of extraction buffer were added to each tube to dissolve the pellets completely.

Finally, the samples were transferred to a 96 well plate and the optical density was read by plate reader at 530 nm. The total collagen was estimated in the same ways of the biochemical assays above.

2.8 Statistical analysis

Unless otherwise stated in the thesis, data was statistically analysed using IBM SPSS statistics program version 24. One-way ANOVA with Tukey's multiple comparisons test was chosen to determine statistical significance between the experimental conditions. All values quoted in the results are mean ± standard deviation except Young's modulus data expressed as mean ± standard error. The value for statistical significance was set to 0.05. P values were denoted as *$p<0.05$, **$p<0.01$, ***$p<0.001$.

CHAPTER 3

Native Sheep Cartilage Characterisation – Investigating Donor Variability

3.1 Introduction

Cartilage is considered avascular, aneural, and has limited capacity for self-repair (Buckwalter, 1992) because Cartilage has sparse cellularity, inactive appearance, and obscure characteristics (Buckwalter and Mankin, 1998b; Mikos *et al.*, 2006; Redman *et al.*, 2005).However, researchers have defined not only the structural arrangement of the tissue and the complexity of the polydisperse matrix components, but a surprisingly active set of metabolic processes (Athanasiou *et al.*, 2009).

The cartilage composition varies depending on location, age and injury or diseased state of the individual (Cremer *et al.*, 1998), but in general, the extracellular matrix (ECM) of the articular cartilage has three main constituents, collagen, proteoglycans, and water. Articular or hyaline cartilage forms the bearing surfaces of the movable joints of the body. Since it is weight bearing it possesses toughness and resilience through which the tissue shows exceptional mechanical and biological properties.

The ECM is suited to weight bear and for the maintenance of the bone surfaces due exclusively to the unique interactions between the contents (collagen, water and proteoglycan). Usually, chondrocytes make up less than 10% of the total volume of the cartilage tissue and are not considered to contribute to the mechanical properties of the tissue (Zhang *et al.*, 2009). The ECM is composed of a tight collagen fibre network which detains the highly hydrophilic gel of aggregated proteoglycan macromolecules. Collagen accounts for approximately 50-60% of the cartilage dry weight, the remaining 40-50% is composed of proteoglycans and cellular material. Intact healthy articular cartilage behaves as a linear viscoelastic solid. This behaviour is due to the regular viscous drag of fluid through the tissue in harmony with the specific properties of the extracellular matrix.

In addition to above, water perfusion across the cartilage surface in response to physiologic loading is thought to play a significant role in the lubrication of joints. The importance of articular cartilage as a bearing surface has led to extensive mechanical and biologic studies of this tissue (Parsons, 2016).

Furthermore, collagen forms a characteristically oriented fibril network. Its function is to determine the tensile strength of the tissue (Cremer *et al.,* 1998) and it was demonstrated that collagen type II alone has the potential to induce and maintain MSCs chondrogenesis (Bosnakovski *et al.,* 2006).

Several methods can be used to compute the tissue's mechanical property (Fulcher *et al.,* 2009; Lawless *et al.,* 2017). There are three kinds of commonly used mechanical testing configurations: (a) unconfined compression which is a commonly used global mechanical test configuration. It is an *in vitro* technique where cartilage sample discs are placed between smooth plates in a compression test machine, (b) confined compression (confined compression test can be used to estimate material parameters, such as the hydraulic permeability using permeable piston and sink the samples in the fluid) and (c) indentation when samples were indented using porous indenters that measure the mechanical property of the different cartilage zone (Figure 3.1).

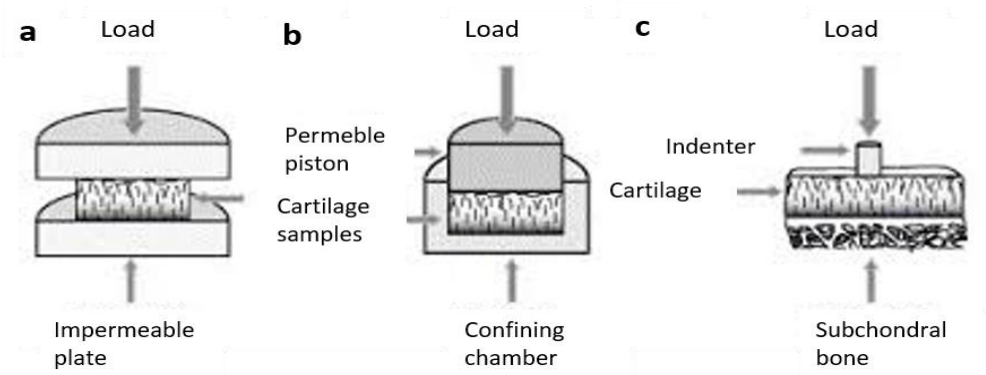

Figure 3. 1:Commonly used mechanical testing configurations. *(a) Unconfined compression (UCC), (b) confined compression (CC) and indentation (c). (Knecht et al., 2006).*

Bose ElectroForce 3200 system which is used in this thesis provide unconfined compression. The mechanical properties of the articular cartilage are considered to be viscoelastic (Hayes and Mockros, 1971; Parsons and Black, 1977) because of the function of aggrecan which carry highly negatively charged carboxyl and sulphate groups. In physiological solution, the negative charges are balanced by an influx of positive ions (Na^{+} and Ca^{+2}). This influx of ions results in an osmotic balance between the proteoglycan and the surrounding synovial fluid lead to formation of a proteoglycan gel that causes cartilage to swell in physiological

saline solutions. This swelling is the reason for low water permeability of cartilage under applied loads the resulting osmosis-based cartilage structure is poro-viscoelastic, which enables the tissue to store and dissipate energy upon mechanical deformation (Eisenberg and Grodzinsky, 1985; Mow *et al.,* 1982). Typical force-displacement curve for an impact test on articular cartilage is showed in Figure 3.2 (Burgin and Aspden, 2008).

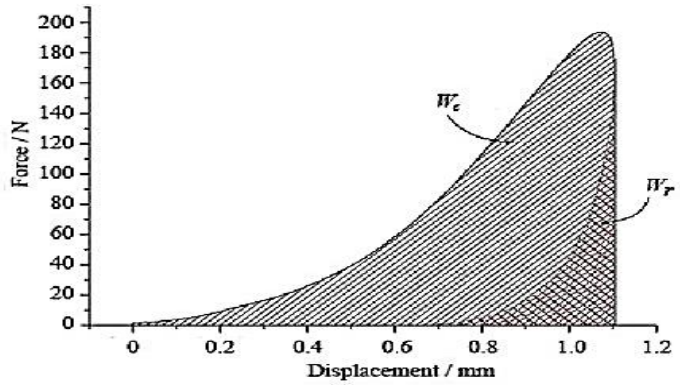

Figure 3. 2: Typical force-displacement curve for an impact test on articular cartilage. *The areas corresponding to the work done in compression, Wc, and in restitution, Wr, are shown hatched (Burgin and Aspden, 2008).*

Investigations have also shown that the mechanical properties of articular cartilage depend on its biochemical composition (Armstrong and Mow, 1982; Ficklin *et al.*, 2007). Mechanical properties of the articular cartilage Young's modulus in MPa for different species is showed in Table 3. 1.

Table 3. 1: Young's modulus of articular cartilage for different species*

References	Species	E [MPa]
(Jurvelin et al., 2003)	Human	0.581
(Jurvelin et al., 1997)	Bovine	0.754 (confined compression) 0.677(unconfined compression)
(Machado et al., 2017)	Swine	0.3886
(Knecht, 2006)	Equine	1.669
(Turner et al., 1997)	Ovine	0.50
(Fermor et al., 2015)	Ovine	1.31
(Peters et al., 2017)	Canine	1.76

*Note: * Young's modulus in these different references were measured with different methods using different mechanical testing configurations according to each reference. The value mentioned to compare our results with the others' results.*

3.2 Aims and objectives

3.2.1 Aims

The aim of this chapter is to study the biochemical and mechanical properties of native adult sheep articular cartilage using post-mortem samples of femurs patella groove cartilage and to study the variations between the different donors' samples.

3.2.2 Objectives

The objectives for this chapter are:

- To determine the mechanical properties of adult sheep articular cartilage by determining the Young's modulus.
- To study the biochemical composition of the native cartilage samples by assessing sGAG, total protein and total collagen content in relation to cell number.
- To study the variations between different donors.
- To study the cartilage structure using different histological stains and immunohistochemistry.

3.3 Methods

3.3.1 Cartilage samples collection

Native sheep cartilage samples were collected from six female sheep directly after euthanasia. The sheep used in this study were non-pregnant English Mule sheep with a skeletally mature age of 2 - 4 years and a weight between 64.5 - 89.5 kg. To allow for donor comparison, the same breed, age group and gender were selected for all individuals. The animals were kindly provided by our collaborator from the veterinary school-Sutton Bonnington Animal Facility at Nottingham University according to the principles of replacement, reduction and refinement (the 3Rs) and animal tissue sharing.

After euthanasia, the stifle joint was dissected, and the articular surfaces was exposed. Then, using an 8 mm diameter biopsy punch (Integra™ Miltex™ REF 33-37 Cat # 12-460-412), cartilage samples of approximately 8 mm diameter and 0.7 -1 mm thickness were collected from the articular surface of the patellofemoral groove of each donor (n = 8-10). The samples were collected from both right and left leg of each donors and kept in ice-cold PBS during transport to the cell culture laboratory at Keele University to perform the tissue analysis as mentioned in Figure 3.3.

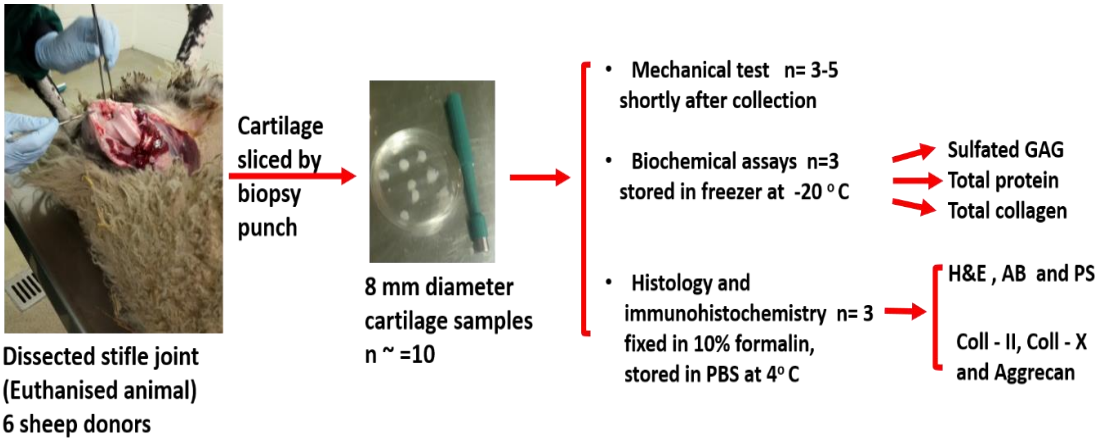

Figure 3. 3: Methodology of chapter 3. *This scheme summarises the steps carried out in chapter 3 for experiments on native sheep cartilage collection and characterisation.*

A fraction of the freshly collected samples was used for mechanical testing (minimum n=3). Meanwhile, the remaining samples were divided into two parts. One of them was stored at -21ºC for biochemical analysis (n=3) and the other samples were fixed with 10% buffered formalin overnight and then stored in PBS at 4º C until using them for histology and immunohistochemistry (n=3).

3.3.2 Mechanical test and Young's modulus

Samples were stored in cold PBS after collection. Compression tests were performed within a few hours of collection. Sample diameter and height were measured using digital calliper and subsequently placed on the platform of the Bose ElectroForce 3200. Tests were performed as described in chapter 2, section 2.7.

Stress-strain curves were plotted, and the Young's modulus was calculated. For all calculations tissue homogeneity was assumed.

3.3.3 Biochemical assays

Sheep cartilage samples were prepared for the biochemical assays. In brief, the whole thickness cartilage from both legs of each sheep donor (n=3) was weighted. The specimens were digested with 1 ml of 50 µg/ml proteinase K in 100 mM ammonium acetate overnight at 60ºC. During this time, the vials were vortex twice. Then a suspension of 0.03 g/ml of native sheep cartilage was prepared from each sample using the known weighted sample stock solutions above. To avoid freeze-thawing cycles, portions of these final concentrations were aliquoted and frozen at -21ºC until use. Sample were analysed to quantify the content of DNA, sulphated GAG, total collagen and total protein, using the specific assays as described in sections 2.6.1-2.6.4, respectively.

3.3.4 Histological and immunohistological staining

Cartilage samples were prepared for histology and immunohistology as previously mentioned in chapter 2, sections 2.4.2. Serial slide sections were used for histological and immunohistological stains. Hematoxylin and Eosin (H&E), alcian blue (AB) and picrosirius red (PS) were chosen for histological assessment of the native sheep cartilage (Sections

2.4.3.1-2.4.3.5). Immunohistological assessment was performed using immune-peroxidase antibody staining for collagen II, collagen X and aggrecan staining (Section 2.4.4).

3.4 Statistical analysis

DNA content, sGAG content, total protein and total collagen content, and their normalisation to the DNA content, were compared using one-way ANOVA with Tukey's multiple comparisons test to determine statistical significance between the six donors. Statistical significance between the right and left leg of each sheep donor was measured using the Student's paired t-test (two-tailed). Analysis was performed using SPSS statistics program version 24. All data are shown as mean ± standard deviation (except Data obtained for Young's modulus were plotted as mean ± standard error). The value for statistical significance was set to 0.05. P values were denoted as *p<0.05, **p<0.01, ***p<0.001.

3.5 Results

3.5.1 Mechanical test and Young's modulus calculation

To allow for displacement of 0.2 mm of the entire specimen thickness, loads ranging between 5-20 N were applied. The load that was applied to the cartilage specimens did not cause visual crack formation. Resulting load-displacement data obtained from the mechanical tester were used to plot the Stress-Strain curves for each sample (Figure 3.4). The compression test displayed graphs of stress-strain, which was identical to the graphs that can be obtained from viscoelastic materials.

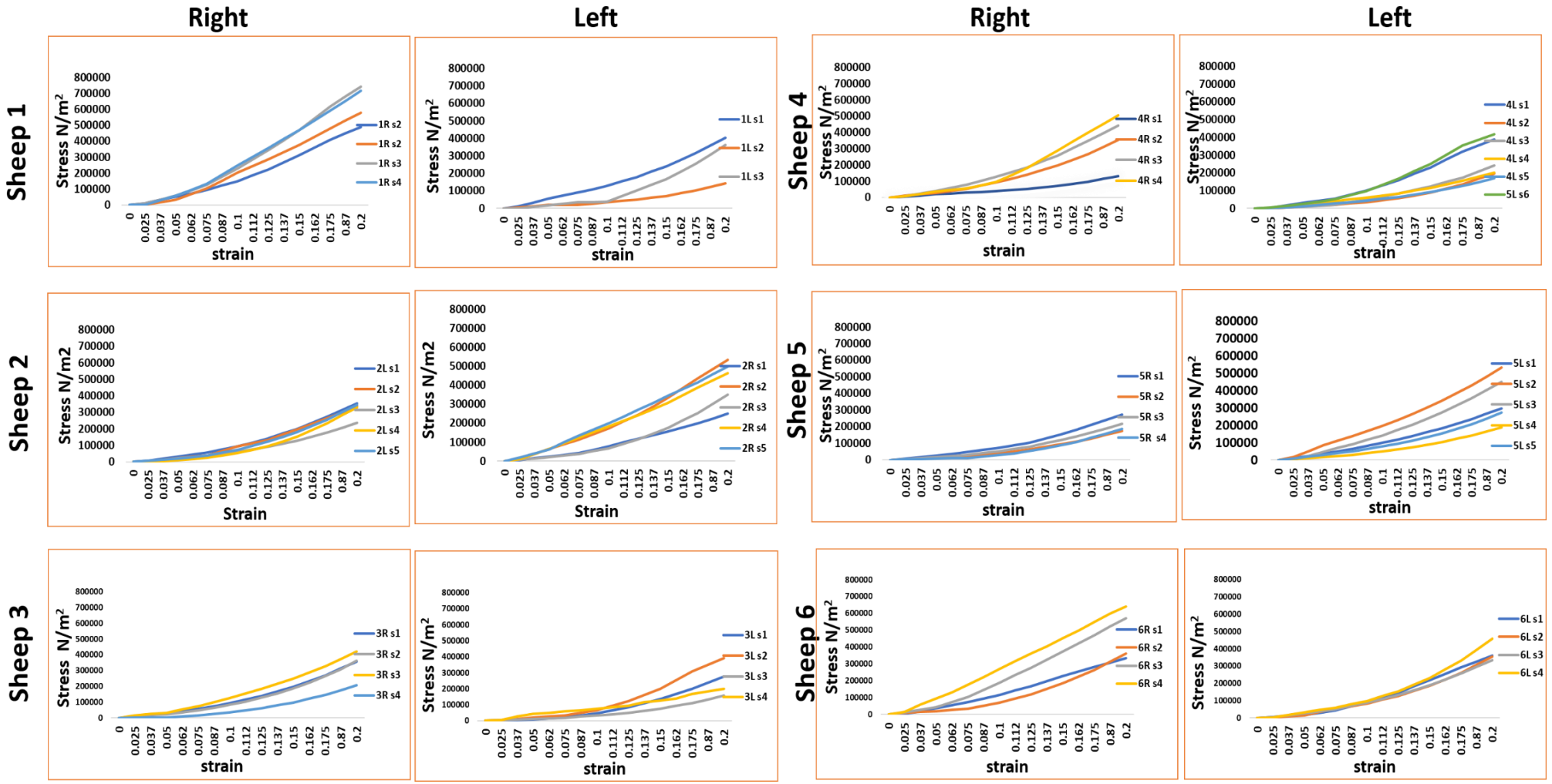

Figure 3. 4: Stress-strain of native sheep cartilage. *Stress-strain curves of native sheep cartilage of right and left legs of each sheep donor. Stress versus strain curves of all donors displayed the viscoelastic properties of the cartilage samples. R= right, L= Left, s = sample number, n=3-5.*

Subsequently, Young's modulus of the native sheep cartilage was computed. This was done by evaluating the slope in stress relative to strain using equation 2.7 (Chapter 2, section 2.7). Data are shown in Figure 3.5, A and B. Young's modulus of the cartilage for each donor were ranged between 0.81 ± 0.045 MPa (sheep 3 left leg) to 1.517 ± 0.196 MPa (sheep 6 right leg). Significant differences were observed when compare the right and left leg of each sheep donors, for the sheep donor 1, 3, 5 and 6 (Figure 3.5, A). However, no significant differences between the six sheep donors were observed (Figure 3.5, B). The measured sheep cartilage Young's modulus from all samples of all donors was 1.257 MPa.

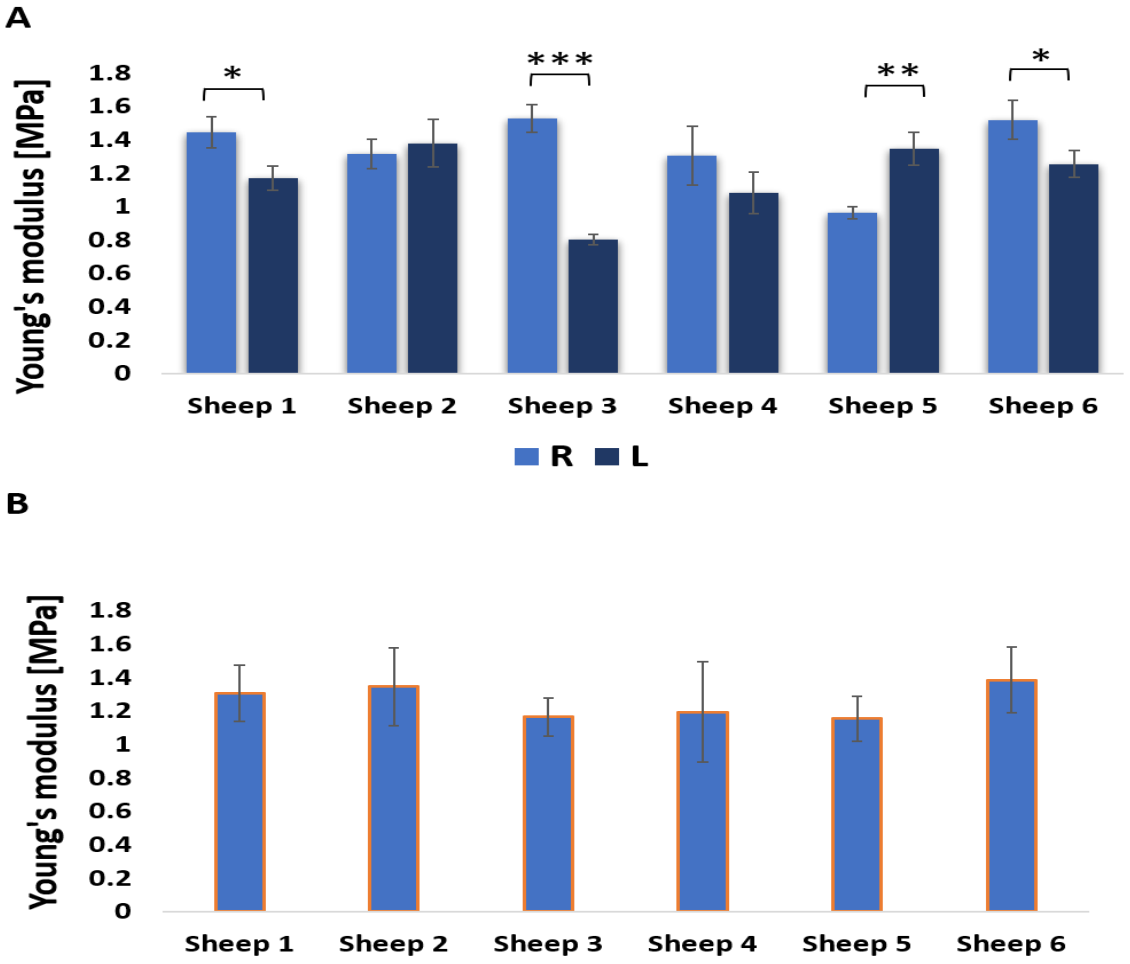

Figure 3. 5: Young's modulus of native sheep cartilage. *Young's modulus of the native sheep cartilage was calculated for six sheep. Data are expressed as mean ± standard error (n=3). Significant differences were observed between left and right legs of sheep 1,3,5 and 6 (A). No Significant differences were observed between the six sheep when gathering the values of the left and right legs of each (B).*

3.5.2 Biochemical composition of native sheep cartilage

Lysates were prepared as described in Chapter 2, section 2.6 and used for the biochemical assays.

3.5.2.1 DNA content

PicoGreen DNA assay was used to quantify the DNA content in the lysates. The overall DNA content of the samples varied between 1.225 ± 0.232 µg/ml (sheep 1 left leg) to 1.896 ± 0.077 µg/ml (sheep 5 left leg). The significant differences in DNA content were observed for sheep 1 versus sheep 4 ($p \leq 0.05$), and 6 ($p \leq 0.01$) only (Figure 3.6). The percentage of DNA content in 1 g cartilage samples was about 0.136 %.

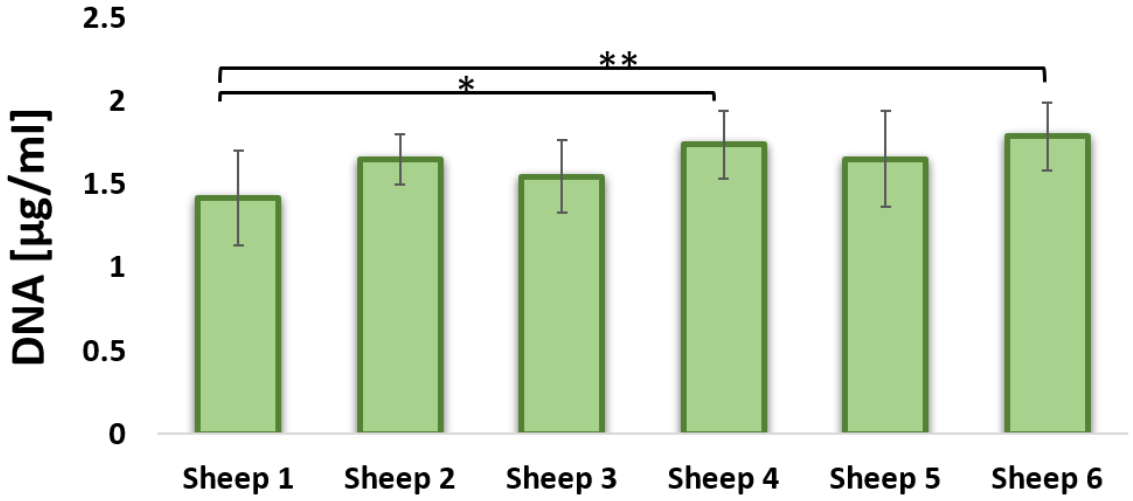

Figure 3. 6: DNA content of native sheep cartilage. *Total DNA content was determined using the PicoGreen assay for all donors following digestion with proteinase K. Significant differences among the six sheep were observed between sheep 1 in comparison to sheep 4 and 6. Data are expressed as mean ± standard deviation, n=6, *p ≤ 0.05, **p ≤ 0.01.*

3.5.2.2 Sulphated Glycosaminoglycan content

Total amount of sGAG was analysed by performing DMMB assay. Samples were analysed in triplicate and the results are shown in Figure 3.7. The sGAG contents obtained from all six sheep ranged between 137.722 ± 10.794 µg/ml (sheep 3 right leg) to 163.500 ± 4.061 µg/ml (sheep 5 left leg). In general, no significant differences were observed for the comparison of all sheep donors. Whereas, significant differences in the sGAG content between right and left legs were observed for sheep 1, 2, 3, 5 and 6. The percentage of sGAG content in 1 g cartilage samples about 15.302 %.

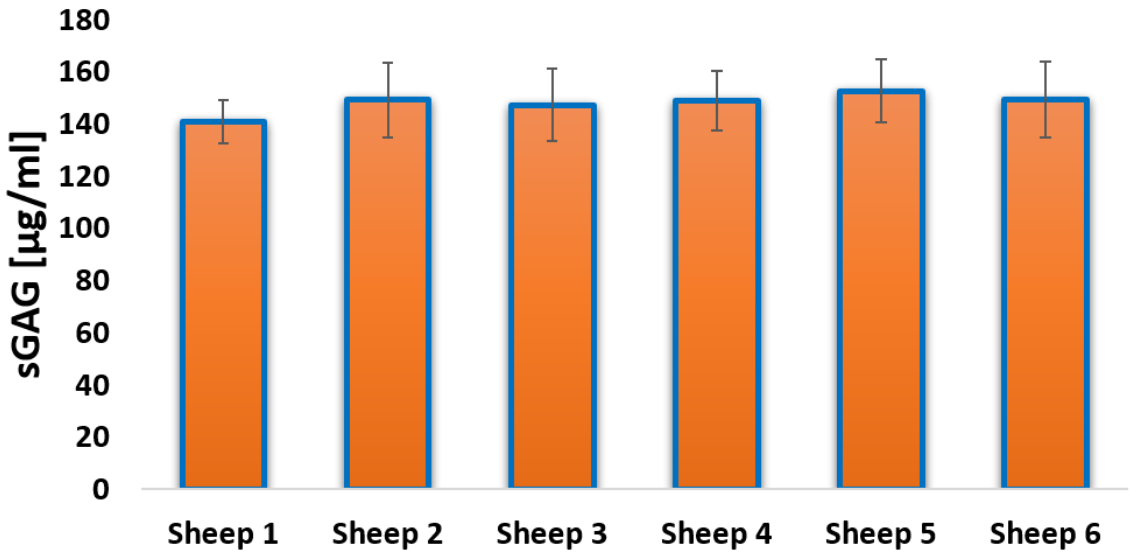

Figure 3. 7: Native sheep cartilage sGAG content. *sGAG content was quantified using DMMB assay. no significant differences among the six donors. Data are expressed as mean ± standard deviation, n=6.*

3.5.2.3 sGAG content normalised to DNA content

To determine the sGAG content in relation to cell number, the sGAG content was normalised to the DNA content of the same samples. The results showed that the normalised sGAG to DNA content (µg/ µg) ranged from 73.238 ± 4.246 µg/µg (sheep 6 right leg) to 119.472 ± 24.428 µg/µg (sheep 1 left leg). No significant differences between the six sheep were observed (Figure 3.8).

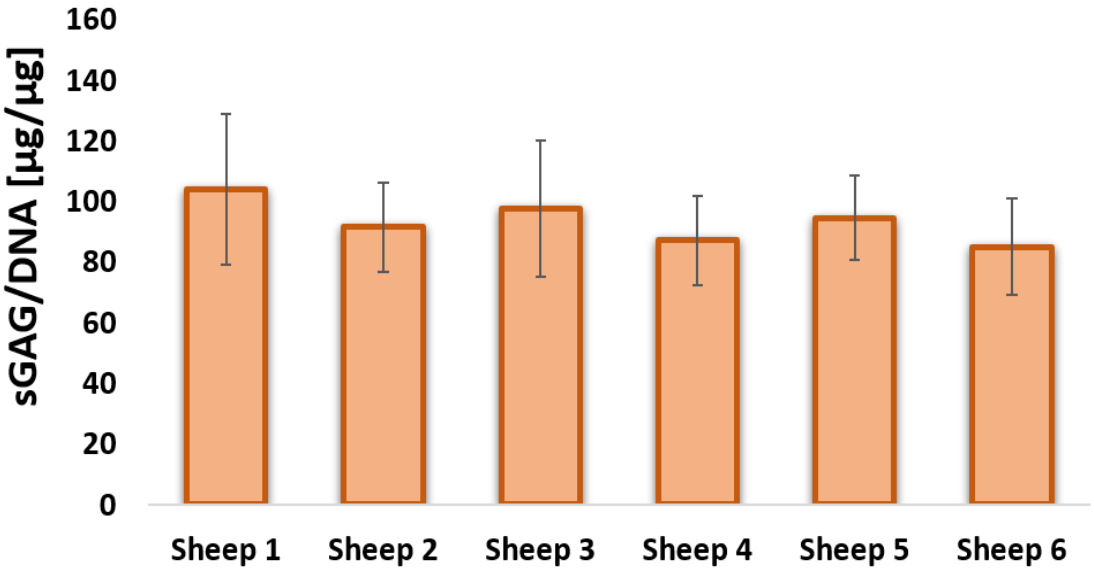

Figure 3. 8: sGAG normalised to DNA content. *The sGAG / DNA content revealed no significant differences between the six sheep donors. Data are expressed as mean ± standard deviation, n=6.*

3.5.2.4 Total protein content

Pierce™ BCA protein assay kit was used for detecting total protein content of the sheep cartilage samples. The total protein ranged from 483.778 ± 66.212 µg/ml (sheep 3 right leg) to 639.334 ± 87.369 µg/ml (sheep 4 right leg). When comparing sheep donors with each other, significant differences were observed for sheep 4 versus sheep 1, 3 and 5, $P \leq 0.05$, $p \leq 0.01$, $p \leq 0.001$ also in between sheep 5 and sheep 6 $P \leq 0.05$ were observed (Figure 3.9). The percentage of the total protein content in 1 g cartilage samples was about 53.753 %.

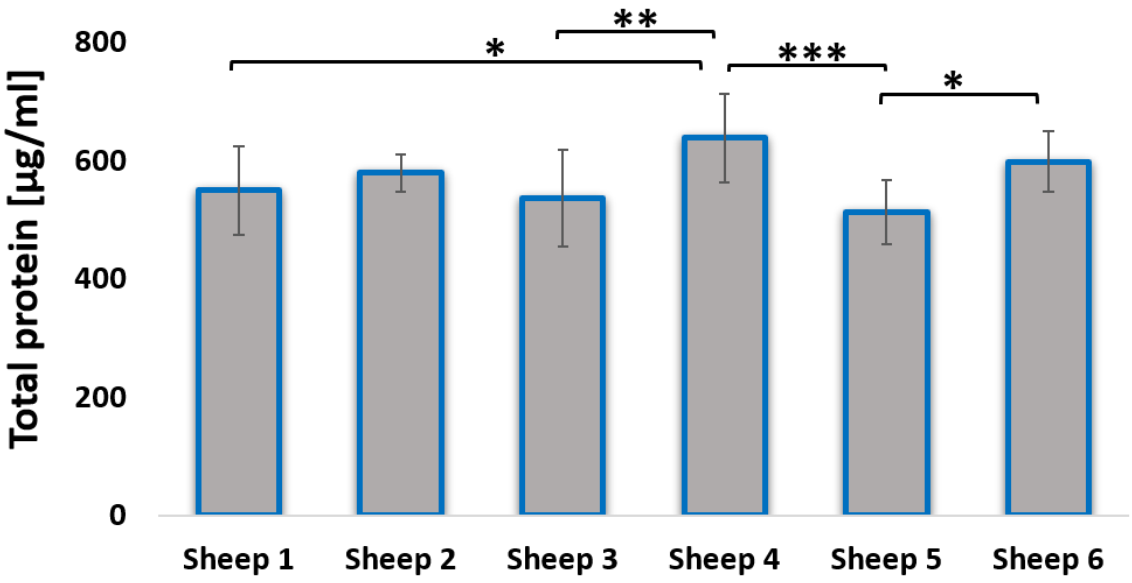

Figure 3. 9: Total protein content of native sheep cartilage. *Total protein content was quantified using BCA assay. The results display significant differences between sheep 4 and sheep 1, 3 and 5 as well as between sheep 5 and 6 were observed. Data are expressed as mean ± standard deviation, n=6, *P ≤ 0.05, **p≤ 0.01, ***p≤ 0.001.*

3.5.2.5 Total protein content normalised to DNA content

Total protein content was normalised to DNA content of the same sample to determine the total protein content in relation to cell number. Data are shown in Figure 3.10. The total protein/ DNA ratio ranged between 276.317 ± 25.004 µg/ µg (sheep 3, right leg) to 469.606 ± 109.728 µg/ µg (sheep 1 left leg). There were no significant differences between the six sheep donors as well as between each sheep's right and left legs.

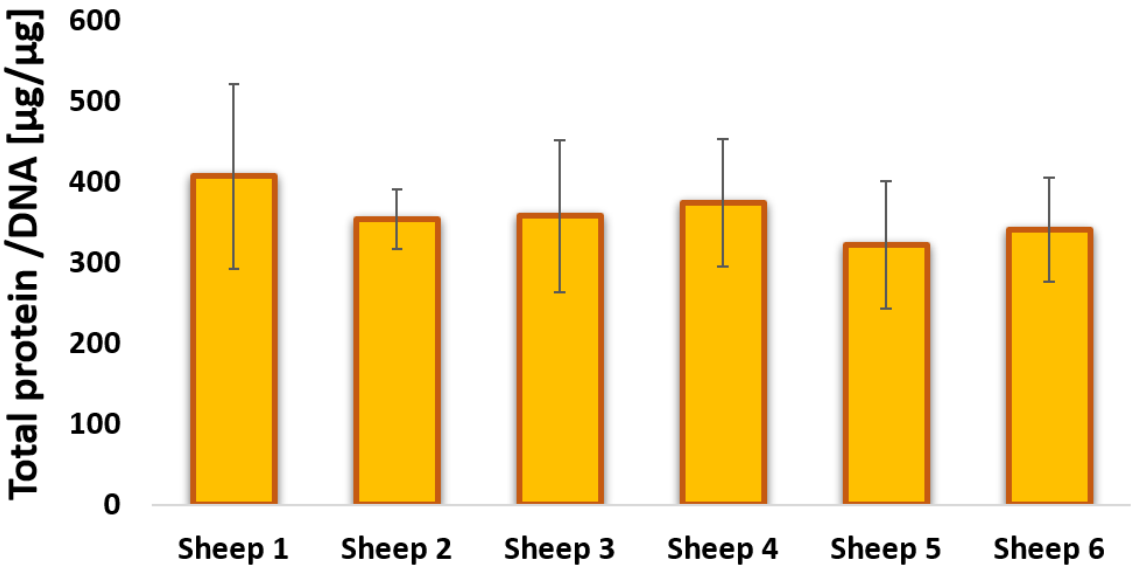

Figure 3. 10: Total protein normalised to DNA content. *The results revealed no significant differences for $p \leq 0.05$ among the six sheep donors as well as between sheep's right and left legs. Data are expressed as mean ± standard deviation, n=6.*

3.5.2.6 Total collagen content

Chondrex Sirius Red collagen detection kit was used to assess the total collagen content of the samples. The amount of total collagen varied between 69.443 ± 8.039 µg/ml (sheep 1 right leg) to 143.778 ± 12.293 µg/ml (sheep 2 left leg). Results showed significant differences among the six sheep donors. Significant differences were observed between sheep 1 compared to sheep 2, 4 and 5. Also sheep 2 versus sheep 3, 5 and 6. In addition to sheep 4 versus sheep 3 and 6 (Figure 3.11). The percentage of total collagen content in 1 g cartilage samples was about 7.716 %.

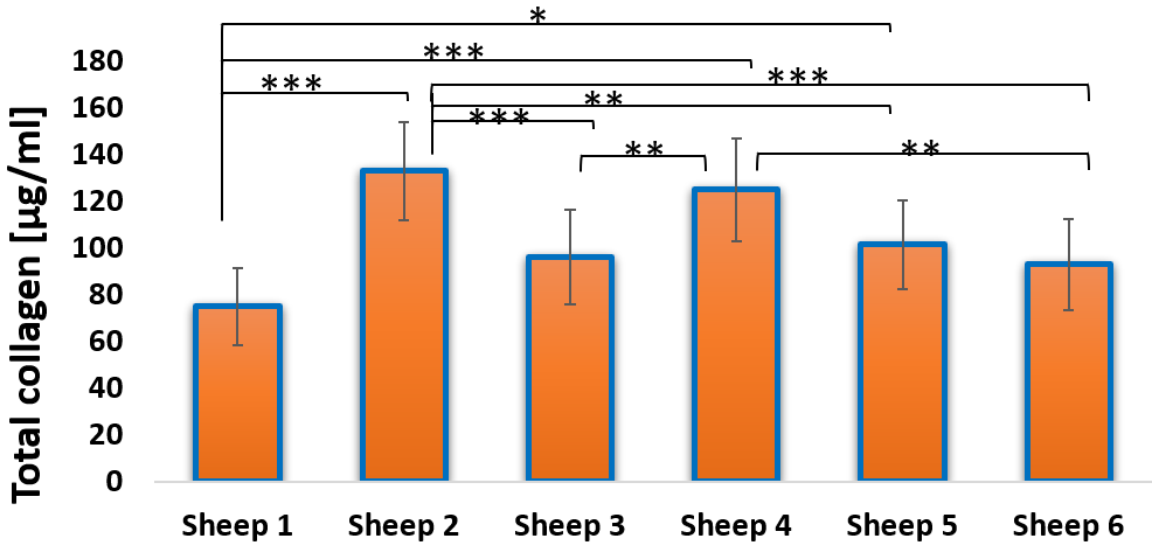

Figure 3. 11: Native sheep cartilage total collagen content. *A) Total collagen content was quantified using sirius red quantitation assay. Significant differences were observed between sheep 1 and sheep 2, 4 and 6; between sheep 2 and sheep 3, 5 and 6. Also in sheep 4 versus 3 and 6. Data are expressed as mean ± standard deviation, n=6, *p ≤ 0.05, **p ≤ 0.01, *** p ≤ 0.001.*

3.5.2.7 Total collagen content normalized to DNA content

To assess the total amount of collagen in relation to cell number, total collagen was normalised to DNA content. Statistical analysis revealed significant differences between the donors. Collagen/DNA ratio comparison between sheep 2 revealed a significant difference compared to sheep 1 and sheep 6 at $P \leq 0.05$. and $P \leq 0.01$ respectively (Figure 3.12).

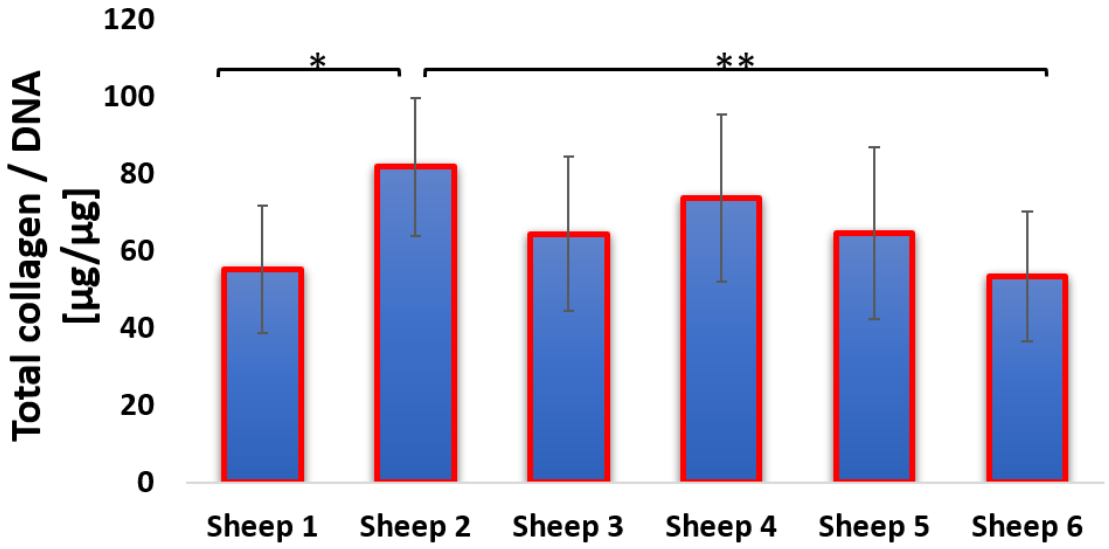

Figure 3. 12: Total Collagen normalised to DNA content. *The results revealed significant differences when comparing sheep 2 with sheep 1 and sheep 6. Data are expressed as mean ± standard deviation, n=6, *p ≤ 0.05 **p ≤ 0.01.*

3.5.2.8 Total collagen content normalized to total protein content

To determine the amount of the collagen in comparison to total protein amount (µg/µg), the total collagen values were normalised to total protein values (Figure 3.13). The results displayed differences between sheep 1 versus sheep 2, 4 and 5 ($P \leq 0.001$) and sheep 2 ($P \leq 0.05$). Meanwhile, sheep 2 showed significant differences with sheep 3 ($P \leq 0.01$) and sheep 6 ($P \leq 0.001$). Sheep 4 showed differences with sheep 6 ($P \leq 0.05$). Finally, sheep 5 versus sheep 6 ($P \leq 0.05$).

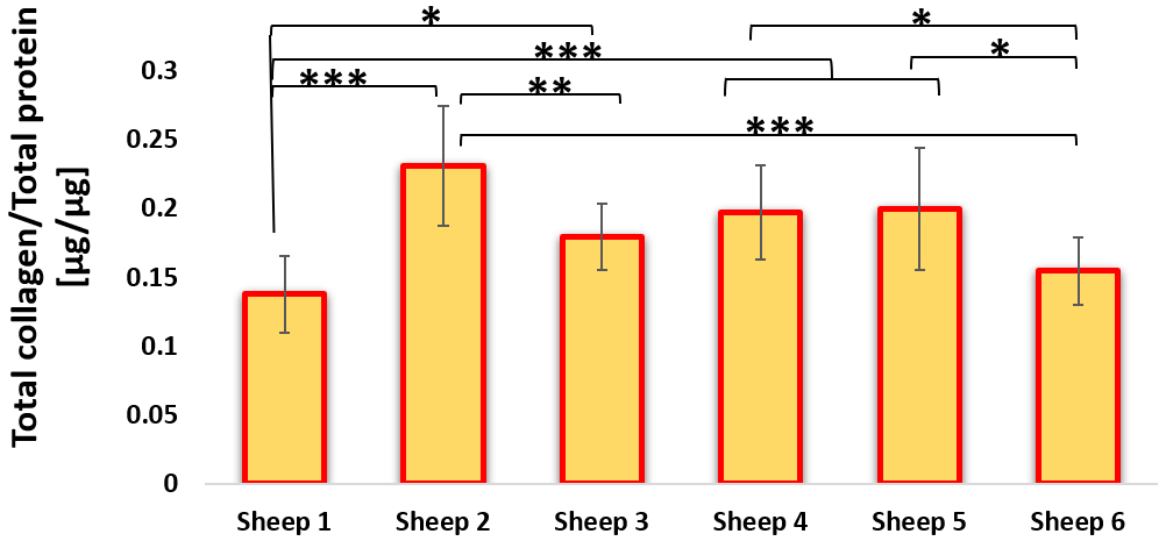

Figure 3. 13: Total collagen content normalised to total protein. *The results displayed statistically significant differences for the comparison of sheep 1 with sheep 2, 3, 4 and 5. Sheep 2 showed significant differences with sheep 3 and 6, and sheep 4 was significantly different from sheep 6. Also in between sheep5 with sheep 6. Data are expressed as mean ± standard deviation, n=6, *p ≤ 0.05, **p ≤ 0.01, *** p ≤ 0.001.*

3.5.3 Histology and Immunohistochemistry

Three histological stains H&E, Alcian blue and Picrosirius red were carried out. Immunohistology was performed to investigate collagen II collagen X and aggrecan.

3.5.3.1 Haematoxylin and Eosin stain

H&E stain was performed as described (Chapter 2, section 2.4.3.1) to determine the histological structure, cell morphology and main layers of the cartilage tissue (Figure 3.14). The sections display the four layers of native cartilage, namely the superficial zone, the middle zone, the deep zone and the calcified zone. The four cartilage zones were identified by cell size, organization, and orientation as indicated in the images. The images also display the morphology of the chondrocyte located in the different cartilage zones. Chondrocytes in superficial zones are spindle in shape and accumulate a high density in the zone (a). Meanwhile, the middle zone (b) and the deep zone (c) often appear interchangeably, and the chondrocytes appear small and rounded with a blue nucleus allocated as a single cell or as a chondrone composed of two or more chondrocytes surrounded by a capsule. The calcified zone appears as the cellular portion of the calcified cartilage interdigitating with the subchondral bone. Chondrocytes in this zone appear big and rounded with deep blue coloured nucleus.

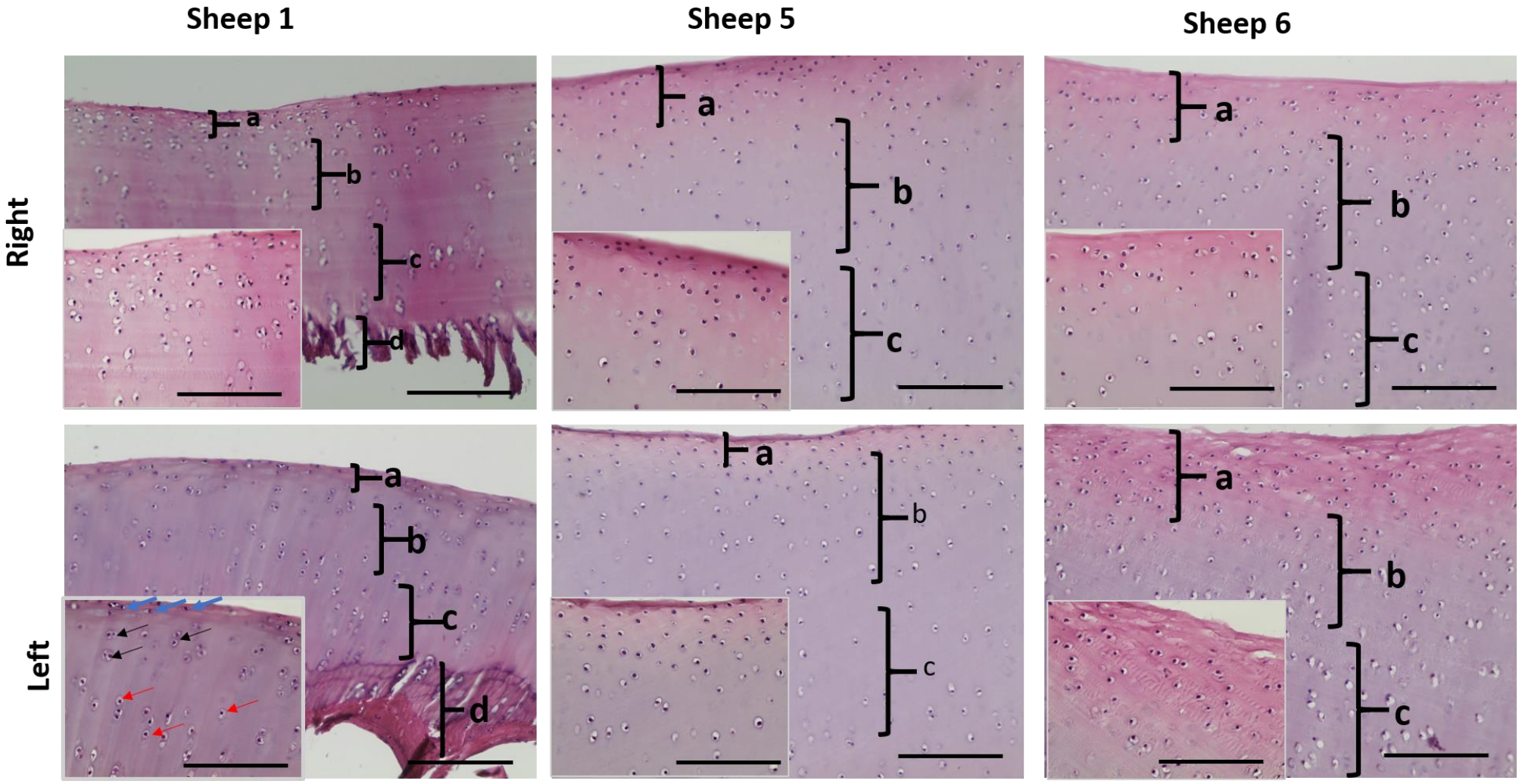

Figure 3. 14: Haematoxylin and Eosin staining of native articular cartilage. *Paraffin sections with a thickness of 7 µm were prepared, stained with H&E stain and imaged by bright field microscopy to illustrate native articular cartilage structure. Full depth cartilage sections show (a) superficial, (b) middle, (c) deep zoon and (d) calcified zone and e subchondral bone (20 x magnification). Different shapes of chondrocytes according to their location are shown in the inserts (blue, black and red arrows) (40 x magnifications). Scale bar = 150 µm.*

3.5.3.2 Alcian blue staining

Alcian blue staining was performed as described (Chapter 2, section 2.4.3.2) to stain the GAG content of the extra cellular matrix of the native sheep cartilage (Figure 3.15). The dye stained the section with blue colour indicating the presence of the GAG in the extracellular matrix (the interterritorial matrix). More intense stain was observed in the Perichondrium (red arrow) and surrounding the chondrocytes and chodron (the black arrows) forming a capsular matrix (territorial matrix).

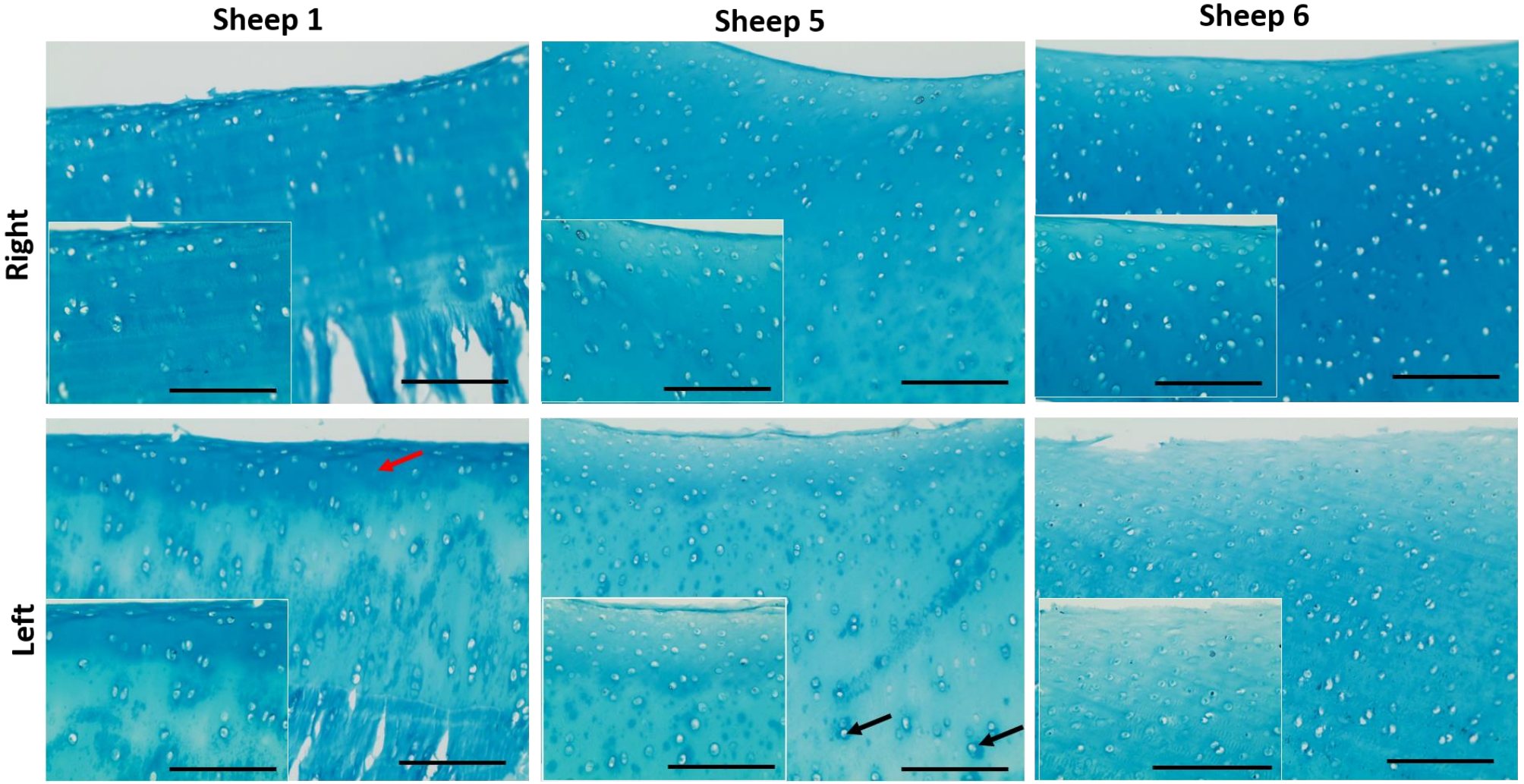

Figure 3. 15: Alcian blue staining of native articular cartilage. *Paraffin sections with a thickness of 7 µm were prepared, stained with alcian blue stain and imaged by bright field microscopy to illustrate native articular cartilage GAG distribution (20x magnification). More intense stains were found in the basal perichondrium (red arrow) and in the pericellular matrix (black arrows) (40x magnifications). Scale bar=150 µm.*

3.5.3.3 Picrosirius Red Stain

Picrosirius red staining was performed as described in chapter 2, section 2.4.3.4 to stain the collagen in the extra cellular matrix. The dye stained the section with pinkish-red colour indicating the presence of the collagen in the intercellular matrix (Figure 3.16). Sections vividly showed variance in the dye intensity. The strongest stains were found for the sheep 6 left leg section. Higher collagen content was found in the basal perichondrium (the black arrows) and the territorial matrix surrounding the chondrocytes (the blue arrows) as indicated by the stronger stain intensity.

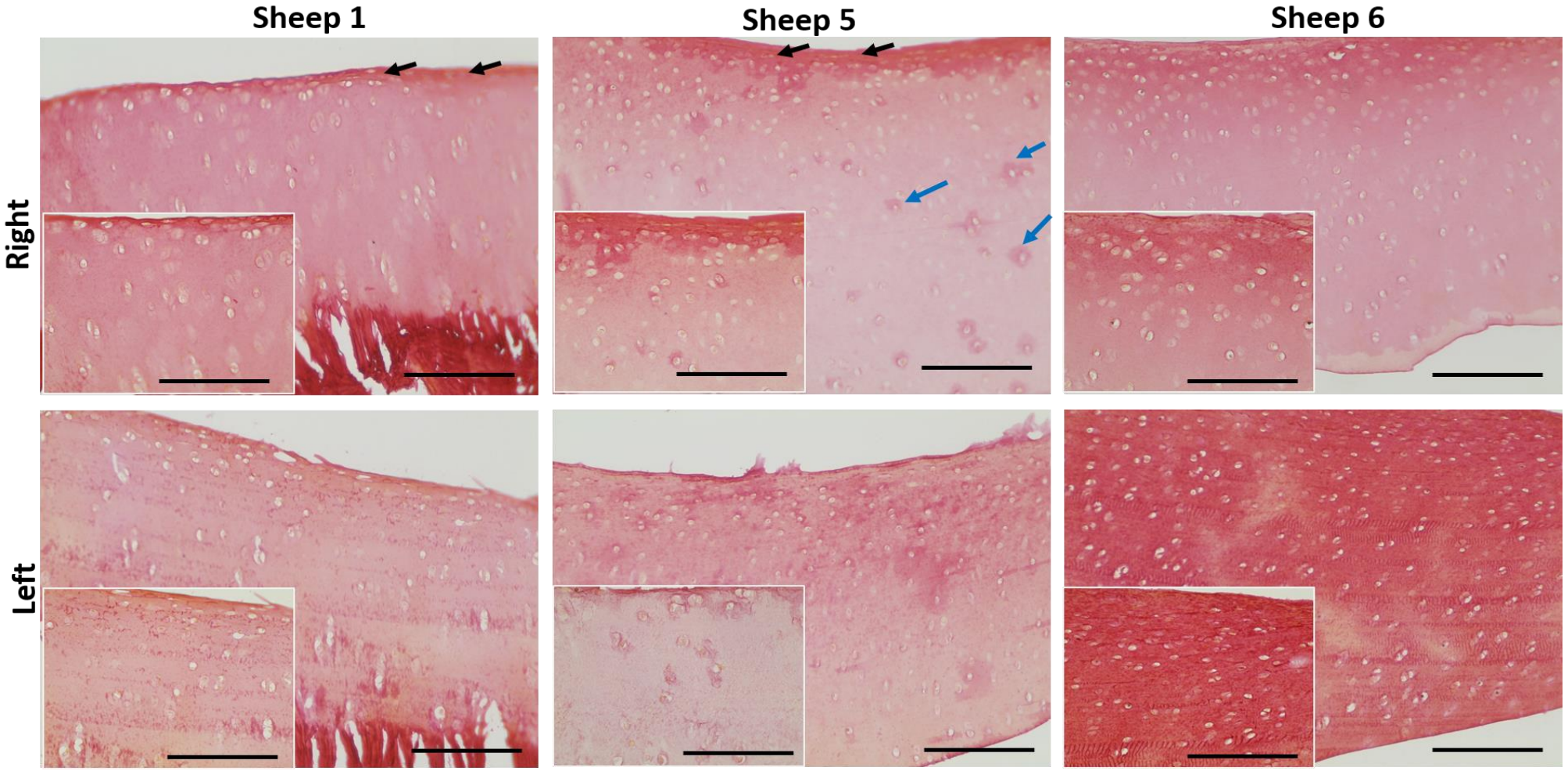

Figure 3. 16: Picrosirius red staining of native sheep articular cartilage. *Paraffin sections with a thickness of 7 µm were prepared, stained with picrosirius red stain and imaged by bright field microscopy to illustrate native articular cartilage collagen distribution. Sections showed variance in the dye intensity. The left leg section for sheep 6 was stained most strongly (20x magnification). The strongest stains were found in the basal perichondrium (black arrows) and surrounding the chondrocytes (blue arrow) (40 x magnifications). Scale bar = 150 µm.*

3.5.4 Immunohistochemistry

Horseradish peroxidase (HRP) was used to immunohistochemically stain the native sheep cartilage. Peroxide/DAB is the substrate chromogen for this enzyme. The antibody-antigen interaction was visualised using chromogenic detection, in which an enzyme conjugated to the antibody cleaves a substrate to produce a coloured precipitate at the location of the protein. Three antibodies for collagen II collagen X and aggrecan were used (Figures 3.17-3.19).

3.5.4.1 Collagen type II immunostaining

The results of the Collagen type II immunostaining of the native sheep cartilage showed an expression of the Collagen type II in the samples. The strongest stain was observed for sheep 6 (right and left leg) (Figure 3.17).

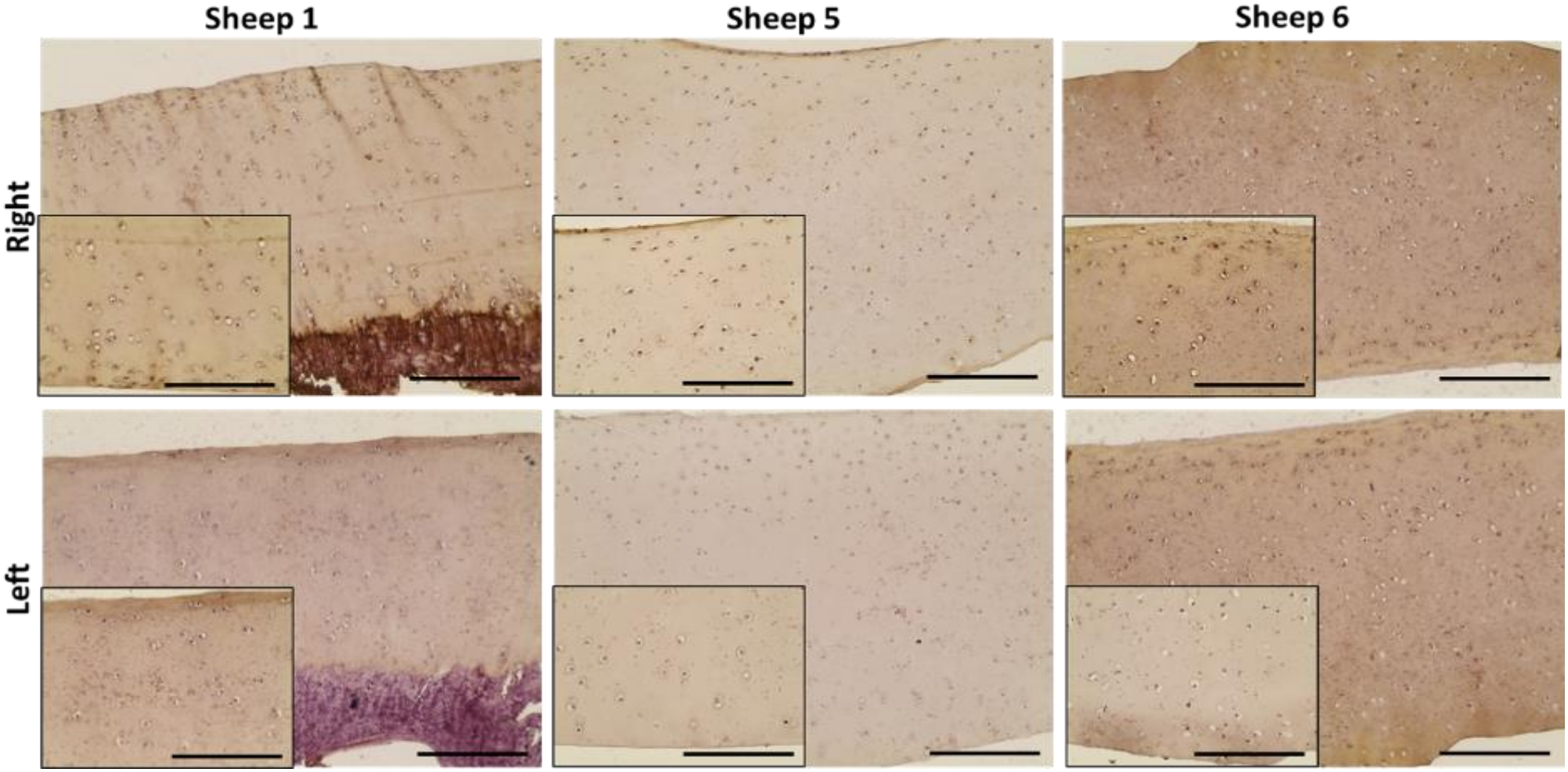

Figure 3. 17: Immuno-peroxidase antibody staining for collagen II of native sheep articular cartilage. *Paraffin sections with a thickness of 7 µm were prepared, stained for collage II and imaged by bright field microscopy to illustrate native articular cartilage collagen II. Sections were positive to the antibody. The strongest stain was observed for sheep 6 (right and left leg) (20 x and 40 x magnifications). Scale bar =150 µm.*

3.5.4.2 Collagen type X immunostaining

The results of the collagen X immunostaining showed that there is collagen X expression in the native articular cartilage. All sections were stained positively especially the superficial layer. The strongest stains were observed for sheep 1 (Figure 3.18).

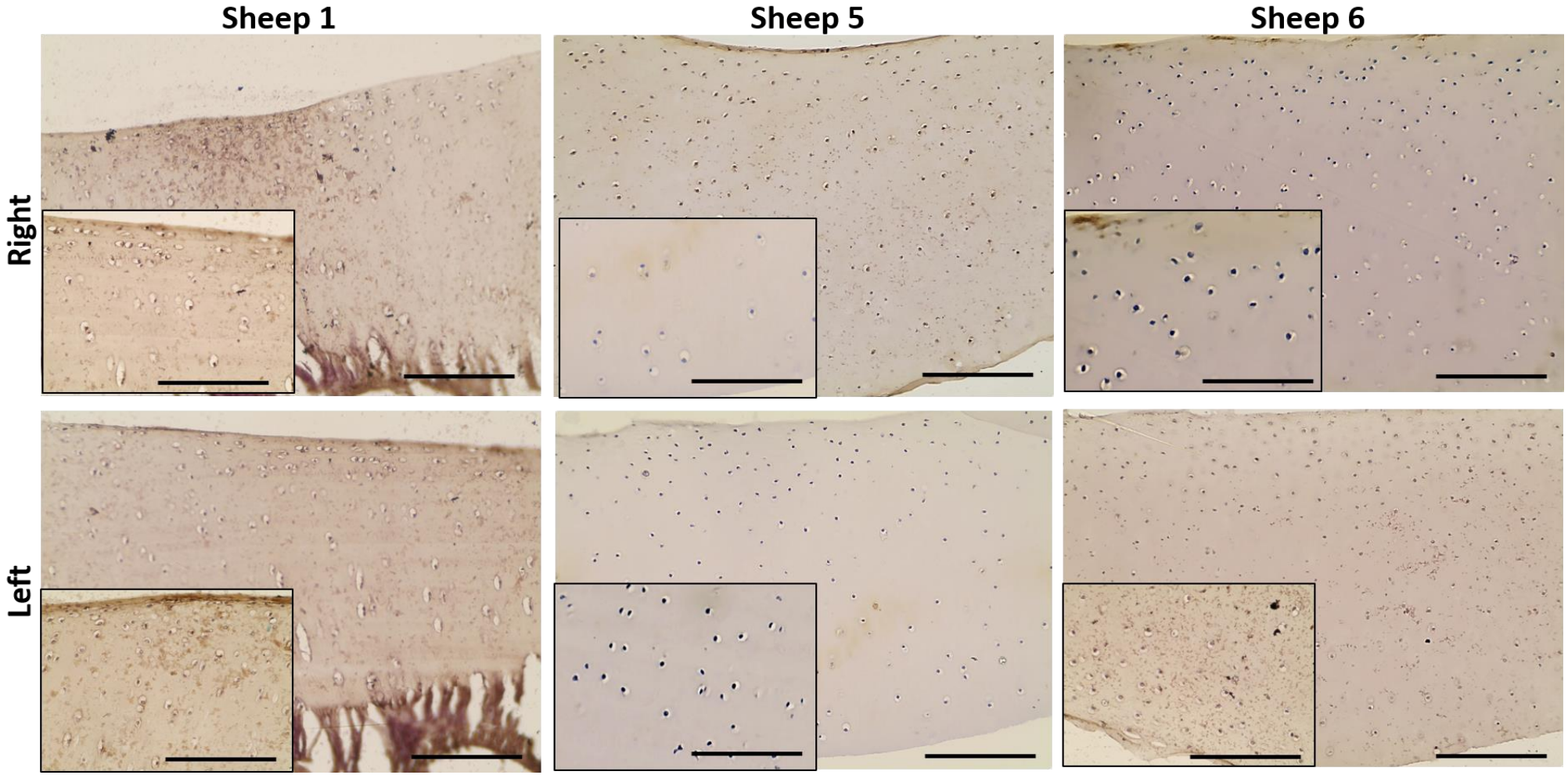

Figure 3. 18: Immuno-peroxidase antibody staining for collagen X of native sheep articular cartilage. *Paraffin sections with a thickness of 7 µm were prepared, stained for collage X and imaged by bright field microscopy to illustrate collagen X in the native articula cartilage. All sections were stained positively, and strongest stains were observed for sheep 1 (left leg) Images were taken at 20 x and 40 x (inserts) magnifications. Scale bar =150 µm.*

3.5.4.3 Aggrecan immunostaining

The results of aggrecan immunostaining showed that there is aggrecan expression in the native articular cartilage. All sections were stained positively. The strongest stains were observed for sheep 6 (left) (Figure 3.19).

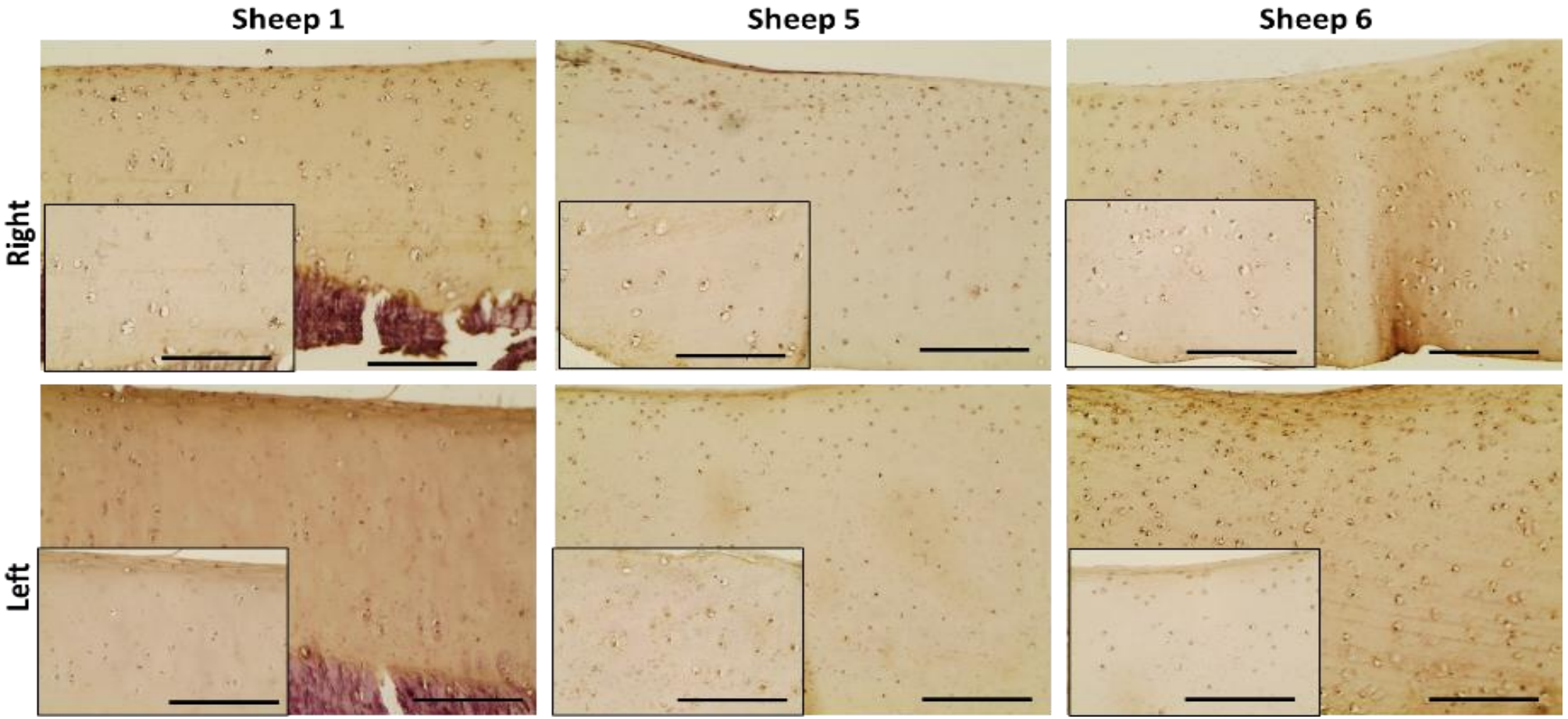

Figure 3. 19: Immuno-peroxidase antibody staining for aggrecan of native sheep articular cartilage*. Paraffin sections with a thickness of 7 µm were prepared, stained for aggrecan and imaged by bright field microscopy to illustrate aggrecan in the native articular cartilage. All sections were stained positive to the antibody. Strongest stain was observed for sheep 6, left leg. Images were taken at 20x magnification and 40 x magnifications. Scale bar=150 µm.*

3.6 Discussion

Articular cartilage is a thin layer of specialized connective tissue with an exceptional viscoelastic characteristic. Its major role is to provide a smooth, lubricated surface to facilitate movement and spread of loads to the underlying subchondral bone (Mccredie, 2010). Articular cartilage is unique in its ability to resist repeated loads. Studying and understanding the normal composition and natural structure in addition to the mechanical properties of the native cartilage is essential prior to presenting any engineered cartilage and making comparison between them.

In this chapter, mechanical properties and biochemical composition were studied including sulphated GAG, total protein and total collagen of native cartilage obtained from animals that have the same characteristics and specifications of the sheep used in the experiments mentioned in later chapters of this thesis.

To study the mechanical properties of the articular cartilage various approaches have been developed. Most of them depend on the stress-relaxation tests, unconfined compression (UCC) and indentation which were performed by a mechanical testing rig such as the Bose ElectroForce 3200 system (Machado *et al.,* 2017).

When the cartilage samples were tested at the micrometre- centimetre scale, the articular cartilage behaved as a non-structured and uniform material. This is widely used as the first approximation which allowing measurement of the overall cartilage stiffness (Loparic *et al.,* 2010). However, most investigators have reported that this stiffness measurements are not sensitive to even substantial changes in cartilage structure associated with aging or early-stage osteoarthritis (Athanasiou *et al.,* 2000; Duda *et al.,* 2004).

Developed methods were modified to study the mechanical properties using well-defined testing approaches, like confined compression (CC) (Mow *et al.,* 1989; Mow *et al.,* 1980) and indentation (Loparic, 2012). In addition, articular cartilage exhibits both tension-compression nonlinearity as well as time-dependent viscoelastic (creep and stress-

relaxation) behaviours (Aagaard *et al.,* 2003; Huang *et al.,* 2003; Mow *et al.,* 1980; Soltz and Ateshian, 2000).

Technology has been developed which allows the use of regional or molecular analysis to study the mechanical properties of the articular cartilage in the different zones, such as the middle or deep zone of sectioned articular cartilage samples. In addition the mechanical properties of the pericellular matrix (PCM) and extracellular matrix (ECM) can be studied using In Situ via Atomic Force Microscopy (Darling *et al.,* 2010).

Depending on the experimental loading conditions, the loading geometry employed by the articular cartilage exhibited a wide range of values of Young's modulus started from ~1 MPa (Loparic, 2012). In this chapter, the computed Young's modulus of the sheep cartilage study of the modulus was about (1.257 MPa) while the Young's modulus of the normal sheep cartilage ranged between 0.39 to 1.10 MPa and 0.14 to 2.00 MPa for the most severe OA grade (Williamson et al 2001). In another study the Young's modulus of the normal sheep cartilage was 1.3 MPa (Kleemann *et al.,* 2007). This study is in line with these findings for Young's modulus of sheep cartilage.

Biochemical assays were used to determine the quantities, relative to wet weight, of the three major constituents of cartilage: sulphated glycosaminoglycan (sGAG) by BMMB assays, collagen by Chondrex sirius red collagen detection assay, total protein by BCA Protein Assay in addition to DNA by PicoGreen assy. Technically on average, each gram of wet cartilage contained 77.7% water, 7.7% collagen, 2.9% sGAG, and 24.9 million cells (Homicz *et al.,* 2003). The calculated components were 7.716 % collagen, 15.302 % sGAG and the 0.211 % DNA.

Haematoxylin and eosin staining were used to determine the general structure of the cartilage tissue, the cartilage zone and cell morphology. In addition, cartilage specific stains like alcian blue staining for GAG and the picrosirius red for collagen were employed. The three stains were equally suitable for the organisation of hyaline cartilage and reflect the normal composition of the native sheep cartilage. The layers of articular cartilage are easiest to

identify in the histological section (Slomianka, 2009). The fibres are not visible on the slides, but the dye intensity concentrated on where the fibrils were concentrating showing the presence of the collagen fibres in specific places like basal perichondrium. For all the stains, no clear differences were observed between the cartilage section of the three chosen donors. However, donor 6 left leg histology had had the highest dye intensity and that may be due to individual variation as there was no specific pathological lesion (Figures 3.14-3.16).

In the literature, type II collagen is normally distributed throughout the cartilaginous zones but is concentrated at higher levels within the superficial zone of cartilage and expressed evenly at the mid and deep zones of cartilage (Wang *et al.,* 2015). Our studies agree with these findings as illustrated by the results obtained from the immunohistology of the native sheep cartilage. A similar result was demonstrated for the aggrecan immunostaining. Both collagen and aggrecan expression was highest in the donor 6 showing a correlation between the extracellular matrix protein expression in individuals. Collagen X was expressed in the native sheep cartilage in low intensity as demonstrated with the immunocytochemistry. The Collagen X was localised to small regions spatially and located in the membrane. Type X collagen is mainly expressed in hypertrophic chondrocytes in cartilage. The expression is usually limited to the hypertrophic zone of the growth plate and in the calcified zone of articular cartilage of long bones (Van Der Kraan and Van Den Berg, 2012). This explain the low intensity of the collagen X expression which indicate the samples were collected from adults but not aged animal donors and there is no clear hypertrophic indication in the cartilage.

All these finding aid in make a vision about biochemical composition of the native cartilage to compare with the output that will be produce through tissue engineering using MICA technology.

CHAPTER 4

Isolation, expansion and characterisation of bone marrow-derived ovine mesenchymal stem cells

4.1 Introduction

Stem cells have been introduced as a possible cell source for orthopaedic tissue engineering. Due to their unique biological properties, mesenchymal stem cells (MSCs) have generated a great amount of interest (Kumar *et al.,* 2015).

According to the International Society of Cellular Therapy (ISCT) MSCs of human or different species) have three characteristics. First, they must be adherent to plastic under standard tissue culture conditions. Second, MSCs must have the capacity to differentiate. Third , they must express certain cell surface markers such as cluster of differentiation (CD) CD73, CD90, and CD105 and lack expression of other markers including CD45, CD34, CD14, CD11b, CD79 alpha CD19 and human leukocyte antigen (HLA-DR) surface molecules (Niwa, 2013).

Although several stem cell sources are currently under investigation, such as umbilical cord blood, amniotic fluid, bone marrow, mobilised peripheral blood, and adipose tissue stem cells, clinical applications are mainly limited to bone marrow and peripheral blood derived MSCs, which can be harvested easily and safely. While the sources, which are complicated to harvest and propose challenges in terms of cell expansion (Burt *et al.,* 2008).

There are some limitations associated with using sheep animal model for orthopaedic studies such as high cost, ethical consideration and quadrupedal gait. However, sheep model are still the best suited animal model for the clinical translation of novel orthopaedic therapies for patients, because sheep are docile compare with other spices, and have similar bone and cartilage structure, biochemical, and mineral composition to humans (Filardo *et al.,* 2018; Martini *et al.,* 2001).

In addition to that, the size and basic anatomy of the sheep skeleton are generally comparable with the human skeleton (Wilke *et al.,* 1997). Hence, orthopaedic implants such as engineered bone or cartilage tissues are commonly tested in sheep models (Filardo *et al.,* 2018; Music *et al.,* 2018). Examples are numerous; testing some biomaterials in orthopaedical research (Potes *et al.,* 2008), segmental bone defect (Pearce *et al.,* 2007),

meniscus repair (Chevrier *et al.,* 2009), shoulder surgery (Turner, 2007), osteoporosis (Turner, 2002), osteopenia (Newman *et al.,* 1995), tendon healing (Weiler *et al.,* 2002).

Ovine MSCs (oMSC), unlike human MSCs (hMSC), are not well studied regarding isolation, expansion, and characterisation. Very few studies investigated the growth characteristics, differentiation, and surface antigen expression of oMSC (Adamzyk *et al.,* 2013).

Same as humans, there are individual variations between different sheep donors. However, despite large donor-dependent variations, standard protocols and media for hMSCs differentiation were first established by Pittenger in 1999 (Pittenger *et al.,* 1999). In contrast, the oMSCs differentiation and characterisation protocols which are still lacking.

4.2 Aims and Objectives

4.2.1 Aims

The aim of this chapter is to understand and control oMSCs behaviour by studying their fate in vitro.

4.2.1 Objectives

The Objectives of this chapter are

- To Isolate, select, expand and store oMSC, selection, expansion and cell storage of oMSCs.
- To select and test media compositions that promote oMSCs differentiation.
- Comparison of the trilineage differentiation potential of thirteen sheep donors' oMSCs.
- Characterisation of oMSCs by expression to specific MSCs epitopes and comparison.

4.3 Materials and Method

The summery of chapter four methodology is shown in Figure 4.1.

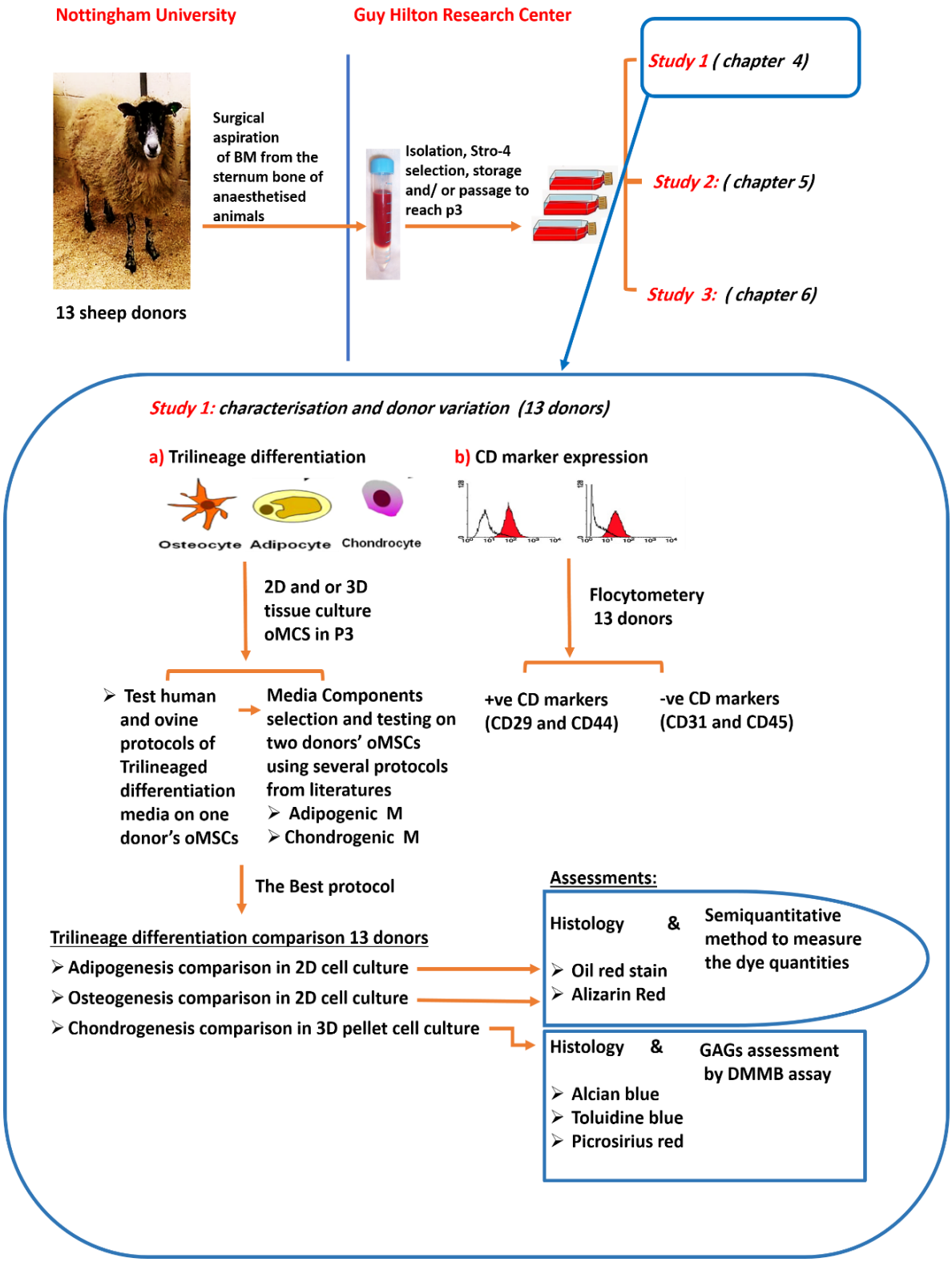

Figure 4. 1: schematic representation of the methodology adopted in chapters 4 - 6. Chapter 4 will be focused on study 1

4.3.1 BM-oMSCs Isolation

BM-oMSCs of thirteen donors were isolated from bone marrow aspirates and Stro-4 selected. The bone marrow aspirates have been surgically collected from the sternum bone of the animal donors (Chapter 2, section 2.2.2.1). These BM-oMSCs were expanded and stored according to general cell culture techniques described in chapter 2, section 2.2.2.2 Cells were used at passages 1-3 (P1-3) for the experiments described in this chapter.

4.3.2 Cell viability of the isolated BM-oMSCs

4.3.2.1 Trypan blue exclusion test of cell viability

The viability of the cells during passaging was determined by trypan blue staining. Hence, cell viability was tested at passage 1, 2 and 3 for donor 13 only. Briefly, after trypisination cells were resuspended in 3 ml basic media. An aliquot of 50 µL of cell suspension was added to an equal amount of trypan blue (dilution factor =2). About 10 µL of this suspension was used for cell counting using a hemocytometer. Trypan blue stains the dead cells dark blue. Whereas living cells will remain unstained as their cell membrane is intact. Both live and dead cells were counted under a light microscope as previously explained in chapter 2, section 2.2.3. This process was repeated four times. The total number of both live and dead cells was calculated by equation 2.4.

Data of live and dead cells was plotted using Excel and statistically analysed using SPSS.

4.3.2.2 Alamar blue assay

To determine metabolic activity of the oMSCs during each passage, alamarBlue® reagent was used. Briefly, BM-oMSCs of donor 13 were seeded at passage 1, 2 and 3 at a concentration of $2X10^4$ cell/well in 24 well plates (n=5). Cells were cultured in basic media overnight to allow attachment. Subsequently, the media was replaced with basic media containing 10 % alamar blue. Cells were incubated for 3 hours at 37ºC, as explain in Chapter 2, section 2.2.2.10. Data are shown as mean ± standard deviation and statistically analysed using SPSS.

4.3.3 Tri-lineage differentiation of BM-oMSCs

oMSCs are characterised by their ability to undergo differentiation into adipocytes, osteocytes and chondrocytes (tri-lineage differentiation capacity). In this case, various differentiation protocols were investigated to encourage oMSCs differentiation. One donor was used in this study to compare a standard protocol shown to be effective to differentiating human MSCs (hMSCs) (Pittenger *et al.,* 1999) and another protocol, which was found to be applicable for oMSCs (kindly offered by Oreffo and his co-workers at the University of Southampton). In order to set this experiment, oMSCs were seeded at P3 at a density of $5X10^3$ cells /well. Cells were cultured using basic media in 24-well plates (n=3) as mentioned in chapter 2, section 2.2.2.7, and incubated for 1-2 days until cells reached 80% confluency. Then, the media was changed to differentiation media. The relevant differentiation media specifying all differentiation components is described in the Table 4.1. Plates were fixed using 10% buffered formalin at day 0, day 7, day 14 and day 21 to perform histological staining.

Table 4. 1: Compositions of differentiation media. *The compositions of differentiation media obtained from protocols for ovine MSCs, and human MSCs adipogenic, osteogenic and chondrogenic differentiation.*

Reagent	**oMSCs protocol**	**hMSCs protocol**
ADIPOGENESIS	**Oreffo et al (not published)**	**(Pittenger *et al.*, 1999)**
Dexamethasone	100 nM	0.5 µM
3-isobutyl-1methylxanthine IBMX	0.5 mM	0.5 mM
Insulin	0	10 µg/ml
Indomethacin	0	100 µM
Rosiglitazone (PPAR-Ɣ agonists)	1 µM	0
FBS	10%	10%
OSTEOGENESIS	**Oreffo et al**	**(Jaiswal *et al.*, 1997)**
Dexamethasone	10 nM	0.1 µM
Ascorbic Acid	0.8 mM	50 µM
β –Glycerophosphate β-GP	10 mM	50 mM
FBS	10%	10%
CHONDROGENESIS	**Oreffo et al**	**(Mckay, 2004)**
Dexamethasone	10 µM	0.1 µM
Ascorbic Acid	50 µM	50 µM
TGF-β3	2 ng/ml	10 ng/ml
ITS	10 µl/ml	10 µl/ml
FBS	0	1% v/v
L-proline	0	40 µg/ml
Sodium Pyruvate	0	10 µl/ml
Media for all recipes:	alpha MEM without L-glutamine	DMEM without L-glutamine high glucose 4.5 mg/ml
L-glutamine for all recipes	1%	1%
P/S for all recipes	1%	1%

4.3.4 Effect of differentiation media composition on adipogenesis and chondrogenesis

When applying either a standard hMSCs protocol or the recommended oMSCs protocol to differentiate oMSCs, the two protocols resulting in osteogenesis. While, limited adipogenesis and chondrogenesis were observed. Therefore, different protocols were tested on oMSCs of two donors to determine the optimal media composition for adipogenesis and chondrogenesis.

4.3.4.1 Testing media composition for adipogenic differentiation

oMSCs from two different donors were seeded at a density of $2X10^4$ cell/ well in 24 well plates (n=3). Here, six different protocols, which previously were tried and tested for sheep and various animal species were tested. The composition of this media is described in Table 4.2.

Table 4. 2: Compositions of different media used to induce adipogenic differentiation in various protocols

Protocol number / Component	(1) Sheep MSCs Oreffo *et al* (not published)	(2) Human MSCs (Pittenger *et al.*, 1999)	(3) Sheep MSCs (Heidari *et al.*, 2013)	(4) Rat MSCs (Crawford *et al.*, 2006)		(5) Mouse MSCs (Markides *et al.*, 2013)	(6) Sheep MSCs (Rentsch *et al.*, 2010)
				Induction	Maintenance		
Dexamethasone	0.1µ M	0.5 µM	0.1 µ M	1 µM	/	1 µM	1 µM
IBMX	0.5 mM	0.5 mM	/	0.5 mM	/	50 µM	0.5 mM
Insulin	/	10 µg/ml	/	10 µg/ml	10 µg/ml	/	1.7 µM
indomethacin	/	100 µM	50 µg/ml	100 µM	/	100 µM	0.2 mM
ITS	/	/	/	/	/	10 µl/ml	/
Ascorbic acid	/	/	50 µg/ml	/	/	/	/
Rosiglitazone	1 µM	/	/	/	/	/	/
Non-essential amino acid (NEAA)	1%	1%	1%	1%	1%	1%	1%
FBS	1%	10%	10%	0	0	10%	10%
Bovine serum albumin BSA	/	/	/	1%	1%	/	/
l-glutamine	1%	1%	1%	1%	1%	1%	1%
P/S	1%	1%	1%	1%	1%	1%	1%
Media	high-glucose DMEM for all recipes						

After cells reached 80% confluence, cells were incubated with 1 ml of the relevant adipogenic differentiation media (n=3) using basic media as control. The plates were observed regularly under a light microscope to identify adipogenic alteration of the oMSCs by accumulation of the lipid droplets in their cytoplasm. Plates were fixed with 10% buffered formalin at day 0, day 7 and day 14 after adding differentiation medium.

4.3.4.2 Testing media composition for chondrogenic differentiation

In this experiment, the monolayer culture was replaced with pellet culture. Therefore, in 1.5 ml centrifuge tubes, cell pellets from two different donors (P3) were created as described in

chapter2, section 2.2.2.8 (n = 6) and incubated at standard culture conditions. Five different protocols were tested. The media compositions of these protocols are given in Table 4.3.

Table 4. 3: Chondrogenic differentiation media compositions. *Compositions of different media used to induce and promote chondrogenic differentiation in various protocols.*

Protocol number / Components	(1) Sheep MSCs Oreffo	(2) Human MSCs (Mckay, 2004)	(3) Sheep MSCs (Heidari *et al.*, 2013)	(4) Rat MSCs (Crawford *et al.*, 2006)	(5) Sheep MSCs (Mrugala *et al.*, 2007)
Dexamethasone	10 µM	0.2 µM	0.1 µM	0.1 µM	/
Ascorbic Acid	50 µM	50 µM	50 µg/ml	50 µg/ml	/
TGF-β3	2 ng/ml	10 ng/ml	/	10 ng/ml	10 ng/ml
TGF-β1	/	/	10 ng/mL	/	/
ITS	10 µl/ml	10 µl/ml	50 µl /mL	10 µl/ml	/
L-Proline	/	40 µg/ml	/	/	/
Sodium Pyruvate	/	10 µl/ml	/	/	/
FBS	/	1%	10%	/	/
BSA	/	/	/	1 mg/ml	/
l-glutamin	1%	1%	1%	1%	1%
P/S	1%	1%	1%	1%	1%
Media	high-glucose DMEM for all recipes				

Cell pellets cultured in proliferation media were used as control. Media was changed every three days over a period of 21 days. After that time the pellets were harvested, fixed and prepared for histological staining (n=3). Chondrogenesis was evaluated histologically by alcian blue for GAG staining. To compare the effect of cell number, pellets were also prepared using $5X10^5$ oMSC/pellet and tested using protocol 3 Table 4.3. At day 21 the pellets were fixed, in this case two histological staining was performed to assess GAG and collagen content of the pellets.

4.3.5 Characterization and comparison of oMSC obtained from thirteen sheep donors

4.3.5.1 Trilineage differentiation

4.3.5.1.1 Adipogenesis of oMSC monolayers

oMSCs of thirteen donors were seeded as monolayers in 24 well plates at a cell density of $2X10^4$ cell/ well (n=3) as mentioned in chapter 2, section 2.2.2.7. Cells were cultured using protocol 4, which resulted in the good adipogenic differentiation among the tested protocols in chapter 2, section 4.3.4. At day 1, day 7 and day 14 cells were fixed with 10% buffered formalin to perform histological analysis. Adipogenesis was assessed semi-quantitatively by de-staining the Oil Red O. Hence, 200 µL of 100% isopropanol were added to each well, incubated for 10 minutes while gently shaking the plates at RT. The absorbance of the eluted dye was measured at 492 nm.

4.3.5.1.2 Osteogenesis of oMSC monolayers

In this experiment, the human protocol for osteogenesis was used (Table 4.1), to compare the responses of the oMSCs of thirteen different donors. Briefly, $2X10^5$ cell/ well were seeded in 6 well plates (n=3). Once cells had reached 90 to 100 % confluence, cells were incubated with 4 ml of osteogenic media (Os M), while the control plate was incubated with basic media (B M). Media were replaced once a week. The monolayer plates were fixed at three time points, day 1, day 14 and day 21. Osteogenesis was evaluated histologically after cells were fixed using 95% methanol for 20 minutes, and then stained with alizarin red stain described in chapter 2, section 2.4.1.2. A semi-quantitative method was used to assess osteogenesis by de-staining the alizarin red using 5 ml of 10% Cetylpyridinum chloride (CPC) for each well. Samples were incubated overnight at RT. The absorbance of the eluted dye was measured at 562 nm.

4.3.5.1.3 Chondrogenesis of oMSC in pellet culture

To compare the chondrogenic potential of the BM-oMSCs 3D oMSC pellets were prepared as explained in chapter 2, section 2.2.2.8. In brief, protocol 3 (Heidari *et al.*, 2013) was

utilized with slight modification. Pellets were prepared using oMSC at to $5X10^5$ cells per pellet (n=6). Pellets were harvested and stored as explained previously (Chapter 2, section 2.2.2.8) at three-time points, day 0, day 14 and day 21 in specific. Chondrogenesis was assessed by GAG quantification and histology.

4.3.5.2 Expression of cell surface markers by flow cytometry

The oMSCs of the thirteen donors were characterised by flow cytometry immunophenotyping (Chapter 2, section 2.3). Therefore, cells at passage 3 were cultured until 80% confluency and then were subjected to flow cytometry to specify CD markers anti CD29, CD44, CD45 and CD31 antibodies as explained in chapter 2, section 2.3. CD29 and CD44 were positive markers and CD45 and CD 31 were negative CD markers. The percentage of cells that were considered positively stained was determined by gating the stained population with a gate that excluded 99% of all isotype control events. Results were plotted in Figure 4.17 and 4.18.

4.4 Statistical analysis

Values for both trypan blue, alamar blue, and also, the results for the trilineage differentiation including adipogenic and osteogenic quantitation, the pellets sGAG content and sGAG/DNA content were plotted as a bar chat. The data was expressed as a mean ± standard division. Data was compared using one-way ANOVA with Tukey's multiple comparisons test to determine statistical significance. Analysis was performed using SPSS statistics program version 24. The value for statistical significance was set to 0.05. P values were denoted as *$p<0.05$, **$p<0.01$, ***$p<0.001$.

4.5 RESULTS

4.5.1 Isolation and expansion of BM-oMSCs

4.5.1.1 Morphology of BM-oMSC

Colonies of fibroblast-like cells were observed attached to the tissue culture plastic at day 3-4 after seeding. Cells exhibited characteristic spindle shape and polygonal morphology (Figure 4.2).

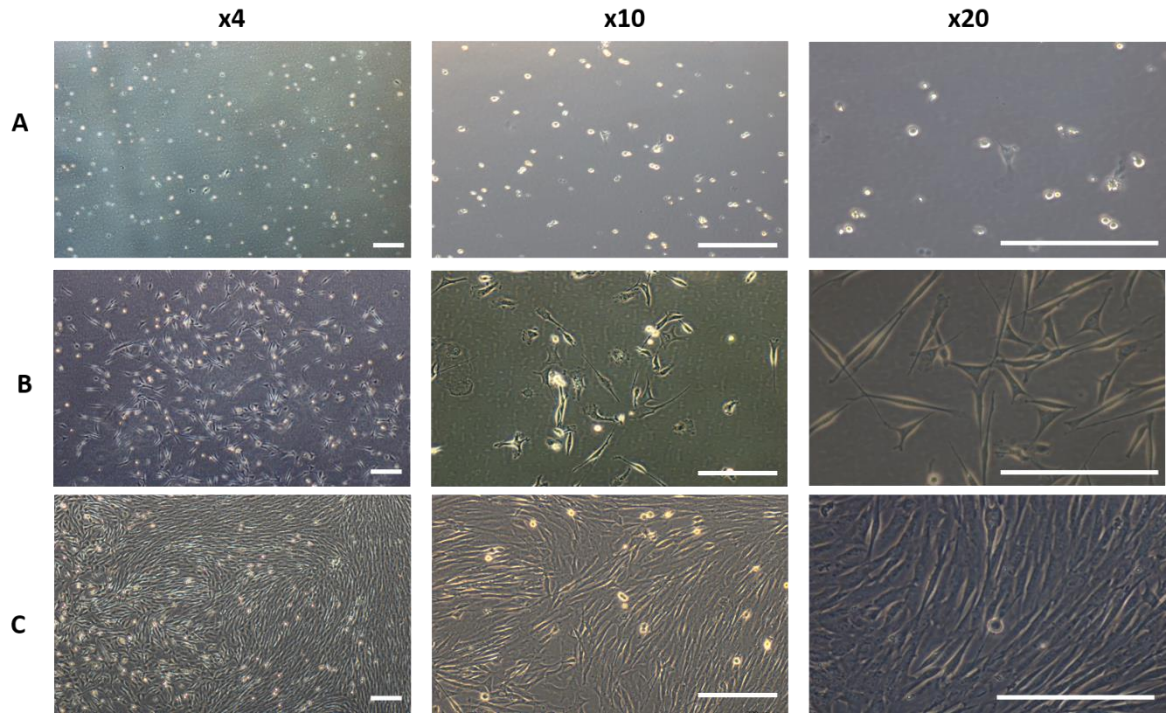

Figure 4. 2: STRO-4 positive isolated B M-oMSC*. Bright field micrographs of STRO-4 positive B M-oMSCs in 2D cell culture at A) 10 % confluence on day 3, B) 50 % confluence on day 7 and C) 90 % confluence on day 9. Cells exhibited characteristic spindle shape and polygonal morphology, scale bar = 300 µm.*

4.5.1.2 Trypan blue exclusion test of cell viability

Quantitation of the cell viability was performed by trypan blue staining of donor 13. The number of live cells increased significantly over three passages ($P \leq 0.001$) from $0.628 \pm 0.098\ 10^6$ cells in passage 1 to about $1.047 \pm 0.135\ 10^6$ cells in passage 2 and $1.295 \pm 0.22\ 10^6$ cells in passage 3. No significant changes in the number of dead cells were observed across the three passages indicating cells vitality and activity during the early passages. The values are expressed as total number of dead and life cells and the percentage of the viability.

The viability (%) was calculated by Equation 2.4 and the results showed no significant differences in the viability percentage between the three passages (Figure 4.3).

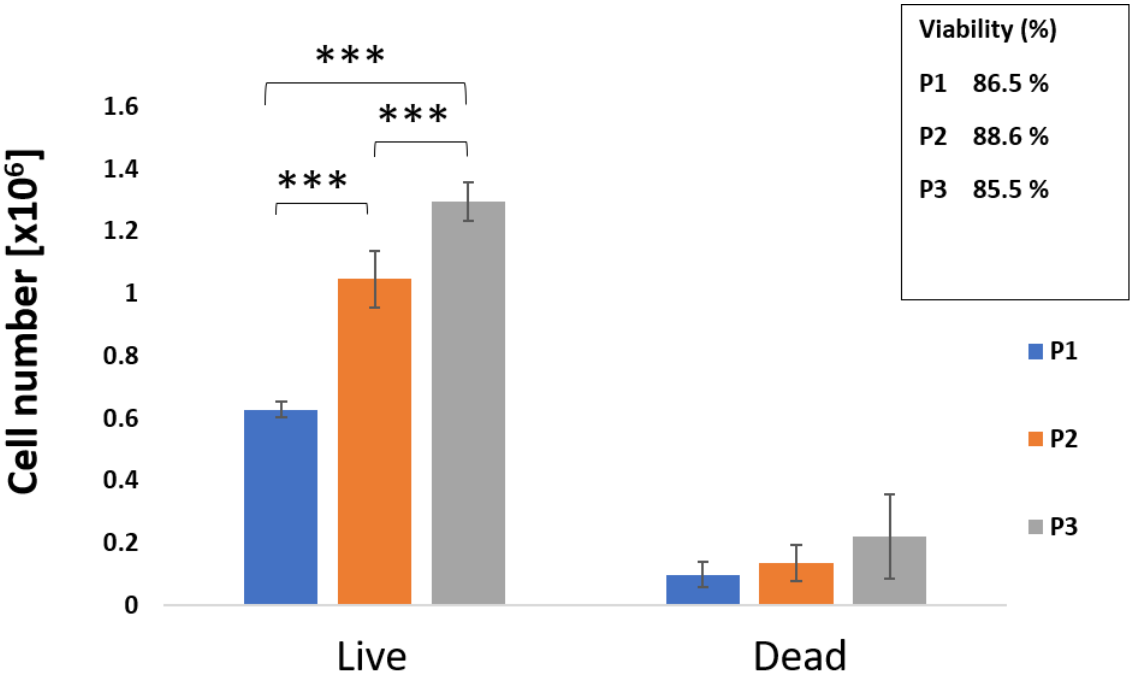

Figure 4. 3: Cell viability using trypan blue. *The numbers of live and dead cells and cell viability (%) of oMSCs was obtained from donor 13 over three passages (P1, P2 and P3) The data are expressed as mean ± standard deviation, n=20, ***p ≤ 0.001.*

4.5.1.3 Metabolic activity assessed by alamar blue

Over three passages, donor 13 oMSCs were assessed for metabolic activity assessed by alamar blue as described in section 4.3.2.2. Significant differences were observed at $P \leq 0.001$ in the metabolic activity of the cells as shown in Figure 4.4. The absorbance of alamarBlue® at 570 nm, using 600 nm as a reference wavelength (normalised to the 600 nm value) revealed increased from 0.32 ± 0.012 (passage 1) to 0.33 ± 0.026 (passage 2) and 0.38 ± 0.003 (passage 3).

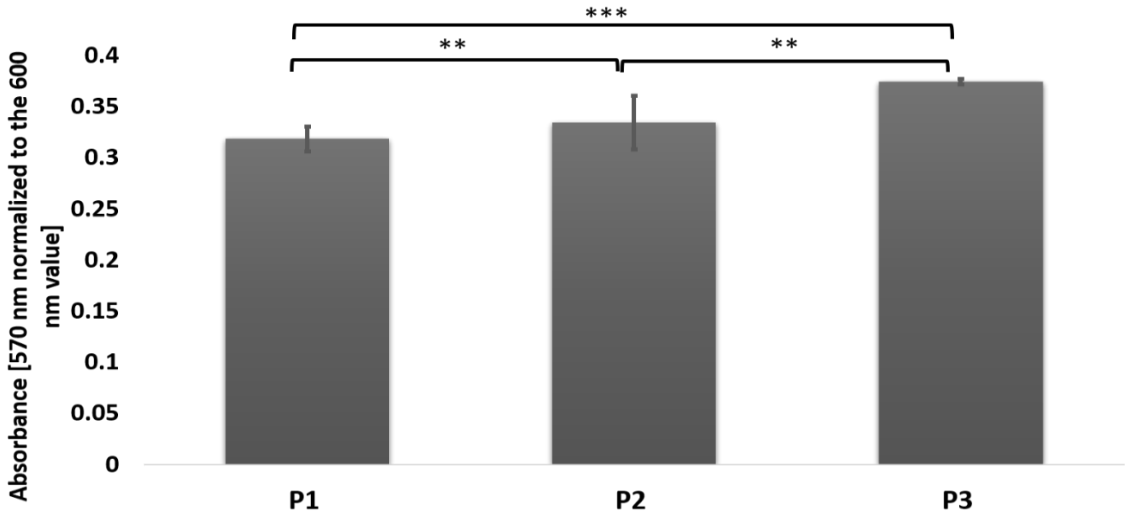

Figure 4. 4: Metabolic activity of BM-oMSC of donor 13. *The absorbance of the alamar blue was read at 570 nm and normalised to a reference wavelength of 600 nm after 3 hours of incubation with BM-oMSCs at passages P1, P2 and P3 (n=8, each). The results were normalised to an acellular blank and data was expressed as mean ± standard deviation, **$p \leq 0.01$ ***$p \leq 0.001$.*

4.5.2 Tri-lineage differentiation capability of isolated BM -oMSCs

Trilineage differentiation was carried out as described in section 4.3.3, on one donor's BM-oMSC to test the differentiation media. Variation in the differentiation capabilities of the cells was observed. Oil Red O staining of the monolayers revealed that the sheep protocol (Table 4.1) promoted adipogenesis initially at day 7, but the differentiation faded after that. Whereas, the human adipogenic differentiation media did not result in a visible cellular response although the monolayer cells seemed to be vacuolated and did not possess the spindle shape of the undifferentiated cells (Figure 4.5 d).

Regarding osteogenic differentiation, both sheep and human protocols drove osteogenesis. However, the human protocol resulted in stronger stain intensity when cells were observed microscopically (Figure 4.5 g-l). Finally, no chondrogenesis was observed for either the sheep and human protocol (Figure 4.5 m-r).

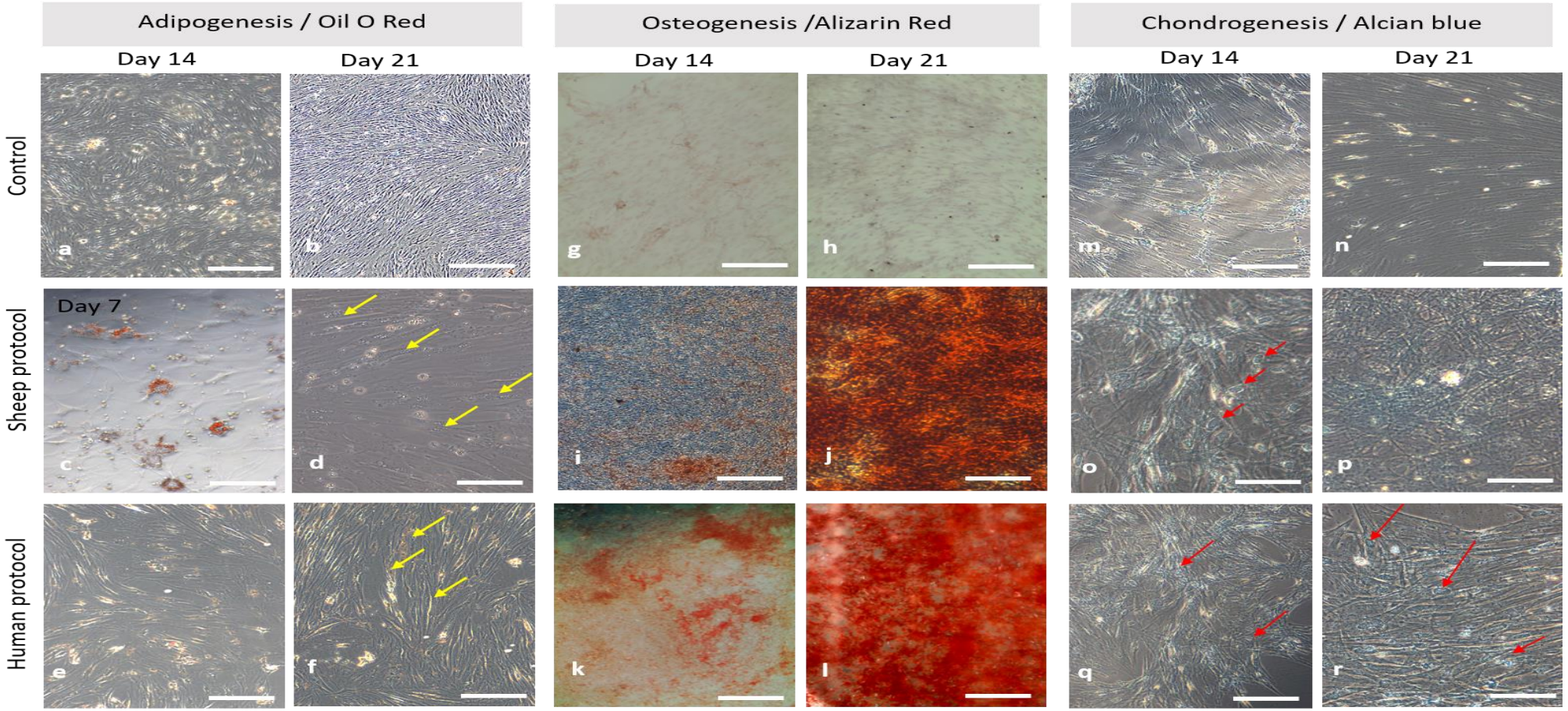

Figure 4. 5: Identifying suitable media compositions for trilineage differentiation of BM-oMSCs. *Bright field micrographs of oMSCs seeded as are shown. Media compositions previously used for human and sheep MSc were to investigate their suitability for trilineage differentiation. Compared with basal media control (a,b), early appearance of adipogenesis on day 7 was observed for the sheep protocol (c), but not on day 21(yellow arrows) (d). There is no clear adipogenesis for the human protocol for both time points, although vacuolated cells (yellow arrows) were observed (e, f). Positive alizarin red stain was observed for osteogenic differentiation in both protocols for each time points (i- l) compared with basal media (g,h) . Stronger stain was detected for the human protocol (k, l). There was no clear chondrogenic differentiation compared with basal media (m,n), despite cells exhibiting chondrocyte features for both time points and protocols (red arrows), (o- r). (Magnification x 10, scale bar = 300 µm).*

4.5.3 Testing media compositions

4.5.3.1 Media composition for adipogenic differentiation

According to the results, all investigated media types drove adipogenesis. However, the degree of differentiation varied. Protocol 3 (Heidari *et al.*, 2013) showed the earliest appearance of adipogenesis at day 4. Comparing the different protocols with each other, the strongest differentiation was observed for protocol 3, followed by protocol 4 (Crawford *et al.*, 2006) and protocol 5 (Crawford *et al.*, 2006; Markides *et al.*, 2013). Whereas, each of the protocols 1, 2, and 6 drove adipogenesis to a lesser degree over the 14 days (Figure 4.6).

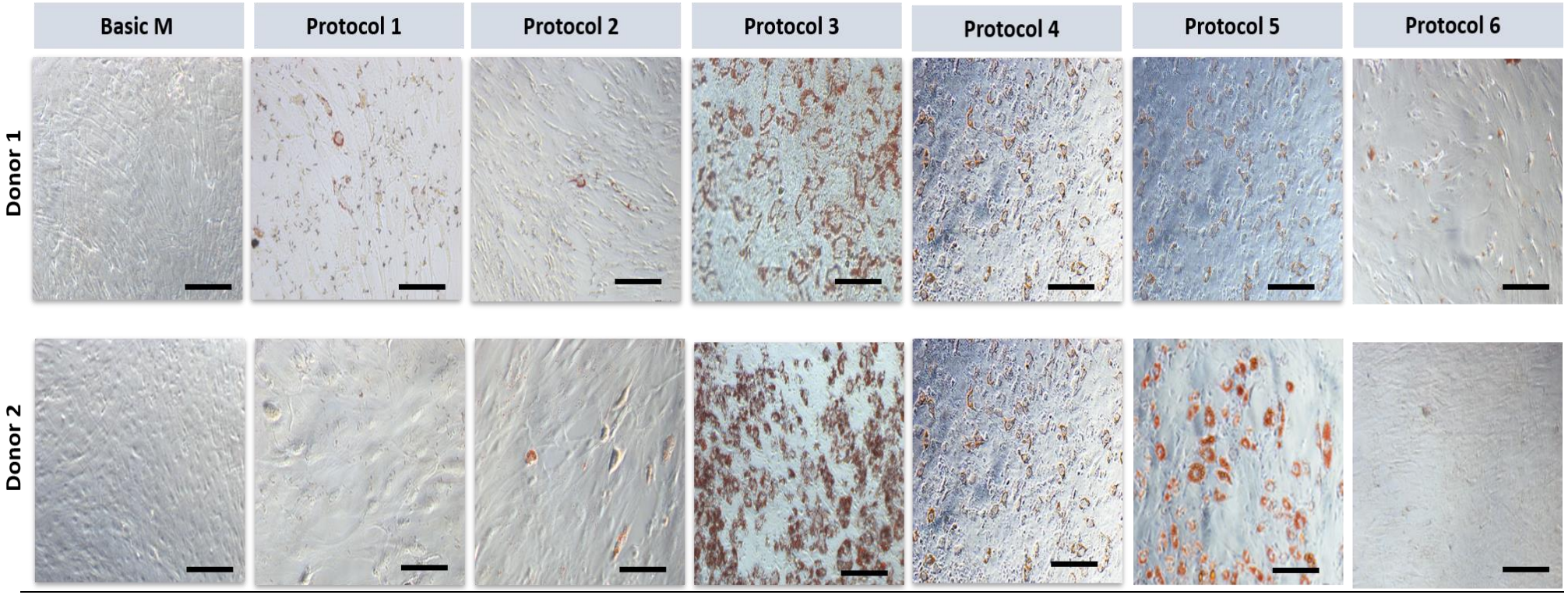

Figure 4. 6 : Adipogenic media selection. *Bright field images of two donors' oMSCs at passage 3 at day 14. oMSCs were seeded in monolayer to compare six different adipogenic differentiation protocols. Oil red O stains revealed that all protocols drove adipogenesis at varying degrees compared the control (oMSC in B M). The best stains were observed for protocol 3 indicating the good differentiation effect on BM-oMSC. Magnification x 10 magnifications, scale bar = 300 µm.*

4.5.3.2 Media composition for chondrogenic differentiation in pellet culture

The results of this experiment confirmed that protocol 3 (Heidari *et al.*, 2013) resulted in the highest level of chondrogenic differentiation, indicated by alcian blue stain, compared to the basic control and other protocols (Figure 4.7 A). Less chondrogenic differentiation was observed for protocol 4 (Crawford *et al.*, 2006) and protocol 2 (Mckay, 2004). Pellets were stained weakly for alcian blue for protocol 5 (Mrugala *et al.*, 2007) confirming low level of chondrogenesis. Regarding protocol 1, pellets could not be obtained during culture which indicated a low integrity of the pellets overall.

The pellets of protocol 3 grew faster and were more robust, especially during histological staining. Hence, the experiment was repeated with one donor using protocol 3 and basic media as control (n=3). Larger number of cells, namely $5x10^5$, were used to form the pellets, which were stained with alcian blue and Sirius red (Figure 4.7 B).

Following these results, protocol 3 was used to carried out the following characterisation experiments discussed in this chapter below.

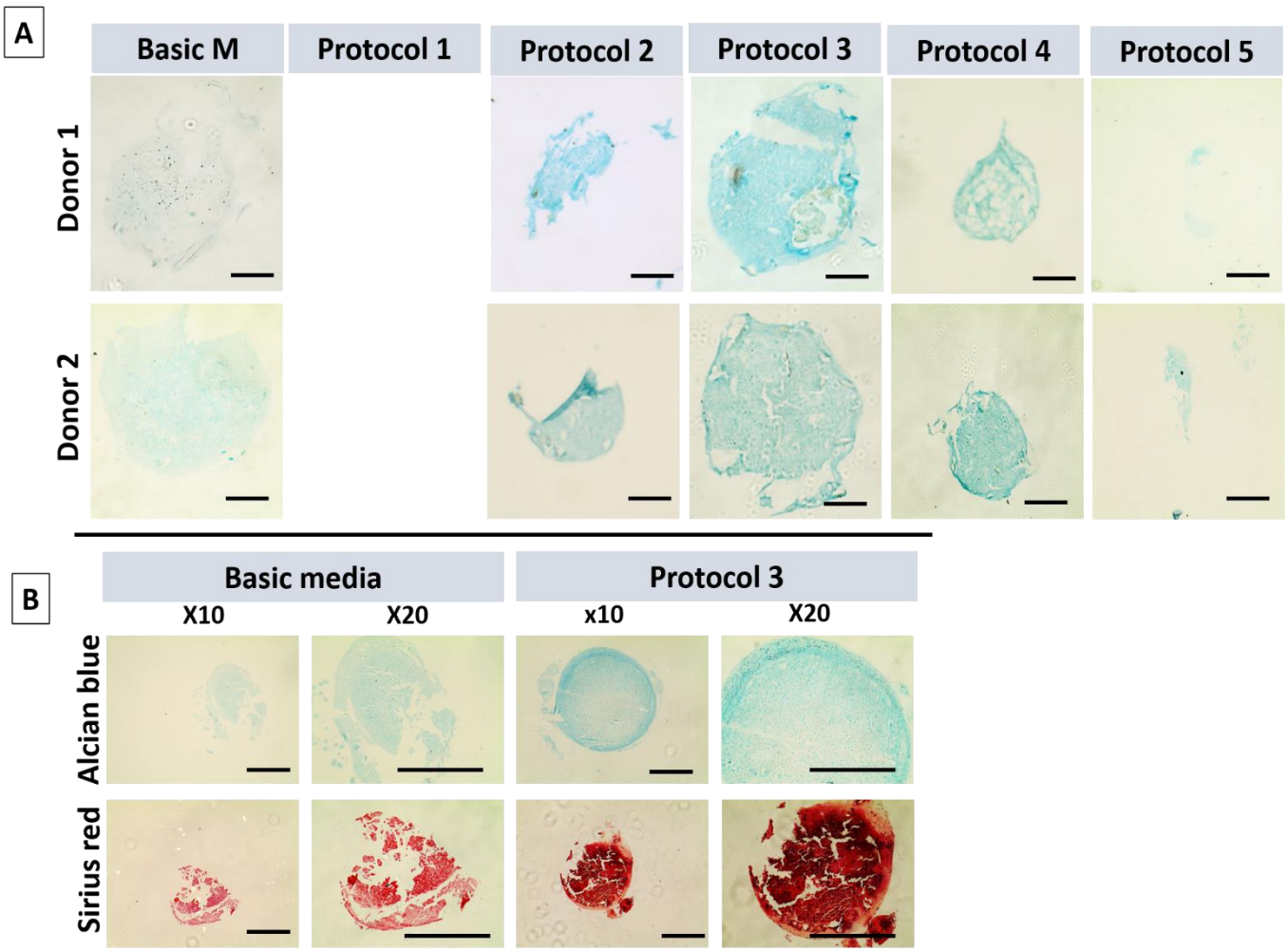

Figure 4. 7: Chondrogenic media selection. *Bright field images of alcian blue-stained 7µm paraffin sections of 3D cell pellets are shown. A) Protocol 3 showed the best chondrogenesis, followed by protocol 4 and 2. Weakest alcian blue stains were observed for protocol 5 as it showed low chondrogenesis. No pellet was obtained from protocol 1. B) Positive alcian blue and Sirius red stain of BM-oMSC pellets prepared with increased cell number confirmed the results obtained from (A). Magnification x10 and x20 magnification, scale bar = 300 µm.*

4.5.4 Characterisation of BM-oMSC of thirteen different sheep donors-a donor variability study

4.5.4.1 Trilineage differentiation potential of BM-oMSC in monolayers

4.5.4.1.1 Adipogenesis differentiation

Oil Red O Stained monolayers oMSCs revealed that the thirteen donors were differentiated towards adipocytes in the different levels at day 10 and day 17 compared to the control groups, which were cultured in B M (Figure 4.8). Microscopic observation revealed different degree of Oil Red O stain indicating variations in adipogenesis. Hense donors were divided into high performing donor (strong Oil Red O stain), medium performing donor (intermediate Oil Red O stain) and low performing donor (weak Oil Red O stain).

This result was confirmed semi-quantitatively by spectrophotometric absorbance at 492 nm of the eluted dye (Figure 4.9). In general, all donors showed significant differences across the duration of the experiment compared to day 1 except donor 6, which revealed a decrease in Oil Red O stain. Significant differences were observed for most absorbance readings when comparing adipogenic medium (Heidari *et al.*) and (B M) at the same time points for each donor. However, when comparing all thirteen donors with each other, noticeable differences were observed among all donors regarding final time points (day17). These results confirmed that each donor was significantly different from some of the other donors, in particular donor 13 which gives the highest degree of the adipogenesis according to absorbance readings of the eluted dye (absorbance of 0.356 ± 0.015). Donor 13 was significant different from all other donors at $P \leq 0.001$. While, the lowest degree of the adipogenesis was observed for donor 6 (absorbance of 0.115 ± 0.022). Figure specific symbols were given to compare the results as the following: (+) is used to compare the significant differences between the treated (Ad M) and control (BM) group of the same time points within the same donor, (*) is used to compare the significance between the three time points for the treated group (Ad M) within each donor, and (1-13) were used to compare the adipogenesis between the thirteen donors at day 17 of the treated group.

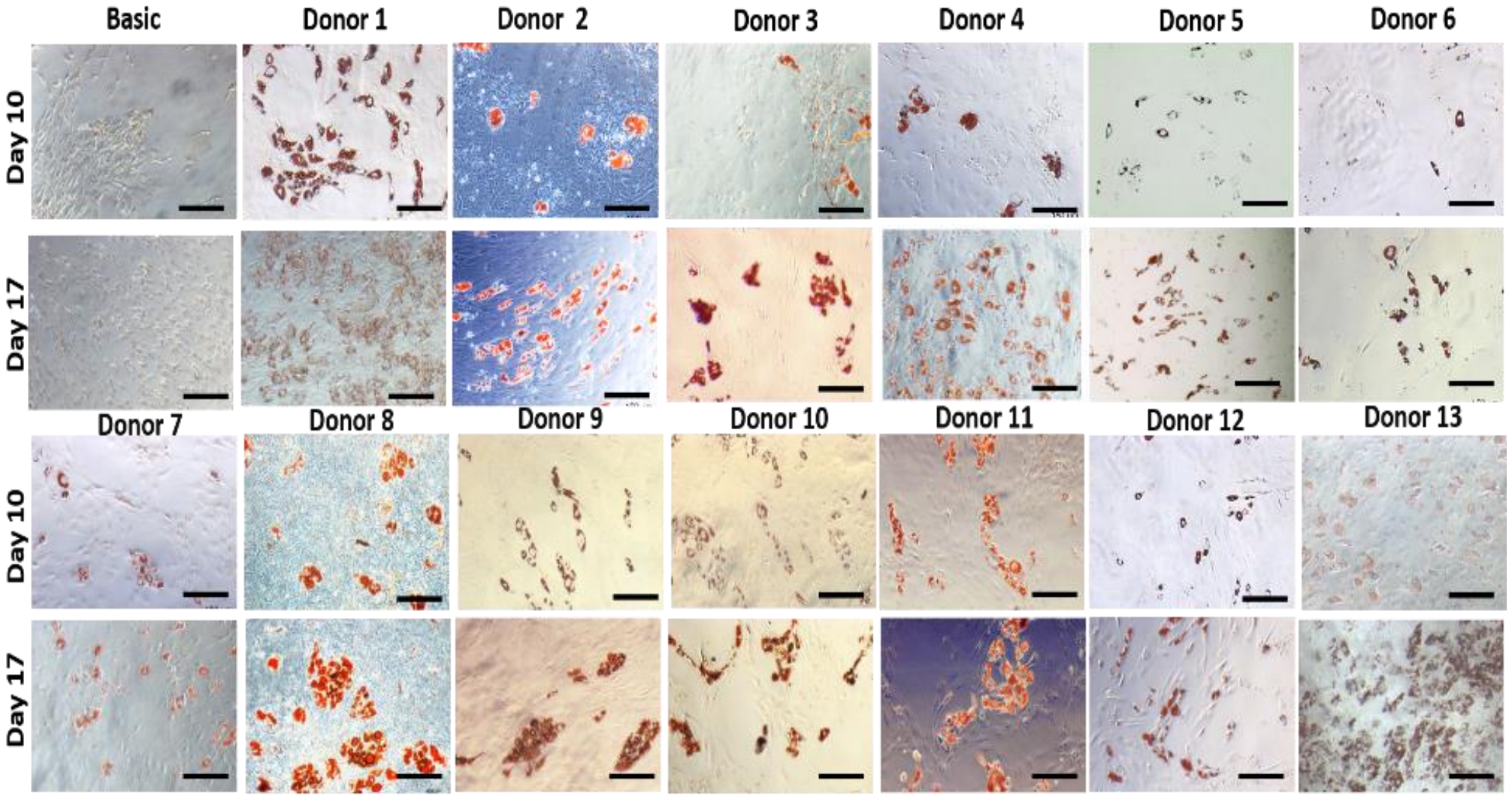

Figure 4. 8: Oil Red O stain of BM-oMSCs in monolayer. *Bright field images oMSCs of thirteen donors at passage 3 were taken on day 10 and day 17. Oil Red O stained monolayers revealed different degrees of adipogenesis ranging from low (donors 5, 6, 9 and 12), moderate (donors 2, 3, 4, 7 and 10) and high (donors 1, 8, 11 and 13) responses to the differentiation media x10 magnification, scale bar = 300 µm.*

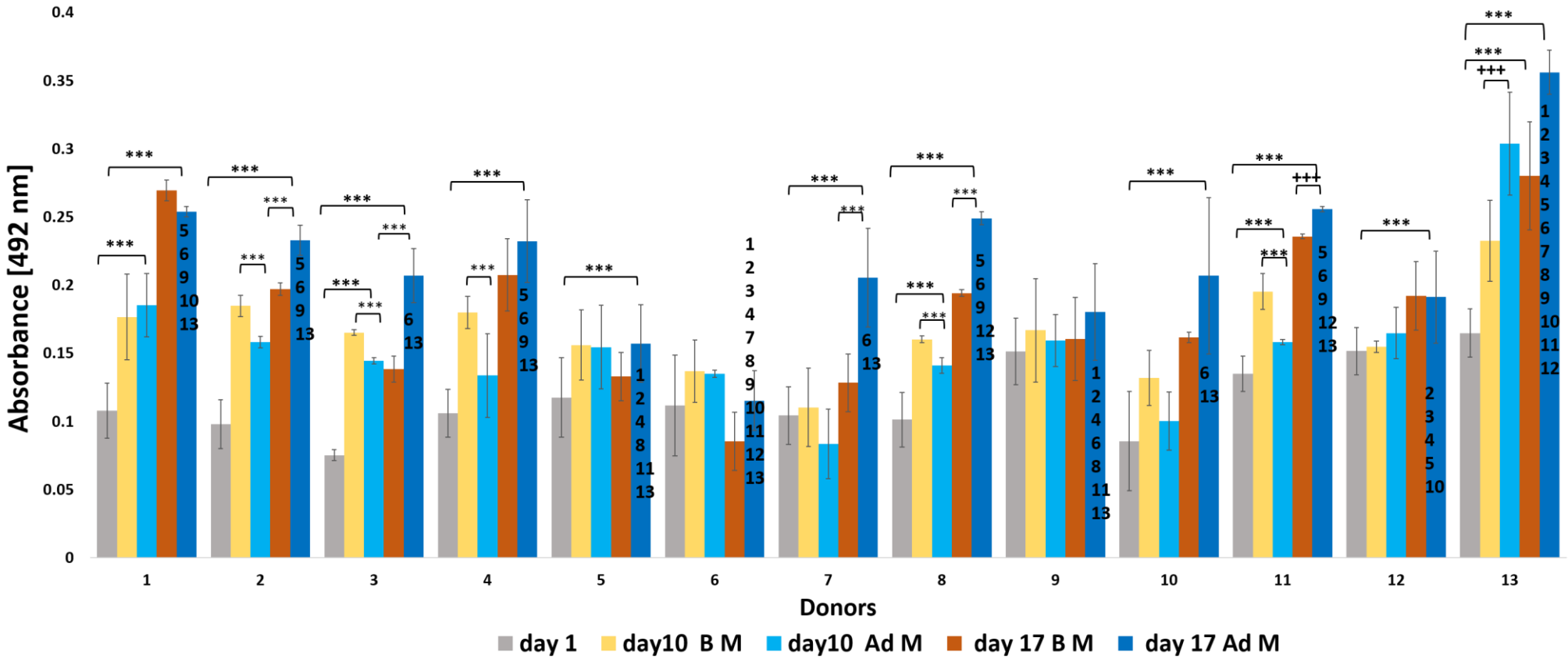

Figure 4. 9: Quantitative measurement of the oMSCs' adipogenic differentiation. *Absorbance at 492 nm of the eluted Oil Red O stained monolayers revealed that the treated group (table 4.2) induced adipogenesis during the experimental time. Donors revealed significant differences at day 10 and day 17 compared to day 1(except donor 6 and donor 9) Significant differences among individual donors were observed, which represent the variances in the ability of each donor to produce adipocytes in response to Ad M across the experimental time. (***) significant differences between the treated and control (B M) for each time point within donor (***) significant difference between the three time points of the treated group for each donor at $p \leq 0.001$, and (1-13) significant differences in the comparison of each donor's adipogenesis performance at day 17 Ad M. Each number represent the donor number in comparison to the other donors at $p \leq 0.001$.*

4.5.4.1.2 Osteogenesis comparison in 2D cell culture

The comparison between the thirteen donors' oMSCs performance to differentiate into osteoblasts was assessed by alizarin red stain of the calcium deposition in the monolayers (Figure 4.10, Figure 4.11). As expected, the histology revealed variances in the performance among the donors regarding the different amounts of calcium that was deposited by the differentiated cells at both time points day 14 and day 21 compared to day 1. The variances ranged from low (donors 3 and 8) to moderate (donors 2,4,6,9, 11, 12 and 13) and high (donors 1, 5, 7, 10 and 12) responses to the differentiation media (Figure 4.10).

This result was confirmed semi-quantitatively by spectrophotometric analysis of the eluted dye at 562 nm absorbance (Figure 4.11). For each donor, significant differences in osteogenesis were observed for day 10 and day 21 compared to day 1 ($P \leq 0.001$). The results showed difference between the treated groups (Os M) compared to the control group (B M) for each time point and each donor. The comparison of the osteogenic performance of all thirteen donors at the day 21 revealed, that donor 8, donor 3 and donor 13 (absorbance 1.192 ± 0.138, 1.508 ± 0.608, and 1.992 ± 0.290 respectively) were low performance donors. While donors 9, 6, 11, 2, 4 and 12 were moderate performers (absorbance 2.232 ± 0.169, 2.238 ± 0.167, 2.294 ± 0.439, 2.316 ± 0.644, 2.465 ± 0.493 and 2.579 ± 0.195 respectively). Lastly, donors 5, 1, 10, and 7 were considered as high osteogenic performers as illustrated by the highest absorbance readings (absorbance 3.067 ± 0.086, 3.099 ± 0.785, 3.160 ± 0.277 and 3.161 ± 0.260 respectively). All absorbance data are shown in Figure 4.11, which showed significant differences between each the treated and the control group of the same time points and between the three time points for the same donor. In addition, significant differences were observed for the overall osteogenesis between the thirteen donors comparing the absorbance readings on day 21 for the treated group. To allow easier comparison and understanding of the graph only non-significant differences are displayed as n.s. significant differences were not displayed. For the comparison of the treated versus the control group at each time point for each donor; and the comparison between of the treated group on day

1, day 14 and day 21 for each donor $P \leq 0.001$ was assumed to be significantly different. (1-13) numbers were used to illustrate the significant differences between each treated (donor's osteogenesis donors' variance at the day 21 Os M).

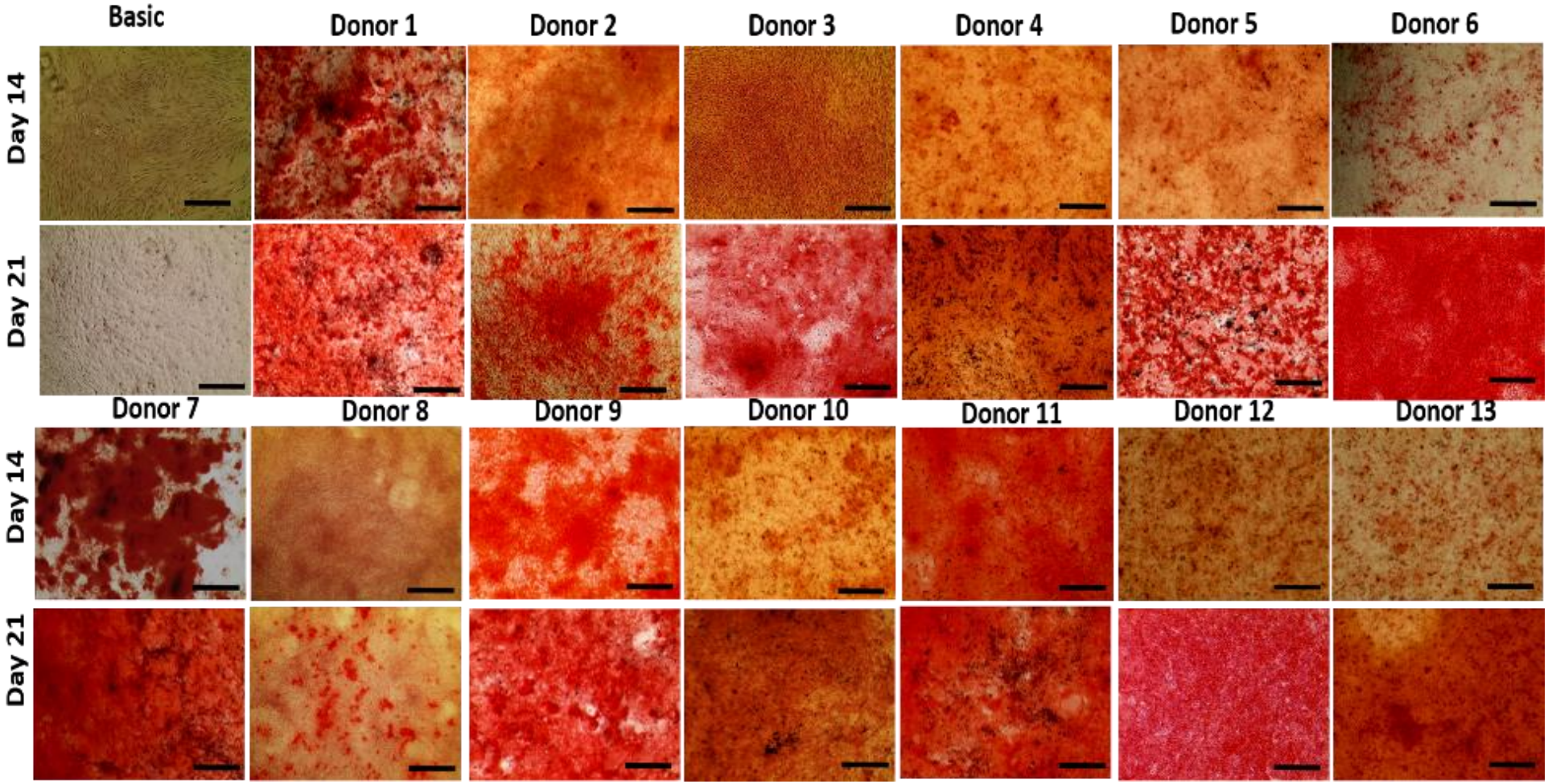

Figure 4. 10: Alizarin Red S stain of BM- oMSCs. *Bright field images of oMSCs of thirteen donors at P3 in monolayers at day 14 and day 21 were taken. alizarin Red S stain revealed different degrees of osteogenesis ranging from low (donors 3 and 8) to moderate (donors 2,4,6,9, 11, 12 and 13) and high (donors 1,5,7 and 10, 12) responses to the differentiation media. Images were taken at x10 magnification, scale bar = 300 µm.*

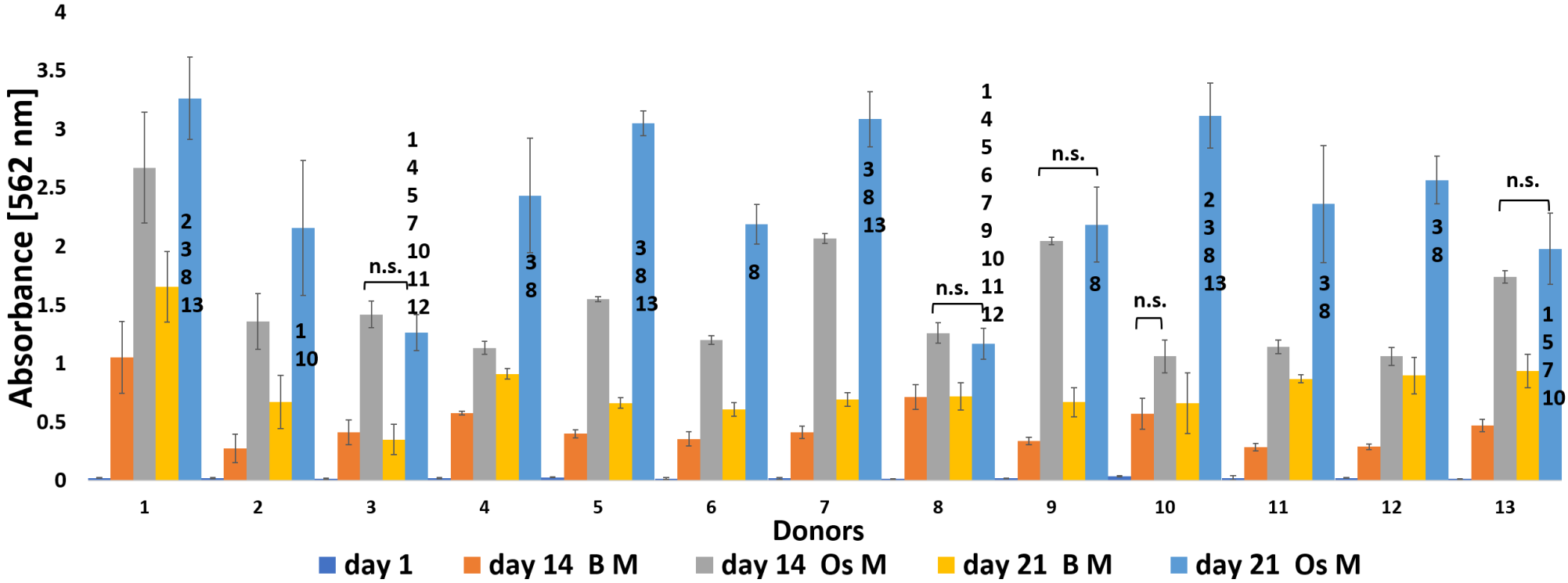

Figure 4. 11: Quantitative measurement of the oMSCs' osteogenic differentiation. *The absorbance of the eluted alizarin Red S dye was measured at 562 nm. Data of the thirteen donors revealed that the treated group (Os M) induced osteogenesis during the experimental time. All donors showed significance differences at day 14 and day 21 compared to day 1Treated groups (Os M) were significantly different from control groups (B M) at the same time point for each donor($p \leq 0.001$). Non-significant differences (n.s.) for all comparisons are shown, which mean all other comparisons were significant at $p \leq 0.001$. Each number represent the donor number in comparison to the other donors at $p \leq 0.001$.*

4.5.4.1.3 Chondrogenesis comparison in 3D pellet culture

The comparison between the thirteen donors' oMSCs performance responding to the chondrogenic media was assessed by histological staining and GAG quantification. Histology revealed chondrogenic differentiation for oMSCs of all thirteen donors treated group (Ch M) compared to the control group (BM) *(*Figure 4.12**).** However, differences can be observed among the donors. The strongest alcian blue and toluidine blue stains were observed for donors 1, 2, 4, and 12. While for the picrosirius red stain the best donors were donors 7 and 13. Using two stains for sGAG alcian and toluidine in this experiment to make a decision which one better to use and can give better histological assessment for sGAG for Chondrogenesis was also assessed quantitatively by assessed the sGAG content in the pellets using DMMB assay. The sGAG content was normalised to the DNA content of the same samples in order to determine the sGAG content in relation to cell number (Figures 4.13-4.15).

Firstly, the DNA was assessed by Quant-iT PicoGreen double stranded DNA assay (Figure 4.16). The results showed a decrease in the DNA amounts of all pellets across the experimental time for both the treated Ch M and the control group B M at day 10 and day 21 compared to day 1. A significant decrease in the DNA content was observed for donor 13 with a drop from 1.149 ± 0.150 µg/ml at day 1 to 0.325 ± 0.025 µg/ml (B M, day 10) or 0.419 ± 0.0824 µg/ml (Ch M, day 10) and 0.1286 ± 0.0164 µg/ml (B M, day 21) or 0.269 ± 0.031 µg/ml (Ch M, day 21) ($P \leq 0.001$). In contrast, donors 6 and 12 which show decreases (but not significant) in the DNA amounts across the three time points. Regarding donor 6 which dropped from 1.634 ± 0.117 µg/ml at day 1 to 0.6144± 0.455 µg/ml for B M or 1.549 ± 0.106 µg/ml for Ch M of day 10; and 0.509 ± 0.0522 µg/ml for B M or 1.281 ± 0.0726 µg/ml for Ch M of day 21. Whereas, donor 12 dropped from 1.645 ± 0.0474 µg/ml at day 1 to 1.099 ± 0.033 µg/ml for B M or 1.108 ± 0.0522 µg/ml for Ch M of day 10; and 0.632 ± 0.023 µg/ml for B M or 1.349± 0.0428 µg/ml for Ch M of day 21.

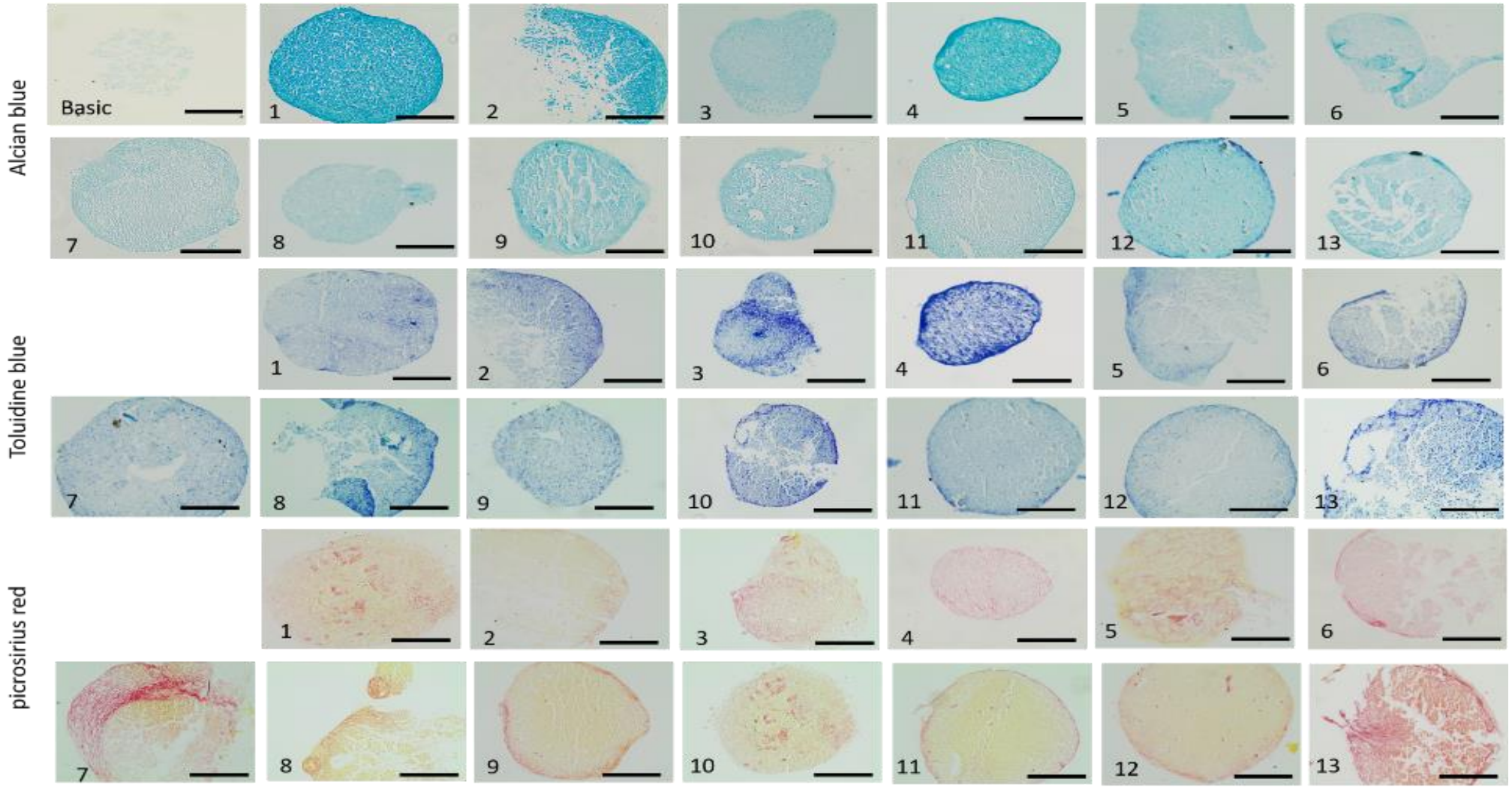

Figure 4. 12: Histological stains of BM-oMSCs pellets. *Histological stains of B M-oMSC pellets for the comparison of chondrogenesis between donors. Three different histological stains were performed on 7µm thick sections of paraffin embedded 3D cell pellets (5x105 cells pelleted in Ch M or B M on day 21). The stains showed variances in the production of GAG (alcian blue and toluidine blue) and collagen (picrosirius red) reflecting the degree of the donors' performance in response to the chondrogenic media. Donors 1, 2, 4 and 12 were considered as high performers in terms of GAG production, while the remaining donors which showed a lower degree of chondrogenesis. Regarding to collagen production donors 7 and 13 performed best. Images were taken at 20 x magnification, scale bar = 200 µm.*

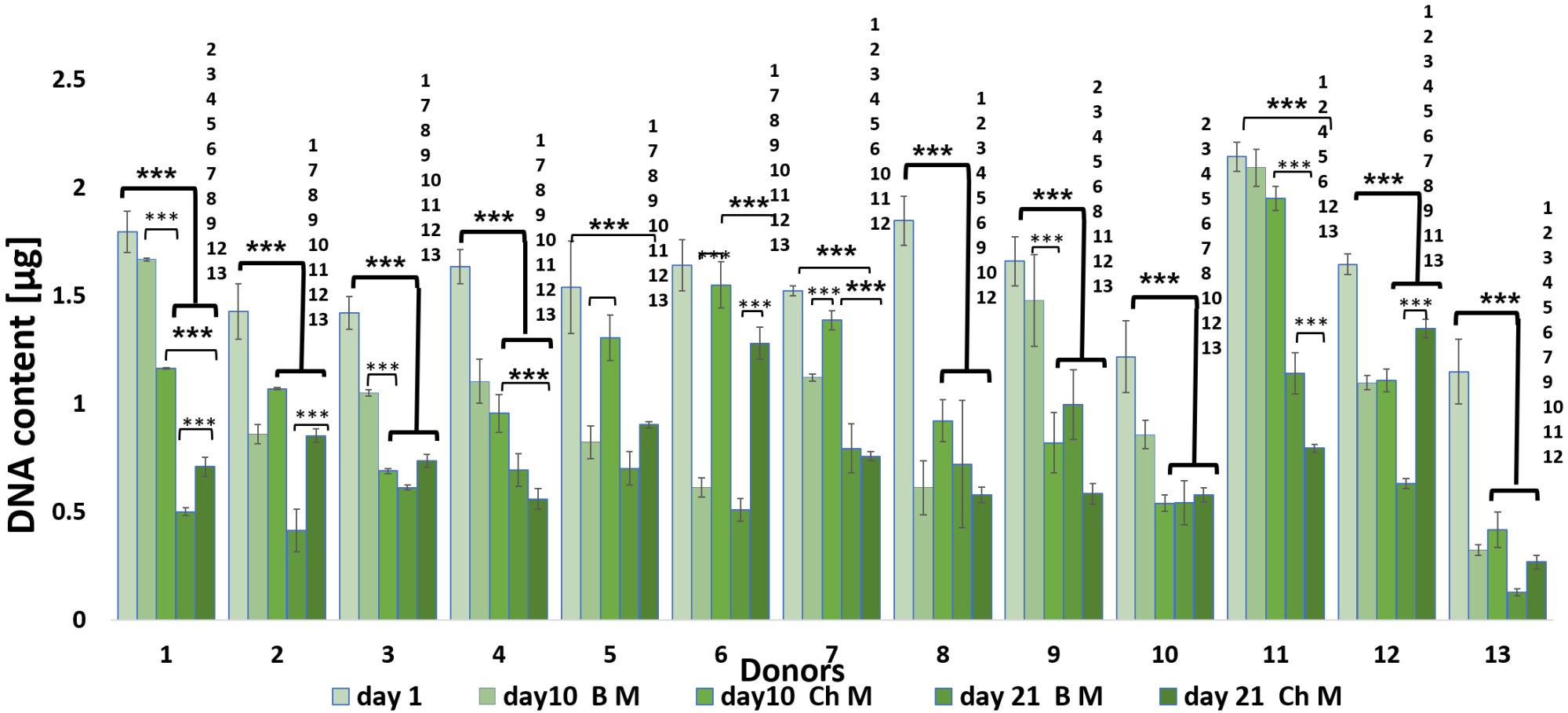

Figure 4. 13: DNA content of oMSC pellets. *Total DNA content was determined using the PicoGreen assay for all cell pellets following digestion with proteinase K. Generally, the results showed a decrease in the DNA amount of the pellets for both treated (Ch M) and control (B M) over 21 days compared to their day 1. The decreases varied from non-significant (donors 5, 6 and 11) or significant in all other donors. (***) significant differences between the treated (Ch M) and control (B M) for each time point for donors, (***) significant difference between the three time points of the treated group for each donor at $p \leq 0.001$. (1-13) significant differences in the comparison of each donor's pellets (DNA content was compared at the day 21 Ch M of each donor with the other donors at the same time point). Each number represent the donor number in comparison to the other donors at $p \leq 0.001$. Data are expressed as mean ± standard deviation, n=3 at $p \leq 0.001$.*

The DMMB assay (Figure 4.14) showed increases in the amounts of sulphated sGAG that were produced by the cell pellets across the time points for all donors. Results are shown in Table 4.4 as mean ± standard deviation. Variances in the degrees of sGAG production across all donors were observed. The amount of the sGAG that was produced gradually increased for donors 1, 2, 3, 5, 10 and 12 from day 1 to day 21. Meanwhile, donors 7, 9, 11, and 13 showed increases in sGAG production at day 10, but the sGAG content dropped until day 21. Whilst, donor 8 did not show any changes in the sGAG production across the time point compared with day 1.

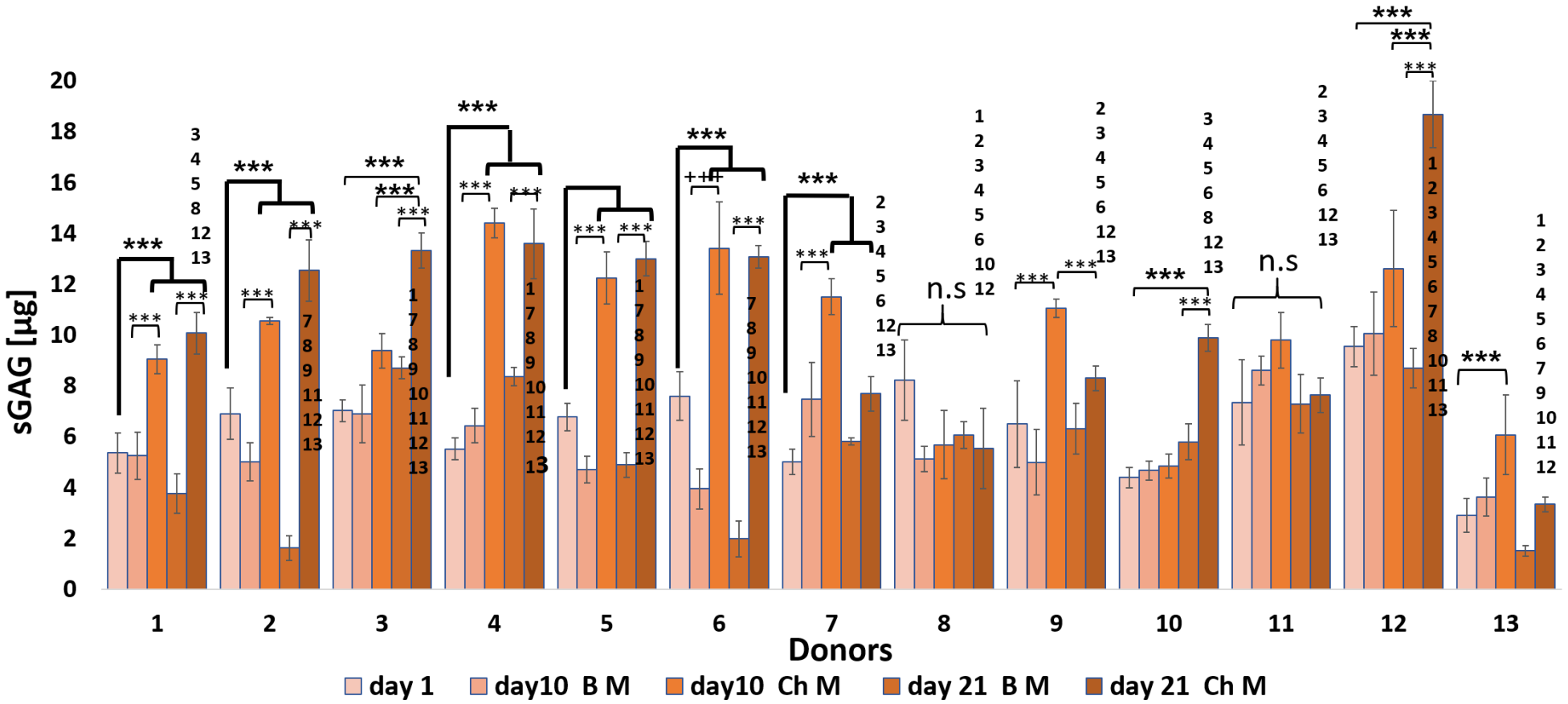

Figure 4. 14: GAG contents of oMSCs pellets. *Total GAG contents were determined using the DMMB assay for all cell pellets following digestion with proteinase K. The results showed significantly increase in the GAG contents at day 10 and day 21 compared with their day 1 of the treated group (Ch M) in most donor. Donors 8, 11, and 13 revealed no significant differences between day 10 and 21 compared with day 1. While the control group did not show increases in the GAG amounts over 21 days. (***) = significant differences between the treated (Ch M) and control (B M) for each time point and donor, (***) = significant difference between the three time points of the treated group for each donor at p ≤ 0.001. (1-13) = significant differences in the comparison of each donor on day 21 Ch M with the other donors at the same time point. Each number represent the donor number in comparison to the other donors. Data are expressed as mean ± standard deviation, n=3 at p ≤ 0.001.*

Table 4. 4: sGAG production before normalization. *The table shows the mean ± standard deviation for all donors cultured in basic medium (B M) and chondrogenic medium (Ch M) on all time points.*

sGAG production [µg]	Day 1	Day 10 B M	Day 10 Ch M	Day 21 B M	Day 21 Ch M	The variance with the time
Donor 1	5.364 ± 0.798	5.250 ± 0.928	9.057 ± 0.568	3.773 ± 0.776	10.080 ± 0.817	↑
Donor 2	6.908 ± 1.015	5.016 ± 0.751	10.556 ± 0.152	1.619 ± 0.491	12.540 ± 1.202	↑
Donor 3	7.023 ± 0.435	6.886 ±1.136	9.386 ± 0.682	8.705 ± 0.435	13.318 ± 0.690	↑
Donor 4	5.522 ± 0.435	6.432 ± 0.682	14.406 ± 0.584	8.363 ± 0.371	13.591 ± 1.364	↓
Donor 5	6.828 ± 0.570	4.437 ± 0.387	12.531 ± 1.180	5.078 ± 0.500	13.391 ± .368	●
Donor 6	7.592 ± 0.955	3.945 ± 0.796	13.41 ±1.822	1.986 ± 0.708	13.075 ± 0.433	↑
Donor 7	5.011 ± 0.507	7.466 ± 1.466	11.500 ± 11.50	5.819 ± 0.131	7.693 ± 0.6786	↓
Donor 8	8.221 ± 1.573	5.110 ± 0.499	5.684 ± 1.350	6.058 ± 0.526	5.537 ± 1.581	↓
Donor 9	6.500 ± 1.706	4.989 ± 1.287	11.064 ± 0.359	6.318 ± 0.980	8.307 ± 0.486	↓
Donor 10	4.328 ± 0.442	4.641 ± 0.424	5.000 ± 0.344	5.937 ± 0.727	9.781 ± 0.536	↑
Donor 11	7.352 ± 1.674	8.602 ± 0.568	9.795 ± 1.098	7.295 ± 1.159	7.636 ± 0.681	↓
Donor 12	9.545 ± 0.799	10.068 ± 1.634	12.613 ± 2.286	8.705 ± 0.776	18.682 ± 1.316	↑
Donor 13	2.900 ± 0.667	3.622 ± 0.756	6.0667 ± 1.565	1.511 ± 0.213	3.344 ± 0.287	↓

↑ gradually increase ↓ incrase by day 10 but decrease by day 21 ● no noticeable changes

To investigate the sGAG in relation to cell number, sGAG contents were normalised to DNA (Figure 4.15). The data was explained in Table 4.5 and same trends were observed as previously described for (Table 4.4). The highest sGAG/DNA was obtained for donor 4, whereas donor 12 showed the lower performance. The remaining donors have maintained their sGAG levels after normalisation. The ability of the donors' oMSCs to produce sGAG was varied across the donors. In general, the amount of sGAG per cell increased progressively until day 21 for all donors. Some donors seemed to produce more sGAG. However, this data was due to a higher number of cells, instead of stronger chondrogenic differentiation. This was observed for donors 6 and 12, which exhibited the highest amounts of sGAG before normalization. Post-normalisation for some donors that were cultured in Ch M were no longer significantly different to B M pellet cultures such as donor 8, donor 12 and donor 13. Normalised sGAG/DNA contents are shown in Table 4.5 as mean ± standard deviations.

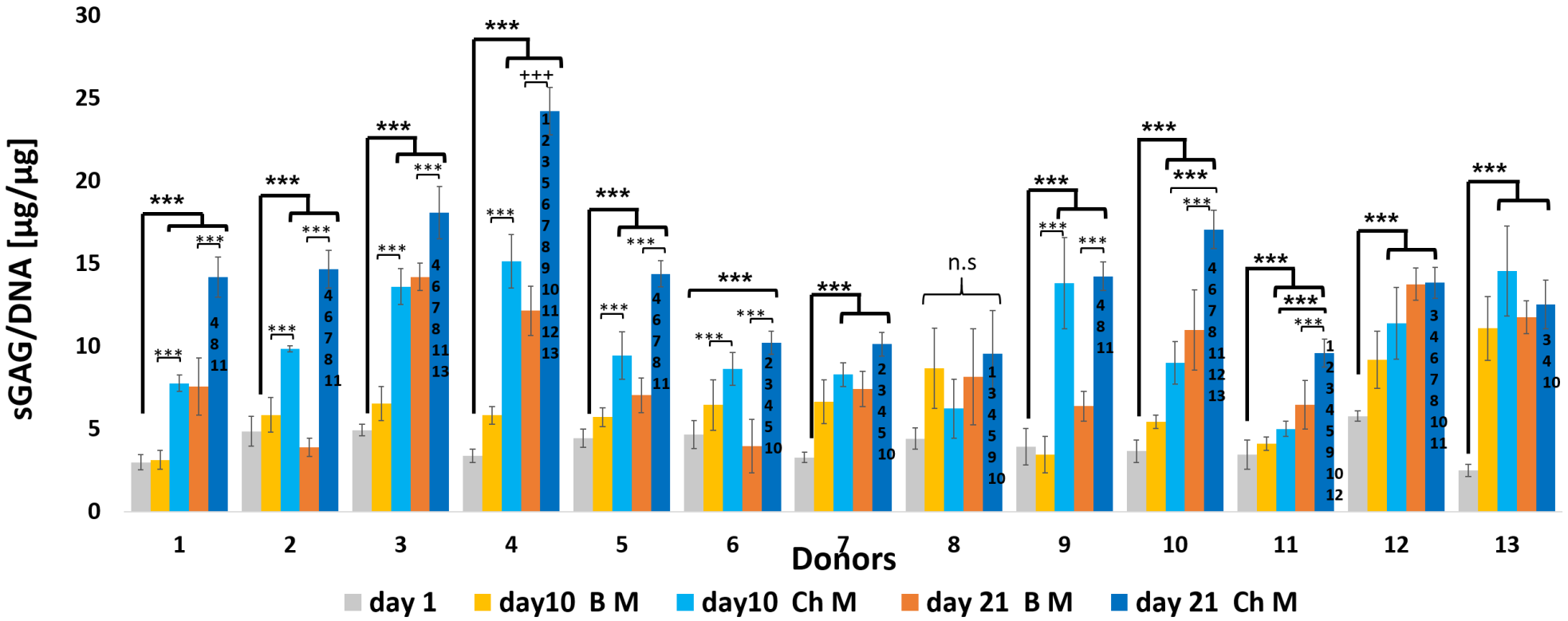

Figure 4. 15: sGAG normalised to DNA content. *Cell pellets GAG content was normalised to DNA. Significant increases were observed at day 10 and day 21 compared to day 1 of the treated group (Ch M) in most donors. Donor 8 revealed no significant differences between day 10 and 21 compared with day 1. (***) = significant differences between the treated (Ch M) and control (B M) for each time point and donor, (***) = significant difference between the three time points of the treated group for each donor at $p \leq 0.001$. (1-13) = significant differences in the comparison of each donor at day 21 for Ch M with all other donors at the same time point. Each number represent the donor number in comparison to the other donors. Data as standard deviation, n= 3 at $p \leq 0.001$.*

Table 4. 5: sGAG contents normalized to DNA contents. *Table shows mean ± standard deviation post-normalisation.*

sGAG/DNA normalization [µg/ µg]	Day 1	Day 10 B M	Day 10 Ch M	Day 21 B M	Day 21 Ch M	The variance with the time
Donor 1	2.993 ± 0.454	3.148 ± 0.559	7.769 ± 0.492	7.565 ± 1.724	14.204 ± 1.210	↑
Donor 2	4.870 ± 0.894	5.855 ± 1.049	9.856 ± 0.171	3.893 ± 0.559	14.678 ± 1.142	↑
Donor 3	4.949 ± 0.346	6.546 ± 1.028	13.616 ± 1.091	14.197 ± 0.826	18.093 ± 1.585	↑
Donor 4	3.393 ± 0.411	5.834 ± 0.537	15.165 ± 1.621	12.168 ± 1.486	24.239 ± 1.437	↑
Donor 5	4.458 ± 0.558	5.727 ± 0.571	9.465 ± 1.436	7.047 ± 1.031	14.390 ± 0.780	↑
Donor 6	4.662 ± 0.850	6.469 ± 1.527	8.658 ± 0.990	3.971 ± 1.609	10.231 ± 0.696	↑
Donor 7	3.287 ± 0.318	6.653 ± 1.324	8.304 ± 0.710	7.444 ± 1.069	10.136 ± 0.732	↑
Donor 8	4.427 ± 0.651	8.680 ± 2.425	6.240 ± 1.785	9.824 ± 4.703	9.551 ± 2.627	●
Donor 9	3.942 ± 1.097	3.448 ± 1.103	13.829 ± 2.743	6.384 ± 0.905	14.244 ± 0.854	↑
Donor 10	3.67 ± 0.687	5.448 ± 0.391	9.003 ± 1.284	10.992 ± 2.436	17.079 ± 1.173	↑
Donor 11	3.449 ± 0.888	4.121 ± 0.406	5.0146 ± 0.451	6.475 ± 1.488	9.606 ± 0.848	↑
Donor 12	5.793 ± 0.323	9.196 ± 1.711	11.408 ± 2.169	13.770 ± 0.972	13.853 ± 0.948	↑
Donor 13	2.511 ± 0.365	11.09 ± 1.936	14.570 ± 2.720	11.755 ± 0.996	12.527 ± 1.469	↓

↑= gradually increase ↓= incrase by day 10 but decrease by day 21 ● = no noticible changes

The summary for the donor variation of the chondrogenesis in the pellet 3D culture, the values of the normalised sGAG to DNA content of the day 21 treated group (Ch M) only was plotted for the all thirteen donors. The graph displayed the variance among the donors in chondrogenesis. The variances between each donor and the others were significant at different levels $P \leq 0.001$, $P \leq 0.01$ $P \leq 0.05$ (Figure 4.16).

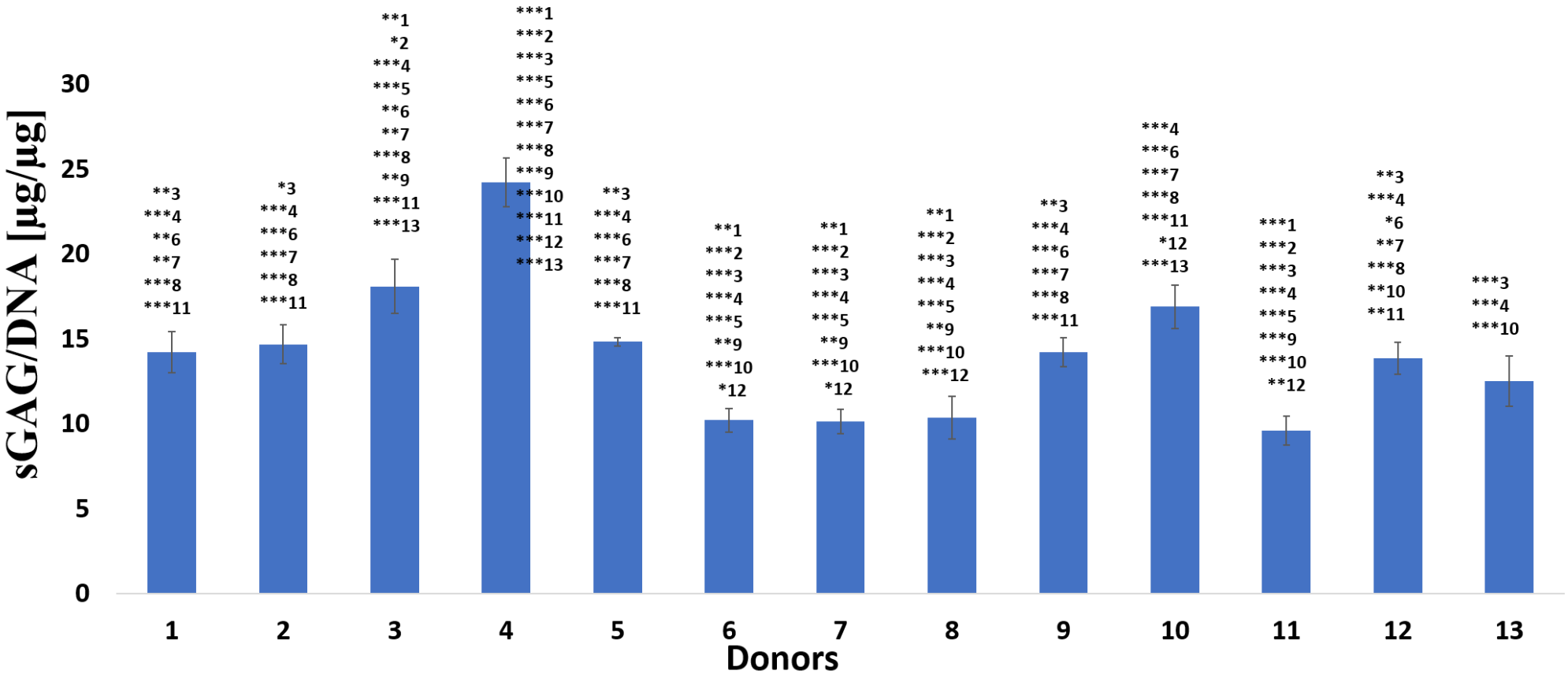

Figure 4. 16: Variation for normalised sGAG content to assess donor variation. *sGAG normalised to DNA content for the day 21 treated group (Ch M) only for the all thirteen donors. The graph displayed the variance among the donors in chondrogenesis. Each number represent the donor number in comparison to the other donors. Data are expressed as mean ± standard deviation, n= 3 at $p \leq 0.001$.*

4.5.4.2 Surface epitope expression

Flow cytometry of oMSCs against a panel of four markers was used to identify oMSCs (Figure 4.17). The results showed most donors were positive for both CD 29 and CD 44, however, differences were observed in the level of expression. CD 29 for example, was more strongly expressed in some donors such as donor 2 (99.93%), donor 4 (96.14%), donor 6 (91.54%) and donor 10 (93.57%). While other donors demonstrated lower expression with less than 50% such as donor 3 (32.28%), donor 8 (35.86%), donor 9 (41.78%) and donor 11 (22.11%). Whereas the remaining donors showed mediocre positive expression such as donor 1 (65.29%), donor 5 (77.45%), donor 7 (72.04%), donor 12 (51.24%) and donor 13 (68.64%). Regarding CD 44, higher positive expressions were observed compared to CD 29. Most donors were strongly positive for CD 44 such as donor 2 (99.73%), donor 4 (90.73%), donor 5 (96.89%), donor 6 (99.60%), donor 7 (96.721), donor 10 (94.43%) and donor 13 (97.70%). While remaining donors showed a mediocre positive expression like donor 3 (89.48%), donor 9 (89.44%), donor 11 (79.21%), or low positive expression like donor 1 (56.61%), donor 12 (53.89%) and donor 8 (48.96%).

In addition, all donors were negative for both CD 45 and CD 31 (Figure 18), which is expected and is used to identify MSCs. For CD 45, most donors showed an expression between 0.32% - 4.63% (less than 10%), except donor 5 (17.76%) and donor 7 (13.41%). While for CD 31, donors expressed the CD marker at levels below 10%, except donor 11 (18.33%). results were shown in Table 4.6, using the recommended scale (Boxall and Jones, 2012) which gave symbols indicating the marker expression level as following −: no expression; +−: <5% expression; +: 5 −50% expression, ++: 50−100% expression.

Table 4. 6 : Number of donors out of 13 have expressed at each level

CD	(-) no expression	(+ -) <5% expression	(+) 5 −50% expression	(++) 50−100% expression
CD 29	/	/	4	9
CD44	/	/	1	12
CD 45	11	2	/	/
CD31	3	7	3	/

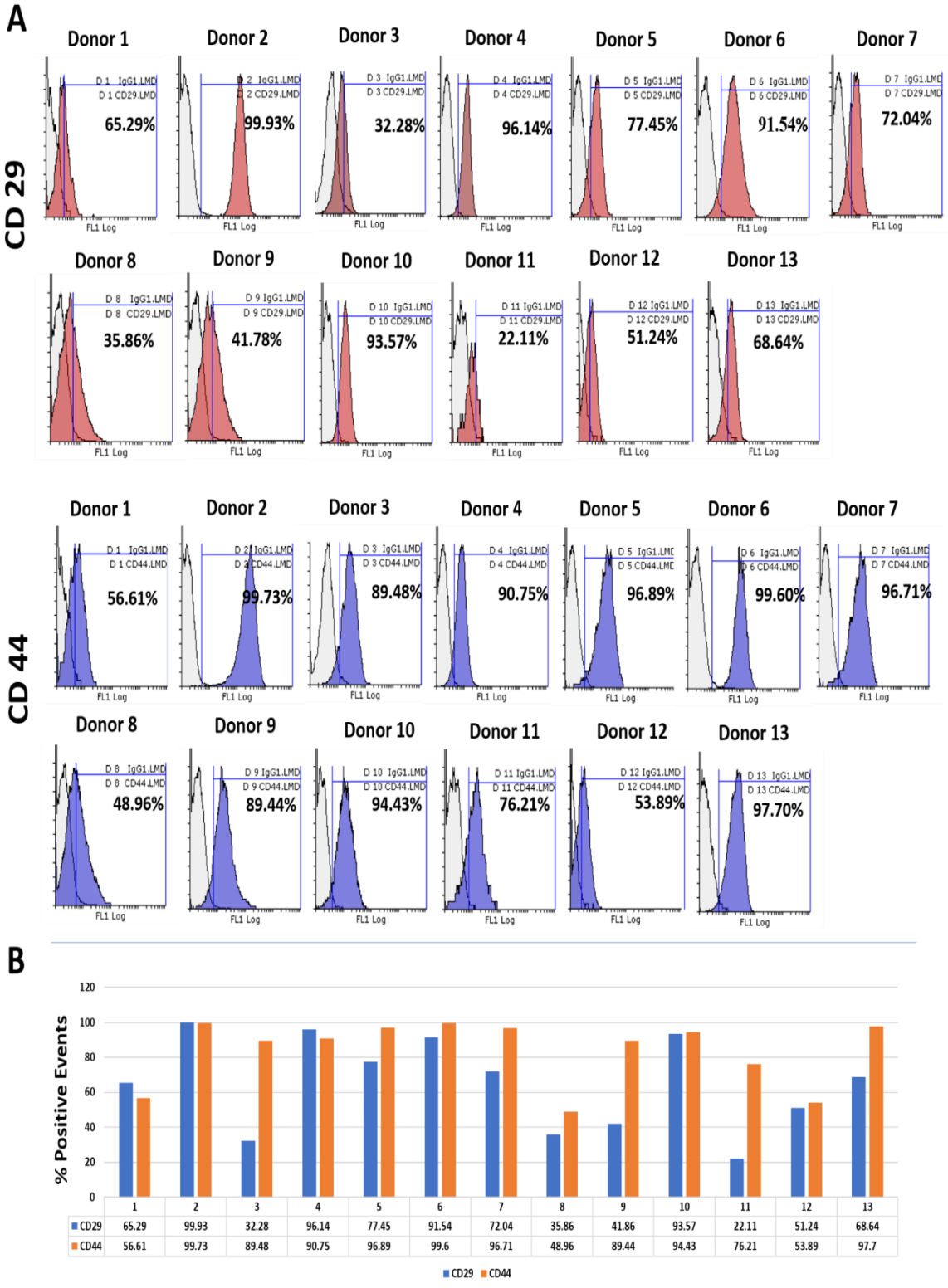

Figure 4. 17 Immunophenotyping of oMSCs for CD 29 and CD 44. *Immunophenotyping of oMSCs. Immunophenotyping of oMSCs for CD 29 and CD 44. oMSCs of all donors were cultured to P3 and 80% confluency in B M. Their expression of CD 29 and CD 44 was assessed to identify their MSCs characteristics. (A) Overlay histograms of each antibody marker, (B) percentage positive cells compared to staining with the IgG1 isotype control. Donors were positive for CD 29 and CD 44. Variations in the expression levels for both CD markers were obtained and ranged between 22.11% - 99.93% for CD 29 and between 48.96 -99.73% for CD 44. The unfilled region is isotype control IgG1, red and blue regions are CD 29 and CD 44 antibody markers, respectively.*

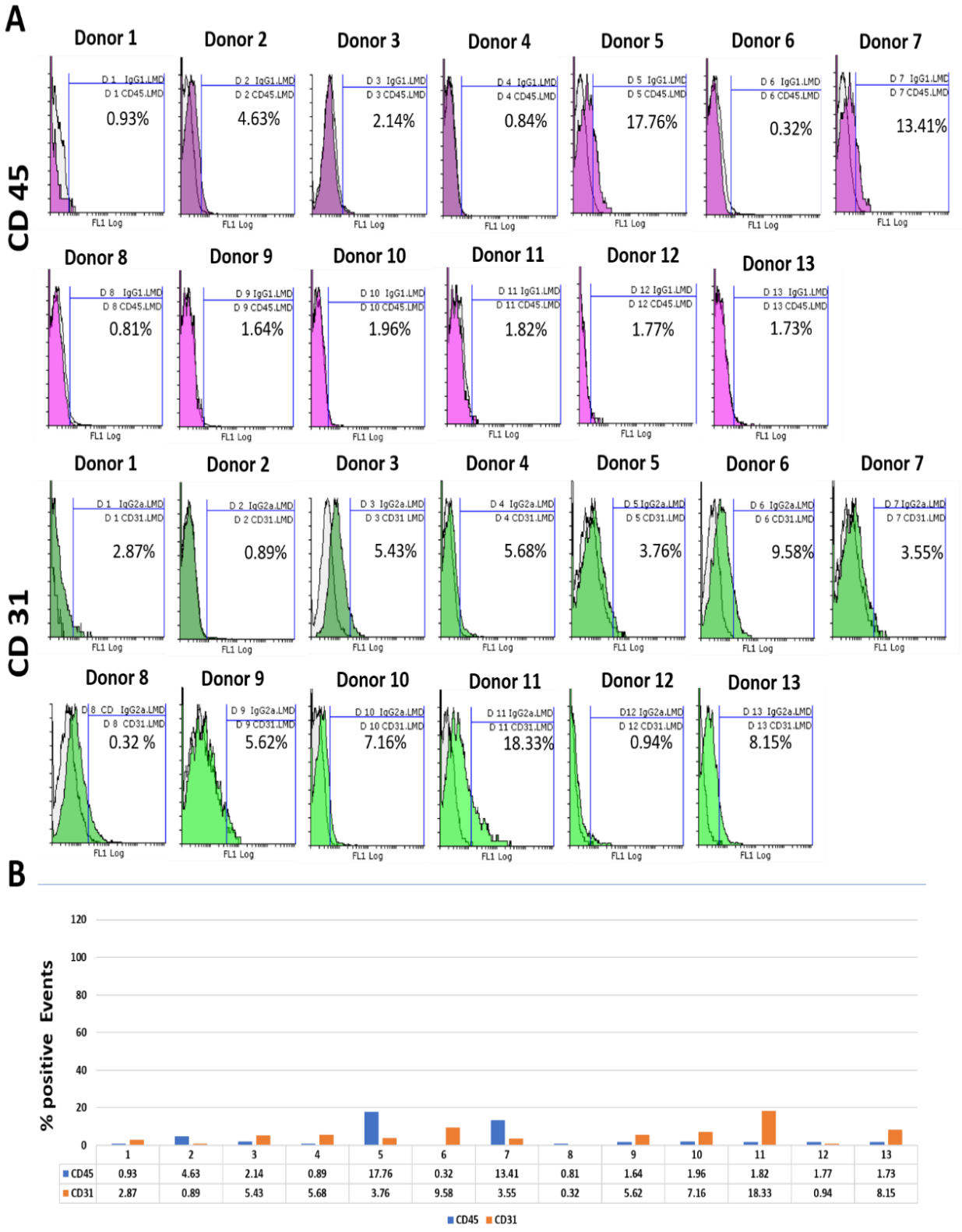

Figure 4. 18: Immunophenotyping of oMSCs for CD 45 and CD 31. *oMSCs of all donors were cultured to P3 and 80% confluency B M. The expression of CD 45 and CD 31 was assessed to identify their MSCs characteristics. (A) Overlay histograms of each antibody marker, (B) positive cells (%) compared to staining with the IgG1 or IgG2α isotype control. As expected, most donors were negative for both CD markers and showed variability in their expression levels, which ranged between 0.32% - 13.41% for CD 45 and between 0.32 - 18.33% for CD 31. Unfilled regions are isotype control IgG1or IgG2α, purple and green regions are CD 45 and CD 31 antibody markers, respectively.*

4.6 Discussion

In recent years, MSCs have emerged as appealing therapeutic agents in the development of skeletal stem cell-based therapies and have demonstrated remarkable clinical potential. A limitation with using MSCs in clinical scenarios is the availability and expansion of these cells to therapeutic numbers. Typically, less than 0.001% of the bone marrows` cell population are characterised as MSCs. Therefore, efforts to enrich the proportion of MSCs are under development.

oMSCs were first isolated from bone marrow in 1994 by Jessop and colleagues. They emphasised that the cells exhibited a fibroblastic morphology and could be induced into adipogenic and osteogenic phenotypes *in vitro* (Jessop *et al.,* 1994). Ever since, oMSCs have been successfully isolated from different sources like; cord blood (Kunisaki *et al.,* 2007) adipose tissue (Fadel *et al.,* 2011), peripheral blood (Lyahyai *et al.,* 2012), liver (Heidari *et al.,* 2013), amniotic fluid (Colosimo *et al.,* 2013), dental pulp (Mrozik *et al.,* 2010), synovial membrane (Godoy *et al.,* 2014), dermis (Cui *et al.,* 2014), hair follicles (Koobatian *et al.,* 2015), and endometrium (Letouzey *et al.,* 2015).

There are multiple sites for harvesting the bone marrow from sheep. In the majority of sheep studies, the iliac bone is preferred site for harvesting of bone marrow (Adamzyk *et al.,* 2013; Mccarty, Gronthos, *et al.,* 2009; Rentsch *et al.,* 2010). However, for this study, the bone marrow aspirate was successfully collected from the sternum bone and adequate quantities of bone marrow was collected (Delling *et al.,* 2012).

Human MSCs can be similarly obtained by taking aspirates of bone marrow from the iliac crest of healthy volunteers (Risbud *et al.,* 2006). In children, the anteromedial face of the tibia is preferred. In all studies above, ovine MSCs exhibit morphological, immunophenotypical and multipotential characteristics similar to those observed in human MSC *in vitro* and *in vivo.* (Mccarty, Grothos, *et al.,* 2009). These results were also confirmed by Rentsch and colleagues (Rentsch *et al.,* 2010).

oMSCs demonstrate a similar morphology to other species of MSCs (Heidari *et al.,* 2013). In this study, we observed that the isolated oMSCs attached to the cell culture plastic after 3 days of incubation under standard cell culture condition. The cells exhibited fibroblast-like morphology with a spindle or triangular-shaped cell bodies, large and ellipse nuclei and growing and growing outward in a "swirling fibroblast-like" pattern. Similar observations were made previously (Heidari *et al.,* 2013). Since the oMSC are smaller than the hMSC (Adamzyk *et al.,* 2013), more ovine cells could proliferate on the same culture area.

STRO-1 is a well-regarded cell surface antigen used in the characterisation of human MSCs populations (Lv *et al.,* 2014). Oreffo and colleagues have shown by selecting with STRO-1, it is possible to enrich the MSC population during cell isolation (Williams *et al.,* 2013). Zannettino et al have developed and characterised an analogous ovine marker, STRO-4, demonstrating efficient enriCh Ment of oMSCs and for this reason implemented in the current study (Gronthos *et al.,* 2009). This study confirmed that when selecting the MSCs with the STRO-4 antibodies, the isolated cells exhibited multilineage differentiation potential and were capable of forming a mineralised matrix, lipid-filled adipocytes, and chondrocytes capable of forming a glycosaminoglycan-rich matrix.

It was shown that prolonged passaging until passage five of oMSCs did not cause changes in the cell viability, cell morphology and cell characteristics typical for MSC. This was also shown by other researchers (Kalaszczynska *et al.,* 2013; Lyahyai *et al.,* 2012). No significant changes were observed for the cell viability obtained from Trypan blue test. However, significant differences were observed when assessing the cell metabolic activity using Alamar blue. This could be due to the nature of the different assays as Trypan blue depends on the number of live/dead cells which increased significantly and gradually without affecting the viability percentage. Whereas, Alamar blue indicates the cell metabolism by using the reducing capacity/ability of living cells to quantitatively measure the proliferation. When cells are alive, they maintain a reducing environment within the cytosol of the cell. In this study, the oMSCs remained healthy and viable and the viability increased significantly

over the three passages. The isolated cells were characterised for the three-lineage differentiation after selection of the differentiation media elements. All donors showed positive differentiation compared to the basal media which contains the essential element for proliferation and expansion. For both adipogenesis and osteogenesis, clear donor's variances was proved through the histology and semiquantitative methods. For chondrogenesis the thirteen donors also showed variances between donors according to the histology and sGAG contents of the pellets. Although each donor population of oMSCs differentiated, there was no clear profile in highly responsive donors between the three lineages. For example, a donor that was highly responsive during chondrogenic differentiation (donor 4), was not necessarily as responsive to osteogenic (donor 1 was the best) or adipogenic differentiation (donor 13 was the best).

The differentiation towards a chondrogenic lineage was monitored using the increase in glycosaminoglycans within the surrounding matrix. It was clear that the DNA content of the pellet decreased with time in Ch M treated group compared with the BM group. However, normalisation of the sGAG to DNA can effectively show that sGAG synthesis increased over the culture period in the chondrogenic media as one would expect. Cell aggregates grown in the basal media did not form cohesive pellets which were fragile and would break up easily whereas cell number has also fallen in the chondrogenic media. Whilst sGAG remained high possibly due to its incorporation in a stable ECM, the number of cells actually contributing to the sGAG may be underestimated whilst sGAG per cell becomes overestimated. Normalisation of the sGAG to DNA can effectively show whether the sGAG synthesis increases on a per cell basis and is a reliable measure when both are increasing or DNA is stable (Dale, 2016).

CD markers have been used to characterise stem cell populations with clear guidelines now in place for establishing genotype and phenotype of bone marrow derived mesenchymal stem cells (Boxall and Jones 2015) However, in our studies we cannot definitely conclude that MSCs resident in different tissues are the same or even very similar. For instance

adipose-derived MSCs express CD 34. (Quirici *et al.,* 2009). Whereas, BM-MSCs do not, W8-B2/MSCA-1 is expressed by BM MSCs but not placenta-derived MSCs (Battula *et al.,* 2007). In our study, we have tested expression to the epitope of the BM-oMSCs for CD 29 and CD 44 and CD 45 and CD 31. Choosing these antibodies was due to several reasons, the main reason was the viability of these antibodies with the cross reaction to sheep cells. In addition, we try to choose some of epitopes that are normally expressed positively (CD 29 And CD 44) and others that normally do not exist on the MSCs or are expressed negatively (CD 45 and CD 31). In a review article, markers for characterisation of Bone Marrow Multipotential Stromal Cells were reviewed from literatures of different animal studies to characterise the MSCs. In this review article wide range of antibodies (antihuman antibodies and some species-specific antibodies) were used in this paper which gave symbols indicating the marker expression level as following −: no expression; +−: <5% expression; +: 5 −50% expression, ++: 50−100% expression (Boxall and Jones, 2012). The results of the CD marker experession of this study confirm this norm for the majority of the donors when the BM-MSCs were positively expressed for CD 29 (4 of 13 donors were +, and 9 of the 13 donors were ++) and CD 44 (1 of 13 donors were +, and 11 of the 13 donors were ++) while negatively expressed for CD 45 (11 of 13 donors were -, and 2 of the 13 donors were +-) and CD 31(3 of 13 donors were -, 7 of the 13 donors were +- and 3 of 13 donor were +).

For the source-dependent and donor-dependent differences of MSC properties. Although bone marrow and adipose tissue are the main sources of the MSCs (Pittenger *et al.,* 1999; Zuk *et al.,* 2002). Many of the perinatal sources, including amniotic membrane and umbilical cord have preference over adult sources due to availability, lack of donor site morbidity, young age of cells, high quantity of cells in the tissue , or high proliferation capacity (Ilancheran *et al.,* 2009) *In vitro* studies comparing MSCs from different sources which mainly illuminated minimal criteria of MSC concluded that MSCs from different sources are similar (Baksh *et al.,* 2007; Barlow *et al.,* 2008; Kern *et al.,* 2006). It is suggested that a better understanding of functional properties indicating the potential impact on future

clinical applications may be achieved by molecular profiling of MSCs [22] (Wegmeyer *et al.*, 2013).

In summary, we have investigated in detail the variability of MSCs derived from sheep and conclude. Sheep are well accepted as pre-clinical models for orthopaedic tissue engineering studies (Mcgovern *et al.*, 2018). Animal models for orthopaedic tissue engineering and modelling disease (Mcgovern *et al.*, 2018). Testing of new purified and expanded MSC based products in large animal models will allow for a thorough pre-clinical evaluation of novel products prior to clinical trials in humans (Bieback *et al.*, 2010).

CHAPTER 5

Chondrogenic Differentiation of oMSC in 3D Hydrogels Under Mechanical Conditioning

5.1 Introduction

Cell based therapy for cartilage repair techniques, either directly injected autologous chondrocytes into the cartilage defect or as engineered cartilaginous grafts using tissue engineering technology, rely on the ex vivo expansion of chondrocytes obtained from small biopsies (Hunziker *et al.,* 2015). However, there are some disadvantages because the matrix-forming capacity of expanded chondrocytes is associated with de-differentiation processes (Von Der Mark *et al.,* 1977; Watt, 1988). In addition, obtaining tissue biopsies from patients can further cause cartilage damage and degeneration (Matricali *et al.,* 2010; Moyad, 2011). Thus, there is interest in alternative cell sources for cartilage regeneration (Oldershaw, 2012) Among the cell sources that have the ability to regenerate cartilage, MSCs are the most favourable because of their multilineage differentiation, immunosuppressive and immunomodulatory capacity as well as cell interaction and growth factor secretion (Zhao *et al.,* 2016). Despite all of the above, there is a shortage of reports on the clinical application of MSCs for cartilage regeneration (Kuroda *et al.,* 2007). This may be due to the fact that MSCs differentiate of into hypertrophic fibrocartilage, which has inferior properties to native hyaline cartilage (Zhao *et al.,* 2016). In addition, there is no standard protocol for the culture of MSCs allowing reproducible and optimal chondrogenic differentiation (Somoza *et al.,* 2014). Studies were directed to control the MSCs behaviour during differentiation towards the chondrogenesis (Spakova *et al.,* 2018).

Recently, a novel remote bio-magnetic activation technique called Magnetic Ion Channel Activation (MICA) has been demonstrated for the control of MSCs behaviour in a preclinical ovine animal study for bone defect repair (Markides *et al.,* 2018). In this chapter, the effect of this technique to promote chondrogenesis of oMSCs after targeting the ion channel (TREK-1) with MNPs and determine if we can culture and differentiate BM-oMSC in chondrogenic growth factor supplemented media. Therefore, cellular three-dimensional

collagen hydrogels were analysed following the same protocols that were used to characterise native sheep cartilage (Chapter 3).

5.2 Aim and objectives

5.2.1 Aim

The aim of this chapter is to investigate the effect of mechanical stimulation using MICA technology on chondrogenic differentiation of the oMSCs by targeting mechanosensitive channel TREK-1 using MNPs.

5.2.2 Objectives

The objectives of this chapter are:

- Comparison of static versus dynamic culture conditions in basic and chondrogenic medium
- To assess the variation between five donor BM-oMSCs to produce cartilaginous matrix in response to chondrogenic media with and without mechanical stimulation.
- To assess the mechanical properties of the engineered cartilage by determining the young's modulus.
- To assess the biochemical composition of the engineered cartilage by determining the sgag, total collagen total protein content relative to total cell number.
- To study the matrix composition of the engineered cartilage through histological stains such as h and e, alcian blue and picrosirius as well as immunohistochemistry for collagen ii collagen x and aggrecan.
- To assess repeatability and reproducibility of the experimental procedures.

5.3 Materials and Method

The summery of chapter five methodology is shown in Figure 5.1.

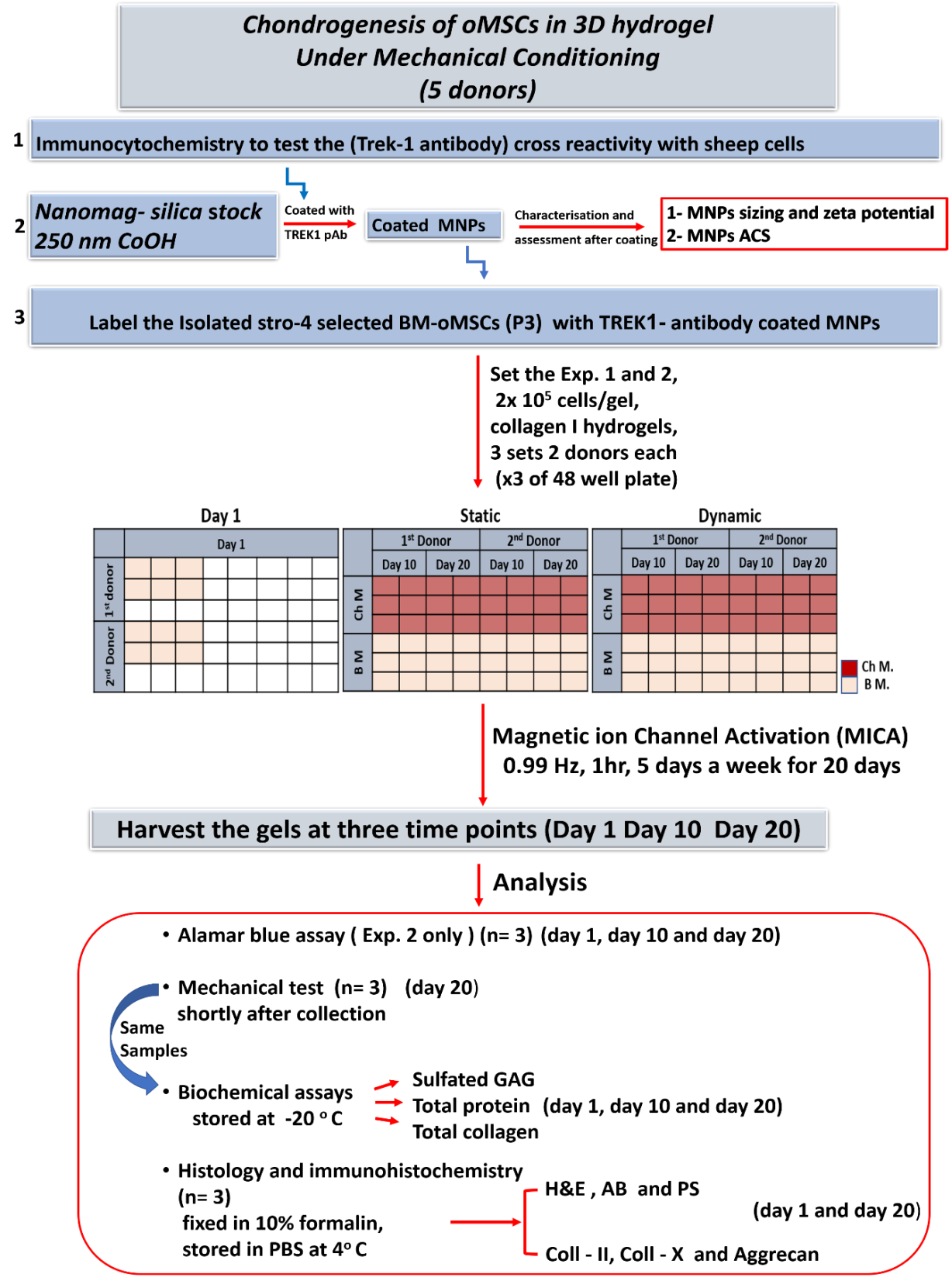

Figure 5. 1: Methodology for chapter 5. *This schematic summarises the experimental steps carried out in chapter 5 for experiment one and two.*

5.3.1. Cross-reactivity of TREK-1 antibody with ovine MSC

The primary TREK-1 antibody was known to react with humans, mouse and rat. Hence, the antibody was tested for ovine cell reactivity by fluorescent immunocytochemistry as described in chapter 2, section 2.5.1 using unlabelled oMSCs as negative control and sheep chondrocytes as positive control.

5.3.2 Magnetic nanoparticles activation and antibody coating

MNPs were coated with antibody as described in chapter 2, section 2.5.1. A stock solution of 10 mg/ml Nanomag suspension was coated with TREK-1 antibody. A final concentration of 1 mg/ml of the antibody- coated MNPs was prepared in 1% BSA. This working solution was stored at 4 ^{o}C until use.

5.3.2.1 Cell labelling with TREK-1 coated MNPs

Three-dimensional hydrogels were prepared from collagen type I to study chondrogenesis of BM-oMSC. Five donors' oMSCs were labelled with the antibody-coated MNPs as mentioned in chapter 2, section 2.5.2. These oMSCs were seeded in collagen gels at a cell density of 2X10^{5} cell /gel (Chapter 2, section 2.2.2.9). Table 5.1 shows the experimental layout for this study.

Table 5. 1: Experimental set up for experiment 1 and 2 for all five donors.

	Plates			Labelled with MNPs	Mechanical stimulation
	Day 1	Static	Dynamic		
EXP 1	B M only	B M	B M	No	No
		Ch M	Ch M	yes	Yes
EXP 2	B M only	B M	B M	yes	No
		Ch M	Ch M	yes	Yes

A slight modification was performed between experiment 1 and 2. In case of experiment 1, the treated group was labelled with the MNPs only, while the control group was left without labelling and mechanical stimulation. Whereas, in experiment 2 all cells were labelled with MNPs for both treated and control group, only the treated group were subjected to mechanical stimulation.

After 24 hours, the gels were imaged using a bright field microscope (EVOS microscope) to assess cell distribution inside the hydrogels. Day 1 gel samples were harvested after 24 hours and fixed for histology or frozen at -20 ^{o}C for biochemical analysis (n = 3). While the remaining gels continued to receive a total media change with either B M or Ch M every 2-3 days until day 20. In addition, after 24 hours the treated group received magnetic stimulation for one hour daily 5 days /week for 20 days, while the control groups were left without stimulation chapter 2, section 2.5.3.

5.4 Statistical analysis

Data for Young's modulus were collected for the both experiments 1 and 2 to compute and specify Young's modulus for the engineered cartilage for each donor. Then, trypan blue, DNA content and GAG, total protein, total collagen content and their normalisation to the DNA content were compared using one-way ANOVA with Tukey's multiple comparisons test to determine statistical significance between each condition. Differences were considered significant for $P \leq 0.05$ $P \leq 0.01$ $P \leq 0.001$. Analysis was performed using IBM SPSS statistics program version 24. All values quoted in the results are mean ± standard deviation except for young's modulus the data were plotted as mean± standard error.

5.5 Results

5.5.1 Trypan blue exclusion test of cell viability

Cell viability of oMSC was assessed by Trypan blue staining during culture at passage 1 to P1-P3. The viability of the oMSCs were calculated using equation 2.4. Results showed increases in the total cell number obtained from each passage, but the dead / live cells ratio. In general, the viability (%) increased from P1 to P2, but then a significant decrease in was observed between the three passages for the five donors. For donor 5, significant difference in cell viability were observed between p2 and p1 and P3 ($P \leq 0.01$). For donor 6 there were significant differences between P3 and p2 ($P \leq 0.05$) and p2 ($P \leq 0.01$). For donor 13 significant difference was found between p1 and p2 ($P \leq 0.05$). There were no differences between the passages for both donor 2 and 8 (Figure 5.2).

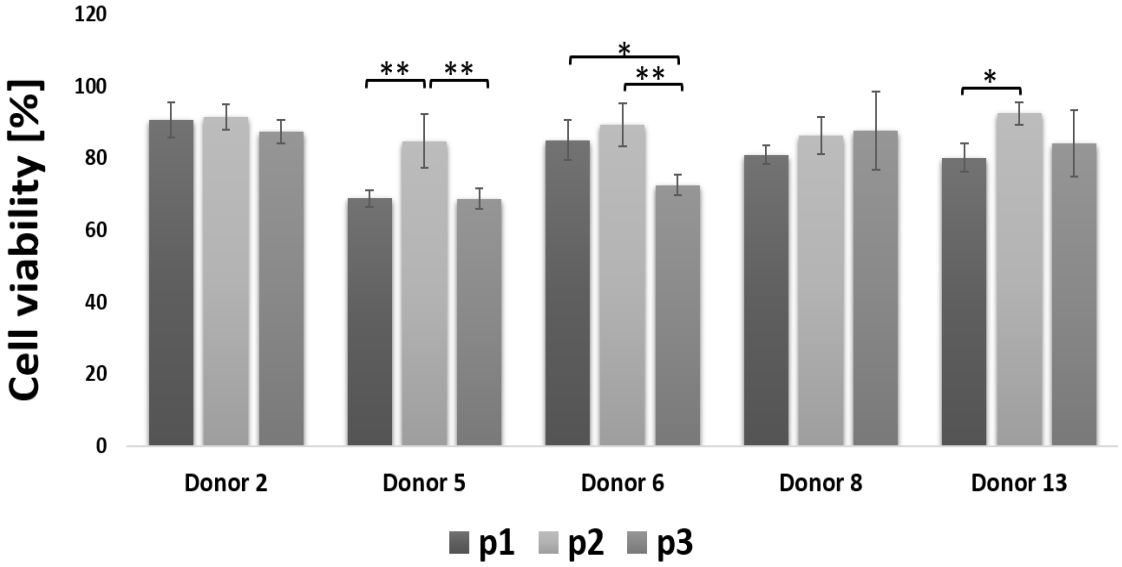

Figure 5. 2: oMSCs cell viability. *Trypan blue was used to assess oMSC viability during passages p1, p2 and p3. Significant differences were observed for three of the five donors, *p ≤ 0.05, ** p ≤ 0.01.*

5.5.2 Alamar blue assay

Cell metabolic activity was assessed by alamar blue. The results showed similarity in the cell viability for each experimental group (Figure 5.3). In general, cell metabolic activities were increased significantly for day 10 and day 20 compared to day 1 ($P \leq 0.001$) (significant not showed). In between day 10 and day 20 in all donors there are no significantly deference in cell viability in B M and Ch M under static or dynamic culture conditions. In the other hand the results showed that the Ch M gels have high cell metabolic activities compare to B M for day 10 and day 20 in both dynamic and static group $P \leq 0.001$. There were no significant differences when comparing the three donors for all conditions in each donor with the parallel conditions of the two other donors the data not showed.

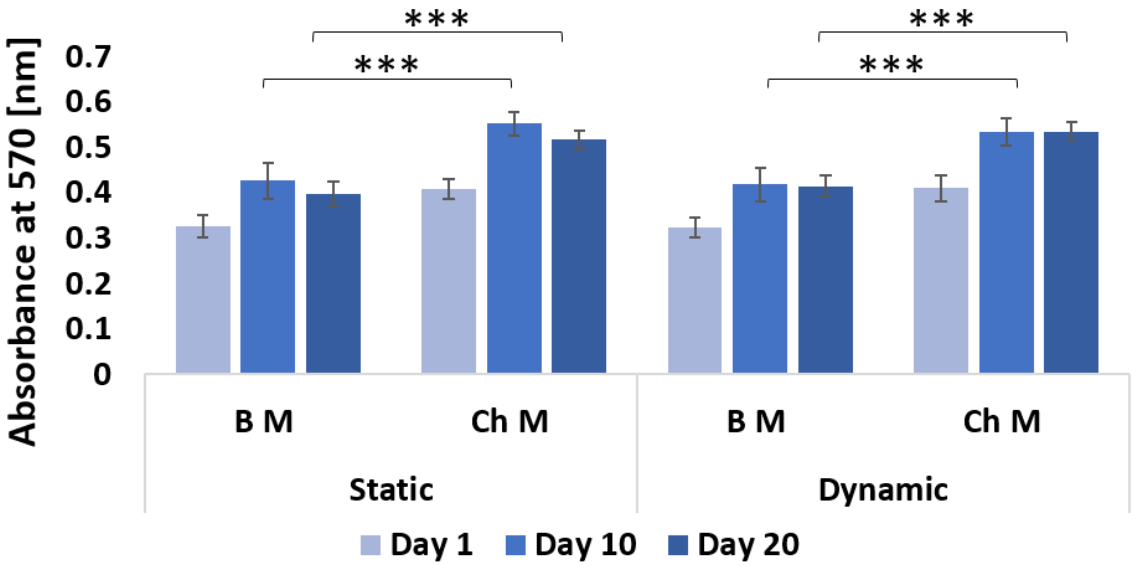

Figure 5. 3: Cell metabolic activity assessed by alamar blue assay. *Generally, significant increases on day 10 and day 20 compared to day 1 ($p \leq 0.001$) for all condition (significance not shown). No significant differences between day 10 and day 20. Significant differences between B M vs. Ch M in both of static and dynamic condition were observed * $p \leq 0.001$.*

5.5.3 Immunocytochemistry to detect TREK-1 antibodies cross reactivity with ovine cells

The immunocytochemistry of both sheep chondrocytes and oMSCs of two experimental donors revealed TREK-1 expression indicating the presence of cross reactivity with sheep cells (Figure 5.4).

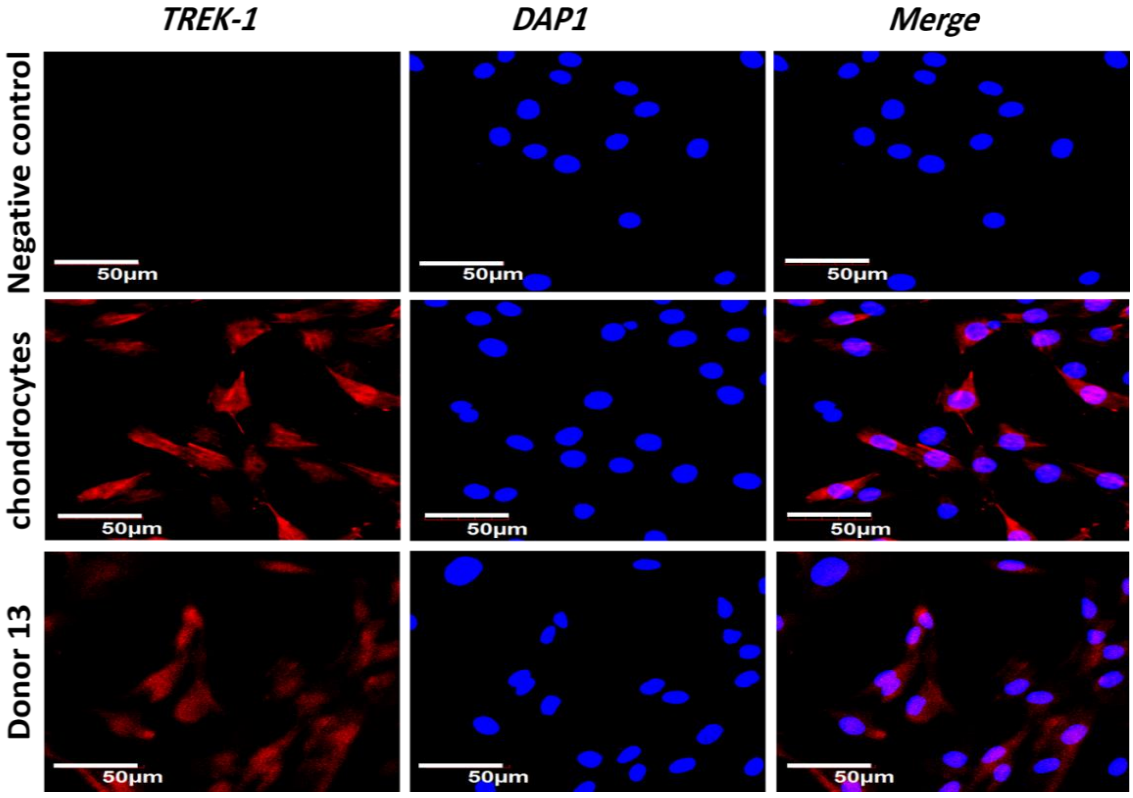

Figure 5. 4: Immunostaining of TREK -1 expression in ovine cells. *Fluorescent micrographs of sheep chondrocytes (P2) and isolated oMSCs (P3) showed positive TREK -1 expression (red) compared to the control. Cell nuclei were counter stained with DAPI (blue). Images were taken using a confocal microscope (CLSM) at 60 x magnification. Scale bars = 50 µm.*

5.5.4 Characterisation of the antibody-coated MNPs

5.5.4.1 MNPs sizing and zeta potential

MNPs size distributions are shown for uncoated MNPs, and TREK-1-coated MNPs (batch 1 and batch 2) (Figure 5.5 A). For uncoated MNPs the particle sizes ranged from around 242 nm to 279 nm (peak at 260 nm). When MNPs were coated with antibodies their size distribution changed. An even broader size distribution was observed for TREK-1-coated (batch 1) MNPs ranging from 174.3 nm to around 955 nm with a peak 344 - 408 nm. Overall, coating MNPs with antibodies resulted in an increase in MNPs diameter. For TREK-1-

coated (batch 2) MNPs, the diameters ranged from below 229 nm to around 4575 nm. Peak was observed at around 912 nm and 1148 nm. While the surface charge of the MNPs (Figure 5.5 B). become more positive from about -31 to -21 mV (uncoated MNPs) to about -26 to +20 mV (batch 1) and about -26 to +20 mV (batch 2) coated MNPs.

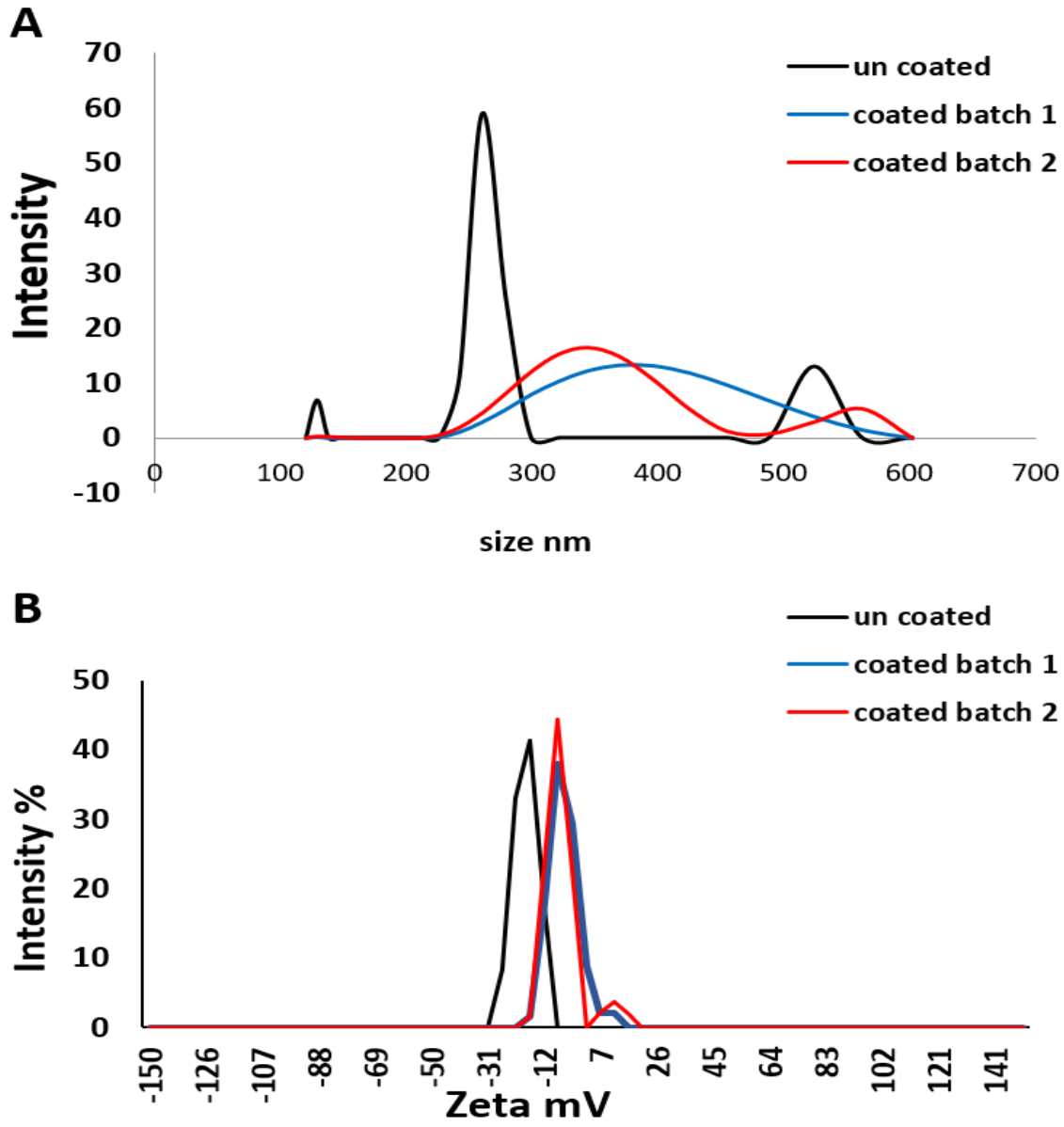

Figure 5. 5: Size and zeta potential of MNPs. *Uncoated and TREK-1coated MNPs (batch 1 and 2) were characterised for (A) size and (B) zeta potential by DLS measurements using Malvern zetasizer. Results illustrate increased size of the MNPs after labelling with the antibodies. Changes in surface charge observed from negative (uncoated) to positive (coated).*

5.5.4.2 MNPs oscillating movement

Magnetic nanoparticles possess the advantage that they can be characterized magnetically in addition to conventional NP characterization techniques to obtain more information regarding the MNPs. The uncoated and the two batches (batch 1 and batch 2) of TREK-1 coated MNPs were characterised for oscillating movement using alternate current susceptometer (ACS) as described in chapter 2, section 2.5.1.2. Results show that there was slight alteration in the chi'' curve for the two batches of TREK-1 coated MNPs from the un-coated. The two batches exhibit a curve almost similar to each other (Figure 5.6).

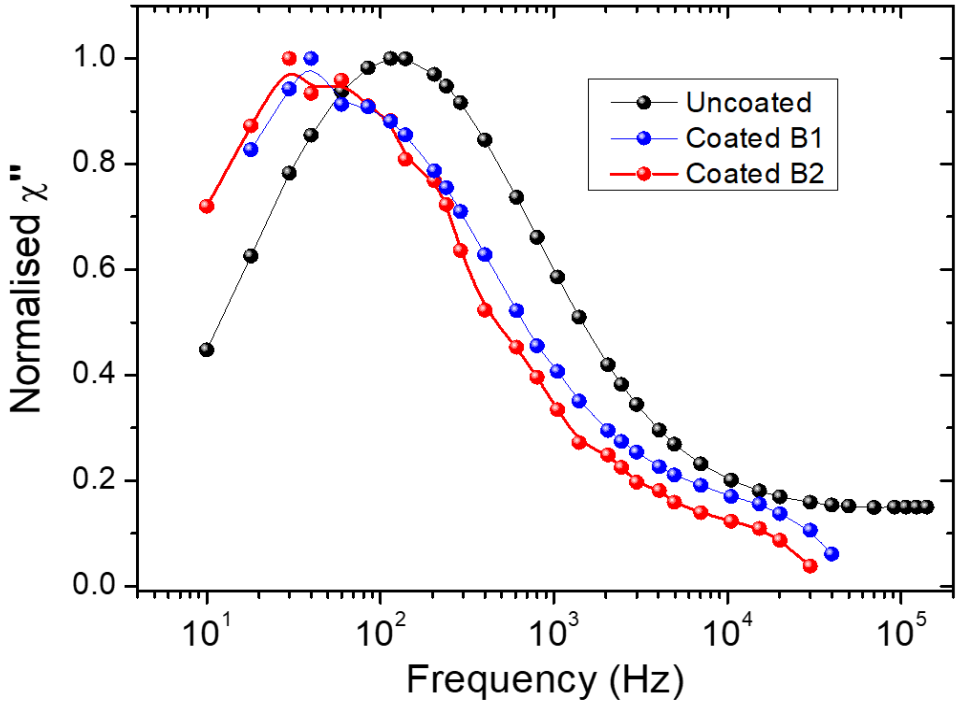

Figure 5. 6: Oscillating movement of MNPs. *The uncoated and the two batches (batch 1 and batch 2) of TREK-1 coated MNPs were characterised for oscillating movement using alternate current susceptometer (ACS). The graph illustrates slight alteration in the chi'' curve for the two batches of TREK-1 coated MNPs from the un-coated. The two batches exhibit identical curve in form almost similar to each other.*

5.5.5 Compression test and Young's Modulus

For both Experiments one and two, Compression tests were performed for the gels cultured dynamically and statically in Ch M at day 20. A displacement of 0.2 mm of the entire specimen thickness was applied resulting in loads ranging between 5-20 N. Stress-strain graphs were plotted and Young's modulus was calculated as described in chapter 2, section 2.8. Although, the stress values of the gel samples required for inducing the deformity or the displacement, were varied from low which need about stress 2000-3000 N/m2 in some samples to high reached 4000 N/m2, that range is lower than that of the cartilage samples, which range between 4000-5000 N/m2 and reach 6000 for some samples chapter 3, section 3.5.1. The dynamic group is generally higher than the static group for all donors in both experiments except donor 2 of the experiment 1 (Figure 5.7) and (Figure 5.8).

Experiment 1

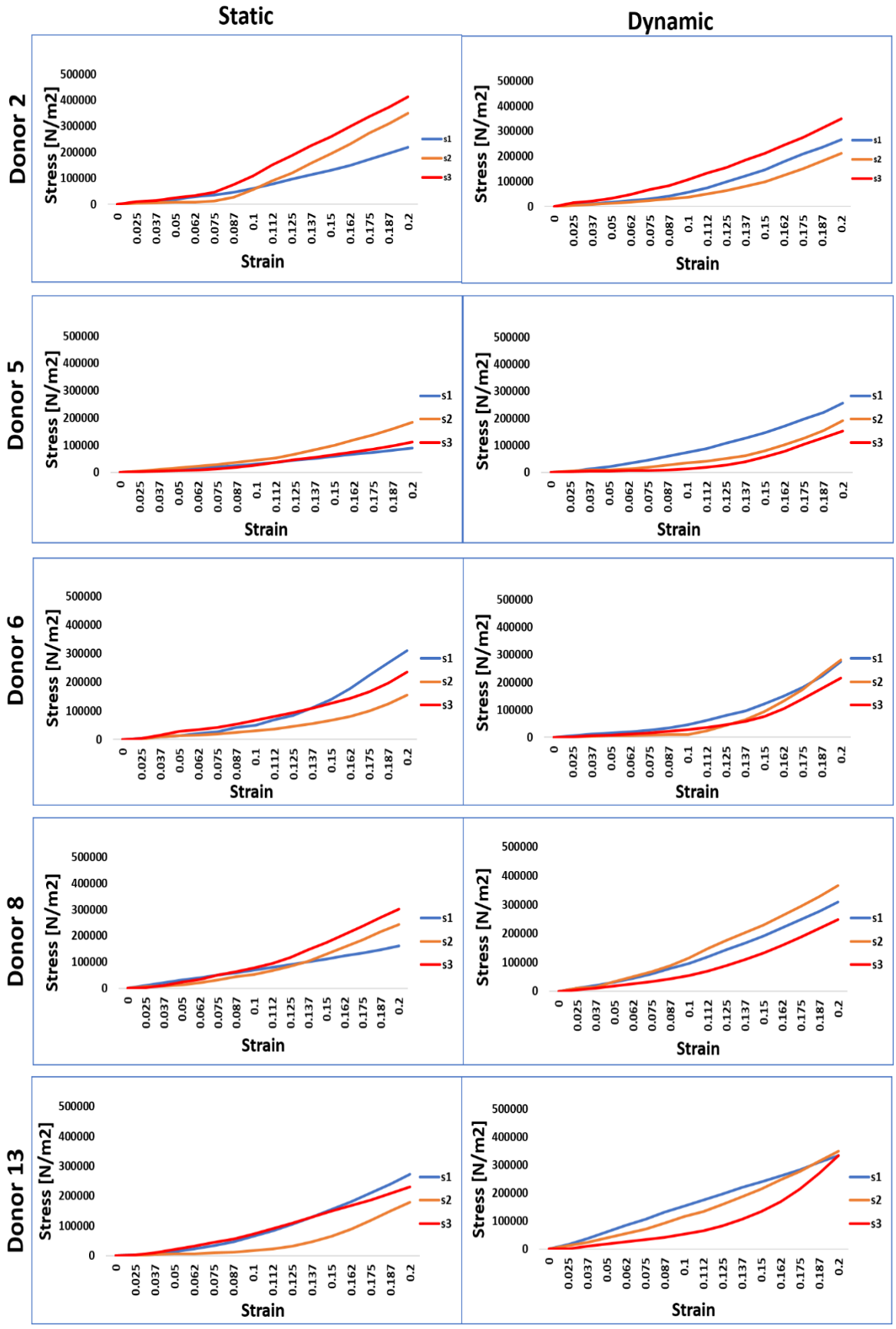

Figure 5. 7: Stress-strain curves for the experiment 1 gel samples. *Stress -strain curves of the gels cultured dynamically and statically in Ch M at day 20. The graph follows similar trends to native sheep cartilages. s= sample number (n=3).*

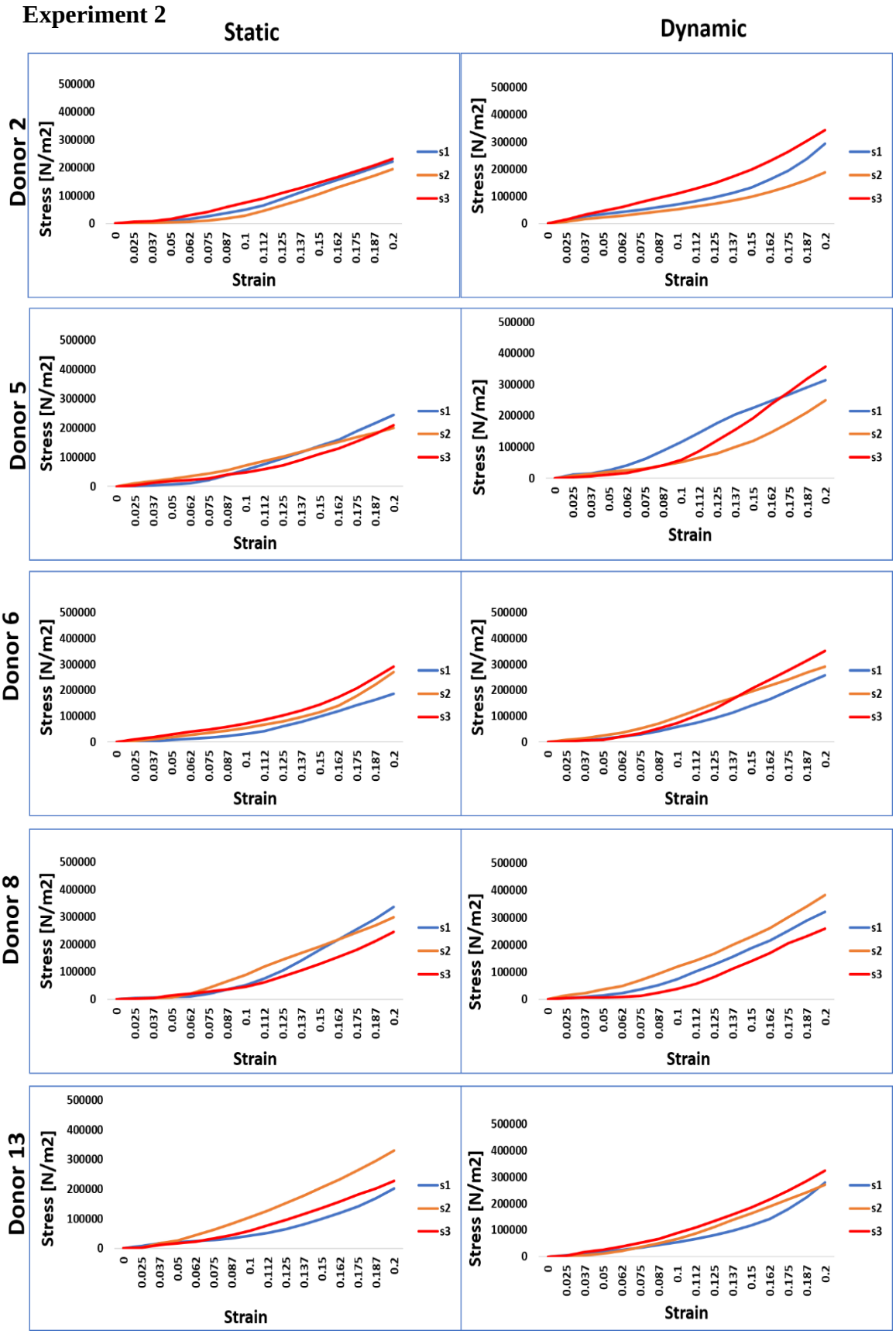

Figure 5. 8: Stress-strain curves for the experiment 2 gel samples. *Stress -strain curves of the gels cultured dynamically and statically in Ch M at day 20. Like experiment 1, the graph follows similar trends to native sheep cartilages. s= sample number (n=3).*

Young's modulus of each sample that was subjected to the compression test was calculated using equation 2.7 (Chapter 2, section 2.7). Data were expressed as mean ± standard error (n = 3) (Figure 5.9). The results showed that Young's modulus was ranged between 0.789 ± 0.183 MPa to 2 ± 0.83 MPa. Significant differences were observed between the static and dynamic group for donor 5 which revealed a significant difference between the static and dynamic group ($P \leq 0.001$) and donor 8 which revealed a significant difference between the static and dynamic group ($P \leq 0.05$). In addition, significant differences ($P \leq 0.05$) were observed when comparing donors with each other, donor 5 was different from each donor 2 donor 13 (static group) and donor 5 with donor 6 (dynamic group). While there were no significant differences between other donors.

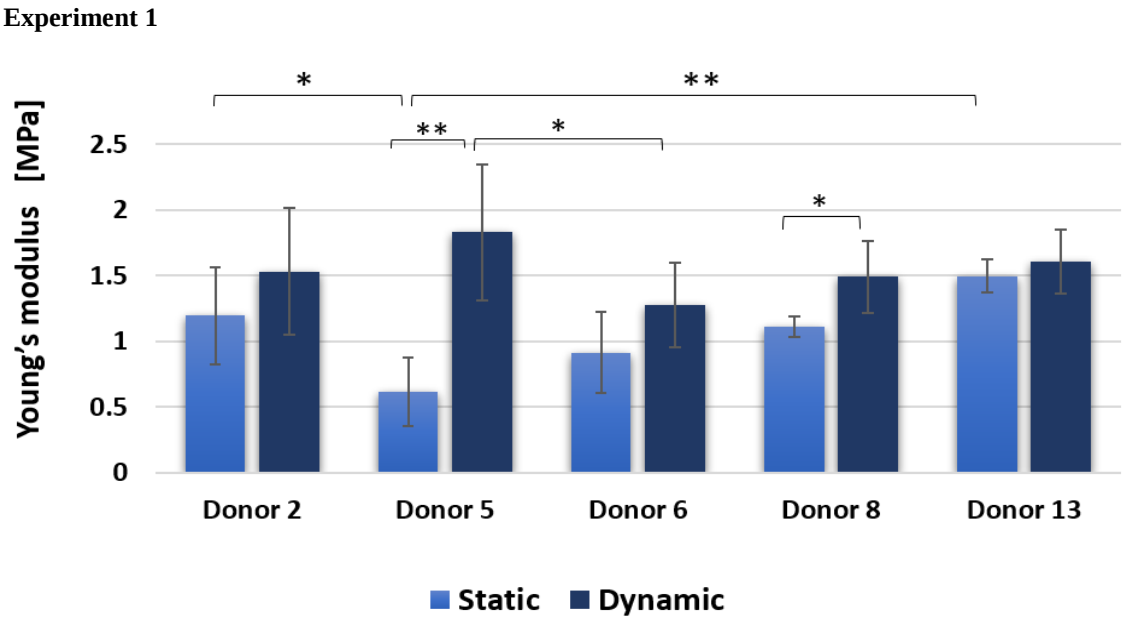

Figure 5. 9: Young's Modulus, Experiment 1*. Young's Modulus of each donor was calculated for Ch M cultured gels, day 20. Significant differences between the static and dynamic group were observed for donor 5 and donor 8 only. For donor variation, the comparison between the donors showed that there were differences of the static group between donor 5 and each donor 2 and 13 and between donor 5 and 6 dynamic group. Data are expressed as mean ± standard error (n = 3) *p ≤ 0.05, **p ≤ 0.01.*

For experiment 2, the computed Young's modulus was ranged between 1.089 ± 0.183 MPa in donor 2 (static) group to 2.12 ± 0.160 in donor 8 (dynamic) group. Significant differences between the static and dynamic group were observed for all donors ($P \leq 0.05$). In addition, when comparing donors with each other, significant differences were observed between donor 8 and each of donor 2, 5 (static), and between donor 8 and 13 dynamic ($P \leq 0.05$) (Figure 5.10).

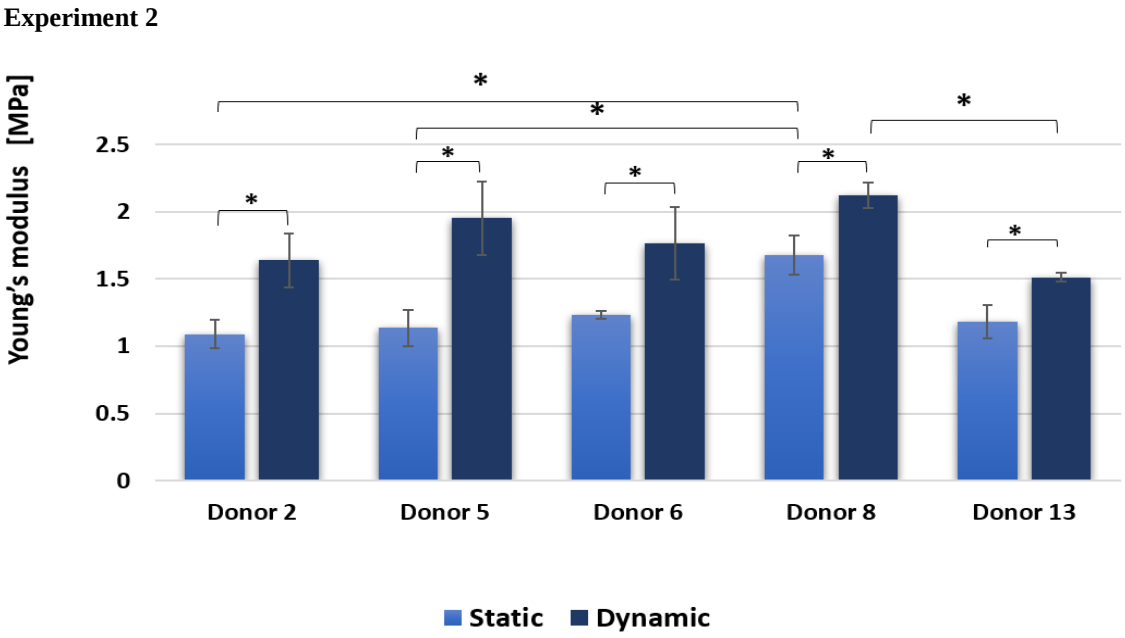

Figure 5. 10:Young's Modulus, Experiment 2. *Young's Modulus of each donor was calculated for Ch M cultured gels, day 20. A significant difference between the static and dynamic group were observed for all donors. For the donor variation, significant differences between donor 8 and each of donor 2 and 5 (static) and between donor 8 and donor 13 (dynamic). Data are expressed as mean ± standard error (n = 3) *p ≤ 0.05, **p ≤ 0.01*

The values of the estimated Young's modulus of native sheep cartilage and the engineered cartilage of both the static and dynamic conditions were compared using one-way ANOVA with Tukey's multiple comparisons test to determine statistical significance between each condition. Differences were significant between the dynamic group with each of the static group ($P \leq 0.001$) and the native sheep cartilage ($P \leq 0.01$). Whereas, there were no significant differences between the estimated Young's modulus between the static group and the native sheep cartilage. The data were plotted as a mean ± standard error (Figure 5.11).

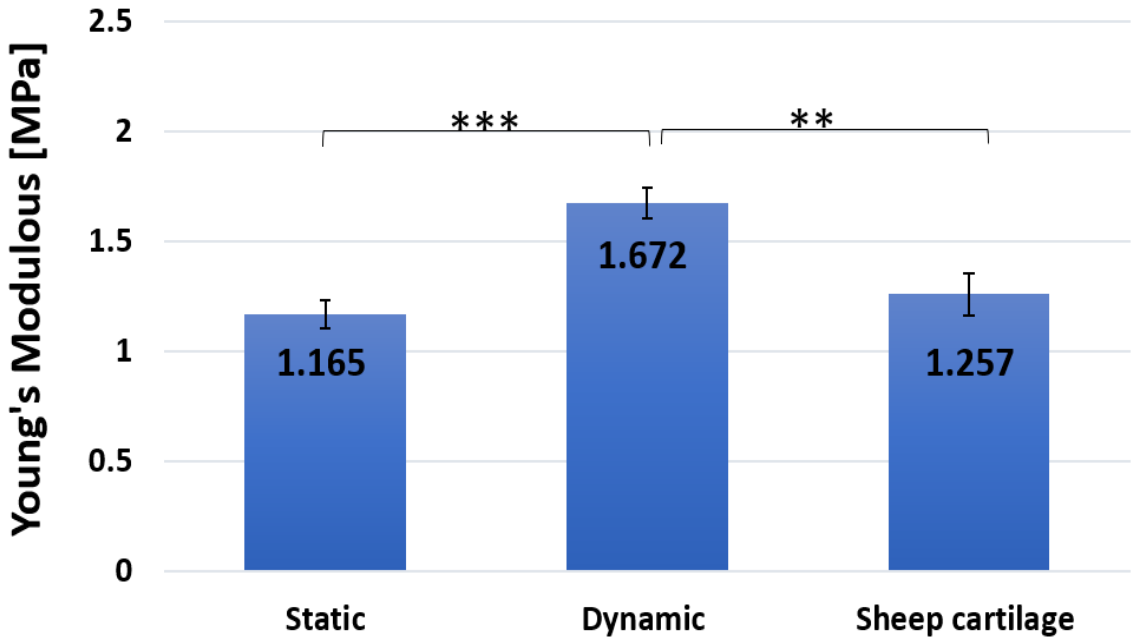

Figure 5. 11: Young's Modulus comparison between the native sheep cartilage and both conditions' engineered cartilage static and dynamic*. The calculated Young's Modulus for Ch M cultured gels, day 20 of each donor of the both experiment 1 and 2 was calculated and compared with the calculated native sheep cartilage from (chapter 3). The differences were significant between the dynamic group and each of the static group and the native sheep cartilage. there were no significant differences between the static group and the native sheep cartilage. The data were plotted as a mean ± standard error (Figure 5.12). For each static and dynamic engineered cartage (n = 5), for native sheep cartilage (n = 6), **p ≤ 0.01, ***p ≤ 0.001.*

5.5.6 Biochemical analysis of the gels

5.5.6.1 DNA content of the gels

PicoGreen assay was used to quantify the DNA content in the gel lysates at day 1, day 10 and day 20 for both experiment 1 and 2 (Figure 5.12), the graph showed, there were significant increases in the DNA contents for the BM gels across the experimental time at day 10 and day 20 compared to day 1. Whereas no significant differences between day 10 and day 20. For the Ch M gels there are no significant differences between the time point. However, the DNA content showed slightly decreases across the time. Comparing BM with Ch M values, there were significant differences between B M and Ch M for both day 10 and day 20 for both static and dynamic groups ($P \leq 0.001$). in addition, there was significant differences ($P \leq 0.05$) between the static and dynamic group for the Ch M at day 20.

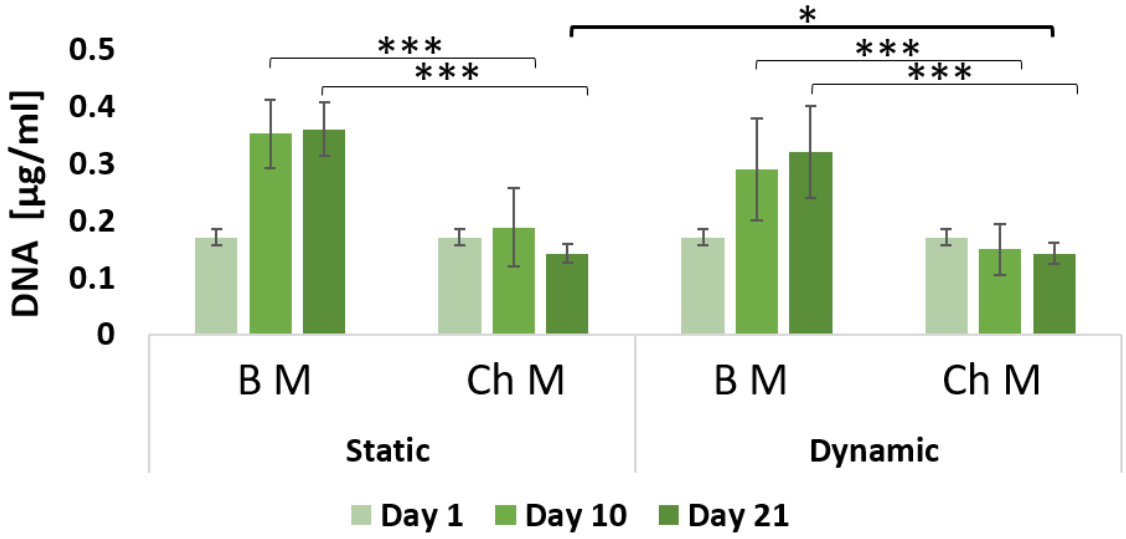

Figure 5. 12: DNA content for experiment 1 and 2. *DNA content of the gel samples was determined using the PicoGreen assay following digestion with proteinase K. The graph showed that DNA content increased significantly at day 10 and day 20 compared to day 1 for all BM gels (significant is not showed. There were significant differences between B M and Ch M for both day 10 and day 20 for both static and dynamic groups). There were significant differences between the static and dynamic group for the Ch M at day 20. Data are expressed as mean ± standard deviation (n = 30). *p ≤ 0.05, ***p ≤ 0.001.*

PicoGreen assay in details, for experiment 1 (Figure 5.13) results showed that the DNA content was significantly increased ($P \leq 0.001$, $P \leq 0.01$ or $P \leq 0.05$) for all B M gels for all donors at day 10 and day 20 compared with day 1 B M. When comparing the day 10 and day 20 of the B M cultured gels there were significant differences in B M dynamic between day 10 and day 20 but not for B M static for all five donors. Meanwhile for Ch M gels, the DNA content was decreased gradually for day 10 and day 20, with some exception in donor 2 and 5 Ch M dynamic which showed initial increases at day 10 then, increases at day 20. Also, donor 6 Ch M static and donor 13 Ch M dynamic which showed the opposite when increased at day 10 and decline in day 20.

For the experiment 2 (Figure 5.14), DNA content significantly increased at day 10 and day 20 for B M gels static and dynamic for all donors. For Ch M cultured gels, the DNA content was clearly varied compared to experiment 1, as the DNA content is significantly increased at day 10 but decrease at day 20 these decreases were not significant for donor 5 and 13 Ch M static day 20 and for day 8 Ch M dynamic day 20.

Experiment 1

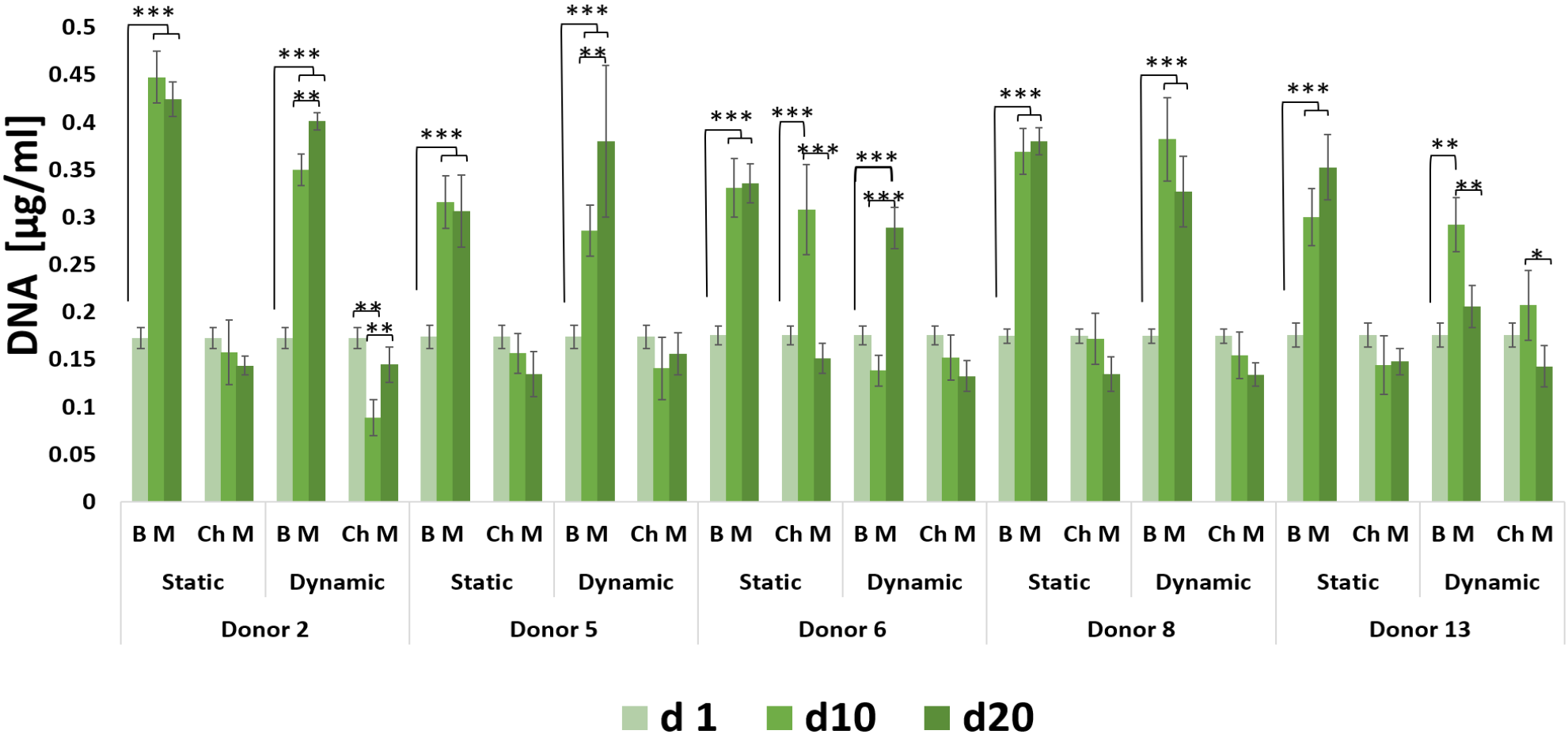

Figure 5. 13: DNA content for experiment 1. *DNA content of the gel samples was determined using the PicoGreen assay following digestion with proteinase K. The graph showed that DNA content increased significantly for all donors at day 10 and day 20 compared to day 1 for all BM gels. For Ch M gels, the DNA content was decreased gradually for day 10 and day 20 in most donors with some exceptions in donor 2 and 5 (Ch M dynamic) which showed initial increases at day 10 then, increases at day 20. And also, donor 6 (Ch M static) and donor 13 (Ch M dynamic) which showed the opposite when increased at day 10 and fill in day 20. Data are expressed as mean ± standard deviation (n = 3). *p ≤ 0.05, **p ≤ 0.01, ***p ≤ 0.001.*

Experiment 2

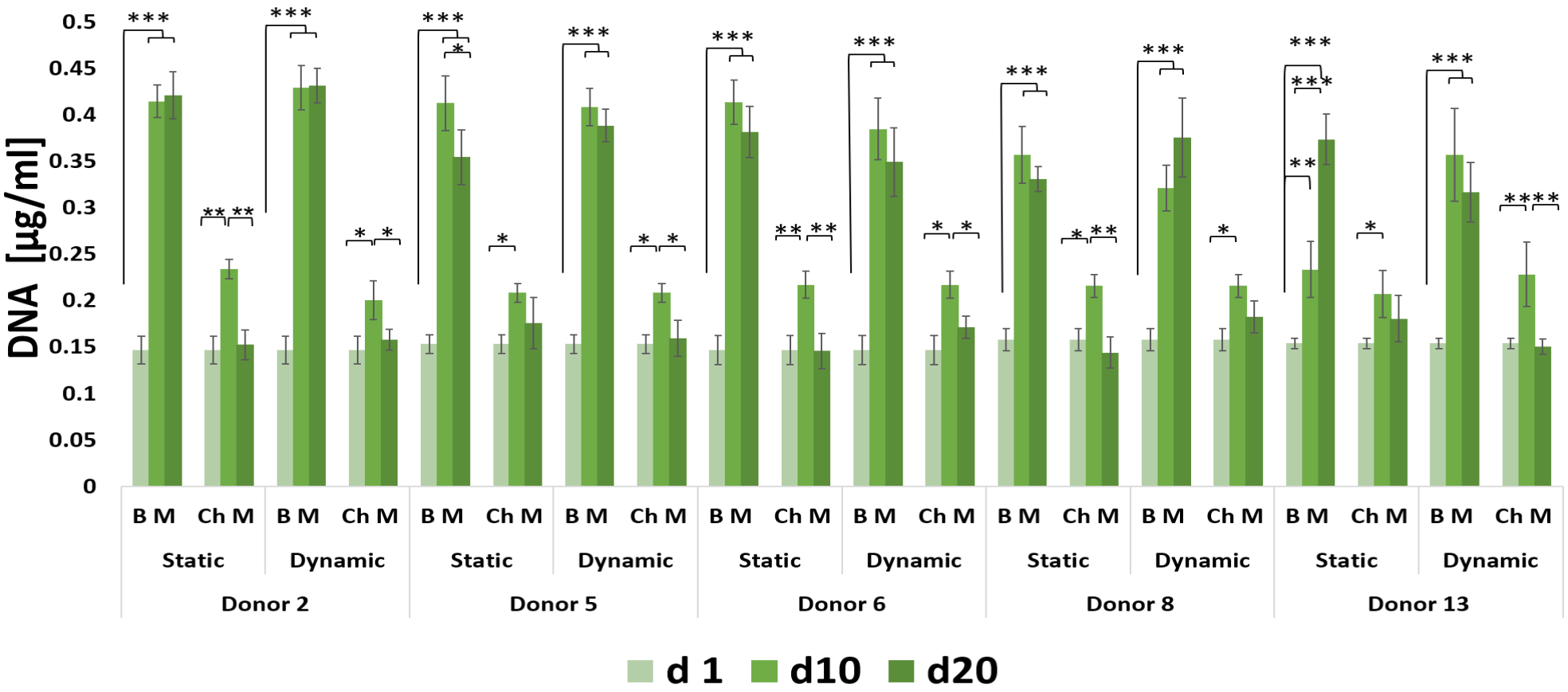

Figure 5. 14: DNA content for experiment 2. *DNA content for experiment 2 samples was assessed by Pico green assay. the graph showed that the DNA content increased significantly for all donors ta day 10 and day 20 compared to day 1 for all BM gels For ChM gels were decreased at day 10, and in some ChM gel was significant, but for day 20, the values was full down to its day 1 level. Data are expressed as mean ± standard deviation (n = 3). *p ≤ 0.05, **p ≤ 0.01, ***p ≤ 0.001.*

5.5.6.2 sGAG content of the gels

The sGAG content was assessed by DMMB assay for both experiment 1 and 2, as described in chapter 2, section 2.6.2. The results for both experiment 1 and 2 (Figure 5.15) showed significant increases (at $p \leq 0.001$.) at day 10 and 20 for static and dynamic compared to day 1. No significant differences were observed between B M and Ch M nor between the both conditions static and dynamic.

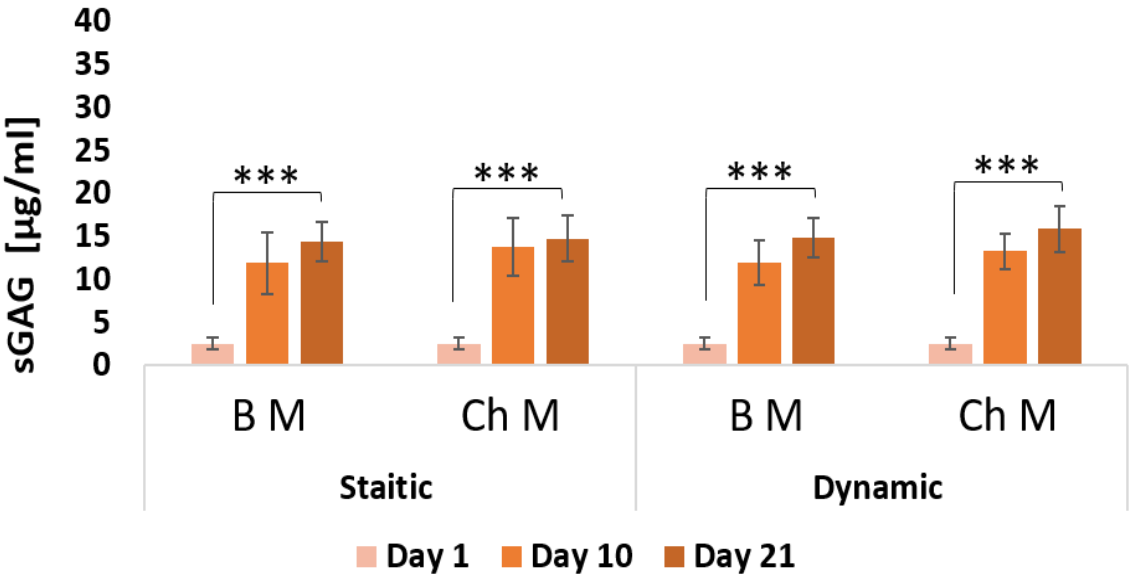

Figure 5. 15: The sGAG content was assessed by DMMB assay. *Graphs showed significant increase at day 10 and 20 for static and dynamic compared to day 1. No Significant differences were observed in B M and Ch M in both conditions at day 20 and day 10. Data are expressed as mean ± standard deviation (n = 30). ***$p \leq 0.001$.*

The results for experiment 1 (Figure 5.16) showed significant increases in the sGAG content at day 10 and 20 compared to day 1, for both static and dynamic groups ($P \leq 0.001$). In addition, significant increases at day 20 compared to day 10 were observed for all samples except for donor 2 and 5 B M dynamic and donor 6 B M, Ch M static.

Donor 6 revealed the lowest values for all conditions compared to the other donors. Whereas, the highest sGAG content was found for donor 5 Ch M dynamic gels. The comparison between static and dynamic groups showed no significant differences between the static and dynamic for each donor. Comparing between donors' performance revealed significant differences between donor 5 Ch M dynamic group and each donor 2, 8 and 13 Ch M dynamic group ($P \leq 0.05$) and donor 6 Ch M dynamic group ($P \leq 0.001$).

For experiment 2 (Figure 5.17), significant increases in the GAG content was observed at day 10 and 20 compared to day 1 for both static and dynamic groups ($P \leq 0.001$). Significant increases at day 20 compared to day 10 was found with some exceptions. The comparison between static and dynamic cultured showed significant differences between the static and dynamic groups for donor 2 ($P \leq 0.05$) and donor 6 ($P \leq 0.001$). The donor comparison for experiment 2 revealed significant differences between donor 6 Ch M dynamic and each donor 5 and 13 Ch M dynamic ($P \leq 0.05$).

Experiment 1

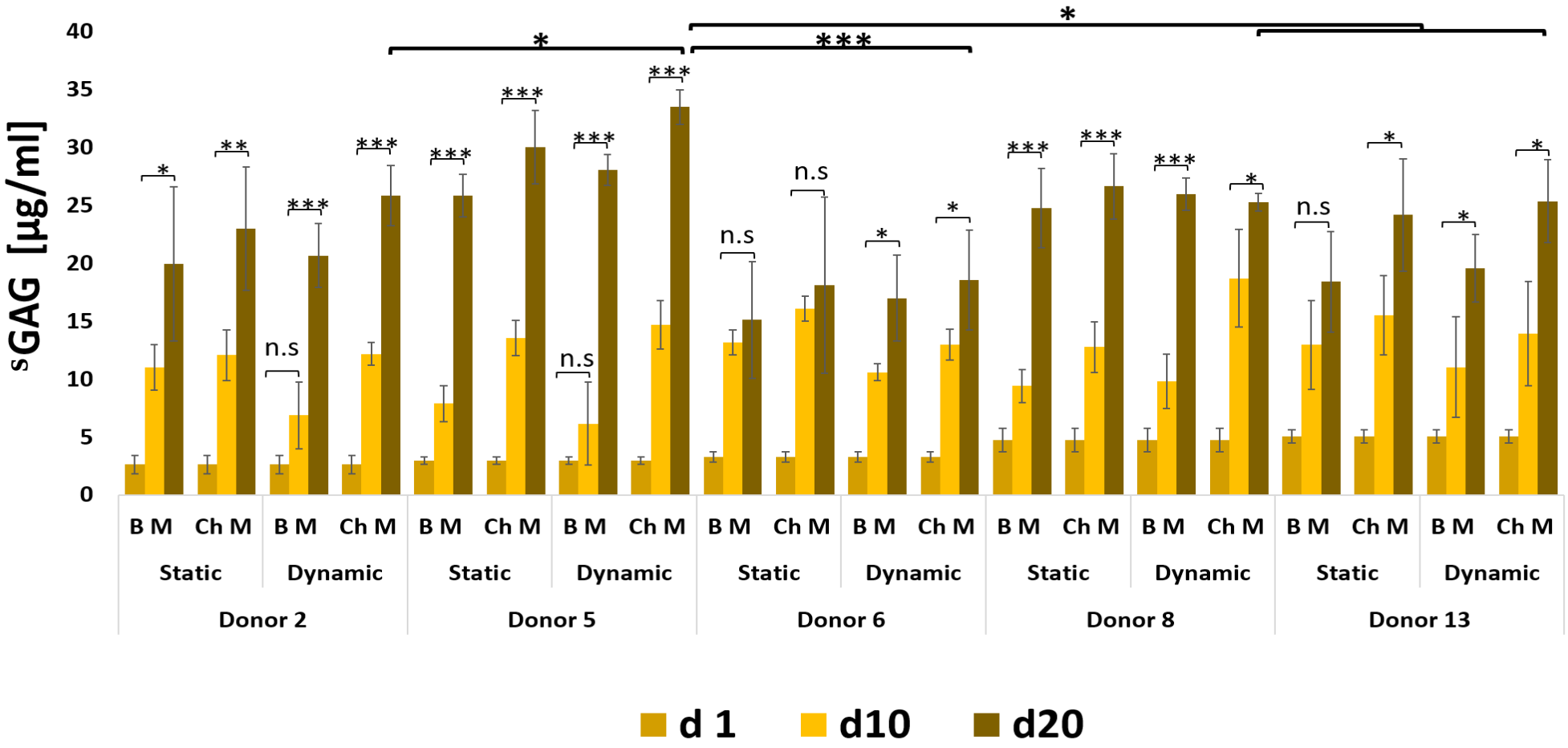

Figure 5. 16: GAG content for experiment 1. *The GAG content was assessed by DMMB assay. Graphs showed a significant increase at day 10 and 20 for static and dynamic compared to day 1 (significance not shown). Significant increases at day 20 compared to day 10 were observed for all samples except for donor 6 (B M and Ch M static) and donor 13 (B M, static). Donor 6 revealed the lowest values for all conditions compared with the other donors, Whereas, the best performing donor is donor 5 (ChM dynamic), which is significantly increased compared to donor 2,6,8 and 13(ChM dynamic) No significant differences were observed between the static and dynamic group of each donor for (Ch M). Data is expressed as mean ± standard deviation (n = 3). *p ≤ 0.05, **p ≤ 0.01, ***p ≤ 0.001.*

Experiment 2

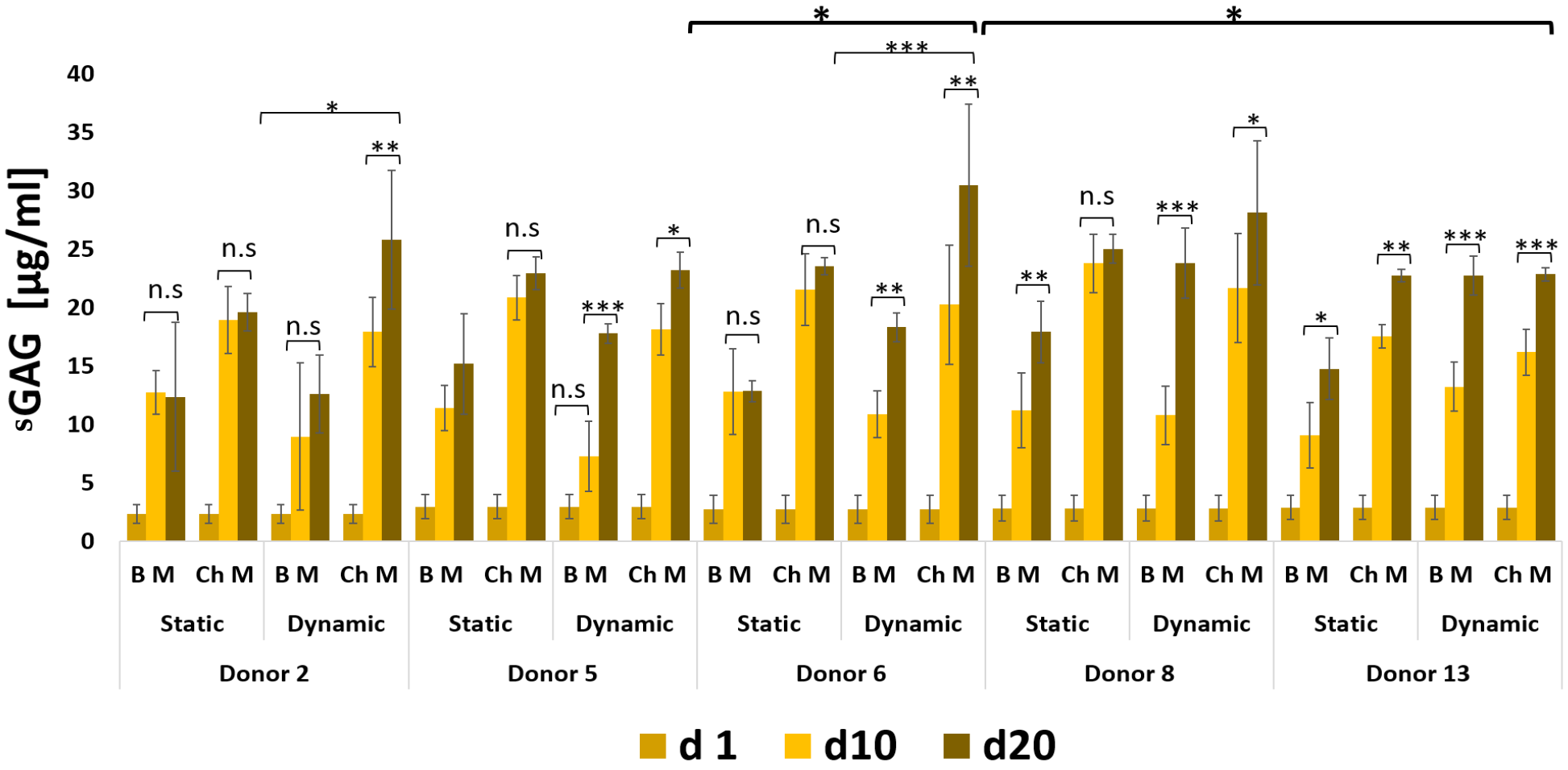

Figure 5. 17: sGAG content for experiment 2. *The GAG content was assessed by DMMB assay Graphs showed significant increase at day 10 and 20 for static and dynamic compared to day 1(significance not shown). There were significant increases in some conditions in day 20 compare to day 10. In contrast to experiment 1 donor 6 (Ch M dynamic) is the best donor's performance which is significantly differed from donor 5 and donor 13 (Ch M dynamic). For comparing the static and dynamic group of each donor there were significant differences between static and dynamic of each donor 2 and 6. Data are expressed as mean ± standard deviation (n = 3). *p ≤ 0.05, **p ≤ 0.01, ***p ≤ 0.001.*

5.5.6.3 sGAG content normalised to DNA content

To determine the sGAG content in relation to cell number, the sGAG content was normalised to the DNA content of the same samples. The results for both experiment 1 and 2 (Figure 5.18) showed significant increases (at $p \leq 0.001$) of the normalised sGAG for the Ch M in both condition static and dynamic at day 10 and day 20 compared to day 1. There were significant differences (at $p \leq 0.001$) between the Ch M and B M for each static and dynamic at day 10 as well as day 20.

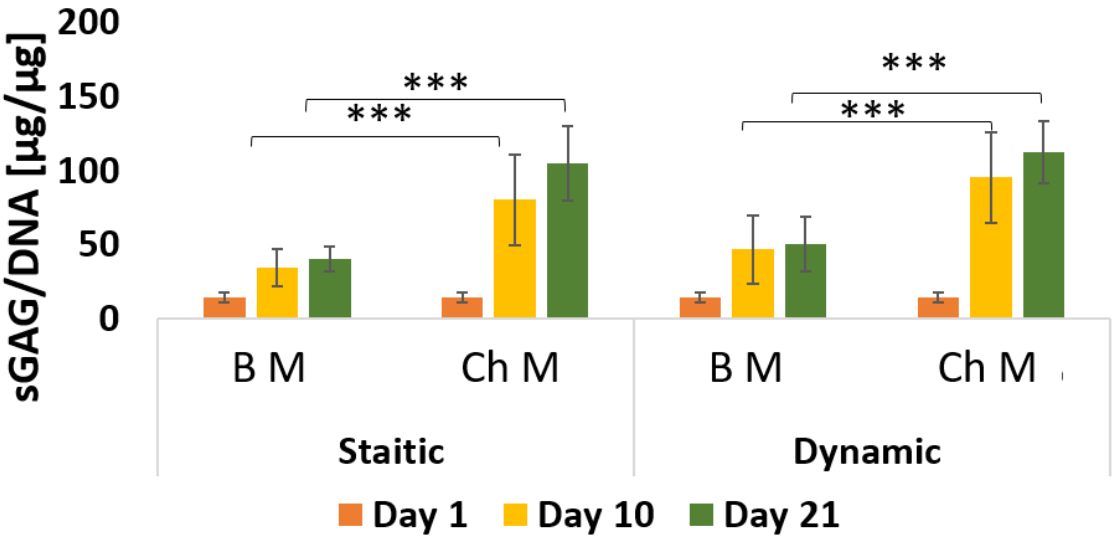

Figure 5. 18: sGAG content normalised to DNA content. *The graph showed significant increases at day 10 and day 20 compared to day 1 for all BM and Ch M (static and dynamic) (the significance not showed). No Significant differences were observed between dynamic and static for Ch M. Data are expressed as mean ± standard deviation (n = 30). ***p ≤ 0.001.*

For experiment 1, (Figure 5.19). The results showed that the normalised values were significantly increased across the experimental time, ($P \leq 0.05$, $P \leq 0.01$ $P \leq 0.001$) for all donors at most conditions, except for B M static for donor 2, 6 and 13, as well as B M dynamic group of donors 13. In general, the Ch M gels values were higher than the B M gels. The highest value was observed for donor 5 Ch M dynamic. While the lowest value was found for donor 6 Ch M dynamic. No significant differences were seen between static and dynamic gels for each donor. For comparing donors' performance, significant differences between the donor 5 Ch M dynamic and donor 6 Ch M dynamic ($P \leq 0.05$).

A similar trend was observed for experiment 2, (Figure 5.20). The results showed that the normalised values were significantly increased over 20 days ($P \leq 0.05$, $P \leq 0.01$ $P \leq 0.001$) for all donors and most conditions except for most of B M gel of the both (static and dynamic). Comparing the static and dynamic group within each donor, donor 2 was the only donor that showed significant difference between the static and dynamic group.

There were no any differences among the donors according to the donors' performance viability.

Experiment 1

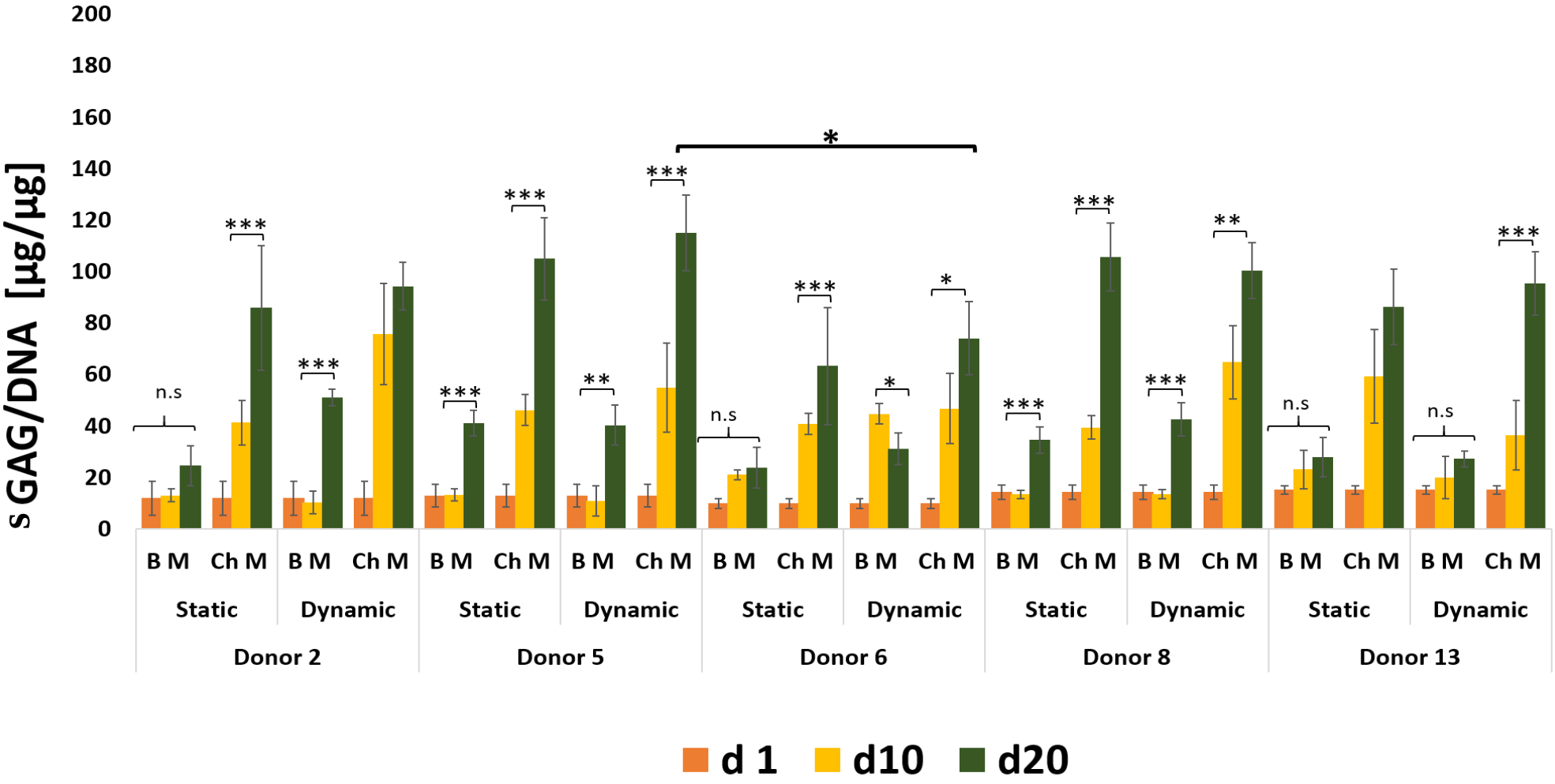

Figure 5. 19: sGAG content normalised to DNA content for experiment 1. *Normalised sGAG was increased across the experimental time ($p \leq 0.001$) for all donors at most conditions (significance not shown), except for BM static group (donor 2, 6 and 13) and BM dynamic (donor 13). There were no significant differences between the static and dynamic group for each donor. Donor comparison revealed significant difference between the donor 5 (ChM dynamic) and the donor 6 (ChM dynamic). Data are expressed as mean ± standard deviation (n = 3). *$p \leq 0.05$, **$p \leq 0.01$, ***$p \leq 0.001$.*

Experiment 2

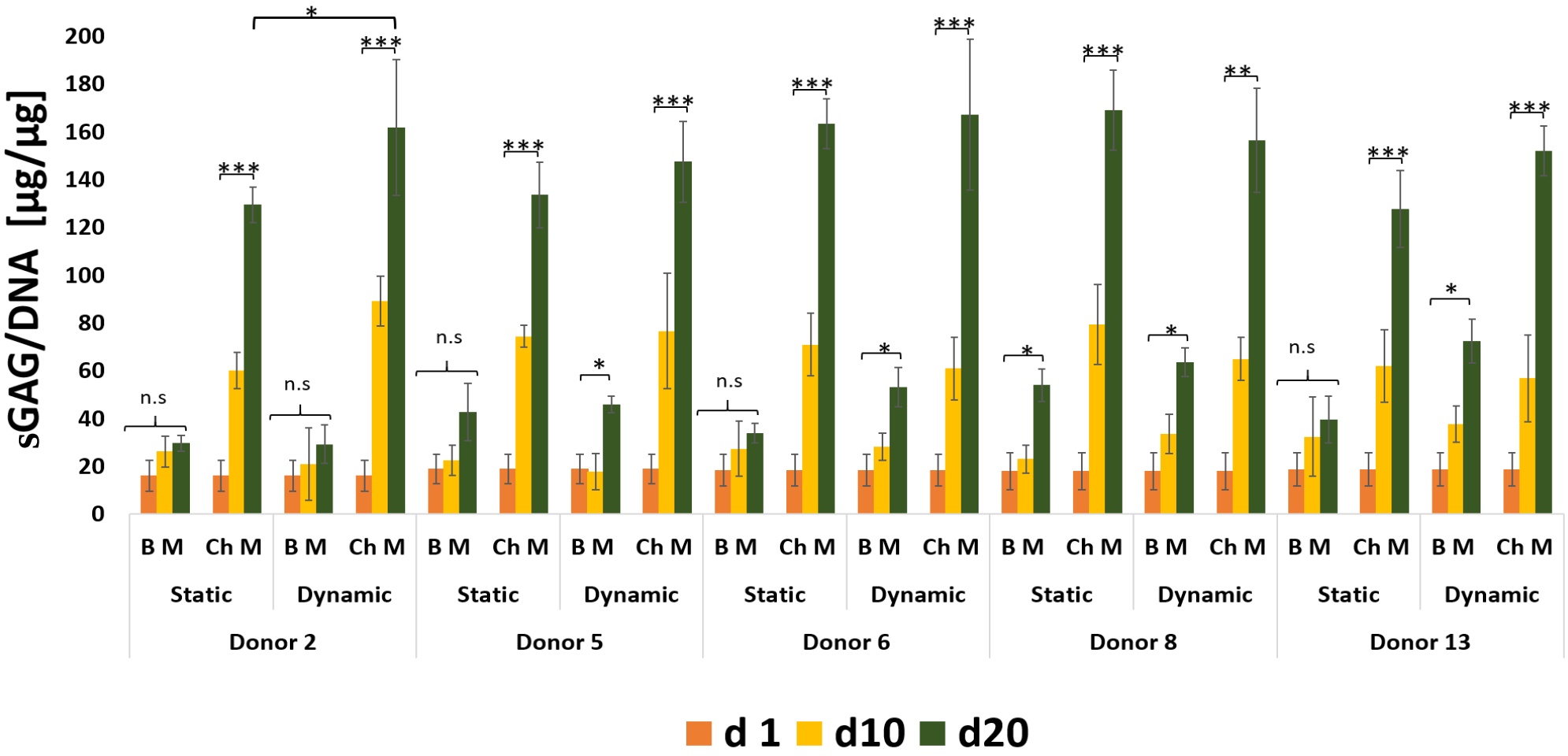

Figure 5. 20: sGAG content normalized to DNA content for experiment 2. *Experiment 2 follows same trends as experiment 1. Normalised sGAG at day 20 was significantly higher than at day 10 and day 1 for all ChM gels (significance not shown). While for the BM gels across time points ranged non-significant to significant ($p \leq 0.05$). Comparing the static and dynamic groups for each donor, significant differences were observed for donor 2. There were no any differences among the donors according to the donors' performance. Data are expressed as mean ± standard deviation (n = 3). *$p \leq 0.05$, **$p \leq 0.01$, ***$p \leq 0.001$.*

5.5.6.4 Total protein content

The total protein content in the gel samples was assessed using BCA Protein Assay. The results for both experiment 1 and 2 (Figure 5.21) showed significant increases (at $p \leq 0.001$) of the total protein for the Ch M in both condition static and dynamic at day 10 and day 20 compared to day 1. While for B M the results were varied. There were significant differences (at $p \leq 0.001$) between the Ch M and B M for each static and dynamic at day 10 as well as day 20. There is a significant difference at ($p \leq 0.05$) comparing the static and the dynamic group of the Ch M at day 20.

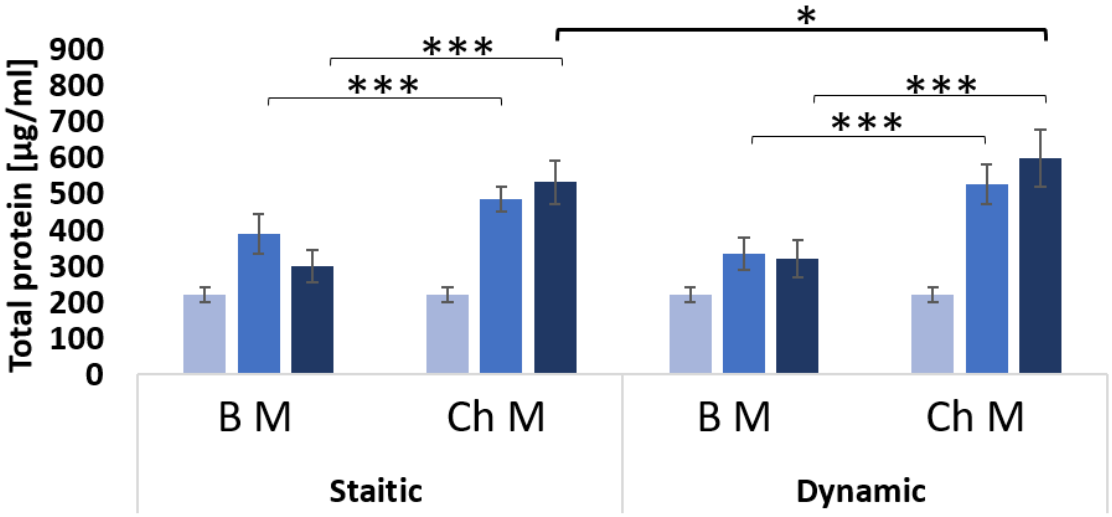

Figure 5. 21: Total protein content*. The total protein content in the gel samples was assessed using BCA Protein Assay, the results showed significant differences in total protein content in day 1 compared to day 10 and day 20 (not shown). In between B M and Ch M in static and dynamic groups the significant differences were found in day 10 and day 20. Between the static and dynamic group there is a significant difference for the Ch M at day 20. Data are expressed as mean ± standard deviation (n = 30). *p ≤ 0.05, ***p ≤ 0.001.*

For experiment 1 (Figure 5.22), the results showed the protein content of the gels was significantly increased at day 10 but decreased either between non-significantly to significantly at day 20. The protein content values dropped in most conditions except donor 13 Ch M static and dynamic. The highest values were observed for donor 2 Ch M dynamic. While the lowest value was in donor 13 Ch M dynamic. For comparing between static and dynamic group, significant differences between the static and dynamic groups were found for donor 2 only. No significant differences were observed when comparing the five donors' performance in experiment 1.

For experiment 2 (Figure 5.23) the increases in the total were progressive and significant at day 10 and day 20 comparing to day 1 ($P \leq 0.001$). For comparing static with dynamic groups, significant differences were observed for donor 2 and donor 8. For donor's comparison, significant differences between the donor 5 Ch M dynamic and donor 6 Ch M dynamic ($P \leq 0.05$) and donor 13 Ch M dynamic ($P \leq 0.001$).

Experiment 1

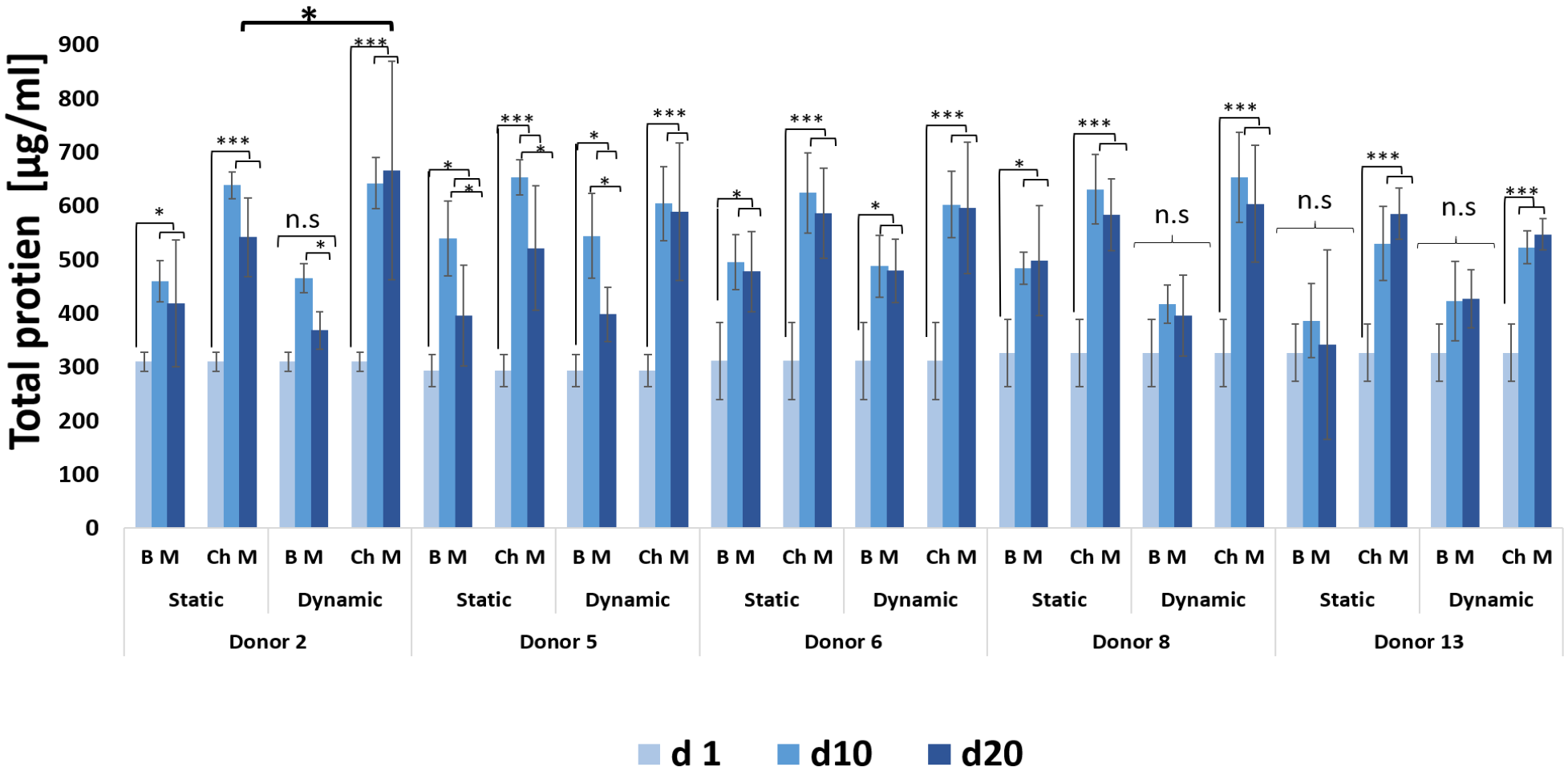

Figure 5. 22: Total protein content for experiment 1. *The total protein content in the gel samples was assessed using BCA Protein Assay, the results showed increasing in total protein content in day 10 samples and stopped at the level or slightly drop at day 20. Significant differences between the static and dynamic groups were found for donor 2 only. There were no differences for the experiment 1 when comparing between donors' performance among the five donors. Data are expressed as mean ± standard deviation (n = 3). *p ≤ 0.05, **p ≤ 0.01, ***p ≤ 0.001.*

Experiment 2

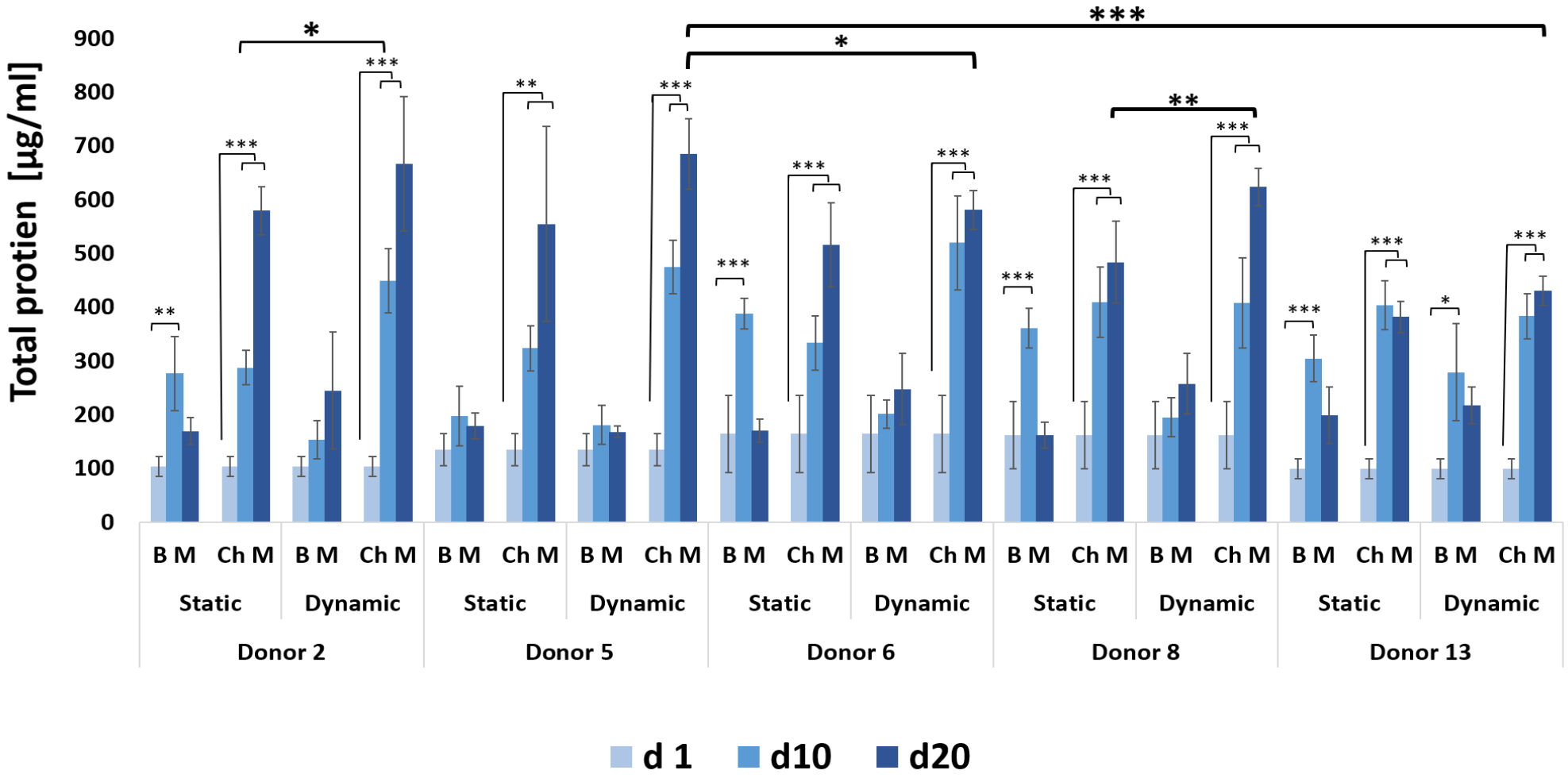

Figure 5. 23: Total protein content for experiment 2. *The total protein content in the gel samples was assessed using BCA Protein Assay, the results showed increasing in total protein content in day 10 and day 20 compare to day 1, the progressive increasing between day 10 and day 20 was significant for all (Ch M gels) . Significant differences between the static and dynamic groups were found for donor 2 only. For donor's comparison significant differences between the donor 5 (Ch M dynamic) and donor 6 and donor 13 (Ch M dynamic). Data are expressed as mean ± standard deviation (n = 3). *p ≤ 0.05, **p ≤ 0.01, ***p ≤ 0.001.*

5.5.6.5 Total protein content normalised to DNA content

The total protein content was normalised to the DNA content of the same samples to determine the total protein content in relation to cell number (Figure 5.24). The results showed that the normalised values were decrease (but not significantly) for the B M whereas significantly increased for Ch M across the experimental times. There were significant differences (at $p \leq 0.001$) between the Ch M and B M for each static and dynamic at day 10 as well as day 20. No significant differences were observed for the Ch M between static and dynamic group at day 20.

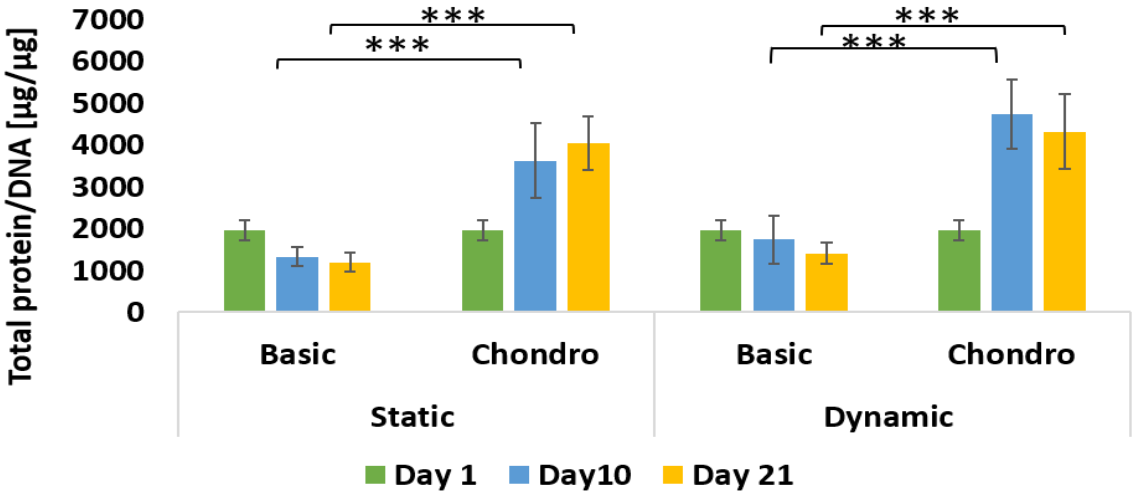

Figure 5. 24: Total protein content normalised to DNA content. *The results showed that the normalised protein/ DNA significantly increased for C hM samples at day 10 and day 20 compare to the day 1. Comparing B M and Ch M, significant differences were observed in day 10 and day 20 in both conditions. There is no significant difference between the Ch M static and dynamic at day 20. Data are expressed as mean ± standard deviation (n = 30). ***$p \leq 0.001$.*

For experiment 1 (Figure 5.25). the normalised protein/ DNA content was significantly increase for Ch M samples at day 10 and day 20 ($P \leq 0.001$) compare to day 1. However, there is no differences between day 10 and day 20. For comparing static and dynamic gels, significant difference was only observed for donor 2. No statistically significant differences were found when comparing the five donors performance at day 20 Ch M.

For experiment 2 (Figure 5.26) normalised protein/ DNA were significantly and progressively increased for Ch M samples at day 10 and day 20, day 20 is significantly higher than day 10 for all donors' Ch M dynamic group ($P \leq 0.001$), but not significant for Ch M static except donor 13. The comparison between static and dynamic gels showed significant difference for donor 2 only. Comparing among the donors, significant differences were found between donors 2 Ch M dynamic and each of donor 5 and 8 Ch M dynamic ($P \leq 0.01$).

Experiment 1

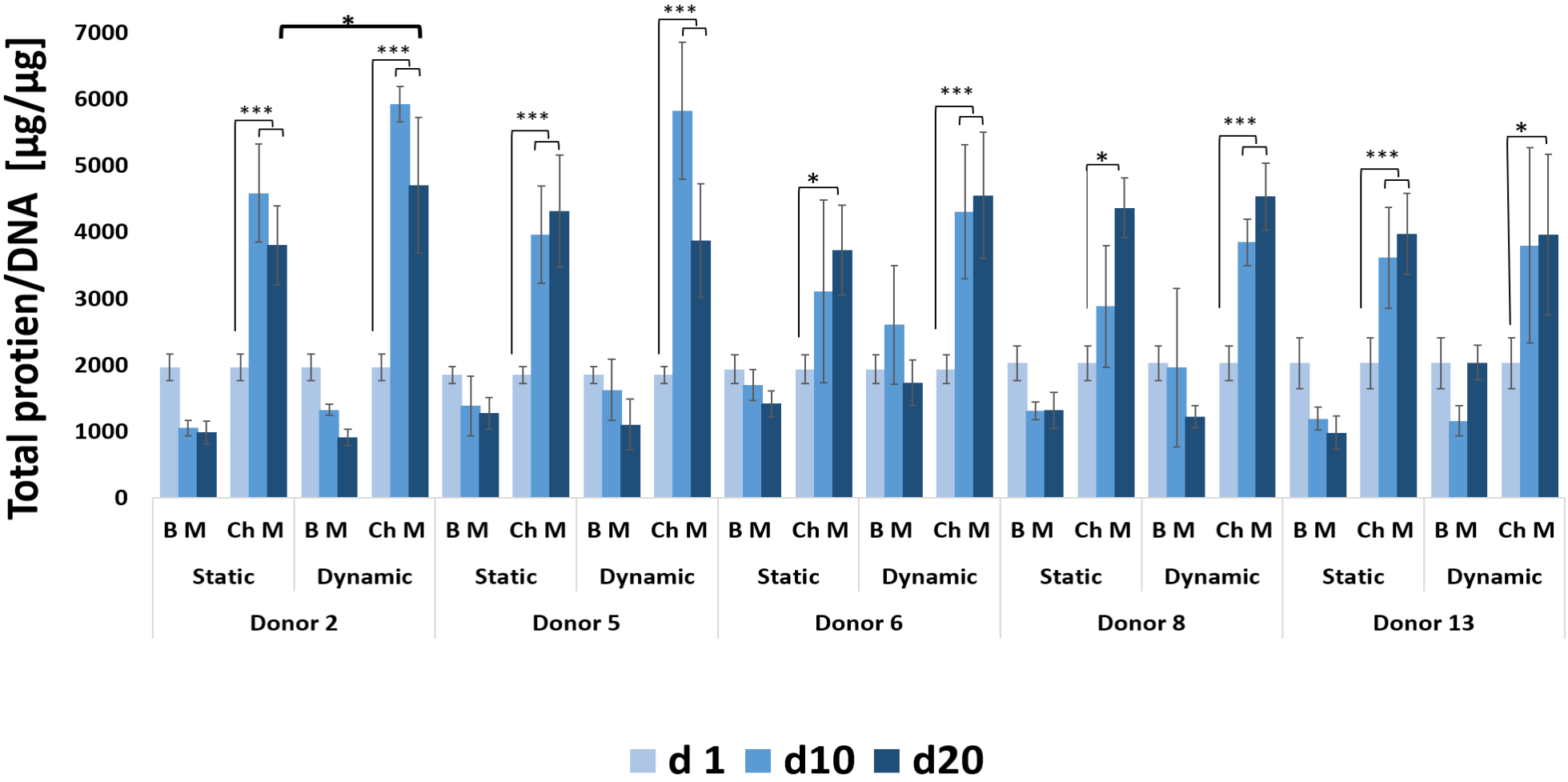

Figure 5. 25: Total protein content normalised to DNA content for experiment 1. *The results showed that the normalised protein/ DNA for experiment 1 was significantly increased for ChM samples at day 10 and day 20 compare to the day 1. No significant differences between day 10 and day 20. For comparing static and dynamic gels, significant difference for the donor 2 was observed. There were no differences comparing between donors' performance among the 5 donors. Data are expressed as mean ± standard deviation (n = 3). *p ≤ 0.05, **p ≤ 0.01, ***p ≤ 0.001.*

Experiment 2

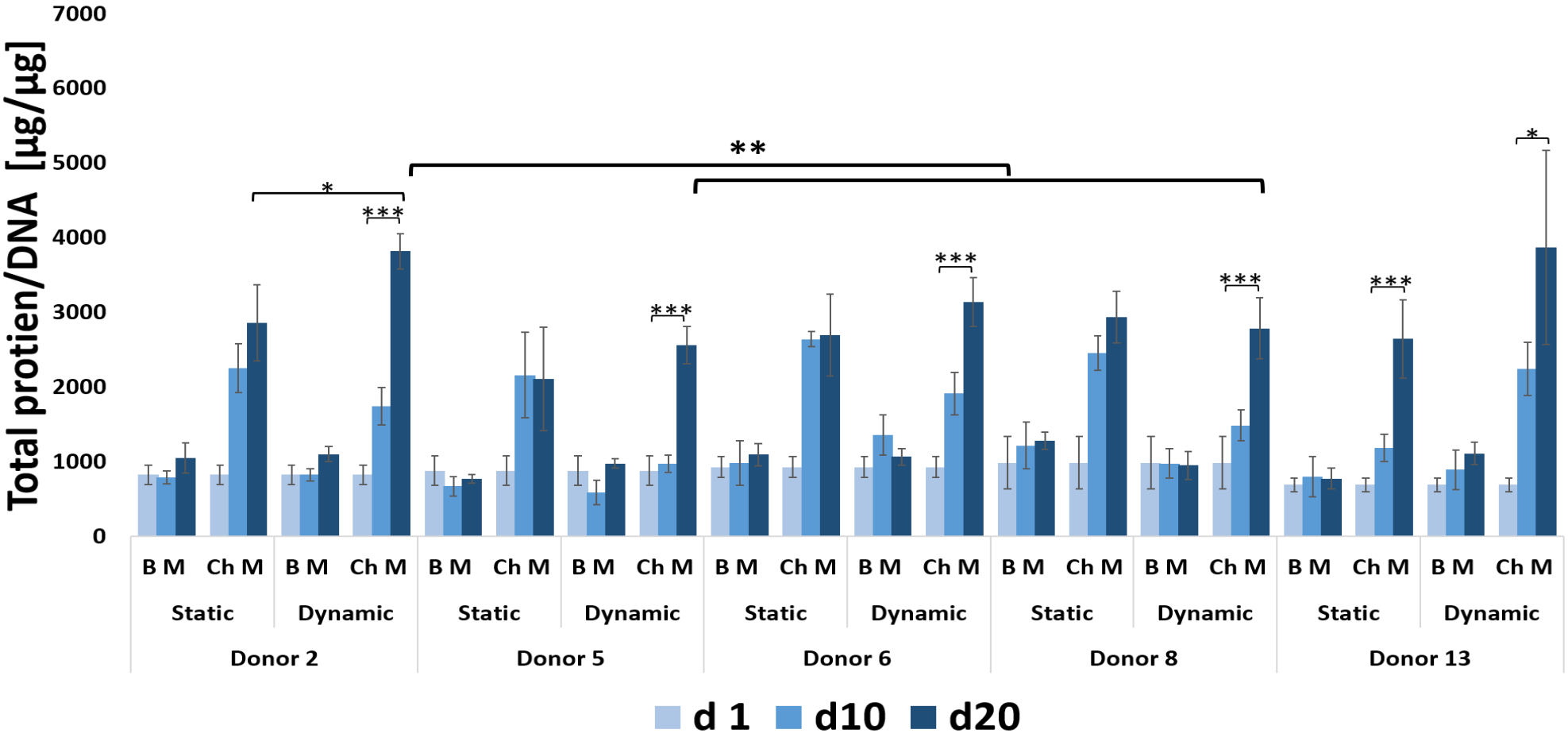

Figure 5. 26: Total protein content normalised to DNA content for experiment 2. *The results showed that the normalised protein/ DNA content for experiment 2 were significantly and progressively increased for ChM samples at day 10 and day 20 compared to day 1. Day 20 is significantly higher than day 10 for all donors' (ChM dynamic), but not significant for ChM static except for donor 13. For comparing static and dynamic gels, significant difference for donor 2was observed. The comparison of individual donors with each other revealed significant differences (for ChM dynamic) between donor 2 and each of donor 5 and donor 8. Data are expressed as mean ± standard deviation (n = 3). *p ≤ 0.05, **p ≤ 0.01, ***p ≤ 0.001.*

5.5.6 .6 Total collagen content

The total collagen content of the oMSCs -seeded gels was assessed using Chondrex Sirius Red Collagen detection Kit (chapter 2, section 2.6.4). The data for experiment 1 and 2 (Figure 5. 27) showed significant increases in total collagen content for ChM ($P \leq 0.01$) across the experimental time. However, there were none -significant drop in the values at day 20 compare to day 10 in Ch M of both static and dynamic group. $p \leq 0.0001$. there were significant differences between Ch M and B M of both static and dynamic condition at day 10 as well as day 20 ($p \leq 0.001$). There is no significant differences between static and dynamic for Ch M at day 20.

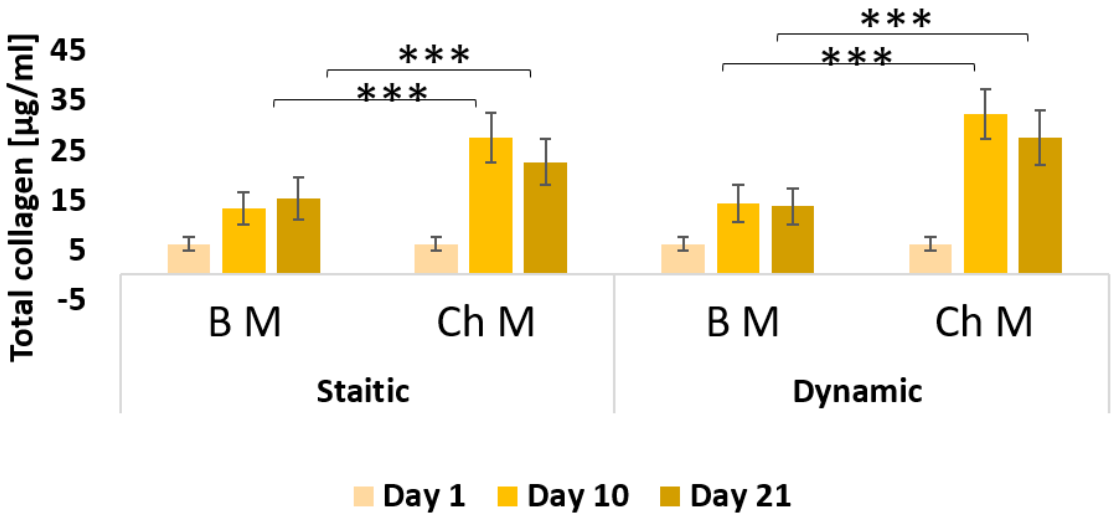

Figure 5. 27: Total collagen content. *The total collagen content of the oMSCs -seeded gels was assessed using Chondrex Sirius Red Collagen detection Kit, the collagen content significantly increased for B M and Ch M at day 10 and day 20 compared to day 1 (significance not shown). Comparing B M and Ch M in static with dynamic gels, significant differences were observed in day 10 and day 20. There were no significant differences between the static and dynamic group for the Ch M at day 10. Data are expressed as mean ± standard deviation (n = 30). ***p ≤ 0.001.*

For experiment 1 (Figure 5.28). the collagen content was significantly increase for Ch M samples at day 10 and day 20 ($P \leq 0.001$). For comparing between static with dynamic gels, significant differences were observed for donor 2 ($P \leq 0.01$). There were no significant differences for the experiment 1 when comparing the five donors' performance with each other.

For the experiment 2(Figure 5.29), the results show significant differences between the day 1, day 10 and day 20 However, most gels dropped at day 20 but not significantly compare to day 10). Comparing static with dynamic gels, significant differences for donor 2, 5, 6 and 8 were found. There were no differences when comparing the five donors' performance with each other.

Experiment 1

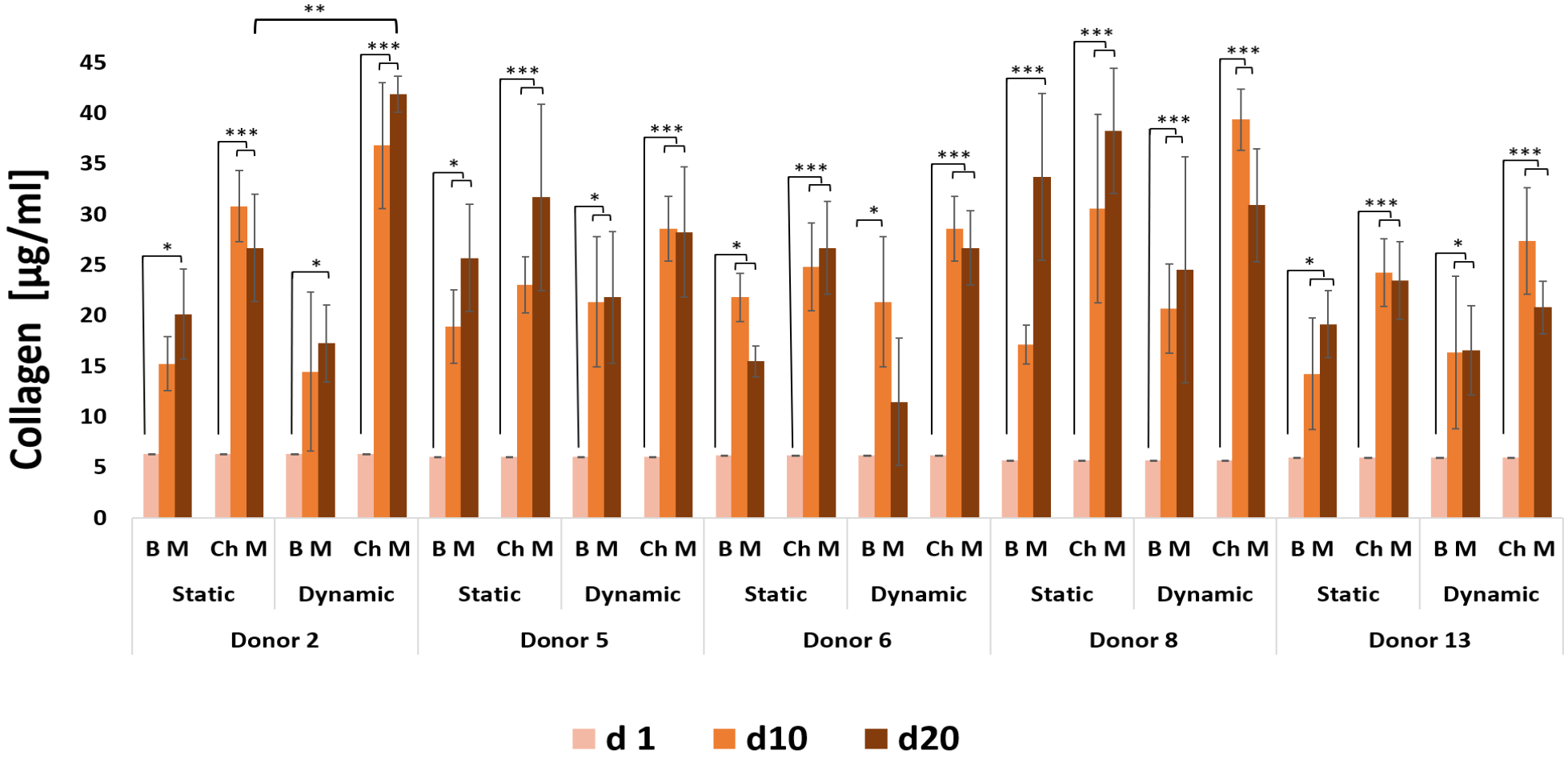

Figure 5. 28:Total collagen content for experiment 1. *The total collagen content of the oMSCs -seeded gels was assessed using Chondrex Sirius Red Collagen detection Kit. The results showed that the collagen content was significantly increase for Ch M samples at day 10 and day 20 compared to day 1. For comparing between static with dynamic gels, significant differences were observed for donor 2 ($p \leq 0.01$). There were no significant differences for the experiment 1 when comparing the five donors' performance with each other. Data are expressed as mean ± standard deviation (n = 3). *$p \leq 0.05$, **$p \leq 0.01$, ***$p \leq 0.001$.*

Experiment 2

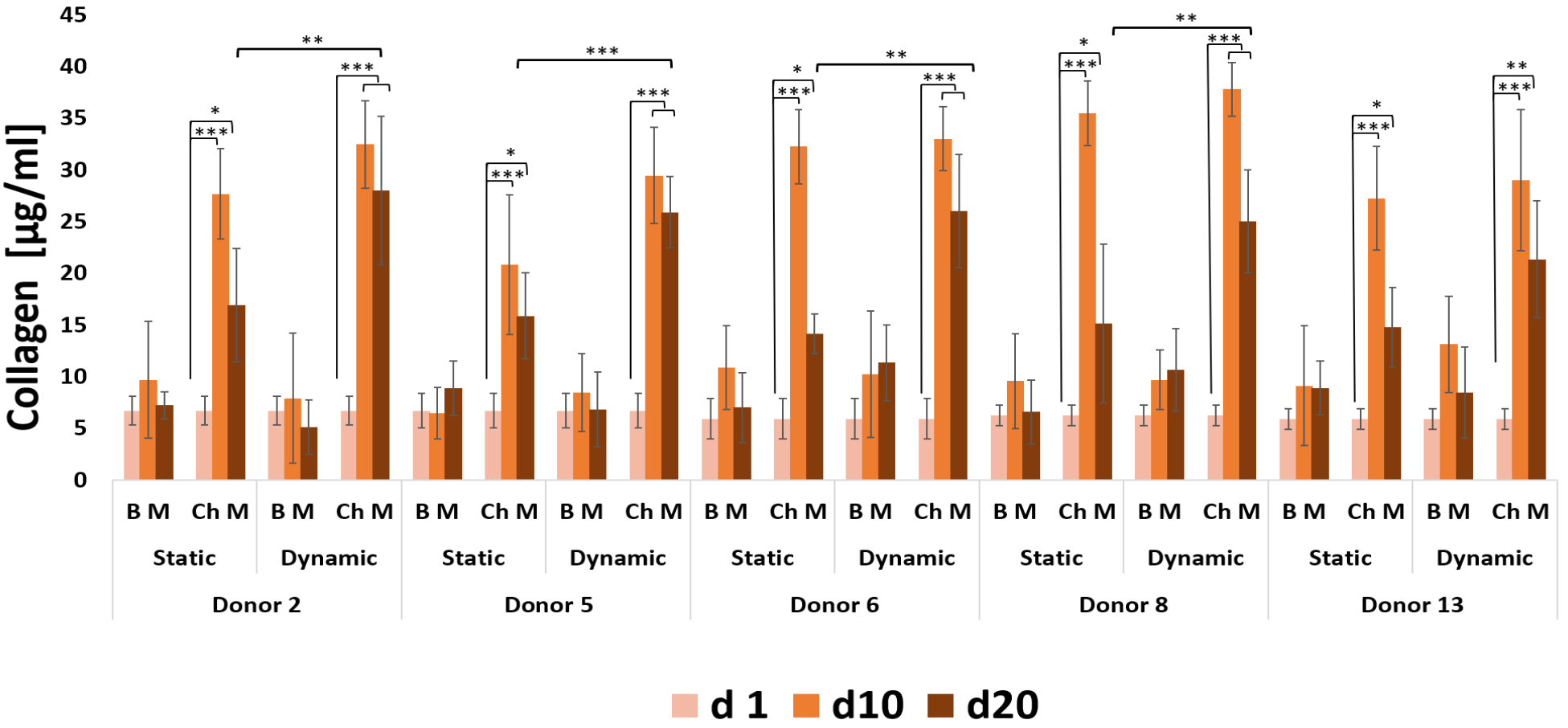

Figure 5. 29:Total collagen content for experiment 2. *The total collagen content of the oMSCs -seeded gels was assessed using Chondrex Sirius Red Collagen detection Kit. The results showed significant differences between the day 1, and each day 10 and day 20. However, most gels dropped at day 20 but not significantly compare to day 10. Comparing static with dynamic gels, significant differences for donor 2, 5 ,6 and 8 were found. There were no differences when comparing the five donors' performance with each other. Data are expressed as mean ± standard deviation (n = 3). *p ≤ 0.05, **p ≤ 0.01, ***p ≤ 0.001.*

5.5.6.7 Total collagen content normalised to DNA content

Total collagen content was normalised to the DNA content of the same samples to determine the total collagen content in relation to cell number. The data for both experiment 1 and 2 were showed in figure 5.30. The results showed no significant differences for the B M gels across the experiment time. Whereas for Ch M gels there were significant differences ($p \leq 0.001$) at day 10 and day 20 compare with day 1. However, there were drop in the normalised collagen for the Ch M static group. There were significant differences between B M and Ch M for both static and dynamic group day 10 day 20. Comparing between the static versus dynamic for Ch M there were significant differences between day 10 ($p \leq 0.05$) as well as day 20 ($p \leq 0.001$).

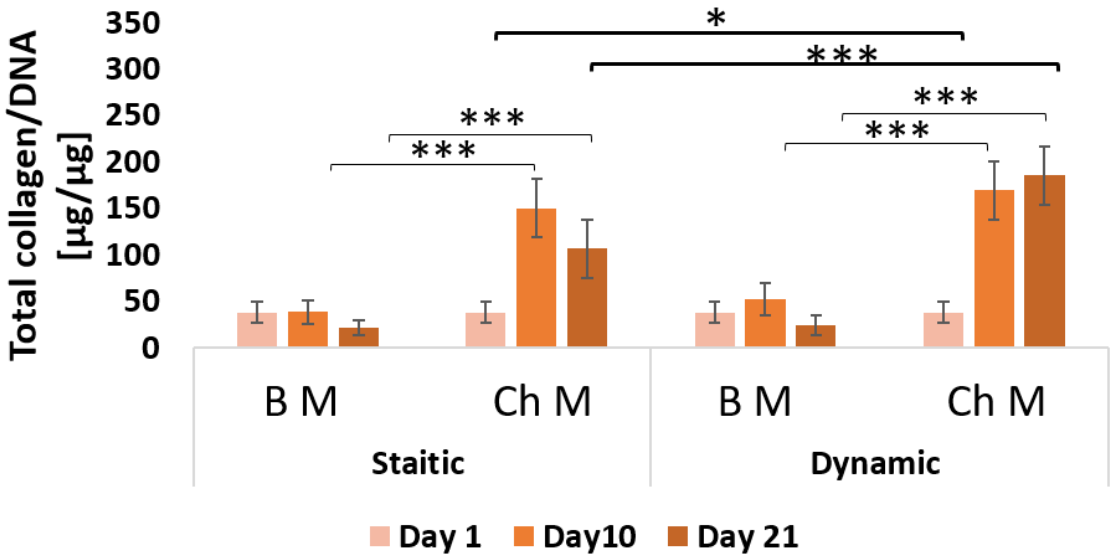

Figure 5. 30: Total collagen content normalised to DNA content. *The normalised collagen/ DNA content significantly increased at day 10 and 20 compared to day 1 for Ch M but not for B M in static and dynamic (significance not shown). There were significant differences between B M and Ch M at both static and dynamic group day 10 day 20. Comparing between the static versus dynamic for Ch M there were significant differences between day 10 as well as day 20. Data are expressed as mean ± standard deviation (n = 30). *$p \leq 0.05$, ***$p \leq 0.001$.*

For experiment 1 (Figures 5.31) the normalised collagen/ DNA content was significant different between day 1, day 10 and 20 ($P \leq 0.001$). Comparing static with dynamic gels showed significant differences for donor 2 and 6 ($P \leq 0.001$) and donor 5 ($P \leq 0.01$). Significant differences were also observed when comparing donors with each other, for donor 2 and each of donor 5, 6, 8 and 13 ($P \leq 0.001$).

For the experiment 2 (Figure 5.32) the results showed significant differences between day 1, day 10 and day 20, for all Ch M static and dynamic gels. For comparing static with dynamic gels, significant differences were observed for donor 2, 5, and 6, ($P \leq 0.001$, $P \leq 0.01$, and $P \leq 0.05$) respectively. Regarding the donors' performance variation of the experiment 2, there were significant differences between donor 2 Ch M dynamic and each of donor 5, 6, 8 and 13 Ch M dynamic ($P \leq 0.001$).

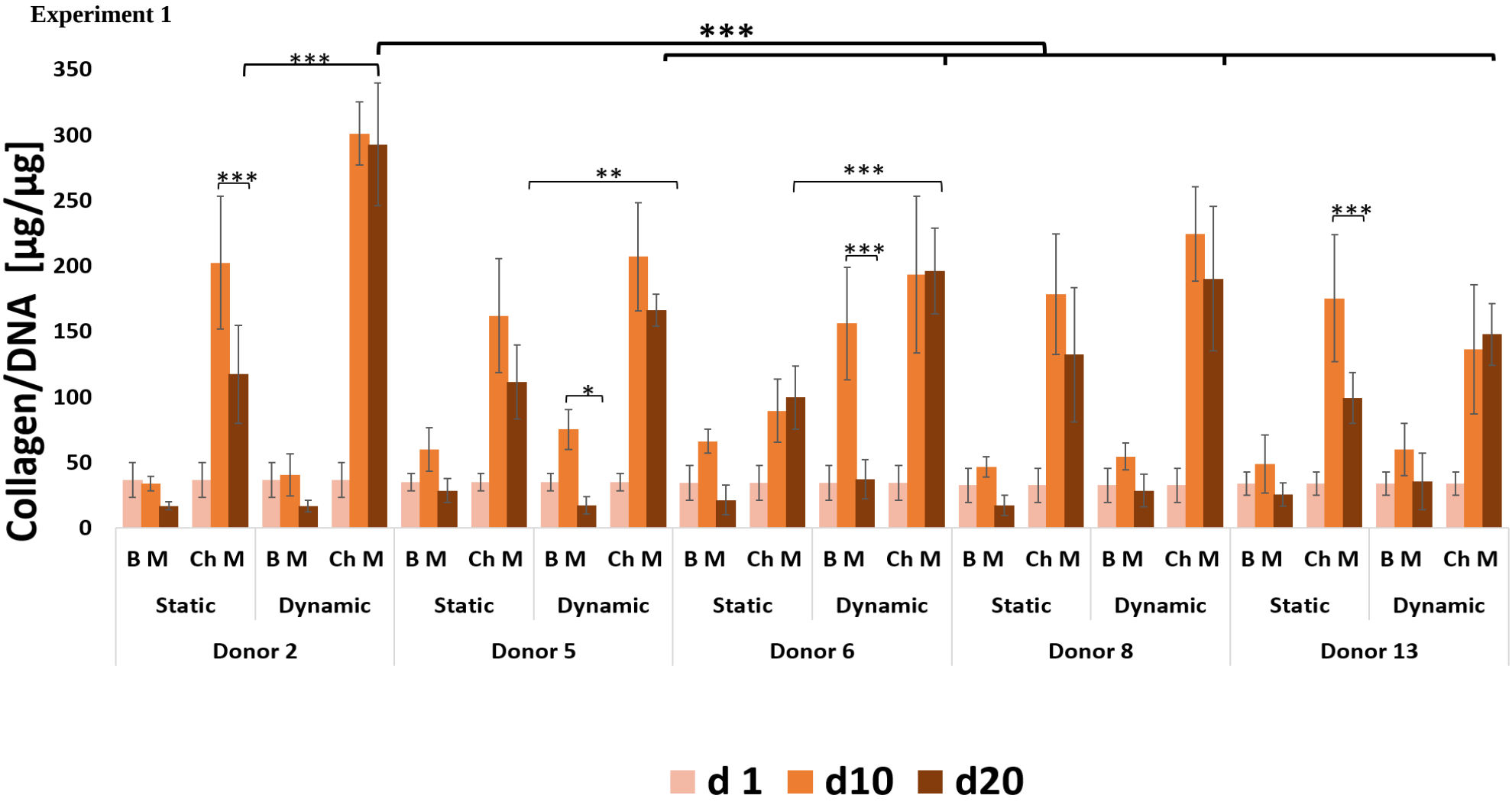

Figure 5. 31: Total collagen content normalised to DNA content for experiment 1. *The normalised collagen/ DNA content was significantly increases, at day 10 and 20 compare to day 1 (significance not shown). Comparing static with dynamic gels, showed significant differences for donor 2, 6 donor 5. Significant differences were also observed when comparing donors with each other for donor 2 and each of donor 5, 6, 8 and 13. Data are expressed as mean ± standard deviation (n = 3). *p ≤ 0.05, **p ≤ 0.01, ***p ≤ 0.001.*

Experiment 2

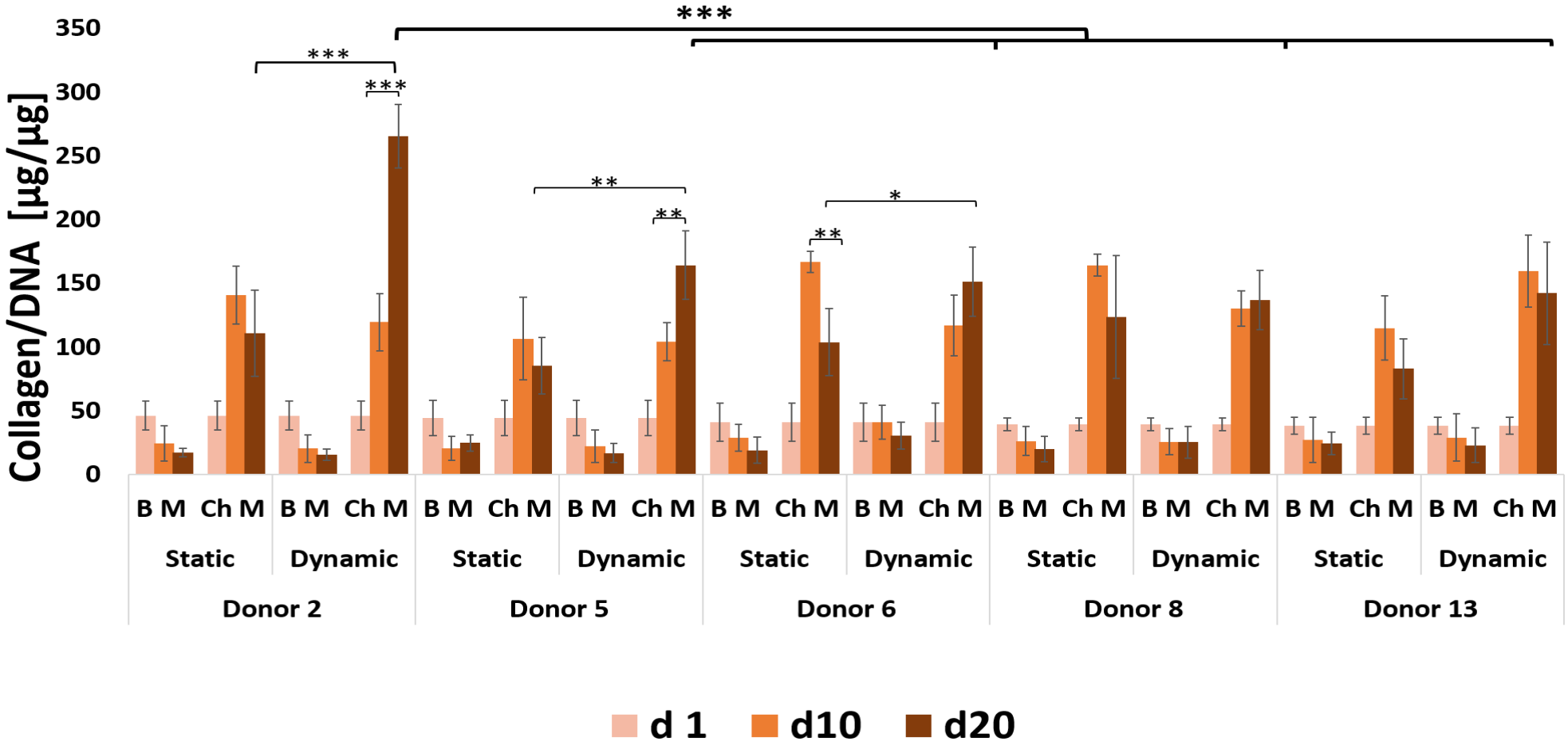

Figure 5. 32: Total collagen content normalised to DNA content for experiment 2. *The normalised collagen/ DNA content was significantly increased, at day 10 and 20 compare to day 1 (significance not shown). For comparing static with dynamic gels, significant differences were observed for donor 2, 5, and 6. Regarding the donors' performance variation, there were significant differences between donor 2 (Ch M dynamic) and each of donor 5, 6, 8 and 13 (Ch M dynamic). Data are expressed as mean ± standard deviation (n = 3). *p ≤ 0.05, **p ≤ 0.01, ***p ≤ 0.001.*

5.5.6.8 Total collagen content normalised to total protein content

Total collagen content was normalised to the total protein content of the same samples to determine the total collagen content in relation to the total protein in the samples. The data for both experiment 1 and 2 were showed in figure 5.33. The results showed no significant differences for the B M gels across the experiment time. Whereas for Ch M gels there were significant increases ($p \leq 0.001$) at day 10 compare with day 1. However, there were drop in the collagen/ protein ratio for the Ch M static and dynamic group at day 20. There were significant differences between B M and Ch M for static group at day 10 and day 20. But for dynamic group there was significant difference only for day 10. Comparing between the static versus dynamic for Ch M there was no significant difference at day 10 and day 20.

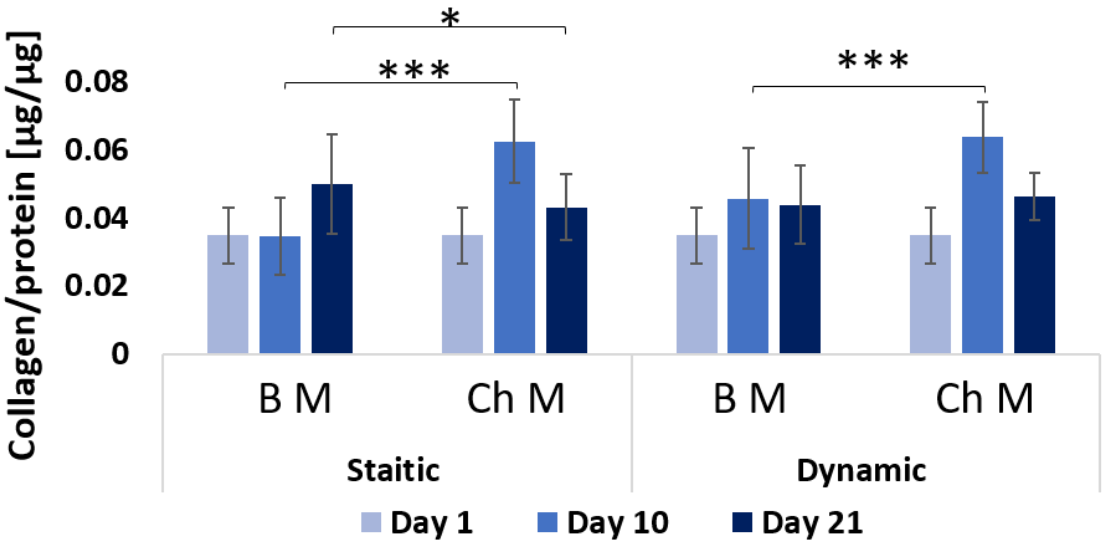

Figure 5. 33: Total collagen content normalised to total protein content. *The normalised total collagen/ total protein content significantly increased at day 10 but decrease for day 20 compared to day There were significant differences between B M and Ch M for static group at day 10 and day 20. But for dynamic group there was significant difference only for day 10. Comparing between the static versus dynamic for Ch M there was no significant difference at day 10 or day 20. Data are expressed as mean ± standard deviation (n = 30). *$p \leq 0.05$, **$p \leq 0.01$, ***$p \leq 0.001$.*

Total collagen content normalised to total protein content for experiment 1 (Figure 5.34), the normalised total collagen/ total protein content was significantly increased, at day 10 and 20 compare to day1 except donor 6 day 20 BM. Comparing static with dynamic gels, showed significant differences for donor 2 only (at $p \leq 0.001$). Significant differences were also observed when comparing donors with each other for donor 2 and 13 (at $p \leq 0.001$).

Total collagen content normalised to total protein content for experiment 2 (Figure 5.35), the normalised collagen/ total protein content was significantly increased, at day 10 but not for day 20 compare to day 1. For comparing static with dynamic gels, significant differences were observed for donor 6. Regarding the donors' performance variation, there were significant differences between donor 5 (Ch M dynamic) and each of donor 8 and 13 (Ch M dynamic).

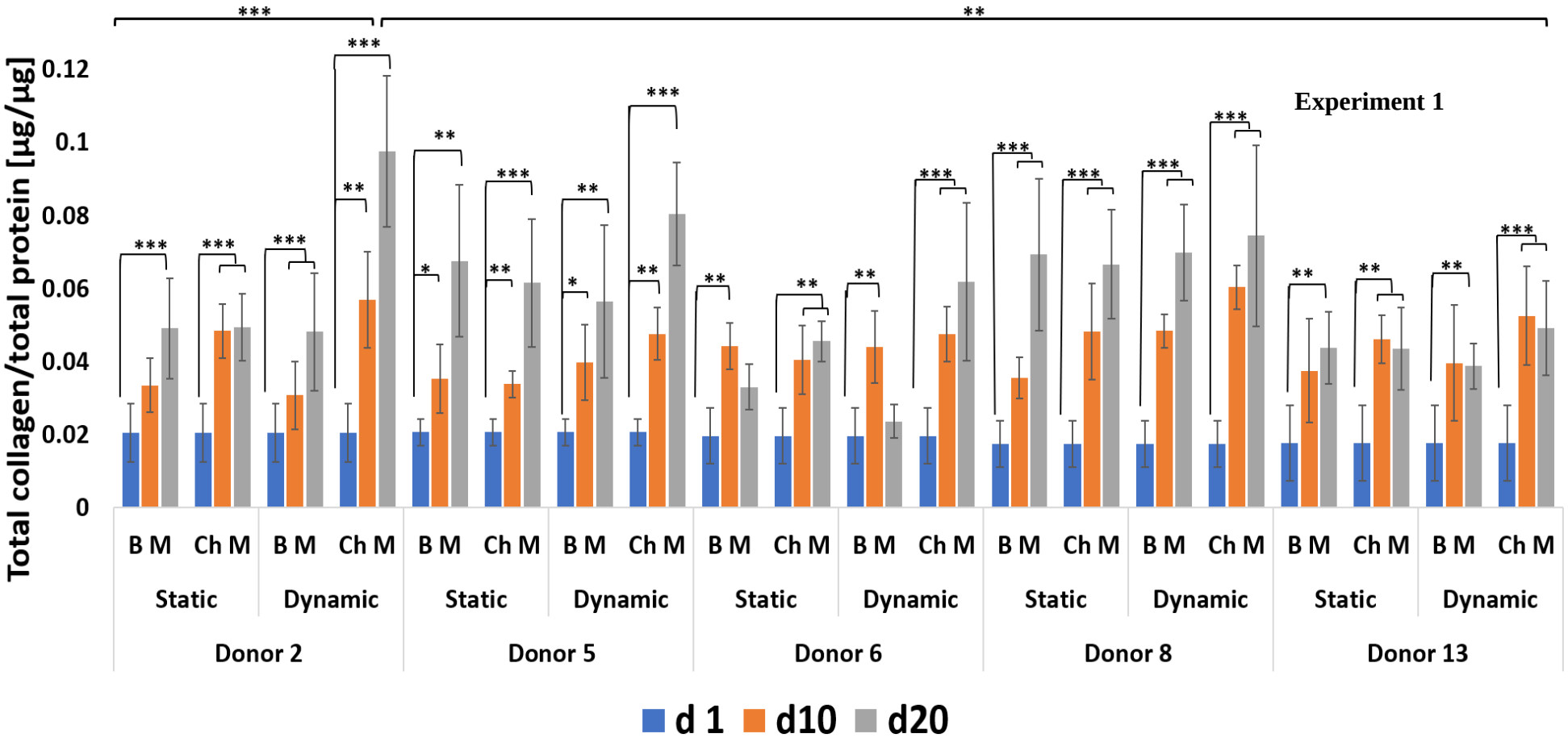

Figure 5. 34: Total collagen content normalised to total protein content for experiment 1. *The normalised total collagen/ total protein content was significantly increased, at day 10 and 20 compare to day1 except donor 6 day 20 BM. Comparing static with dynamic gels, showed significant differences for donor 2 only. Significant differences were also observed when comparing donors with each other for donor 2 and 13. Data are expressed as mean ± standard deviation (n = 3). *p ≤ 0.05, **p ≤ 0.01, ***p ≤ 0.001.*

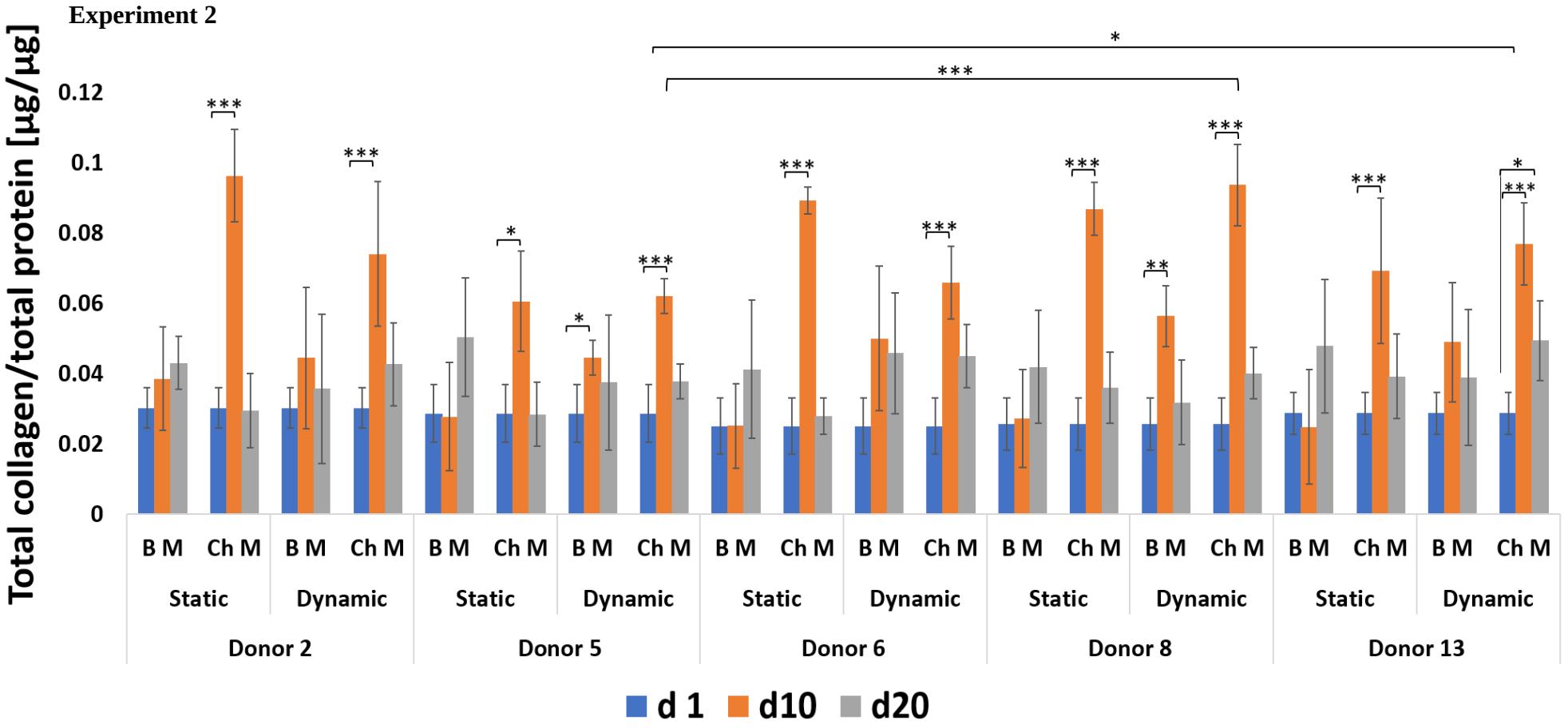

Figure 5. 35: Total collagen content normalised to total protein content for experiment 2. *The normalised collagen/ total protein content was significantly increased, at day 10 but not for day 20 compare to day 1. For comparing static with dynamic gels, significant differences were observed for donor 6. Regarding the donors' performance variation, there were significant differences between donor 5 (Ch M dynamic) and each of donor 8 and 13 (Ch M dynamic). Data are expressed as mean ± standard deviation (n = 3). *p ≤ 0.05, **p ≤ 0.01, ***p ≤ 0.001.*

5.5.8 Histology and immunohistology

5.5.8.1 Staining of native sheep cartilage and acellular gels

In order to compare the histological and immunohistology stains of the 3D collagen gels, a positive (native sheep cartilage) and negative control (acellular gel) were prepared and stained using same histological and immunohistological staining that used for experimental gel (Figures 5.36 and 5.37).

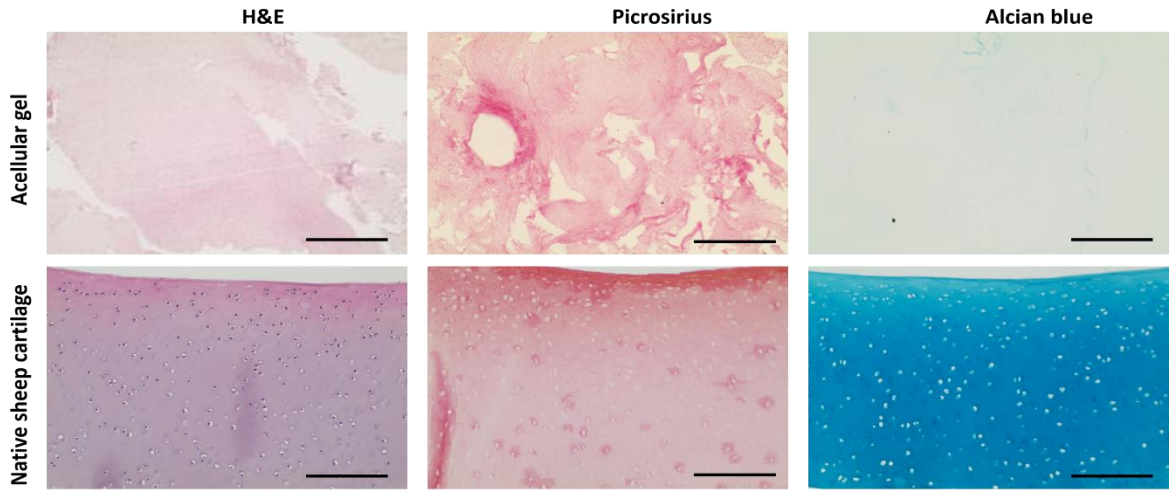

Figure 5. 36: Negative and positive control for histology. *Bright field micrographs of the histological stains H&E, Picrosirius and Alcian blue of 7 µm paraffin sections of an acellular gel and native sheep cartilage were taken at x20 magnification, scale bar = 150µm.*

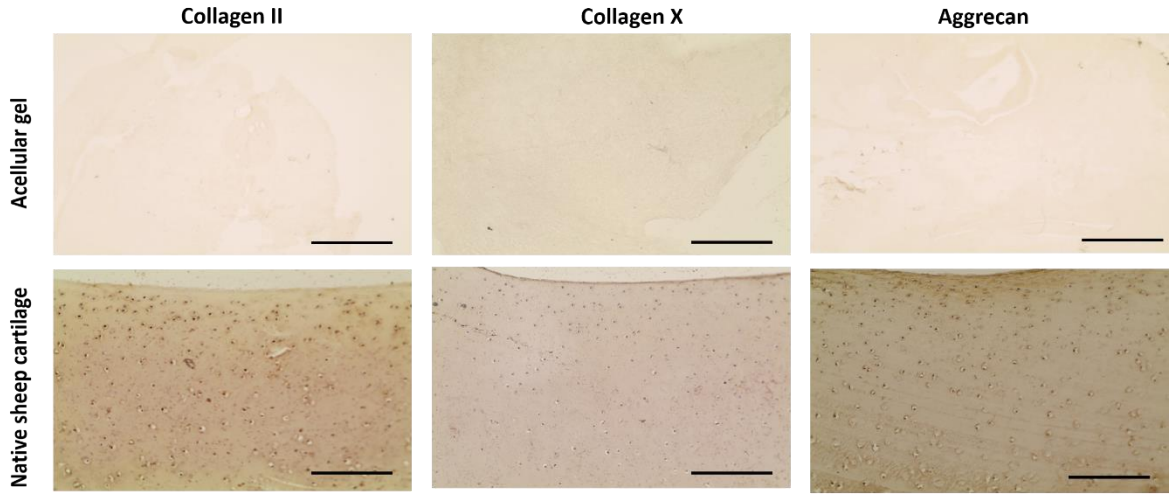

Figure 5. 37: Negative and positive control for immunohistology. *Bright field micrographs of immunohistology stains for collagen-type II, collagen type-X and aggrecan of 7 µm paraffin sections of an acellular gel and native sheep cartilage were taken at x20 magnification, scale bar = 150µm.*

5.5.8.2 Hematoxylin and eosin staining (H & E)

The bright field micrographs of H and E staining for both experiment 1 (Figure 5.38) and experiment 2 (Figure 5.39) on day 20 revealed differences between B M and Ch M treated gels. The B M gels showed minimal staining of the extracellular matrix compared to Ch M in either the dynamically or statically cultured group for the both experiments. No clear differences were observed for Ch M treated gels cultured under dynamic and static conditions for experiment 1, except for donor 5, for which the Ch M gels were stained more intense.

In general, for experiment 2 less H & E stain intensity for all experimental conditions was observed compared to experiment 1. In contrary to experiment 1, where Ch M and B M treated gels were stained similarly intense for dynamic and static conditions, stronger stains were observed for the Ch M dynamic treated groups in experiment 2.

Experiment 1

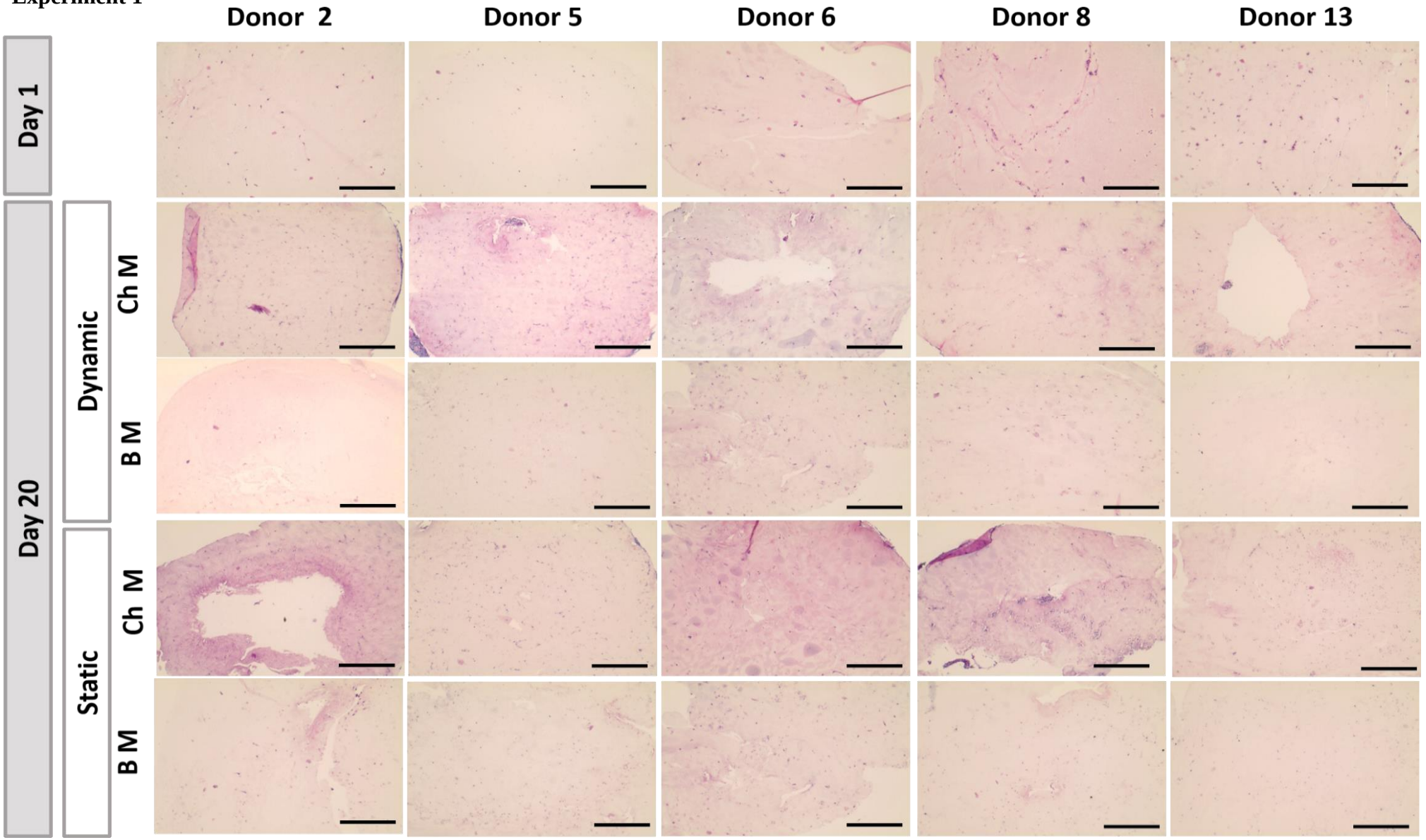

Figure 5. 38: H &E staining for experiment 1. *Bright field micrographs of 7 µm paraffin sections of oMSCs seeded gels were taken for day 1 and day 20. Gels were cultured under dynamic and static conditions and treated with either chondrogenic (Ch M) or basic (BM) media. Images were taken at 10x magnification. Scale bar = 300 µm.*

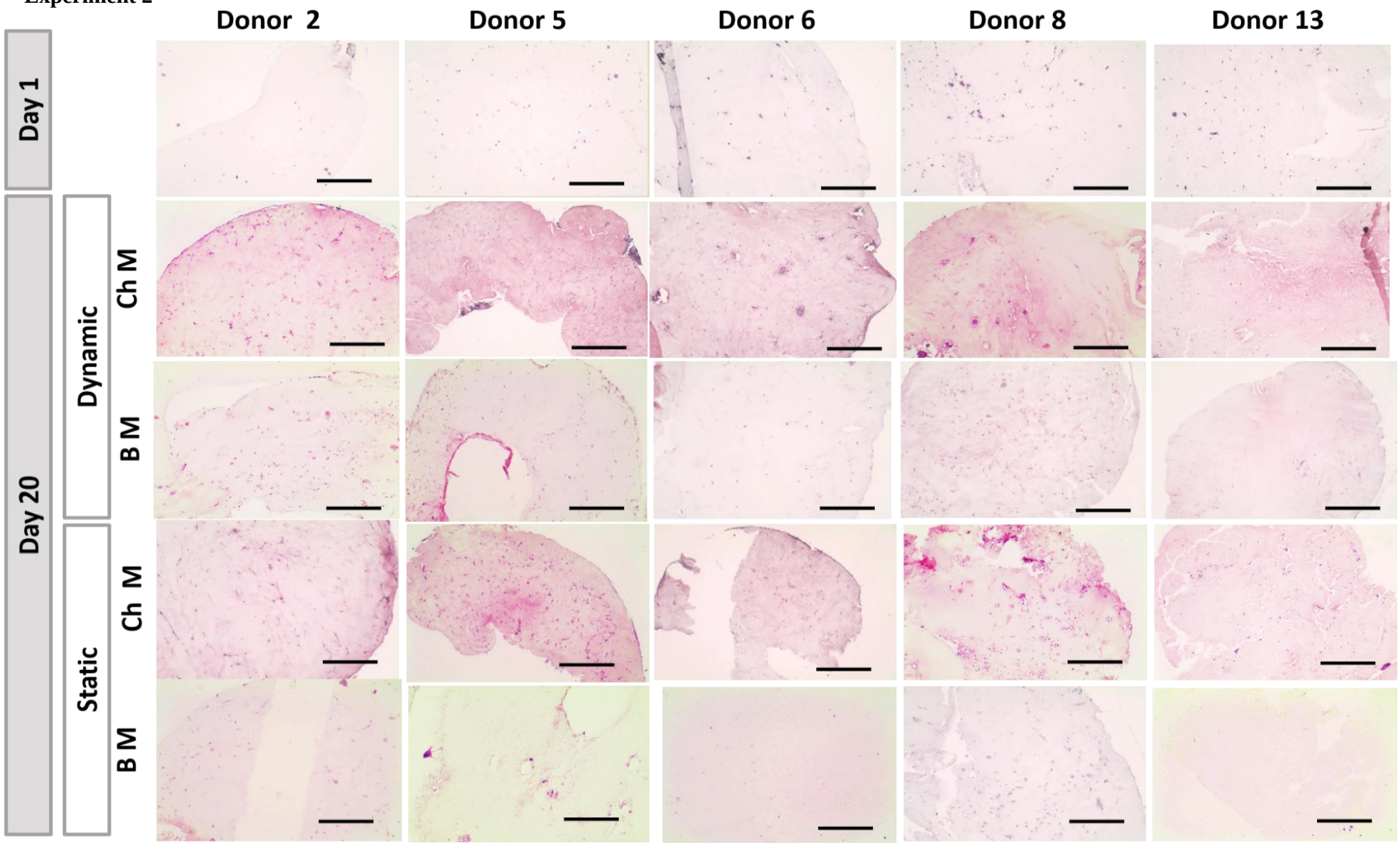

Figure 5. 39: H &E staining for experiment 2. *Bright field micrographs of 7 µm paraffin sections of oMSCs seeded gels were taken for day1 and day 20. Gels were cultured under dynamic and static conditions and treated with either chondrogenic (Ch M) or basic (BM) media. Images were taken at 10x magnification. Scale bar =300 µm.*

5.5.8.3 Picrosirius Red staining for the assessment of total collagen in collagen gels

Similar observation to H&E staining were made for Picrosirius Red staining (Figure 5.40). For both experiment 1 and 2, there are clear differences between the Ch M treated and the B M gels for both static and dynamic culture conditions were observed. Ch M treated gels exhibited a highly intense red colour, which indicates the presence of higher collagen content.

Variances in stain intensity between the 2, 5, 6, 8 and 13 were observed for the comparison of all B M treated gels with all Ch M treated gels for both experiment 1 and 2. For experiment 1, the strongest stain was observed for donor 2 (dynamic, Ch M) and donor 8 (static, Ch M) compared to the other donors. While donor 13 showed the lowest stain intensity for both Ch M and B M indicating lower collagen concentrations compared to the other donors. For B M some donors show higher intensity of the Picrosirius Red staining in dynamic group compared to other donors, for example donor 5 and donor 8 (experiment 1) and donor 6 and donor 8 (experiment 2).

Similar observations were made for experiment 2 (Figure 5.41). Strongest stains were observed for donors 2, 5 and 6 (Ch M dynamic and static) compared to donor 8 and 13

Experiment 1

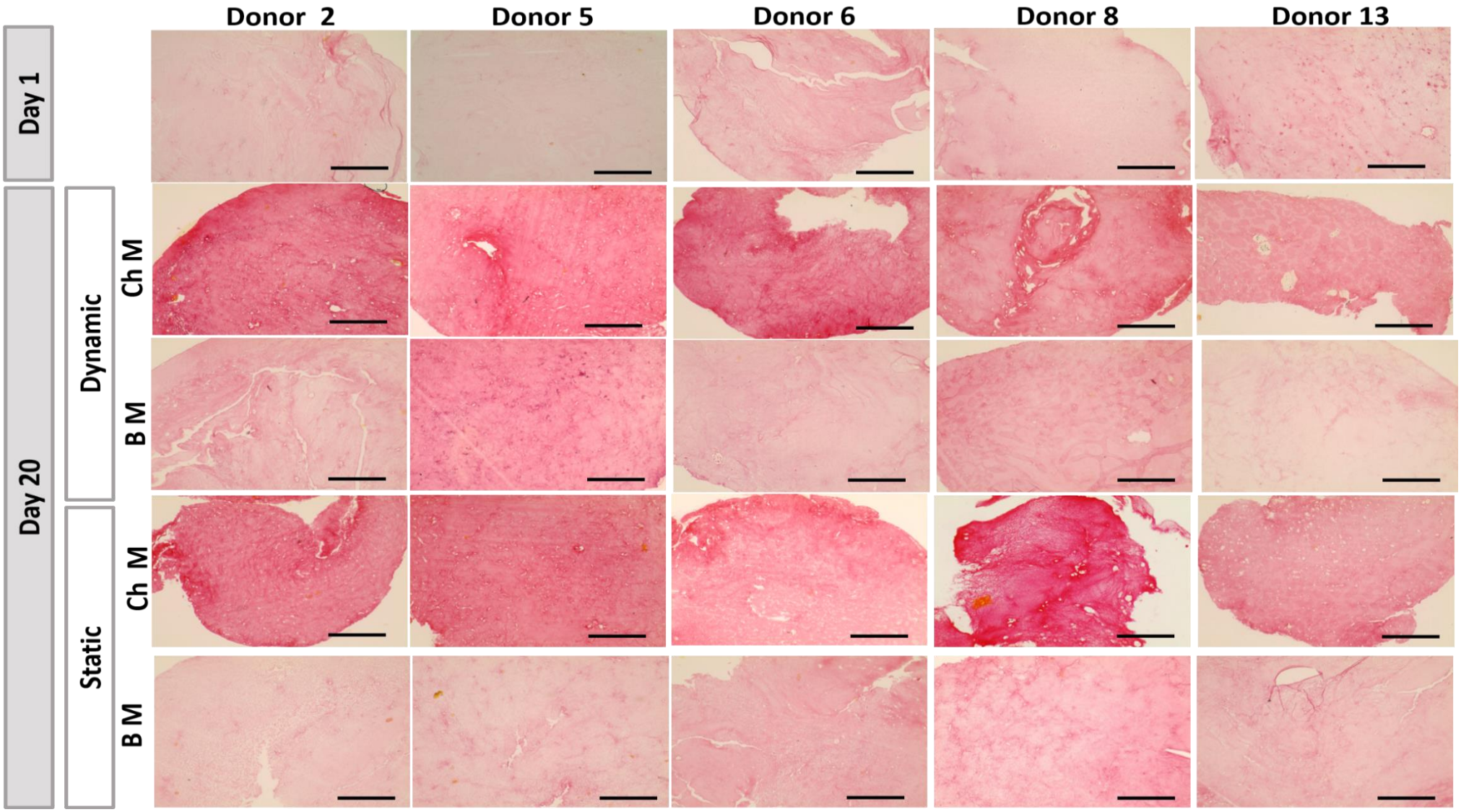

Figure 5. 40: Picrosirius Red staining for experiment 1. *Bright field micrographs of 7 µm paraffin sections of oMSCs seeded gels were taken for day 1 and day 20. Gels were cultured under dynamic and static conditions and treated with either chondrogenic (Ch M) or basic (BM) media, images were taken at 10x magnification. Scale bar = 300 µm.*

Experiment 2

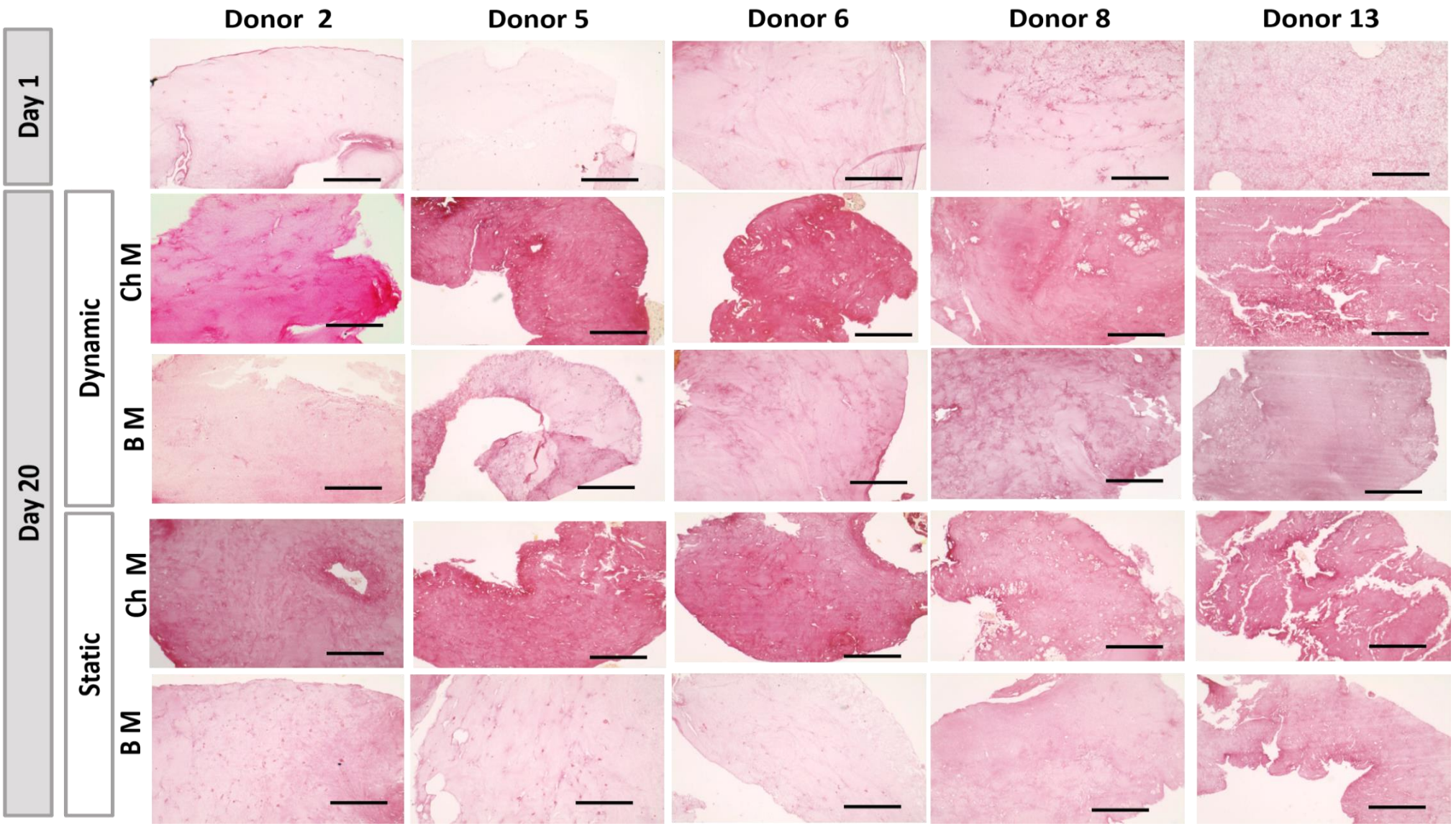

Figure 5. 41: Picrosirius Red staining for experiment 2. *Bright field micrographs of 7 µm paraffin sections of oMSCs seeded gels were taken for day 1 and day 20. Gels were cultured under dynamic and static conditions and treated with either chondrogenic (Ch M) or basic (BM) media, images were taken at 10x magnification. Scale bar = 300 µm.*

5.5.8.4 Alcian Blue staining for the assessment of GAG in collagen gels

There were noticeable differences between B M and Ch M treated gels for both static and dynamic culture conditions. Donor 2, 5, and 6 showed the strongest Alcian blue stains for experiment 1 (Ch M static and dynamic). Whereas, donor 8 and 13 exhibited the lowest stain intensity (Figure 5.42). The intensity of the Alcian blue stain directly correlates with the amount of GAG produced in the gels. Stronger stains represent higher GAG concentrations.

For experiment 2 (Ch M dynamic and static) gels for donors 5 and 6 were stained strongest followed by donor 2 and 8. Donor 13 exhibited the lowest GAG production (Figure 5.43).

For all donors in both experiments all B M gels showed only weak Alcian blue stain and no clear differences between the gels for all donors in both static and dynamic condition were observed.

Experiment 1

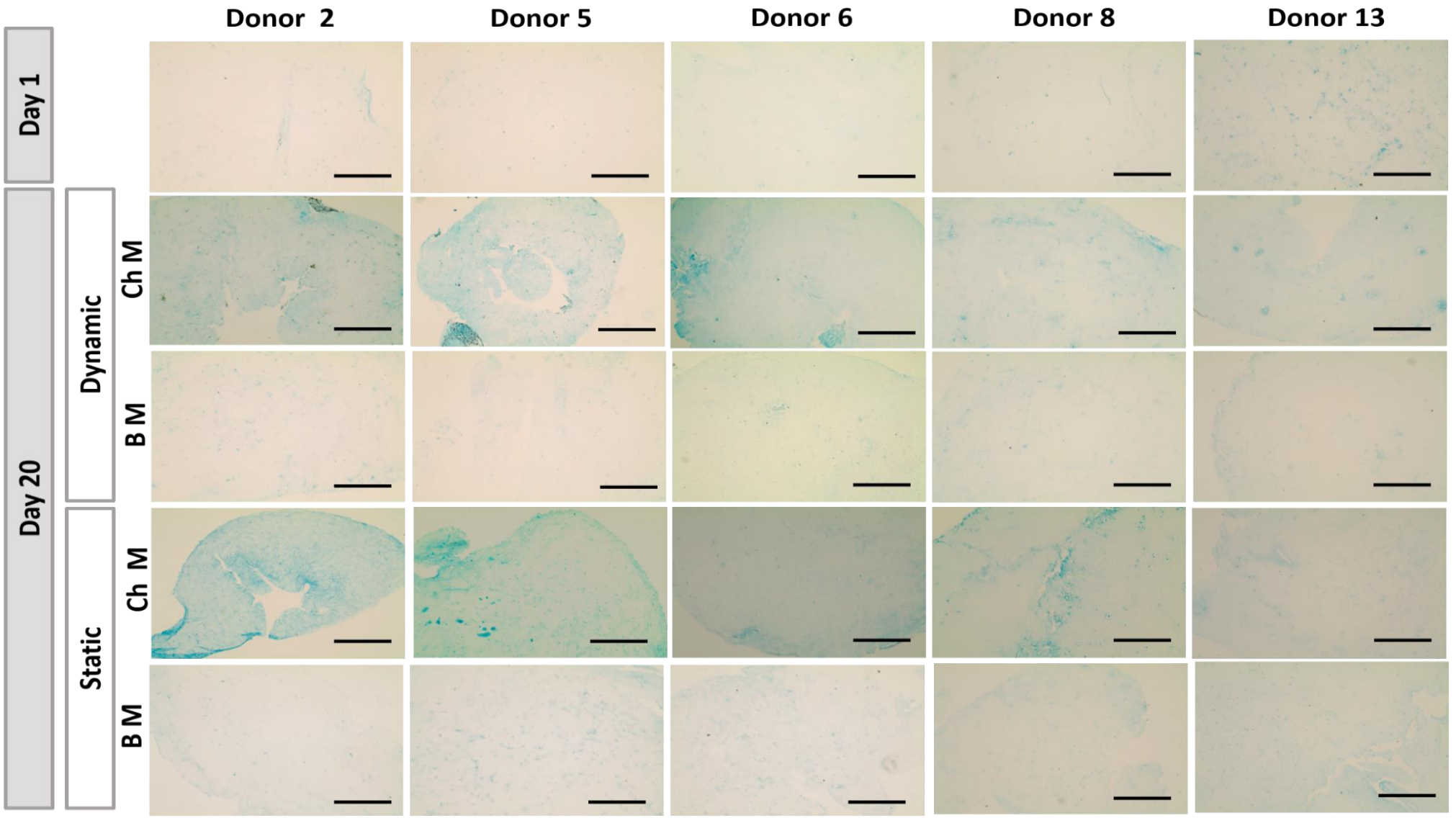

Figure 5. 42: Alcian blue staining for experiment 1. *Bright field micrographs of 7 µm paraffin sections of oMSCs seeded gels were taken for day 1 and day 20. Gels were cultured under dynamic and static conditions and treated with either chondrogenic (Ch M) or basic (BM) media, images were taken at 10x magnification. Scale bar = 300 µm.*

Experiment 2

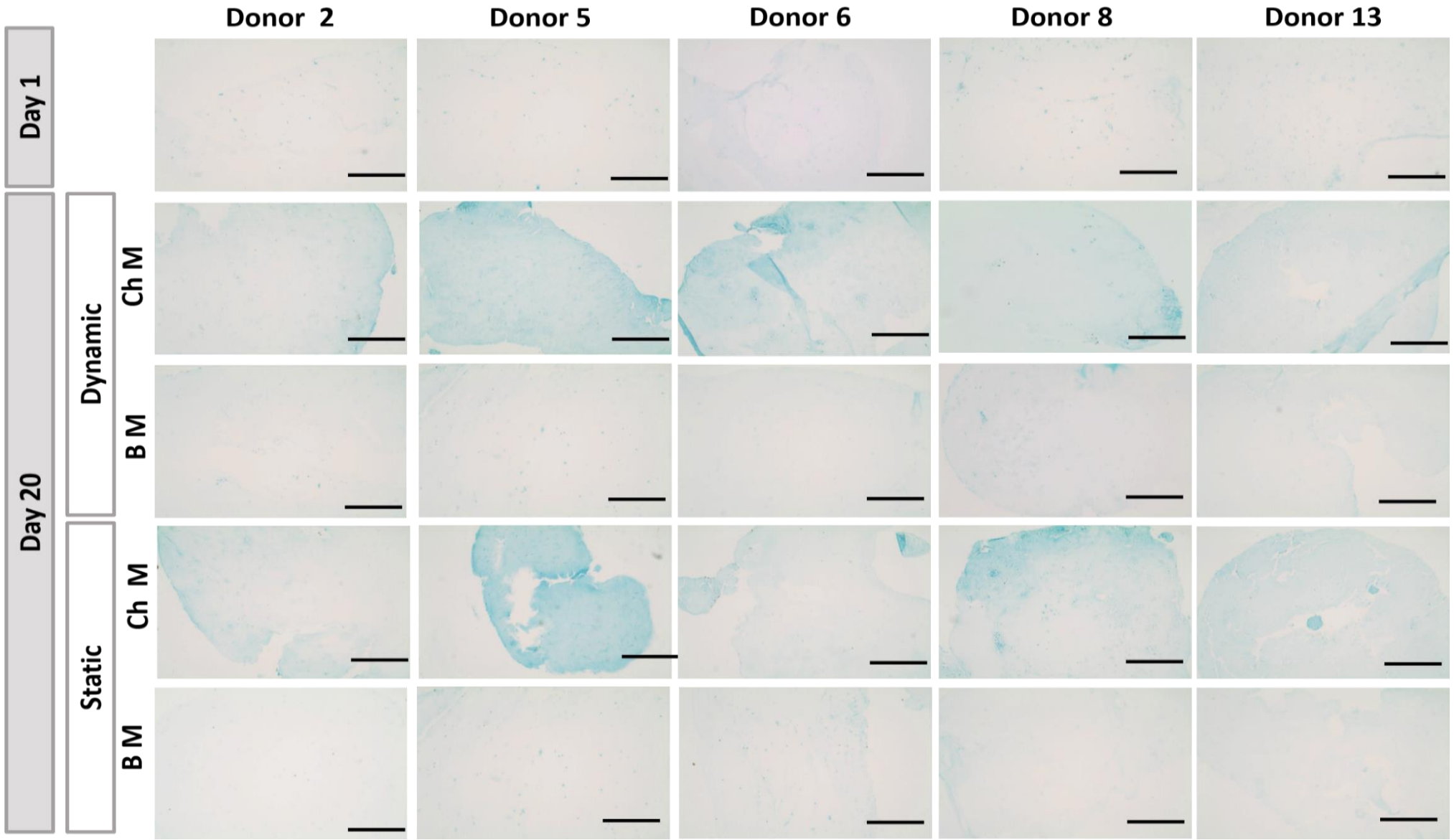

Figure 5. 43: Alcian blue staining for experiment 2. *Bright field micrographs of 7 µm paraffin sections of oMSCs seeded gels were taken for day1 and day 20. Gels were cultured under dynamic and static conditions and treated with either chondrogenic (Ch M) or basic (BM) media, images were taken at 10x magnification. Scale bar = 300 µm.*

5.5.8.5 Collage type-II immunostaining

An enzymatic method using horseradish peroxidase (HRP) was used to carry out immunohistochemical staining of paraffin sections of the gels. The results revealed that Type II collagen expression markedly higher in both experiments for the Ch M gels than the B M gels for all conditions. However, experiment 1 was in general better than experiment 2.

For experiment 1 (Figure 5.44), he gels showed that collagen type-II expression for the both static and dynamic conditions compare with day 1. But in different degrees some differences could be notice between the Ch M treated of the static and dynamic group especially for donor 5 and donor 13 (Ch M dynamic) which have higher dye intensity than (Ch M static)

For experiment 2 (Figure 5.45)., collagen type-II expression was less than experiment 1, and the Ch M groups were almost higher than B M groups for both static and dynamic condition. Experiment 2 showed less variances between donors for (Ch M static) of the five donors whereas for (Ch M dynamic) the results showed that donors 5, 8 and 13 (Ch M dynamic) is higher than donors 2 and 6 of the same condition.

Experiment 1

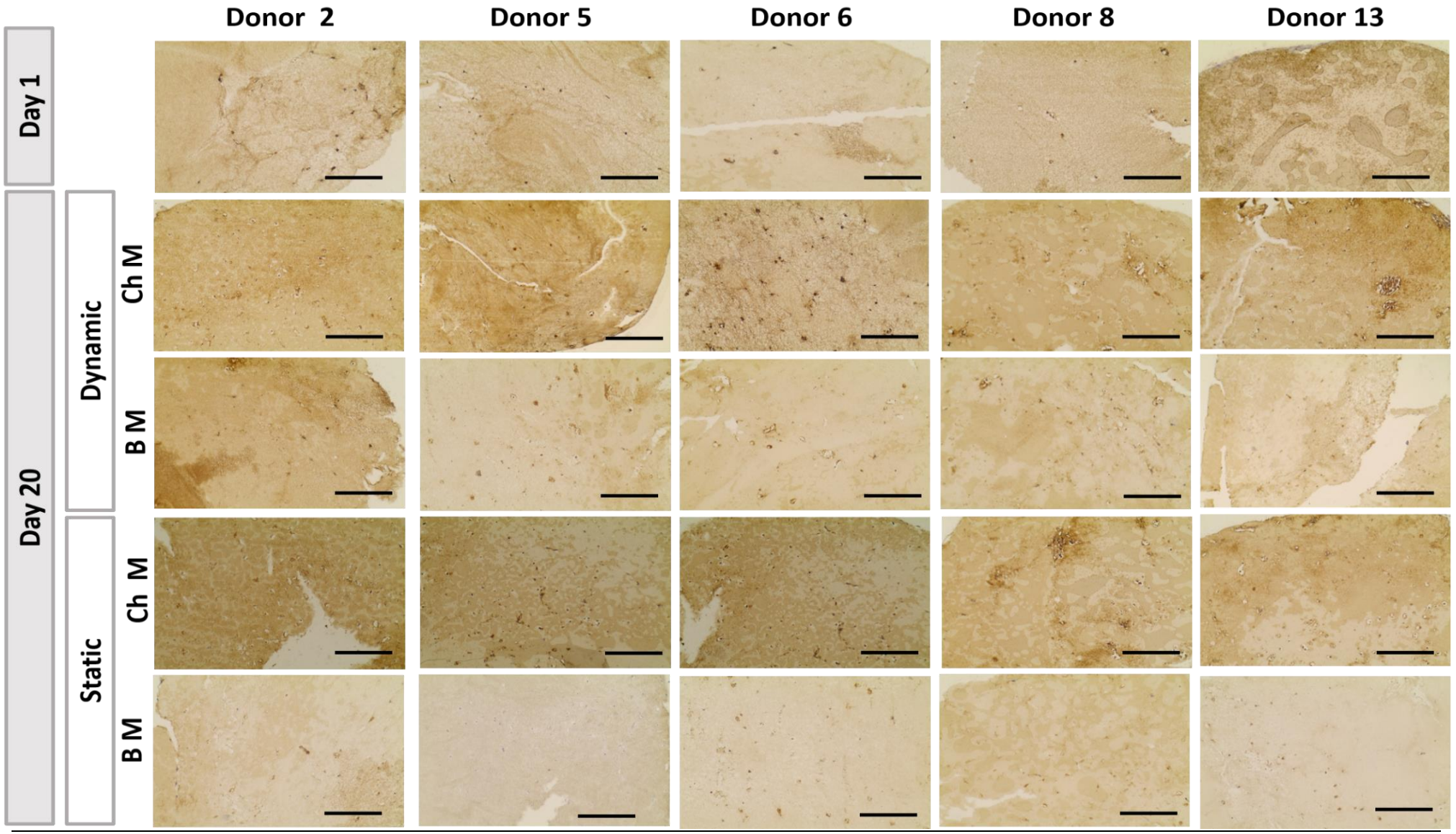

Figure 5. 44: Collagen type-II expression immunostaining for experiment 1. *Bright field micrographs of collagen type-II staining of 7 µm sections, paraffin section of oMSCs seeded gel samples at day1 and day 20. Gels were cultured under dynamic and static conditions and treated with either chondrogenic (Ch M) or basic (B M) media, images were taken at 10x magnification. scale bar = 300 µm.*

Experiment 2

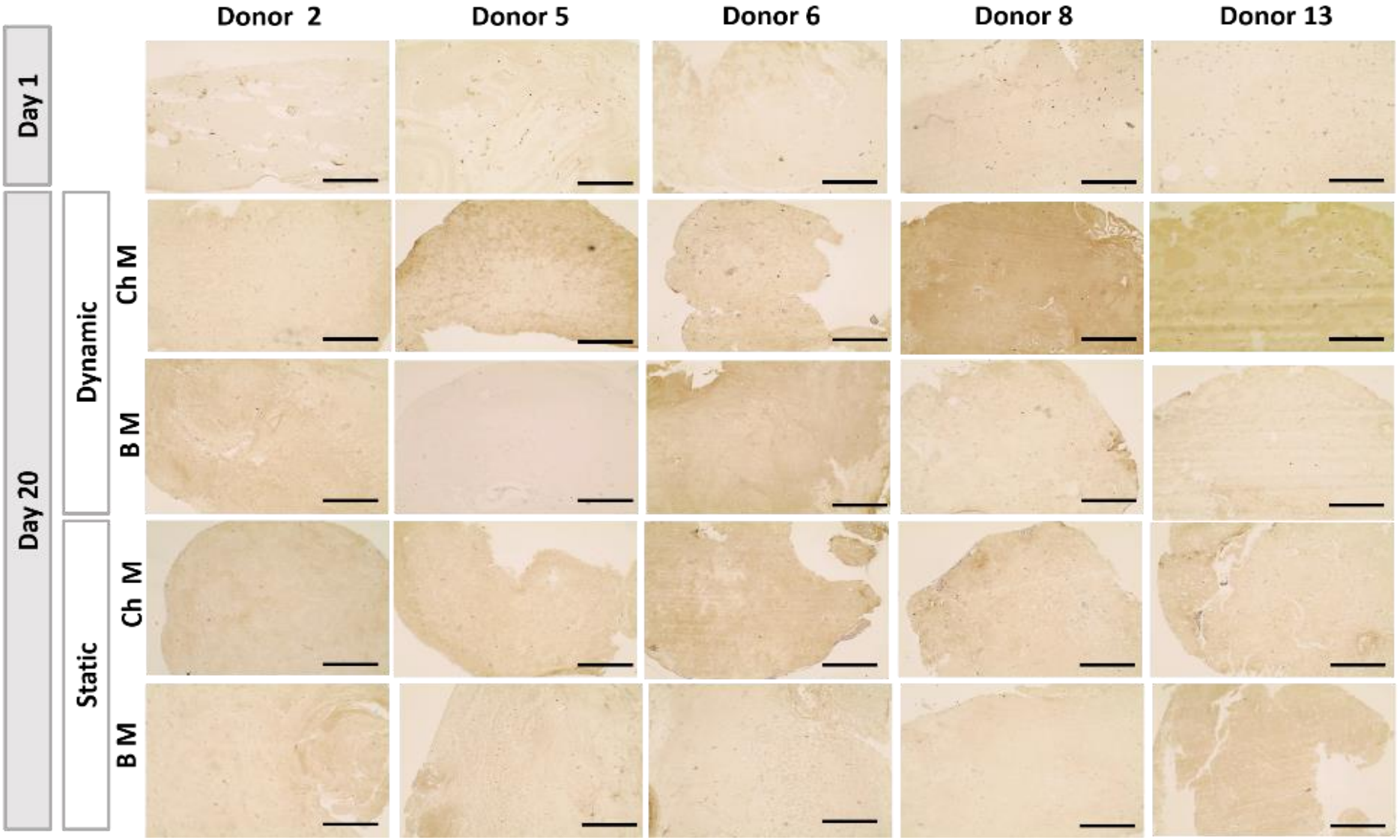

Figure 5. 45: Collagen type-II immunostaining for experiment 2. *Bright field micrographs of collagen type-II immunostaining of 7 µm sections, paraffin section of oMSCs seeded gel samples at day 1 and day 20. Gels were cultured under dynamic and static conditions and treated with either chondrogenic (Ch M) or basic (BM) media, images were taken at 10x magnification. scale bar = 300 µm.*

5.5.8.6 Collagen type-X immunostaining

All gels for experiment 1 and 2 did not show collagen type-X expression when stained using horseradish peroxidase (HRP) immunostaining, compared to the negative control (not labelled with the collagen type-X antibodies) (Figures 5.46 and 5.47).

Experiment 1

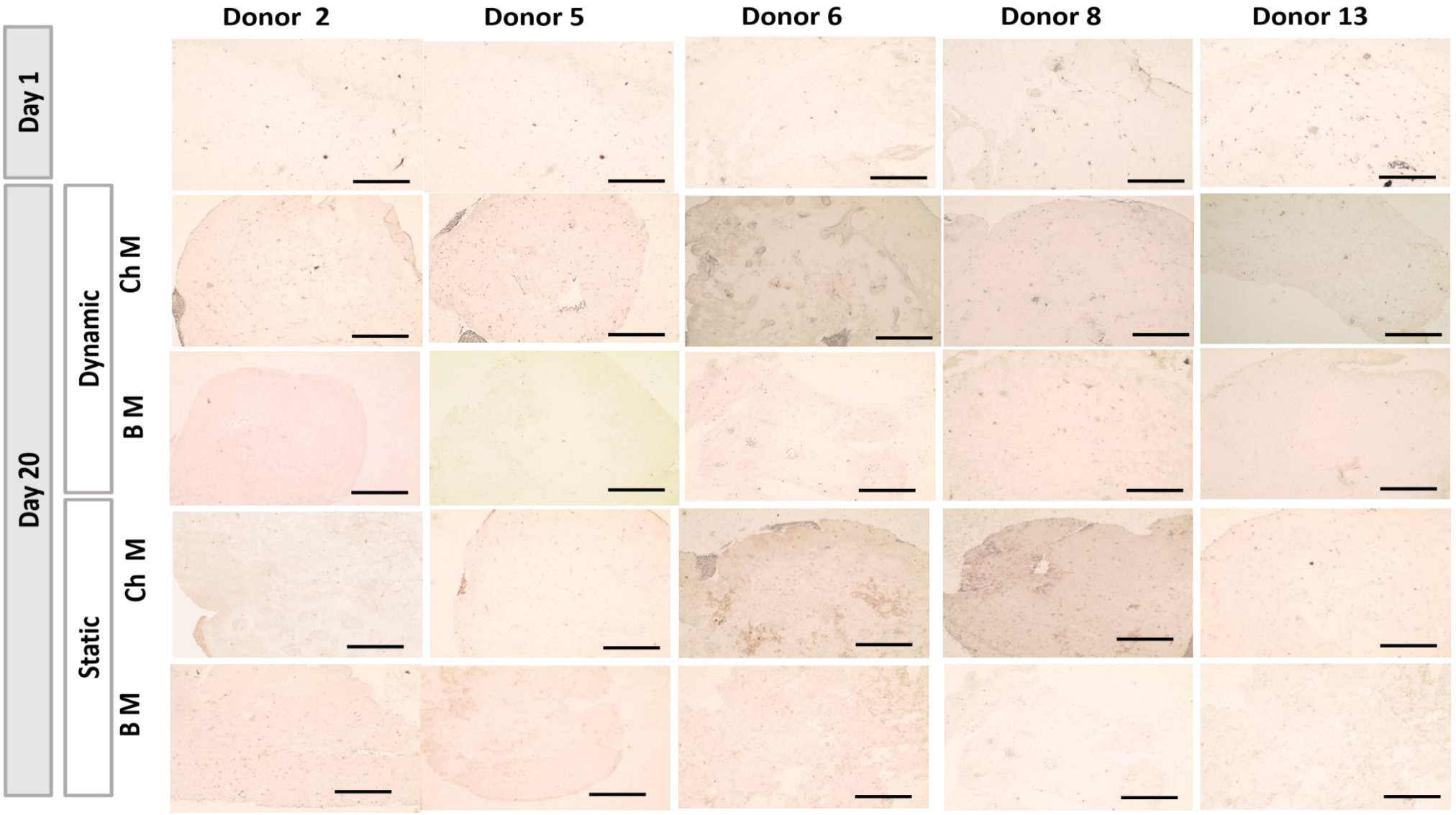

Figure 5. 46: Collagen type-X immunostaining for experiment 1*. Bright field micrographs of collagen type-X immunostaining of 7 µm paraffin sections, paraffin embedded of oMSCs seeded gel samples at day1 and day 20. Gels were cultured under dynamic and static conditions and treated with either chondrogenic (Ch M) or basic (BM) media, images were taken at 10x magnification. Scale bar = 300 µm.*

Experiment 2

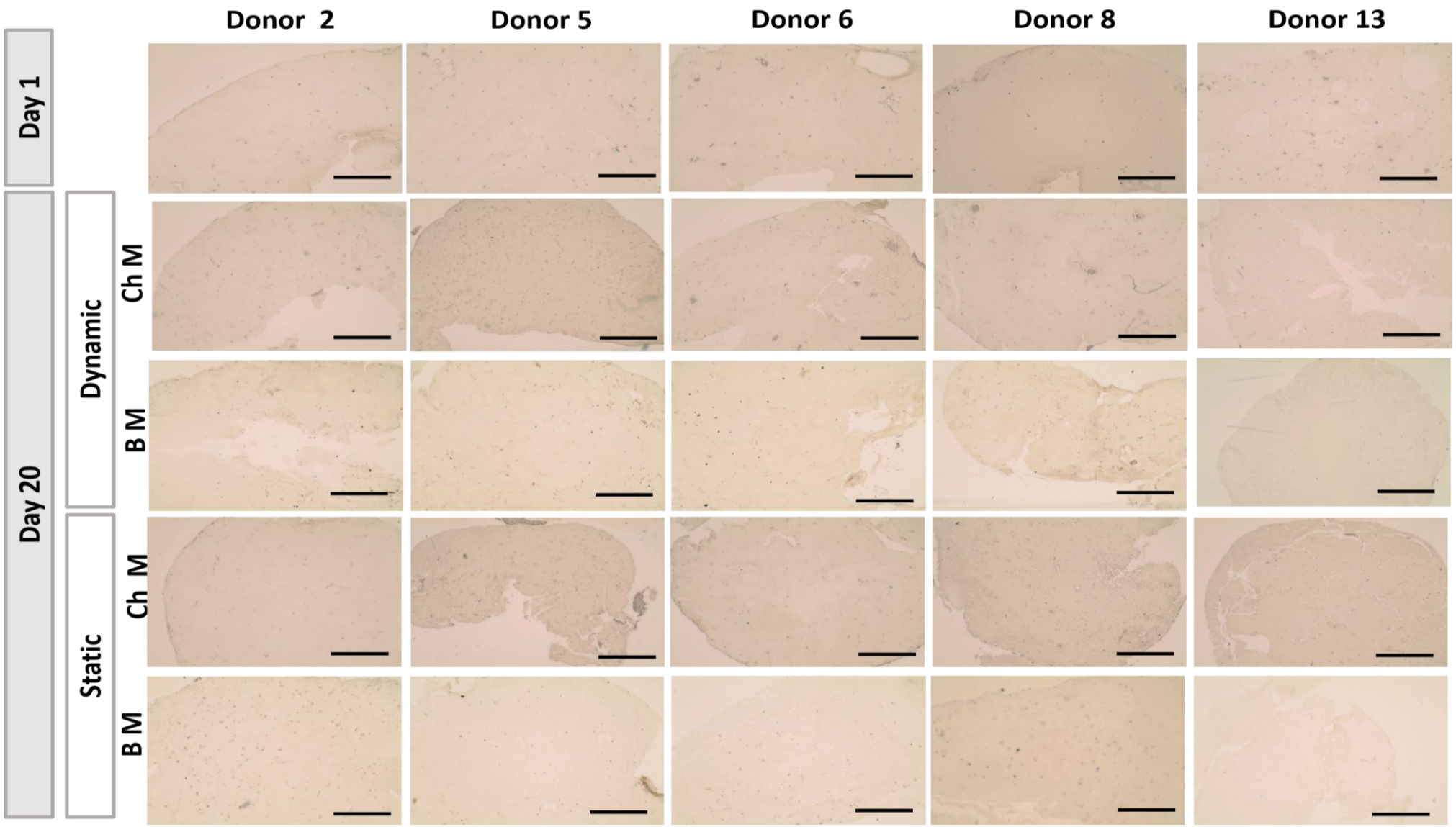

Figure 5. 47: Collagen X immunostaining for experiment 2. *Bright field micrographs of Collagen X immunostaining of 7 µm paraffin sections, of oMSCs seeded gel samples at day 1 and day 20 in two conditions dynamic and static, 20. Gels were cultured under dynamic and static conditions and treated with either chondrogenic (Ch M) or basic (BM) media, images were taken at 10x magnification. Scale bar = 300 µm.*

5.5.8.7 Aggrecan immunostaining

Aggrecan staining for experiment 1 (Figure 5.48) revealed positive stain for the (Ch M) treated gels compare with day 1, In this experiment donors showed almost similar intensity for Ch M treated gels both static and dynamic condition. The interesting observation of the B M treated gels of the dynamic condition regarding to donor 2 and 5 was expressed aggrecan more than other donors of the same condition, in particular the edges of the gels. Experiment 2 (Figure 5.49) is also revealed a positive stain for the (Ch M) treated gels compare with day 1donors 2 and 5 (Ch M dynamic) and donor 5 (Ch M static) showed the best expression to the aggrecan.

Experiment 1

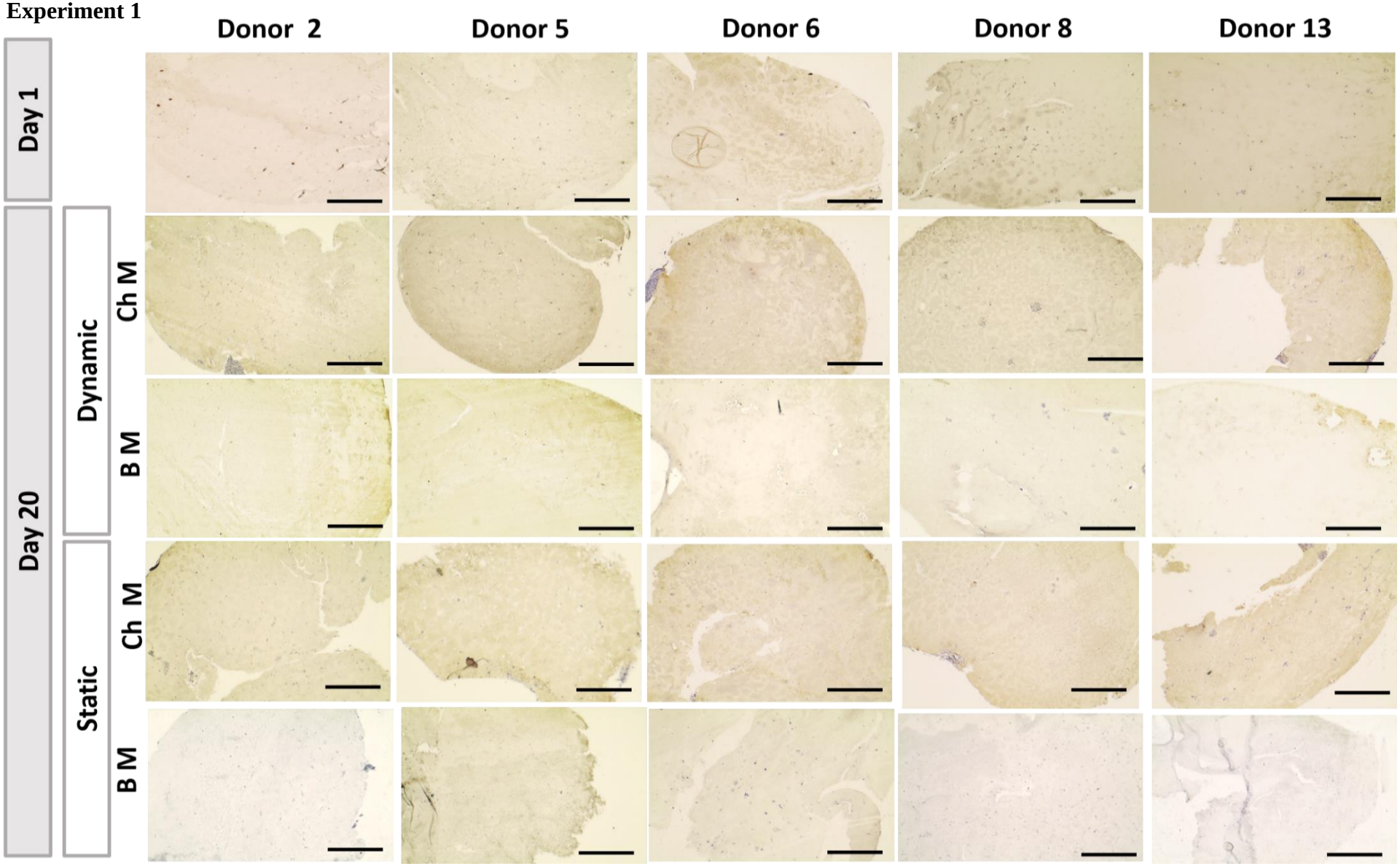

Figure 5. 48: Aggrecan immunostaining for experiment 1. *Bright field micrographs of aggrecan immunostaining of 7 µm paraffin sections, of oMSCs seeded gel samples at day1 and day 20 in two conditions dynamic and static. Gels were cultured under dynamic and static conditions and treated with either chondrogenic (Ch M) or basic (BM) media, images were taken at 10x magnification. Scale bar = 300 µm.*

Experiment 2

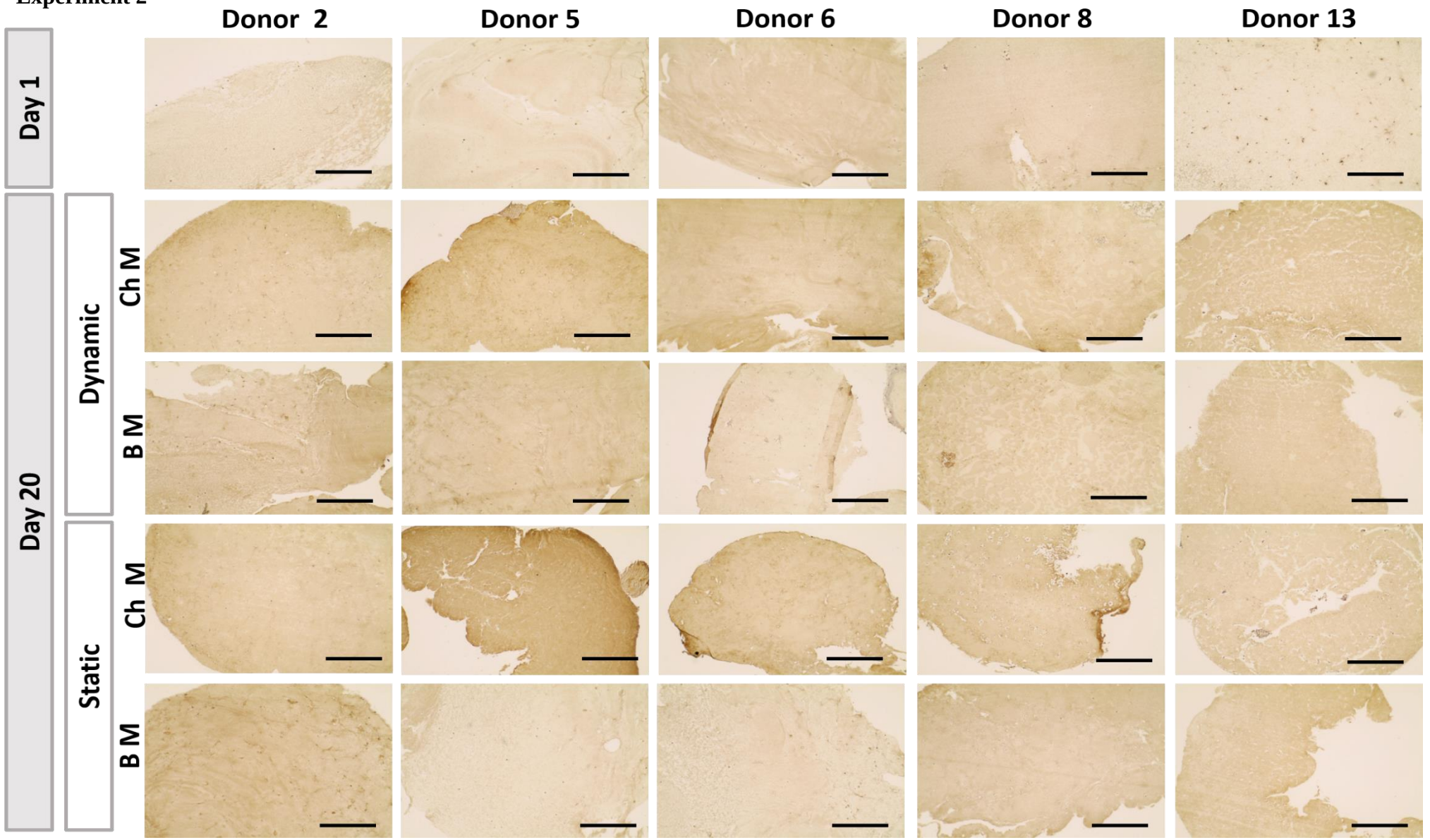

Figure 5. 49: Aggrecan immunostaining for experiment 2. *Bright field micrographs of aggrecan immunostaining of 7 µm paraffin sections, of oMSCs seeded gel samples at day1 and day 20 in two conditions dynamic and static. Gels were cultured under dynamic and static conditions and treated with either chondrogenic (Ch M) or basic media (BM), images were taken at 10x magnification. Scale bar = 300 µm.*

5.6 Discussion

Several methods have been used to support chondrogenesis of BM-MSCs for articular cartilage and fibrocartilage tissue engineering with distinct advantages and disadvantages to each method (Lo Monaco *et al.,* 2018). However, there are tremendous challenges for developing an optimal engineered cartilage. It is believed that tissue engineering of articular cartilage will overcome the present restrictions of surgical treatment by introducing efficient regeneration in the defect region (Park and Cho, 2010).

Magnetic Nanoparticles have many applications in various fields of science, technology and medicine see (Pankhurst *et al.,* 2003) for a detailed review. MNPs can be functionalised with biomolecules such as peptides and antibodies and used to target, stimulate and subsequently activate specific mechano-sensitive cell receptors and signalling pathways. Remote activation is achieved by applying an oscillating external magnetic field to cause a translational torque in the MNPs which is then transduced to the target mechanosensitive protein (Hughes *et al.,* 2005). In previous studies, remote mechano-activation of the ion channel, TREK-1 has been shown to remotely deliver directed mechanical stimuli to promote osteogenesis (Cartmell *et al.,* 2002; Hughes *et al.,* 2007; Hughes *et al.,* 2008). In this study, we have tested this technology for promoting chondrogenesis of oBM-MSCs to differentiate into chondrocytes with the aid of chondrogenic media in a 3D hydrogel cell culture.

The efficiency of the coating of the magnetic nanoparticles with antibodies was first assessed by examining changes in magnetic nanoparticle characteristics. The antibody coating process resulted in an increase in particle size relative to uncoated particles. This increase in size could be attributed to the protein layer around the coated MNPs. In addition, the relative increase in MNPs surface charge might also be attributed to the presence of protein on the particle surface. Previous work has also shown that particle coating with antibodies alters particle surface charge in a similar manner (Hu *et al.,* 2014).

The oMSCs of the donors that have been chosen for this study were tested for the cell viability by Trypan blue staining during culture at passage 1 to 3. In general, the viability (%) increased from P1 to P2. Although, the differences between the three passages were significant for 3 of 5 donors, all donors kept their viability and the ability to proliferates until passage 3. These results agreed with the studies of (Adamzyk *et al.,* 2013). The growth curve and doubling time were determined by counting the cell numbers after each passage, for 1–5 passages where the proliferation decreased after passage 3.

Cell metabolic activity using alamar blue assay was showed significantly increased across the experimental time at day 10 and day 20 compare to day 0. the results have also showed consistency in the cell activity for each experimental group in general. However, when return to the PicoGreen assay results there is a significant decrease in cell number of the Ch M gels compare with B M (Figures 5.15.and 5.16), that means the oMSCs cells which have differentiated into chondrocytes (in the Ch M) have kept their metabolic activity or increased and being active more than the un differentiated in the B M gels. in converting the blue resazurin (alamar blue reagent) is reduced to resorufin, which is a red colourimetric indicator (Bonnier *et al.,* 2015). And that is may due to the highly active new chondrocytes in the Ch M gel and the low activity of the over confluent of the undifferentiated oMSCs in B M gels. There were no significant differences when comparing the five donors for all conditions in each donor's oMSCs metabolic activity.

The results showed a noticeable difference in gross morphology between the Ch M and B M treated gels as the Ch M gels were solid in the texture, concave disc-like shape and sinking in the fluid indicating the accumulation of ECM. While in contrast, the BM exhibited the opposite characteristics as identified in chapter 4. However, no gross differences can be observed between the dynamic and the static group of the Ch M and B M treated group.

Bose Electro Force 3200 mechanical testing machine has been successfully used to measure the mechanical properties of different materials. This approach has been used to characterise the viscoelastic properties of natural tissues (Barnes *et al.,* 2016; Burton *et al.,* 2017; Fulcher

et al., 2009; Temple *et al.*, 2016) and orthopaedic implants (Lawless *et al.*, 2018; Lawless *et al.*, 2017). This unconfined ramp-hold compression was considered a suitable experiment to obtain the mechanical properties of the collagen gels as well as the native cartilage, as it is a simple experiment to perform to those thin samples (Andriakopoulou, 2016). In this study, the gel samples gave similar mechanical properties to the native sheep articular cartilage and the curves obtained from stress-strain data were similar to that of native cartilage tissue. The computed Young modulus of the gel samples for both static and dynamic groups was compared with the native sheep cartilage. And the results showed that the native sheep computed Young modulus value (1.257 MPa) was higher than static group (1.165 MPa). However, this value is lower than dynamic group gels (1.672 MPa) (Figure 5.14) which may indicate that the dynamic condition provided by MICA enhanced chondrogenesis.

A limitation of this study was that native cartilage samples were a disc larger in diameter than the gel samples and that may affect the estimated Young modulus according to the physical thermotical that the pressure is related to the area, because the same force can have a very different effect depending on the area over which it is exerted. Area is typically measured in units of meters squared (m^2). Since pressure is calculated by dividing force by area, it has units of Newtons per meter squared (N/m^2), and this unit is given a new name, Pascals (Pa) 1 Pa = 1 N/m^2.

In this study, we have considered the use of MICA technology for the applications which has been designed to remotely deliver directed mechanical stimuli to individual cells in culture or within the body, to promote osteogenesis (Aagaard *et al.*, 2003; Cartmell *et al.*, 2002; Hughes *et al.*, 2007; Markides *et al.*, 2018). The potential of this technique was tested for chondrogenesis. The chondrogenic capacity was assessed by the production of ECM (sGAG, total collagen and total protein). The results showed that the Ch M treated gel produced a significant amount of the cartilaginous matrix compared with B M treated group which showed that the responses of the oMSCs to the chondrogenic inducing elements in the Ch M. Although there are previous reports of accelerated metabolic activity of

chondrocytes exposed to mechanical cues. (Grad *et al.,* 2012; Han *et al.,* 2007), with the MICA technology we did not see a consistent response in all the ovine donors. The total amounts of sGAG, total collagen and total protein produced by the cells during culture was enhanced in mechanically stimulated gels for potentially only three donors out of the five donors. This demonstrates what has been reported previously by (Markides *et al.,* 2018) showing variation in responses between sheep in their tri-lineage potential.

According to the histological staining for cartilage ECM specific stain (alcian blue for GAG and picrosirius for collagen), the stained paraffin sections of the tested groups exhibited chondrogenic differentiation for all Ch M gels for both dynamic and static compared to B M. The cells began to lose their phenotype from fibroblast-like spindle shapes to rounded and surrounding with ECM. Some selective paraffin samples were investigated for the calcium deposition in the gel sections using alizarin red (Appendix Figure A.1). This indicated that MICA stimulation did not promote osteogenic differentiation.

Chondrogenesis is usually assessed using markers of the chondrocyte phenotype, including type II collagen and aggrecan, in addition to type X collagen which had being used as a marker of late stage chondrocyte hypertrophy, (type X collagen would be interesting in this context because it is associated with endochondral ossification and it can indicate the type of cartilage that is produced) (Mwale *et al.,* 2000; Nelea *et al.,* 2005). In our studies, we confirmed a positive expression for chondrogenic markers collagen II and aggrecan. However, there is no expression for the hypertrophic marker collagen X. This may be due to the length of the culture period where this marker is not observed at this early stage.

CHAPTER 6

Comparison of TREK-1 versus TRPV4 for the induction of chondrogenesis in oMSC-seeded collagen gels under mechanical conditioning

6.1 Introduction

TRPV4 is expressed in chondrocytes and has been shown to significantly upregulate Sox9-dependent reporter activity and loss of TRPV4 function is associated with joint arthropathy and osteoarthritis. In addition, during chondrogenesis of mesenchymal stem cells, the expression pattern of TRPV4 was similar to the expression patterns of chondrogenic marker genes such as Aggrecan and collagen type-II (Cao *et al.,* 2018). In cartilage, TRPV4 has a key role in chondrocyte mechanotransduction and osmosensation. Blocking TRPV4 in chondrocytes closes the anabolic response to mechanical loads, meanwhile activating TRPV4 mimics the response of the mechanical loading. TRPV4 was identified as a regulator of chondrogenic differentiation. O'Conor and his group have proved that inhibition of this osmotic channel during mechanical loading prevented acute, mechanically facilitated the systemisation of proanabolic and anticatabolic genes (O'conor *et al.,* 2014). The goal of this study was to examine the hypothesis that TRPV4 on the oMSCs can be stimulated by MICA after labelling the cells with TRPV4 antibody-coated MNPs and can differentiate towards chondrogenesis.

6.2 Aim and objective

The aim of this chapter is to investigate the effect of mechanical stimulation using MICA technology on chondrogenic differentiation of the BM-oMSCs by targeting TRPV4 mechanosensitive channel in comparison with TREK-1 using MNPs.

The objectives this chapter are

- To study the effect of TRVP-4 activation on chondrogenesis using MICA technology
- To compare chondrogenesis of TREK-1 and TRVP4 targeted BM-oMSC under static and dynamic conditions
- To assess the variance among three different BM-oMSC donors to produce a cartilaginous matrix in response to chondrogenic and basic media.
- To assess the mechanical properties of the engineered cartilage by determining the Young's modulus.
- To assess the biochemical composition of the engineered cartilage by determining the sGAG, total collagen total protein content relative to total cell number.
- To study the matrix composition of the engineered cartilage through histological stains such as H and E, alcian blue and Picrosirius as well as immunohistochemistry for collagen II collagen X and aggrecan.

6.3 Materials and Methods

6.3.1 Compare TREK-1 versus TRPV4 activation

The oMSCs of three donors were cultured to passage 3 and divided into two parts, one part was labelled with TRPV4- coated MNPs and the other part was labelled with TREK-1 - coated MNPs. Cells were seeded in rat tail collagen type I hydrogels at a density of $2X10^5$ cells/gel. The experimental protocol from the TREK-1 experiment was adopted in this experiment (Chapter 5, section 5.3.1). The two groups of antibody-labelled oMSCs were subdivided into two experimental groups, namely statically and dynamically cultured groups. Cells were further cultured with either chondrogenic media (Ch M) or basic medium (B M). Gels were assessed for cell metabolic activity (alamar blue) on day 1, day 10 and day 20 (n = 3), mechanical properties (compression testing, n = 4) gel samples were harvested at day 1 and day 20 and fixed for histology or frozen at -20 oC for biochemical analysis (n = 3). Summary of the experimental procedures performed in Chapter 6 is showed in Figure 6.1.

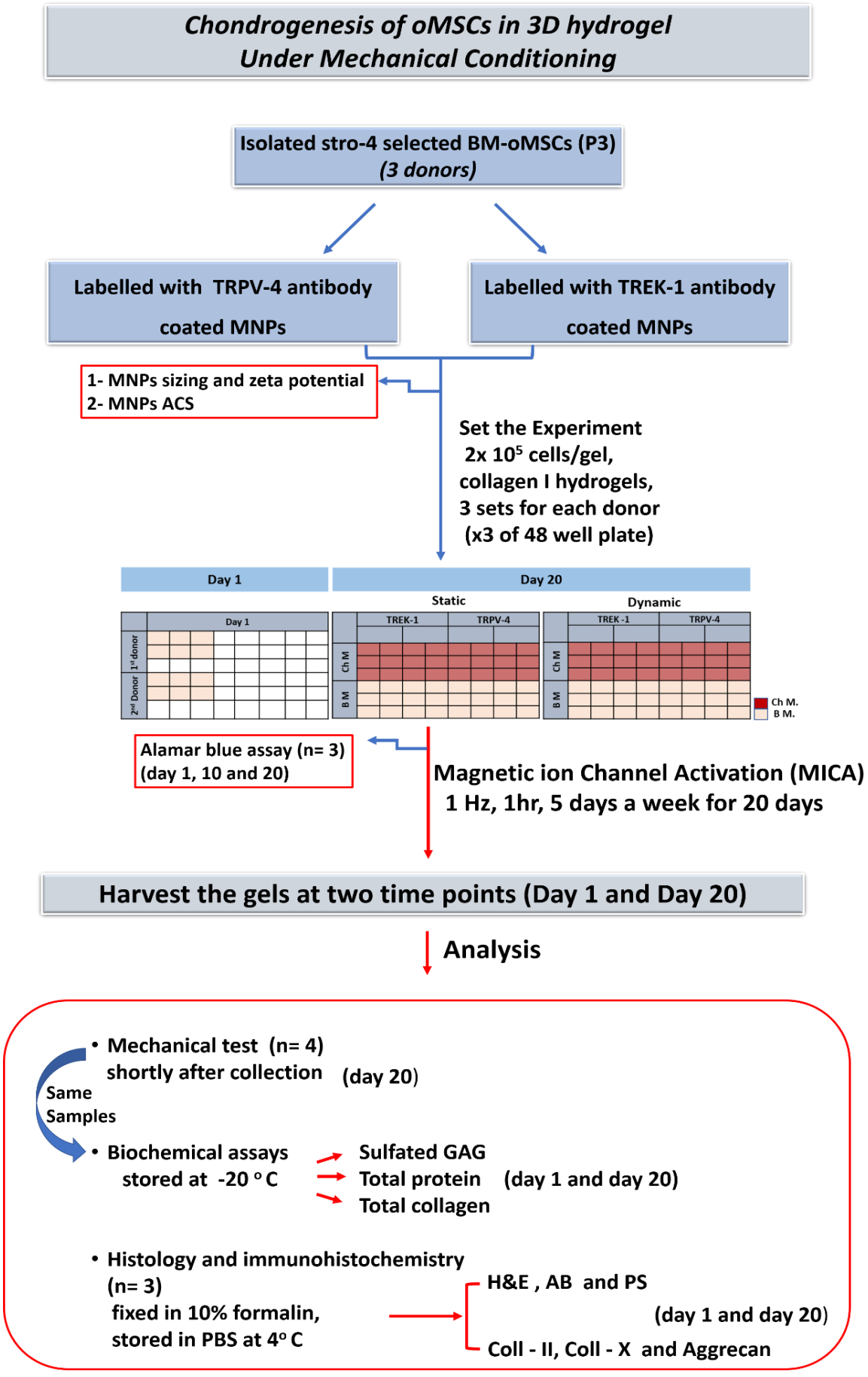

Figure 6. 1: Methodology for chapter 6. *This schematic summarises the experimental steps carried out in chapter 6.*

6.3.2 Cross-reactivity of TRPV4 antibody with ovine MSC

The primary TRPV4 antibody used in this study primarily reacted with humans, mouse and rat. Hence, the antibody was tested for ovine cell reactivity by fluorescent immunocytochemistry as described in chapter 2, section 2.5.1 using unlabelled oMSCs as negative control and sheep chondrocytes as positive control.

6.3.3 Antibody coating of magnetic nanoparticles

MNPs were coated with antibodies as described in chapter 2, section 2.5.1. For this experiment, a stock solution of 10 mg/ml Nanomag suspension was coated with TRPV4 or TREK-1 antibodies. Antibody-coated MNPs were prepared to a final concentration of 1 mg/ml in 1% BSA. The working solutions of both TRPV4 and TREK-1 coated MNPs were subjected to MNPs characterisation before and after coating and were stored at 4°C until use.

6.3.4 Cell labelling with antibody-coated magnetic nanoparticles

oMSCs for donors 2, 6 and 13 were divided into two parts and labelled either with the TRPV4 or TREK-1 antibody-coated MNPs as mentioned in chapter 2, section 2.5.2. The antibody-labelled oMSCs were then seeded in 3D collagen I hydrogels at a cell density of $2X10^5$ cell /gel as described in chapter 2, section 2.2.2.9.

6.3.5 Alamar blue assay

AlamarBlue® cell viability reagent was used to assess cell viability. The assay was performed on day 1, day 10 and day 20 (n = 3 for each condition) as explain in chapter 2, section 2.2.2.10. Data was shown as mean ± standard deviation and statistically analysed using SPSS (Section 6.3).

6.3.6 Mechanical testing and Young's modulus

Samples were subjected to compression test shortly after harvesting at day 1 and day 20 (n = 4 each). Sample diameter and height were measured using digital callipers. Gels were placed on the platform of the mechanical tester (Bose, ElectroForce 3200). Tests were performed as described in chapter 2, section 2.7. The mechanical test was performed for Ch

M-fed gels only, because gels cultured in B M did not consolidate throughout the experiment. Analyses was performed to compare TREK-1 and TRPV4 labelled MNPs in both static and dynamic culture conditions at day 20.

Stress-strain curves were plotted, and the young's modulus was calculated as described in chapter 2, section 2.7. For all of the calculations, tissue homogeneity was assumed. Data was shown as mean ± standard deviation and statistical analyses was performed using SPSS (section 6.3).

6.3.7 Biochemical assays

To perform biochemical assays, samples were digested with 1 ml of 50 µg/ml proteinase K in 100 mM ammonium acetate overnight at 60°C. During this time, the vials were vortexed twice. The digested samples were aliquoted and frozen at -21^{o}C until use. Samples were analysed to quantify the content of DNA, sulphated GAG, total collagen and total protein using the specific assays as described in chapter 2, sections 2.6.1-2.6.4 respectively.

6.3.8 Histology and immunohistology

Samples were prepared for histology and immunohistology as previously mentioned in chapter 2, section 2.4.2. Serial gel sections with a thickness of 7 µm were prepared for histological and immunohistological stains for day 1 and day 20. Hematoxylin and Eosin (H&E) stain, Alcian blue (AB), and Picrosirius red (PS) were chosen for histological assessment of the gel samples (Chapter 2, sections 2.4.3.1-2.4.3.5). Immunohistological assessments were performed using immune-peroxidase antibody staining for Collagen type II, collagen type X and aggrecan staining (Chapter 2, section 2.4.4).

6.4 Statistical analysis

Data for Young's modulus, DNA content and sGAG, total protein, total collagen content and their normalisation to the DNA content were compared using one-way ANOVA with Tukey's multiple comparisons test to determine statistical significance between each condition. Differences were considered significant for $P \leq 0.05$. Analysis was performed

using IBM SPSS statistics program version 24. All values quoted in the results are mean ± standard deviation at day 20, Ch M for both TREK-1 and TRPV4 groups. Both static and dynamic conditions were analysed for the donors' performance and comparison between donors and conditions.

6.5 Results

6.5.1 Cross-reactivity of TRPV4 antibody with ovine MSC

Immunocytochemistry staining of both sheep chondrocytes and oMSCs of two experimental donors revealed TRPV4 expression, indicating cross reactivity of the TRPV4 antibody with sheep cells and hence confirming the antibodies suitability for this experiment (Figure 6.2).

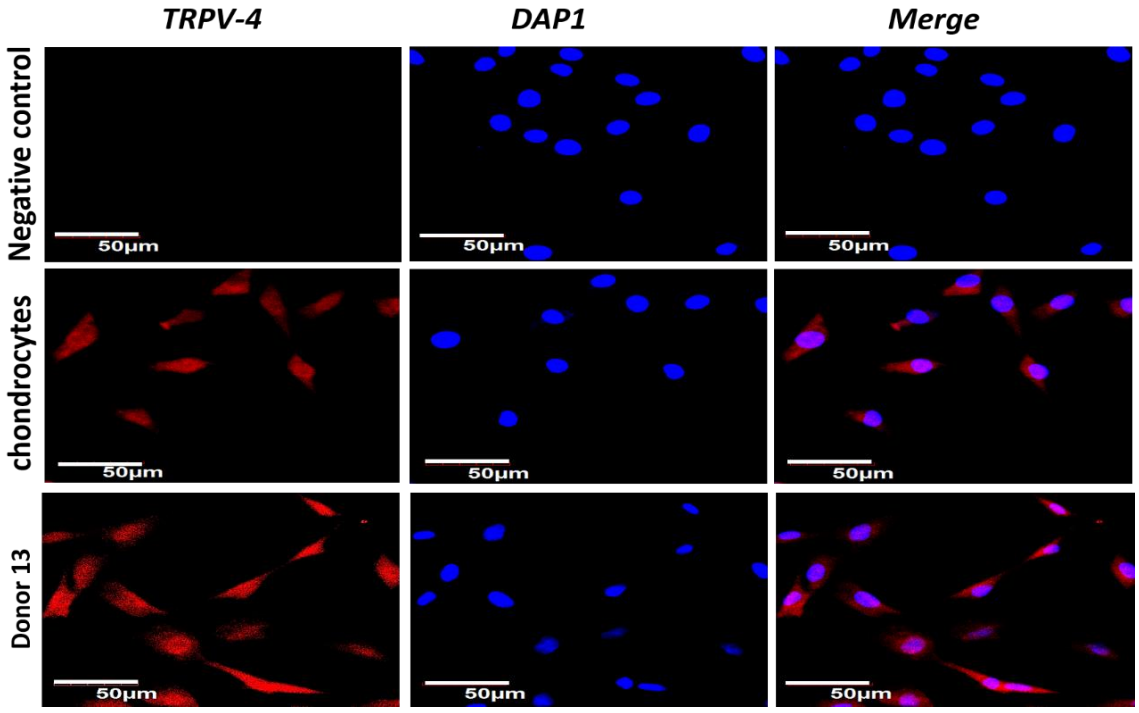

Figure 6. 2: Immunostaining of TRPV4 expression in ovine cells. *Fluorescent micrographs of sheep chondrocytes (P2) and isolated oMSCs (donor 13, P3) showed positive TRPV4 expression (red) compared to the control. Cell nuclei were counter stained with DAPI (blue). Images were taken using a confocal microscope (CLSM) at 60 x magnification. Scale bars = 50 µm.*

6.5.2 Characterisation of the antibody-coated MNPs

6.5.2.1 MNPs sizing and zeta potential

MNPs size distributions are shown for uncoated MNPs, TRPV4-coated and TREK-1-coated MNPs (Figure 6.3A). For uncoated MNPs the particle sizes ranged from around 290 nm to 344 nm (peak at 321 nm). When MNPs were coated with antibodies their size distribution changed. For TREK-1-coated MNPs diameters ranged from below 100nm to around 1200 nm. Two peaks were observed at around 290 nm and 600 nm. An even broader size distribution was observed for TRPV4-coated MNPs ranging from 145 nm to around 1300 nm with a peak at ~350 nm. Overall, coating MNPs with antibodies resulted in an increase in MNPs diameter.

While the surface charge of the MNPs become more positive from about -31-17 mV (uncoated MNPs) to about -21 to +7 mV (TRPV4 coated) and about -17 to +7 mV (TREK-1 coated MNPs (Figure 6.3 B).

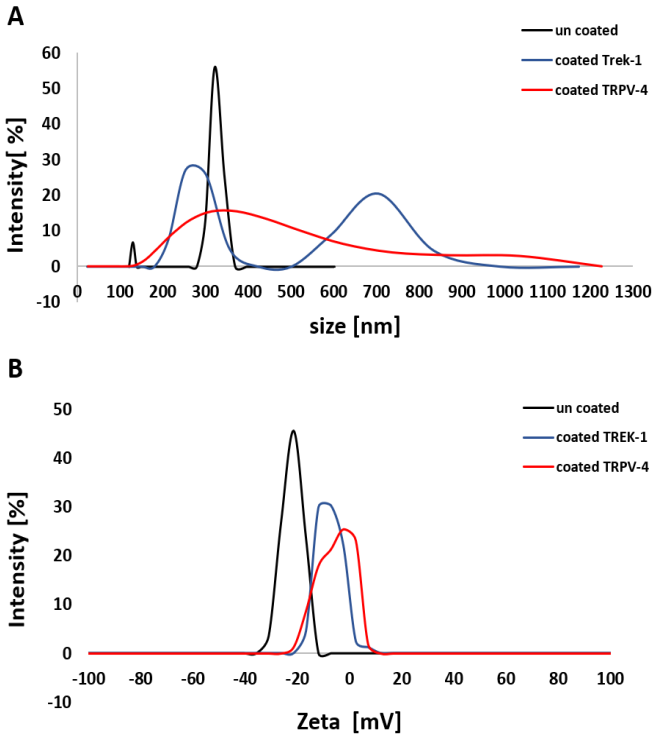

Figure 6. 3: Size and zeta potential of MNPs. *Uncoated and coated MNPs (TRPV4 and TREK-1) were characterised for (A) size and (B) zeta potential by DLS measurements using Malvern zetasizer. Results illustrate increased size of the MNPs after labelling with the antibodies. Changes in surface charge observed from negative (uncoated) to positive (coated).*

6.5.2.2 MNPs oscillating movement

Magnetic nanoparticles possess the advantage that they can be characterized magnetically in addition to conventional NP characterization techniques to obtain more information regarding the MNPs. The TREK-1 and the TRPV4 coated MNPs were characterised for oscillating movement using alternate current susceptometer (ACS) (Figure 6.4). Results show that there was slight alteration in the chi'' curve for the TRPV4 coated MNPs, but not for TREK-1 which exhibited a curve almost similar to the uncoated MNPs.

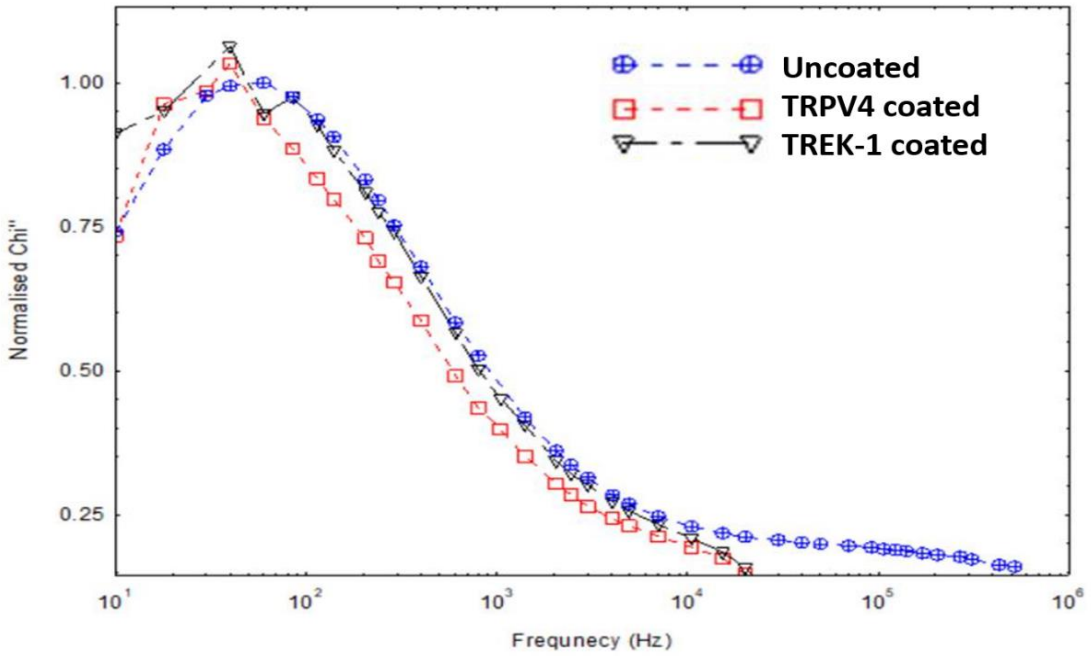

Figure 6. 4: Oscillating movement of MNPs*. Uncoated and coated MNPs (TRPV4 and TREK-1) were characterised for oscillating movement by Alternate Current Susceptometer (ACS). The graph illustrates slight alteration in the ch'' curve for the TRPV4coated MNPs but not for TREK-1 which exhibit a curve almost similar to the uncoated MNPs.*

6.5.3 Assessment of cell metabolic activity using alamar blue assay

Cell metabolic activity was assessed by alamar blue. The results showed consistency in the metabolic activity for each experimental group (Figure 6.5). Generally, cell metabolic activity increased across the experimental time at day 10 and 20 compare to day 1 ($P \leq 0.001$) (significance not shown). In addition, day 10 was significantly higher in cell viability than day 20 for all Ch M cultured gels for both TREK-1 and TRPV4-coated MNPs under static and dynamic culture conditions ($P \leq 0.001$). No significant differences were observed for B M in all conditions between day 10 and 20. Comparing between the TREK-1 group and TRPV4 there was no significant differences in cell metabolic activity between the two groups.

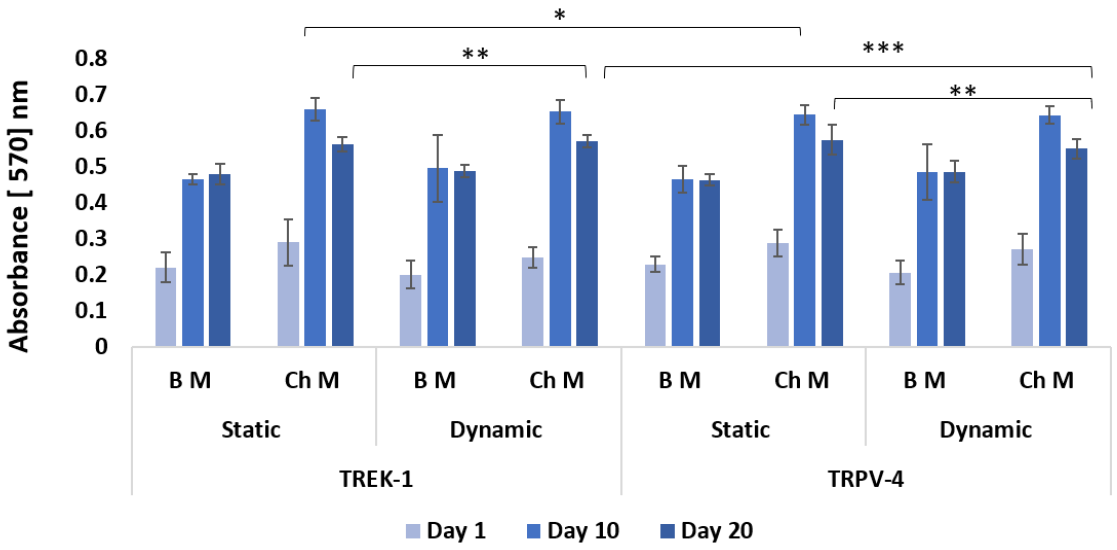

Figure 6. 5: Cell metabolic activity assessed by alamar blue assay. *Cell metabolic activity significantly increased for both ion channel groups TREK-1 and TRPV-4 at day 10 and 20 compare to day 1 for all conditions (significance not shown) There were a significant difference comparing the static and dynamic group within each ion channel. Significant difference was also observed when compare the TREK-1 with TRPV4 regarding to Ch M of each static and dynamic. *p ≤ 0.5, **p ≤ 0.01. ***p ≤ 0.001.*

6.5.4 Compression test and Young's Modulus

Compression tests were performed for gels cultured dynamically and statically in Ch M at day 20. A displacement of 0.2 mm of the entire specimen thickness was applied resulting in loads ranging between 5-20 N. Stress-strain graphs were plotted (Figure 6.6). The TRPV4 dynamic groups revealed the highest values that need for the compression test (stress in N/m^2) than the static, reflecting the solidity of samples. For TREK-1 groups this result was true except donor 13 which showed that the stress strain curves in static group.

Subsequently, Young's modulus was calculated using equation 2.7 in chapter 2, section 2.7 and plotted in Figure 6.7. The graph showed that regarding TRPV4 there is a significant difference between the static and dynamic group for all three donors, for donor 2 ($P \leq 0.01$), for donor 6 ($P \leq 0.01$), and for donor 13 ($P \leq 0.001$). Whereas, there was no significant difference between the groups when comparing dynamic versus static condition. Regarding to differences between the three donors, significant differences were observed ($P \leq 0.001$), between the TRPV4 dynamic group of the donor 13 with TRPV4 dynamic group of each donor 2 ($P \leq 0.01$), and 6 ($P \leq 0.05$). In addition to the significant difference ($P \leq 0.001$) with donor 13 TREK-1 dynamic group.

To summarise the data and compute young modulus of the engineered cartilaginous samples for the three donors the data was plotted as two categories TREK-1 group and TRPV4 group both static and dynamic each. Data was analysed for mean ± standard error. In a same way all static and / or dynamic samples were plotted in a bar chart to estimate the overall young's modulus of the engineered cartilage under the two conditions and the two categories (Figure 6.8).

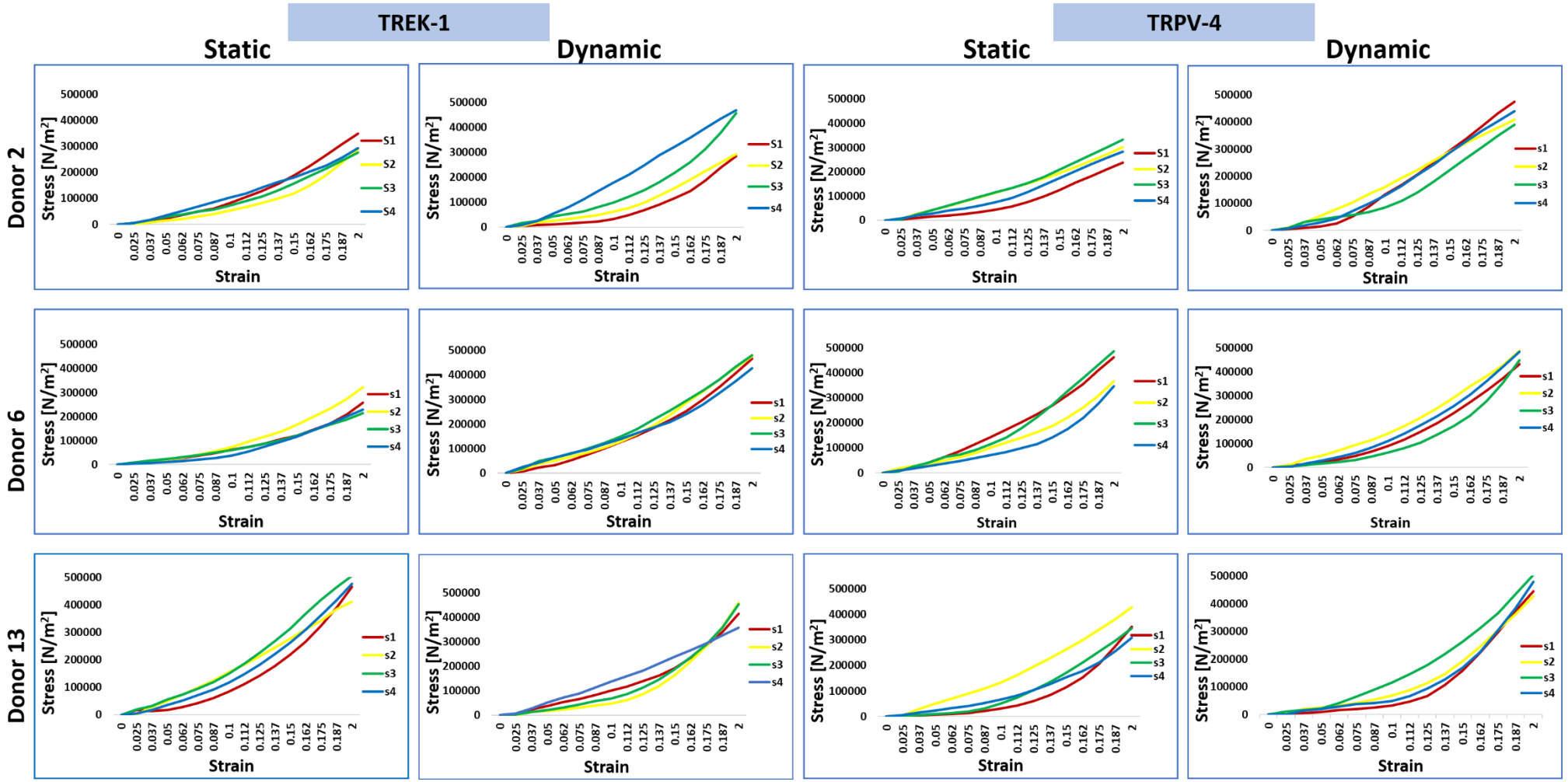

Figure 6. 6: Stress - strain curves of cellular 3D collagen gels. *Stress- strain curves displayed the mechanical properties of the samples. Generally, the TRPV4 dynamic group were higher than static groups, except for donor 13, which displayed the opposite trend in TREK - 1 group. s = sample number (n = 4).*

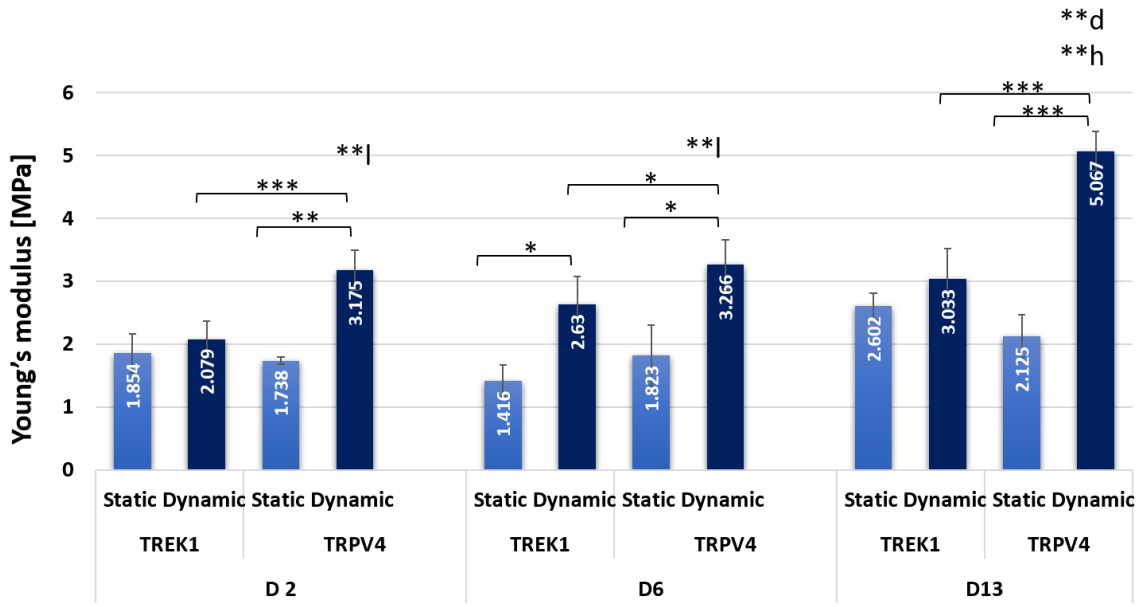

Figure 6. 7: Young's modulus of oMSc-seeded hydrogels on day 20 Ch M only. *Young's modulus was calculated for Ch M treated gels on day 20 only for all experimental groups of the three donors. Significant differences were observed between static and dynamic for TRPV4 group of all donors. Meanwhile, donor 6 was the only one to show significant differences for TREK-1. Also, for the donor variance significant differences between the TRPV4 with TREK-1 dynamic group of the donor 13 and both donors 2 and 6. Data are expressed as mean ± standard error (n = 4). d, h, and l represent statistically significant difference for: donor 2 (Ch M dynamic TRPV4), donor 6 (Ch M dynamic TRPV4), and donor 13(Ch M dynamic TRPV4) respectively * p ≤ 0.05, **p ≤ 001, ***p ≤ 0.001.*

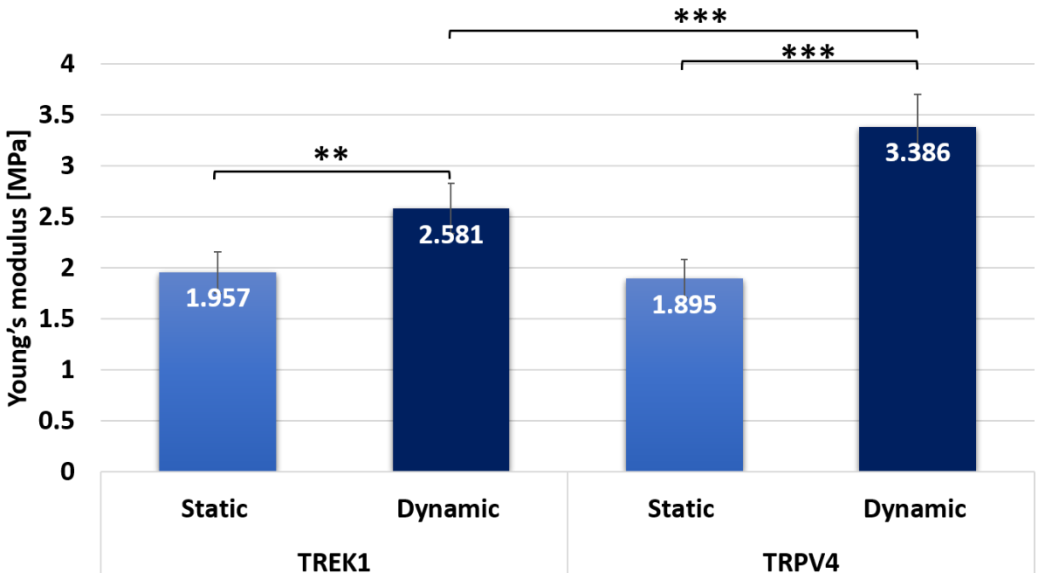

Figure 6. 8: Young's modulus graph of TREK-1 vs TRPV4*. The data of oMSCs-seeded hydrogels of all three donors on day 20 for Ch M only was analysed. The graph displays the significant differences between static and dynamic group for both TREK-1 and TRPV4. The graph also displays that Young's modulus of the TRPV4 dynamic is significantly higher than TREK-1 dynamic group **p ≤ 001. ***p ≤ 0.001.*

6.5.5 Biochemical analysis of oMSC response

6.5.5.1 Quantification of DNA content

PicoGreen assay was used to quantify the DNA content in the gel lysates at day 1 and day 20 (Figure 6.9). In general, the results showed that there is a significant increase in the DNA content indicating increase in the cell number of the B M for all experimental groups in day 20 compared to day 1at $p \leq 0.001$ (the significant was not showed). Whereas, there were decreases but not significant in the cell number for Ch M.

There are differences comparing between the Ch M groups of the dynamic vs static within each group (TREK -1 $p \leq 0.01$ and TRPV 4 $p \leq 0.05$). Significant difference was also observed when compare the TRPV4 with TREK-1 regarding to Ch M of each static $p \leq 0.01$ and dynamic $p \leq 0.05$.

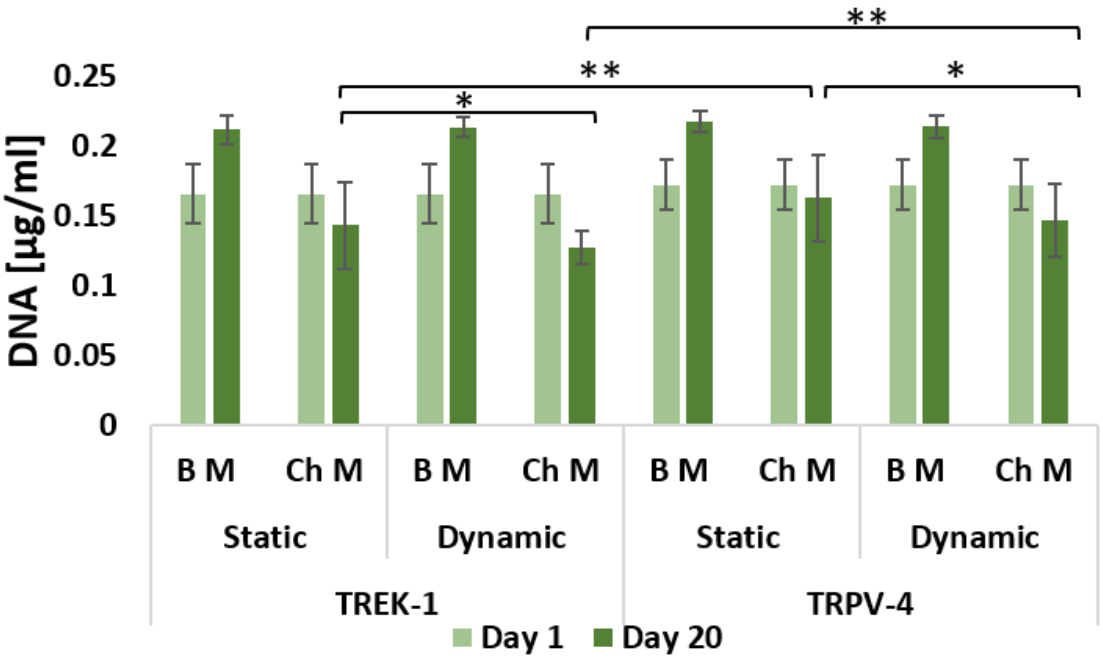

Figure 6. 9: Quantification of DNA content in oMSc-seeded collagen gels of TREK-1 vs TRPV4 group. *DNA content of the gel samples was determined using PicoGreen assay following digestion with proteinase K. The DNA content increased significantly over 20 days for B M gels (significance not shown). Whereas, the DNA content in Ch M gels decreased but not significantly for experimental conditions. There were significant differences while comparing the static and dynamic group within each ion channel. Significant differences were also observed when compare the TRPV4 with TREK-1 in regard to Ch M of each static and dynamic * $P \leq 0.05$, ** $P \leq 0.01$.*

These results confirmed individually for each donor (Figure 6.10) when the DNA contents were significantly increased across the experimental time for the most B M gels that cultured statically and/or subjected to mechanical stimulation. However, the DNA content for the Ch M cultured gels were decreased, except for TRPV4 static (Ch M gel) for the donor 2, which significantly increased ($P \leq 0.001$) over 20 days compared to day 1. For comparing between the static and dynamic group of the all experimental conditions, donor 2 static and dynamic was significantly different ($P \leq 0.001$).

For comparison between the three donors, donor 2 (Ch M dynamic, TREK-1) was different from each donor 6 and 13 (Ch M dynamic, TREK-1). ($P \leq 0.01$) also, donor 2 (Ch M static, TRPV4) was different from each donor 6 and 13 (Ch M static, TRPV4).

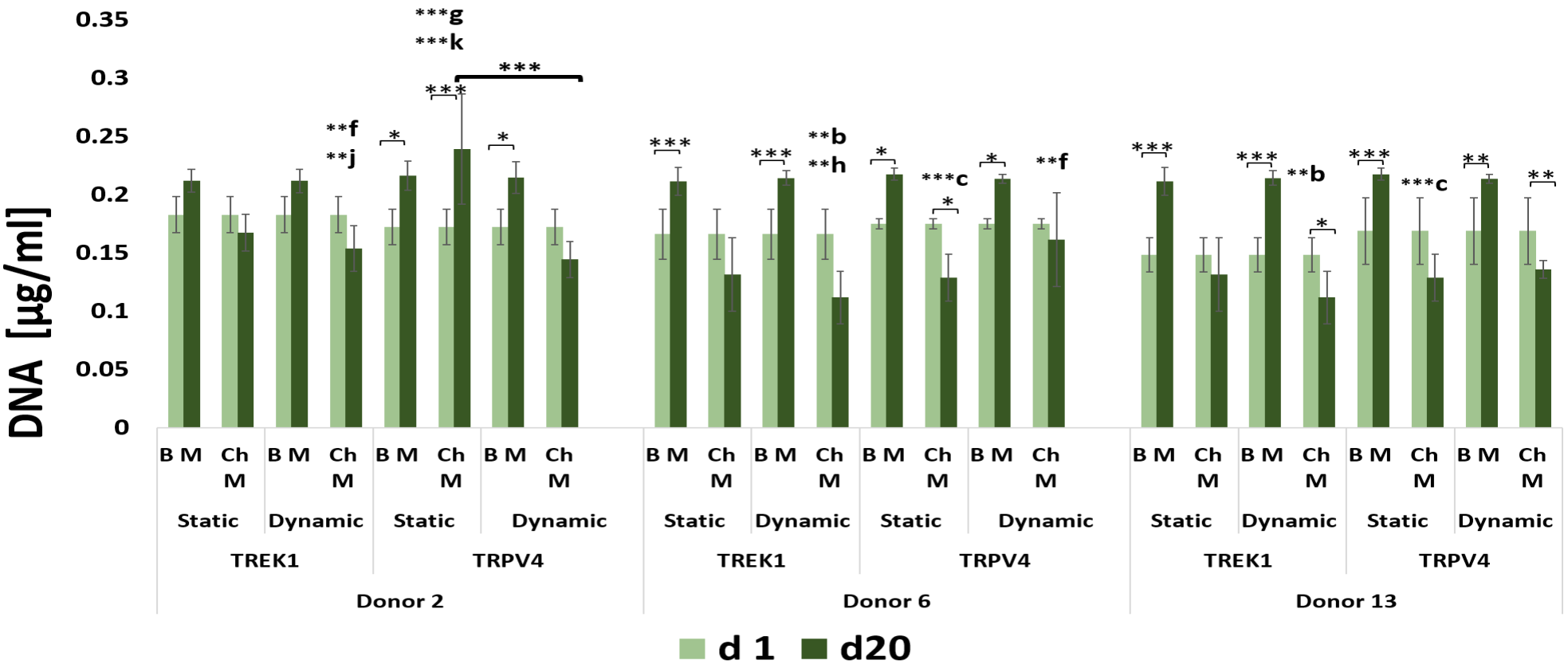

Figure 6. 10: Quantification of DNA content in oMSc-seeded collagen gels. *DNA content was determined using PicoGreen assay following digestion with proteinase K. The DNA content increased significantly over 20 days for most B M gels. Whereas, the DNA content in Ch M gels decreased significantly for experimental conditions except donor 2 static TRPV4 group. Significant differences were observed between donor 2 (Ch M dynamic TREK-1) and each donor 6 and donor 13 (Ch M dynamic TREK-1) as well as donor 2 (Ch M static TRPV4) with each donor 6 and donor 13 (Ch M static TRPV4). d, h, j, and l represent statistically significant difference for: donor 2 (Ch M dynamic TRPV4), donor 6 (Ch M dynamic TRPV4), donor 13 (Ch M dynamic TREK-1) and donor 13(Ch M dynamic TRPV4) respectively. Data are expressed as mean ± standard deviation (n = 3). * $p \leq 0.05$, ** $p \leq 0.01$, *** $p \leq 0.001$.*

6.5.5.2 Quantification of sGAG content in oMSC-seeded collagen gels

The sGAG content was assessed by DMMB assay for all the three donors' data (Figure 6.11). Data showed significant differences between day 1 and day 20 for all conditions ($P \leq 0.001$). (significance not shown). Significant differences were observed when compare static and dynamic group of TRPV4 but not for TREK-1. In addition, a significant difference was observed when comparing TRPV4 versus TREK -1 ($P \leq 0.01$).

These results confirmed individually for each donor (Figure 6.12). when data showed significant differences between day 1 and day 20 for all conditions of the three donors ($P \leq 0.001$), except for the B M gel dynamic TREK-1group ($P \leq 0.01$). No significant differences when compare static and dynamic group of each TREK-1 and TRPV4. For comparison between the three donors, there are 0significant differences between donor 13 (Ch M dynamic TRPV4) with each of donor 2 and 6 (Ch M dynamic TRPV4) ($P \leq 0.05$).

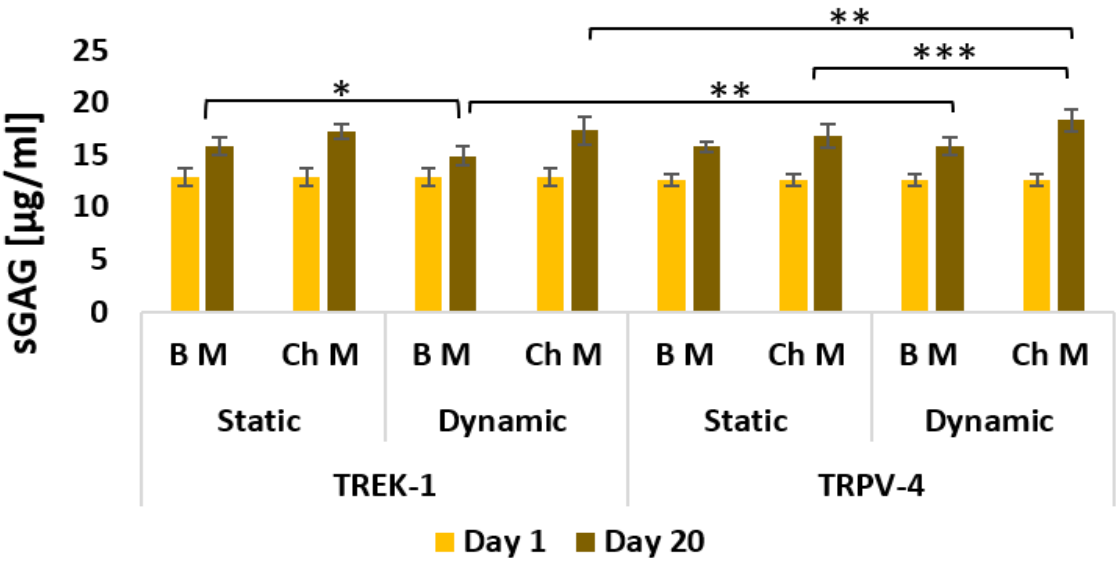

Figure 6. 11: Quantification of sGAG content in oMSc-seeded collagen gels of TREK-1 vs TRPV4 group. *The sGAG content was determined using DMMB assay following digestion with proteinase K. sGAG contents significantly increased at day 20 for all experimental conditions compared to day 1 (significance not shown).*

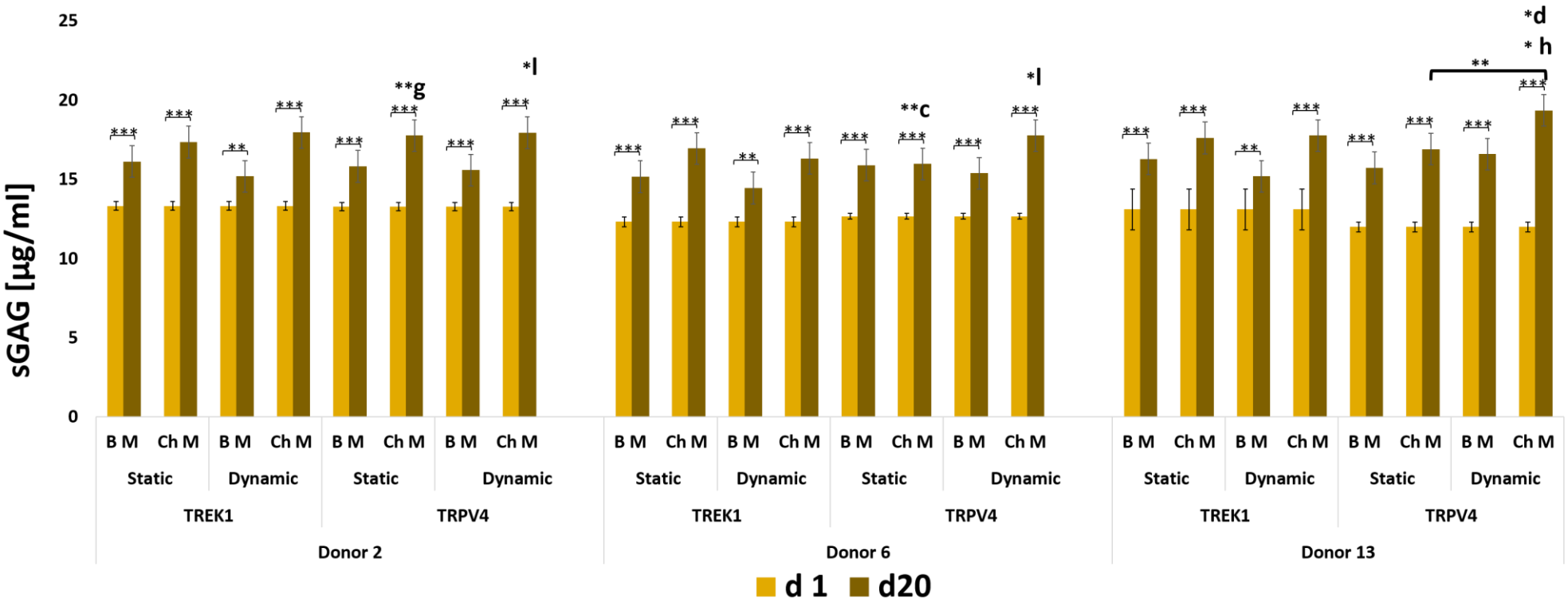

Figure 6. 12: Quantification of GAG content in collagen gels. *The GAG content was determined using DMMB assay following digestion with proteinase K. GAG contents were significantly increased at day 20 for all experimental conditions. Significant differences between donor 2 (static Ch MTRPV4) and donor 6 (static Ch M TRPV4) as well as between donor 13 (dynamic Ch M TRPV4) and donor 2 (dynamic Ch M TRPV4) and donor 6 (dynamic Ch M TRPV4). (c, d, g, h and l) represent statistically significant difference form: donor 2 (Ch M static TRPV4), donor 2 (Ch M dynamic TRPV4), donor 2 (Ch M dynamic TRPV4), donor 6 (Ch M dynamic TRPV4) and donor 13(Ch M dynamic TRPV4) respectively. Data are expressed as mean ± standard deviation (n = 3). * p ≤ 0.05, **p ≤ 001, ***p ≤ 0.001.*

6.5.5.3 sGAG content normalised to DNA content

The sGAG content was normalised to the DNA content of the same samples to determine the sGAG content in relation to cell number (Figure 6.13). The results showed that for all donors and experimental conditions the normalised sGAG for Ch M cultured gels significantly increased ($P \leq 0.001$) (significance not shown), but for B M there were no significant differences. On the other hand, there is a significant difference between the static and dynamic of the TRPV4. Interestingly there is a significant difference between static group between Ch M of the TRPV4 and Ch M of the TREK-1($P \leq 0.01$).

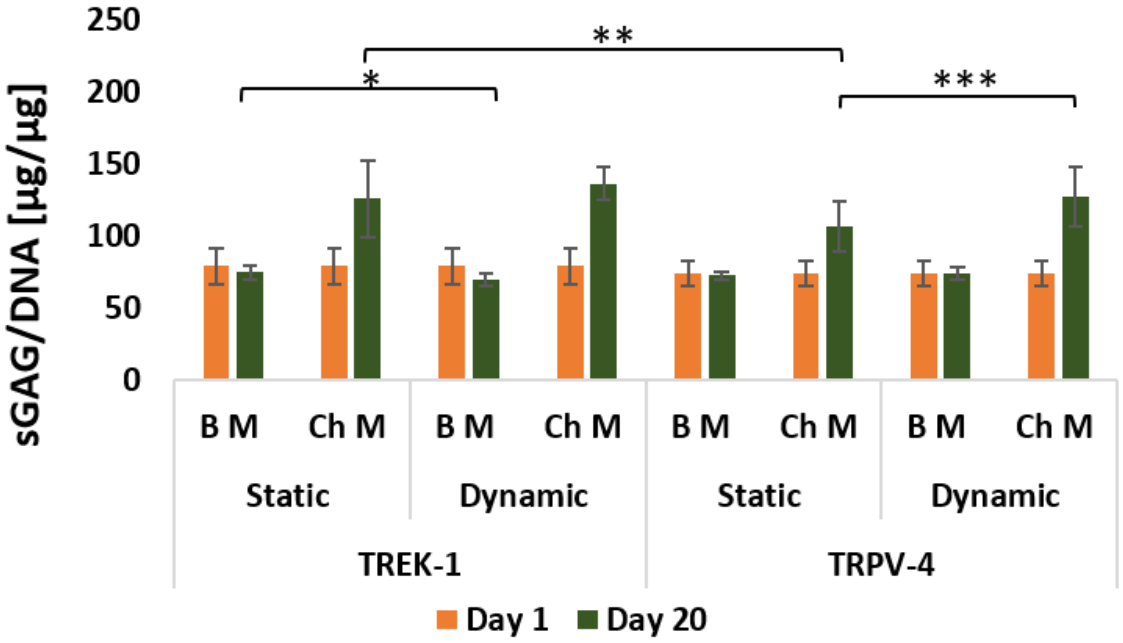

Figure 6. 13: sGAG content in oMSc-seeded collagen gels of TREK-1 vs TRPV4 group. *sGAG in relation to cell number increased significantly for gels cultured in Ch M for all time points (significance not shown). No significant increases were observed for gels cultured in B M. There is a significant difference between the static and dynamic of the TRPV4. Comparing TREK-1 versus TRPV4, there was a significant difference between the static group but not the dynamic group of them * $p \leq 0.05$, **$p \leq 001$***$p \leq 0.001$.*

These results confirmed individually (Figure 6.14). for each donor when the results showed that for all donors and experimental conditions the normalised GAG content for Ch M cultured gels was significantly increased ($P \leq 0.001$) except for donor 2 (Ch M static TRPV4). While for B M gels, no significant differences were observed over 20 days.

Comparing dynamic with static group of the donors, there was significant difference between static and dynamic of the TRPV4 group for the donor 2 only.

When comparing between the three donors, following significant differences were observed: Donor 2 (Ch M static TREK-1) significantly different with donor 13 (Ch M static TREK-1) ($P \leq 0.05$), Donor 2 (Ch M dynamic TREK-1) significantly different with donor 13(Ch M dynamic TREK-1), Donor 2 (Ch M static TRPV4) significantly different with donor 6 and 13 (Ch M static TRPV4) ($P \leq 0.01$) and donor 6 (Ch M dynamic TRPV4) significantly different with donor 13 (Ch M dynamic TRPV4).

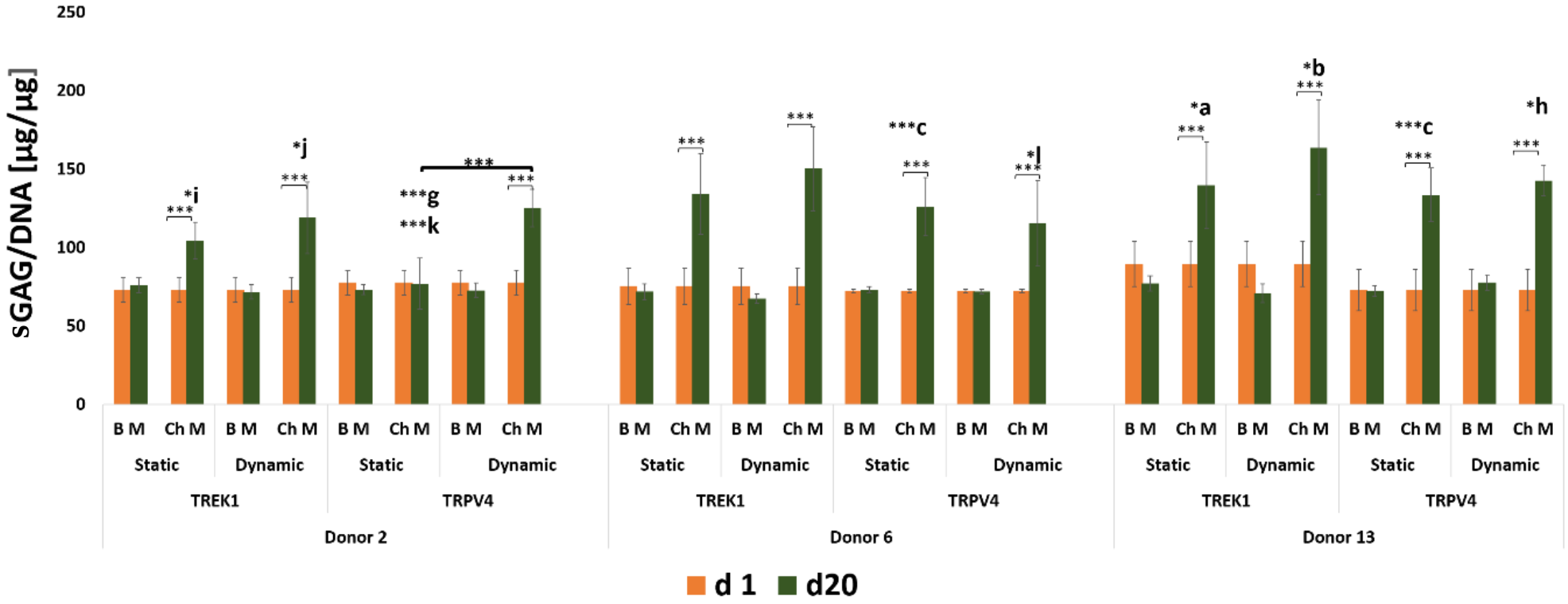

Figure 6. 14: sGAG content normalized to the DNA content. *sGAG in relation to cell number increased significantly for gels cultured in Ch M for all time points, except donor 2 (Ch M, static, TRVP4). No significant increases were observed for gels cultured in B M. Results further revealed significant differences between donor 2 (Ch M static TREK-1) and donor 13 (Ch M, static TREK – 1);between donor 2 (Ch M dynamic TREK – 1) and donor13 (Ch M dynamic TREK – 1); between donor 2 (Ch M static TRPV4) and donor 6 and donor 13 (Ch M static TRPV4;, as well as between donor 13 (Ch M dynamic TRVP4) and donor 6 (Ch M dynamic, TRVP4). a, b, c, g, h, i, j, k and l represent : donor 2 (Ch M static TREK-1), donor 2 (Ch M dynamicTREK-1), donor 2 (Ch M static TRPV4), donor 6 (Ch M static TRPV4), donor 6 (Ch M dynamic TRPV4), donor 13 (Ch M static TREK-1), donor 13 (Ch M dynamicTREK-1), donor 13 (Ch M static TRPV4)and donor 13 (Ch M dynamic TRPV4). Data are expressed as mean ± standard deviation (n = 3), * p ≤ 0.05, **p ≤ 001***p ≤ 0.001.*

6.5.5.4 Quantification of total protein content of oMSC-seeded collagen gels

The total protein content in the gel samples was assessed using BCA Protein Assay (Figure 6.15). There are significant increases in the total protein content (µg/ml) at day 20 compared to day 1 for all Ch M gels ($P \leq 0.01$). (significance not shown), but not for B M gels. Comparing the static and dynamic group within each experimental group (TREK-1 and TRPV4), there is significant difference within TRPV4 ($P \leq 0.001$), but not within TREK-1 group. The graph also displayed significant differences between TRPV4 and TREK-1 in regard to dynamic versus dynamic and static versus static group ($P \leq 0.05$).

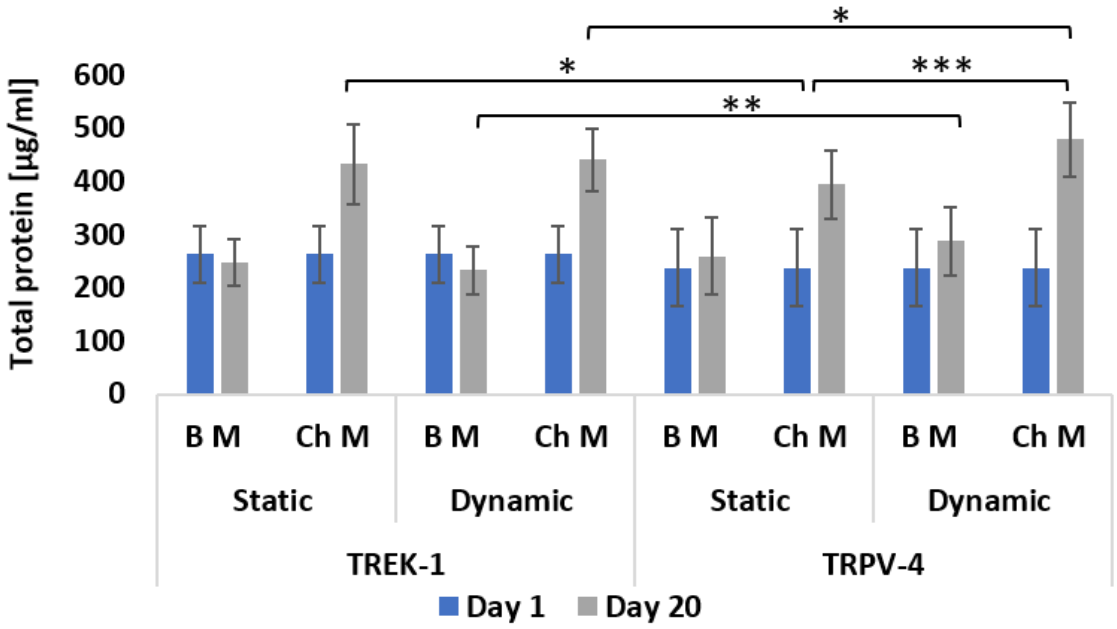

Figure 6. 15: Total protein content in oMSc-seeded collagen gels of TREK-1 vs TRPV4 group. *Total protein content in the gels was assessed using BCA Protein Assay, following digestion with proteinase K. Total protein concentrations significantly increased for all Ch M groups (significance not shown). No significant differences were observed for all B M groups. * p ≤ 0.05, **p ≤ 001***p ≤ 0.001.*

Individually, the results confirmed by significant increases in the total protein content (μg/ml) at day 20 compare with day 1 for all Ch M gels and most of B M gels. Comparing the different culture conditions with each other, no significant differences were found between the dynamic and static groups for both TREK-1 and TRPV4 labelled cells cultured in Ch M. Significant differences in the chondrogenic performance were found as follow: Donor 2 (Ch M static TREK-1) is significantly different from donor 13(Ch M static TREK-1) ($P \leq 0.01$), donor 2 (Ch M dynamic TREK-1) is significantly different from donor 13($P \leq 0.001$), donor 6 (Ch M static TREK-1) is significantly different from donor 13 (Ch M static TREK-1) ($P \leq 0.001$) and donor 6 (Ch M dynamic TREK-1) is significantly different from donor 13 (Ch M dynamic TREK-1) (Figure 6.16).

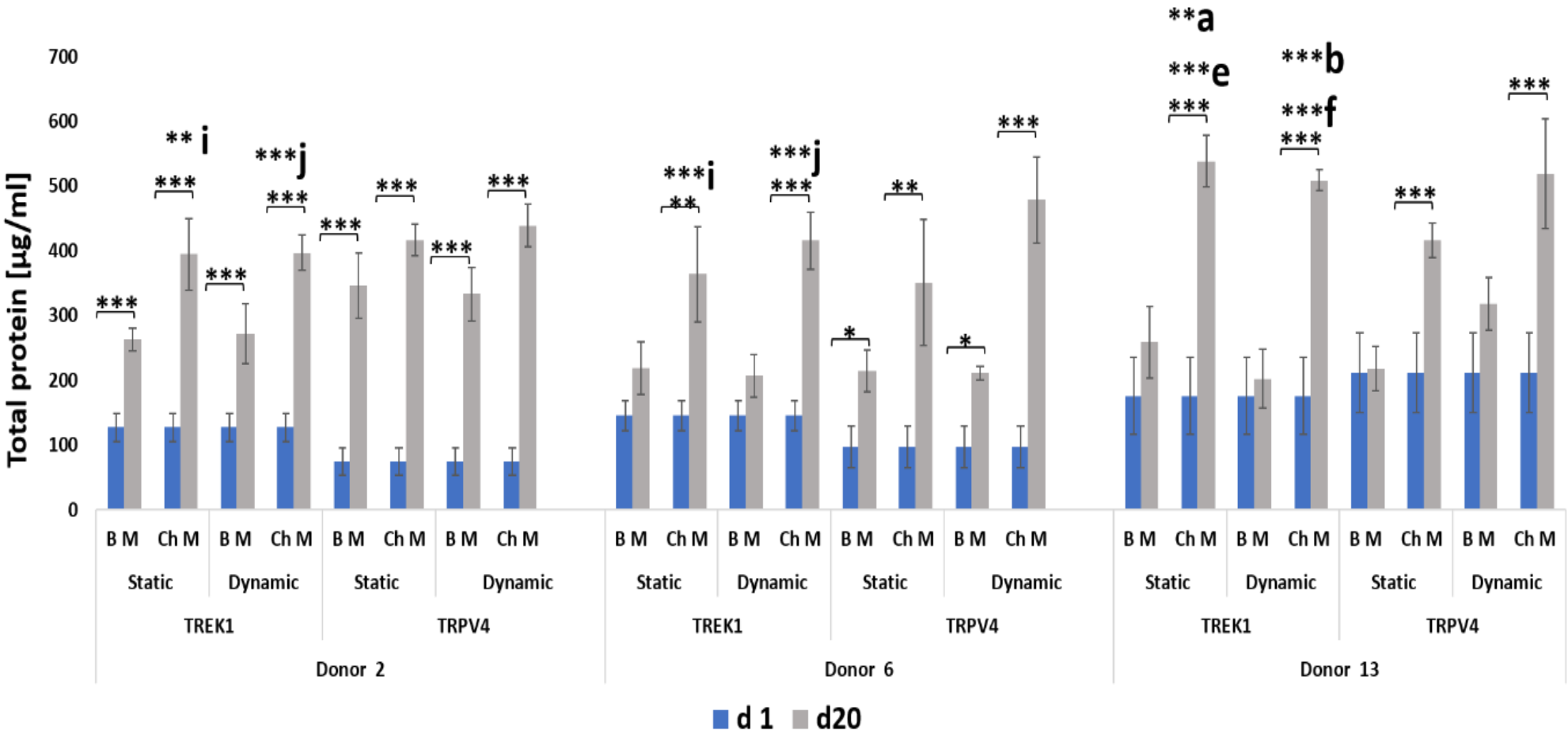

Figure 6. 16: Total protein content. *The total protein content in the gels was assessed using BCA Protein Assay, following digestion with proteinase K. Total protein concentrations significantly increased in all Ch M groups but less in the B M group for the both T REK - 1 and TRPV4 in all three donors. a, b, e, f, i and j represent statistically significant difference for: donor 2 (Ch M static TREK-1), donor 2 (Ch M dynamicTREK-1), donor 6 (Ch M static TREK-1), donor 6 (Ch M dynamicTREK-1), donor 13 (Ch M static TREK-1) and donor 13 (Ch M dynamicTREK-1) respectively. Data are expressed as mean ± standard deviation (n = 3). * p ≤ 0.05, **p ≤ 001, ***p ≤ 0.001.*

6.5.5.5 Total protein content normalised to DNA content

The total protein content was normalised to the DNA content of the same samples to determine the total protein content in relation to cell number (Figure 6.17). In general, the normalised values showed increasing in the normalised data across the experimental time comparing to day 1 for Ch M gels but not for B M. Comparing the Ch M group of each condition, there is a significant difference between Ch M dynamic and Ch M static ($P \leq 0.001$) for TRPV4 group. Whereas, there is no significant difference between Ch M dynamic and Ch M static for TREK-1 group. In the other hand there was no significant differences for Ch M of the dynamic group between the TRPV4 and TREK-1.

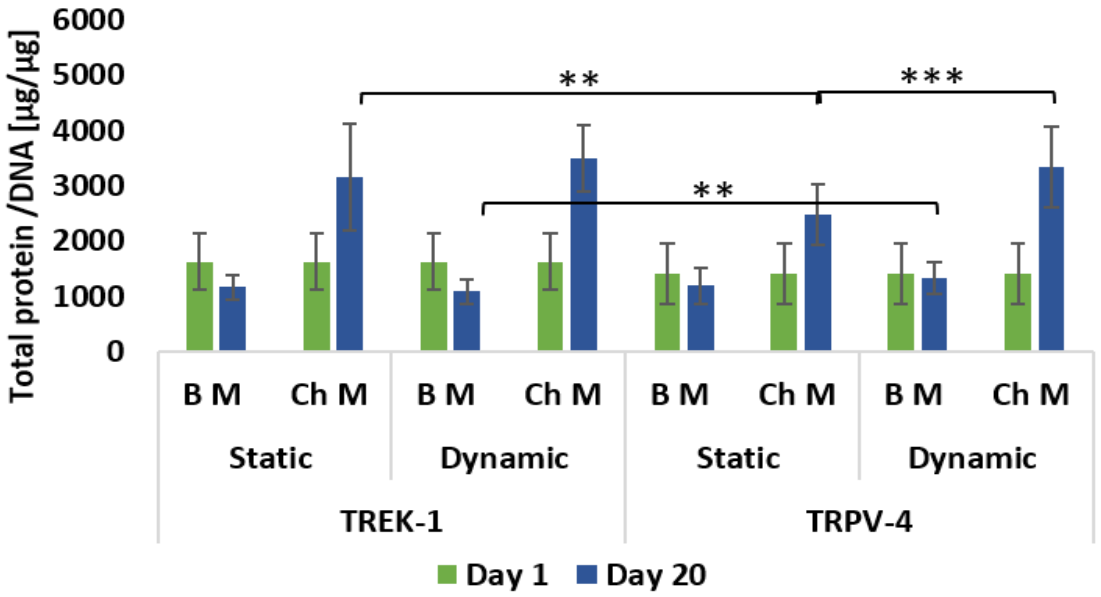

Figure 6. 17: The total protein content normalised to the DNA content of TREK-1 vs TRPV4 group. *The normalised values showed increasing in the normalised data across the experimental time comparing to day 1 for Ch M gels but not for B M. comparing the Ch M group of each condition, there is a significant difference between Ch M dynamic and Ch M static for TRPV4 group. No significant difference between Ch M dynamic and Ch M static for TREK-1 group was observed. No significant differences for Ch M of the dynamic group between the TRPV4 and TREK-1. **p ≤ 001, ***p ≤ 0.001.*

These results confirmed individually for each donor, when the results showed that the increases were significant for $P \leq 0.001$ in all Ch M cultured gels of all condition (Figure 6.18). However, the B M results of the TRPV4 group showed increases in the normalised protein value, for donor 2 and donor 6 (static and dynamic) but they were not as high as for the Ch M gels. Comparing static with dynamic group, significant differences were observed for donor 2 for TRVP4 ($P \leq 0.001$). While, for donor 6 and 13 no significant differences were observed between the dynamic and static groups for both TEK-1 and TRPV4.

Comparing between donors, donor 13 (Ch M static TREK-1) was significantly different from donor 2 (Ch M static TREK-1) and donor 6 (Ch M static TREK-1) ($P \leq 0.001$). Donor 2 (Ch M static TRPV4) was significant different from donor 13 (Ch M static TRPV4) ($P \leq 0.01$). Donor 2 (Ch M static TRPV4) was significant different from each donor 6 and 13 (Ch M static TRPV4) ($P \leq 0.001$).

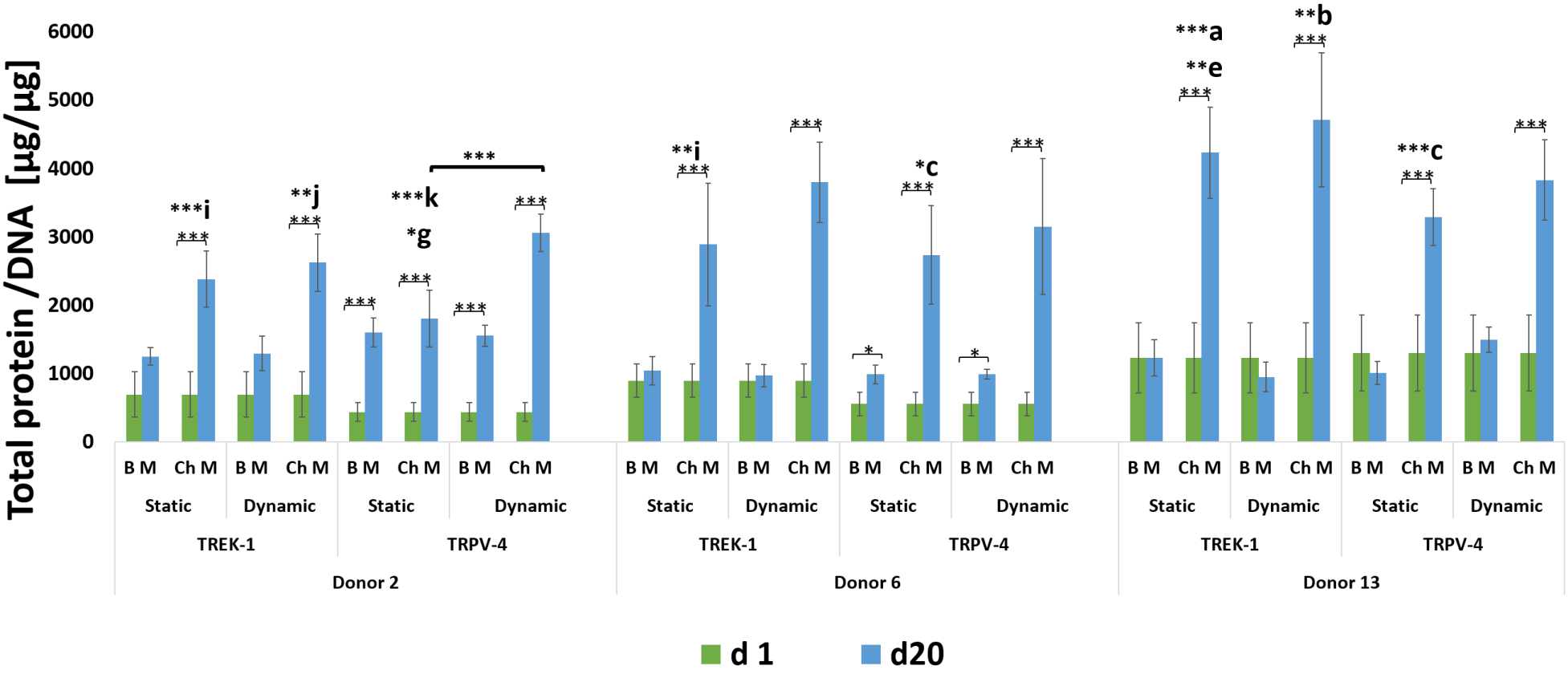

Figure 6. 18: The total protein content normalised to the DNA content. *Significant increases across the time points were observed for Ch M, but not B M for all donors and culture conditions, except donor 2, which showed an increase in the B M of both static and dynamic of the TRPV4 compare with day 1. a, b, c, e, g, i, j and k, represent statistically significant differences for: donor 2 (Ch M static TREK-1), donor 2 (Ch M dynamicTREK-1), donor 2 (Ch M static TRPV4), donor 6 (Ch M static TREK-1), donor 6 (Ch M static TRPV4), donor 13 (Ch M static TREK-1), donor 13 (Ch M dynamicTREK-1) and donor 13 (Ch M static TRPV4) respectively. Data are expressed as mean ± standard deviation (n = 3). * $p \leq 0.05$, ** $p \leq 001$, *** $p \leq 0.001$.*

6.5.5.6 Total collagen content

The total collagen content in the gel samples was assessed using Chondrex Sirius Red Collagen detection Kit as described in chapter 2, section 2.6.4. Data are shown in Figure 6.19. The increases in the collagen production across the experimental time were significant for Ch M dynamic group. Significant differences were found between the dynamic and static groups for both TREK-1 ($P \leq 0.001$) and TRPV4 ($P \leq 0.05$) labelled cells cultured in Ch M.

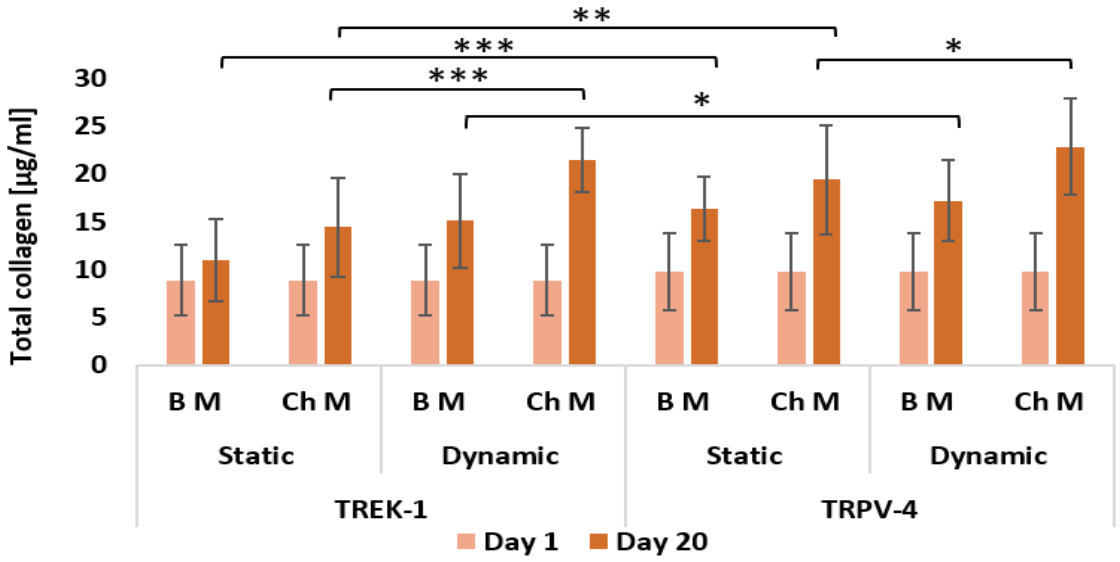

Figure 6. 19: Total collagen content of TREK-1 vs TRPV4 group. *The graph showed significant increases in the collagen production across the experimental time for Ch M dynamic group. Significant differences were found between the dynamic and static groups for both TREK-1 and TRPV4) labelled cells cultured in Ch M. * $p \leq 0.05$, **$p \leq 001$, ***$p \leq 0.001$.*

These results confirmed individually for each donor (Figure 6.20). Significant increases were observed for the comparison of day 1 (Ch M gels) with day 20 (Ch M gels) for both dynamic and static cultured gel ($P \leq 0.001$). However, the B M gels for the TRPV4 dynamic and static group showed increases in the total collagen value for the donors 2 and 13 ($P \leq 0.01$). In addition, increased total collagen concentrations were observed for the B M TREK-1 dynamic group of donors 2 and donor 6 ($P \leq 0.01$). Significant differences were revealed when comparing the dynamic and static group for the both TREK-1 and TRPV4 for donor 6, but not for other donors (donor 2 and donor 13). There were no significant differences among the three donors regarding to their performance of the collagen production.

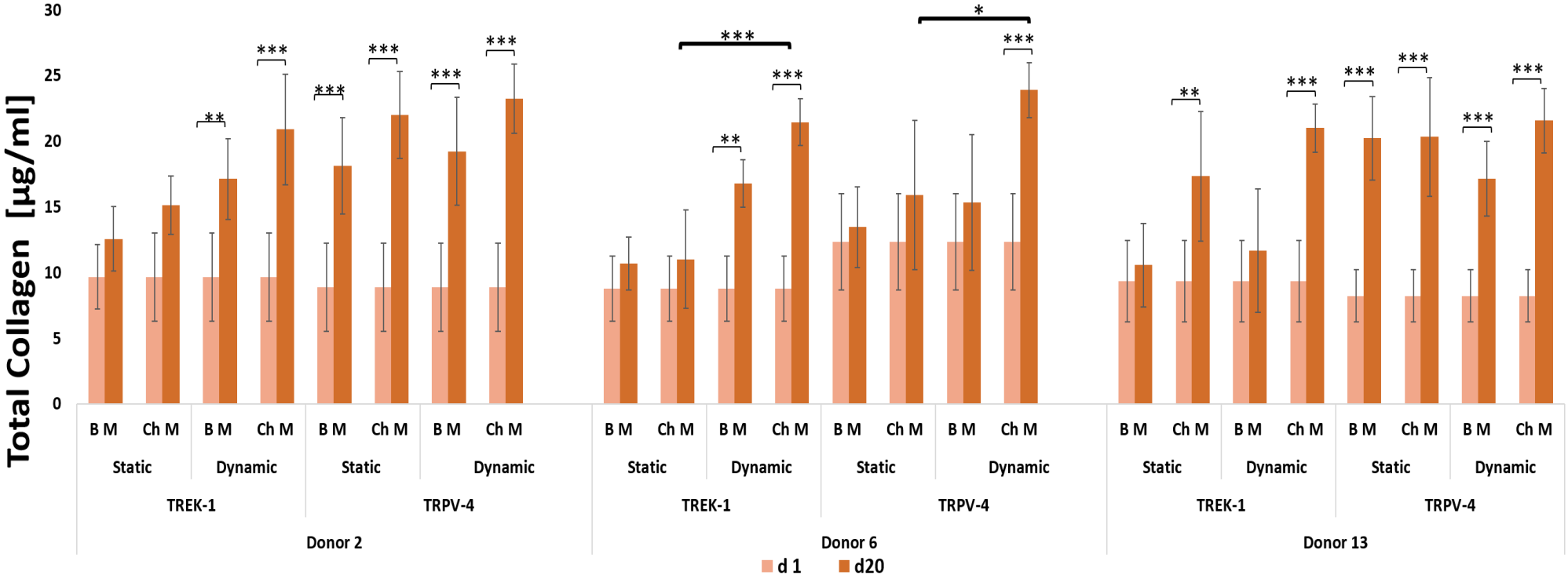

Figure 6. 20: Total collagen content. *The total collagen content in the gel samples was assessed using Chondrex Sirius Red Collagen detection Kit, following digestion with proteinase K. Statistically significant increases were observed at day 20 for all dynamically and some statically cultured gels. The B M gels of the dynamic TRPV4 group showed increases in total collagen for donors 2 and 13 in addition to the B M of the dynamic TREK-1 group for donors 2 and 6. There are significant differences when comparing the dynamic and static group for the both TREK-1 and TRPV4 for donor 6, but not for t donor 2 and donor 13. There were no significant differences among the three donors regarding to their collagen production. Data are expressed as mean ± standard deviation (n = 3). * p ≤ 0.05, **p ≤ 001, ***p ≤ 0.001.*

6.5.5.7 Total collagen content normalised to DNA content

The total collagen content was normalised to the DNA content to determine the total collagen content in relation to cell number (Figure 6.21). Overall, across the experimental time the increases in the normalised DNA value were significant in dynamic group of both TREK-1 and TRPV4 ($P \leq 0.001$). Statistically significant differences were found between the static and dynamic group within each TREK-1($P \leq 0.001$) and TRPV4 ($P \leq 0.01$) group.

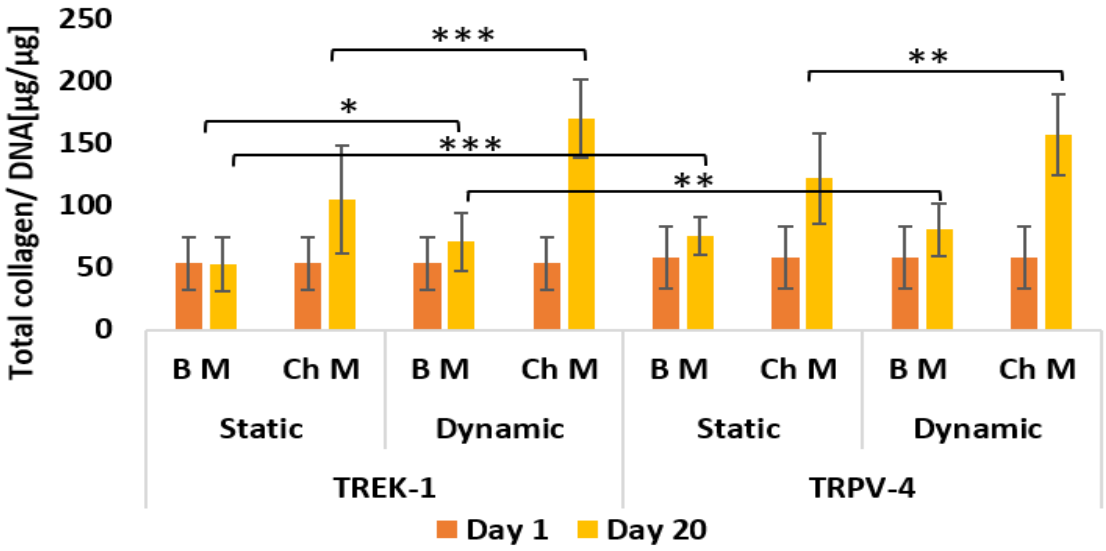

Figure 6. 21: Total collagen content normalised to the DNA content of TREK-1 vs TRPV4 group. *Across the experimental time the increases in the normalised DNA value were significant in dynamic group of both TREK-1 and TRPV4. Differences were found between the static and dynamic group within each TREK-1and TRPV4 group. * $p \leq 0.05$, ** $p \leq 001$, *** $p \leq 0.001$.*

Individually for each donor (Figure 6. 22), the results showed higher levels of normalised collagen for the dynamic Ch M groups compared to the static groups for donor 2, 6 and 13. Statistically significant differences were found for Ch M static gels of donors 2 for both TREK-1 and TRPV4, and for the donor 6 and 13 for TREK-1 ($P \leq 0.001$).

Comparing static with dynamic group, significant differences between static and dynamic group were observed for each donor 2 (for TREK-1 and TRPV4) ($P \leq 0.001$). donor 6 ($P \leq 0.001$).and 13 ($P \leq 0.01$). (for TREK-1 only).

The comparison of all donors with each other revealed significant differences between donor 2 (Ch M dynamic TREK -1) and donors 6 and 13 (Ch M dynamic TREK -1) ($P \leq 0.001$).

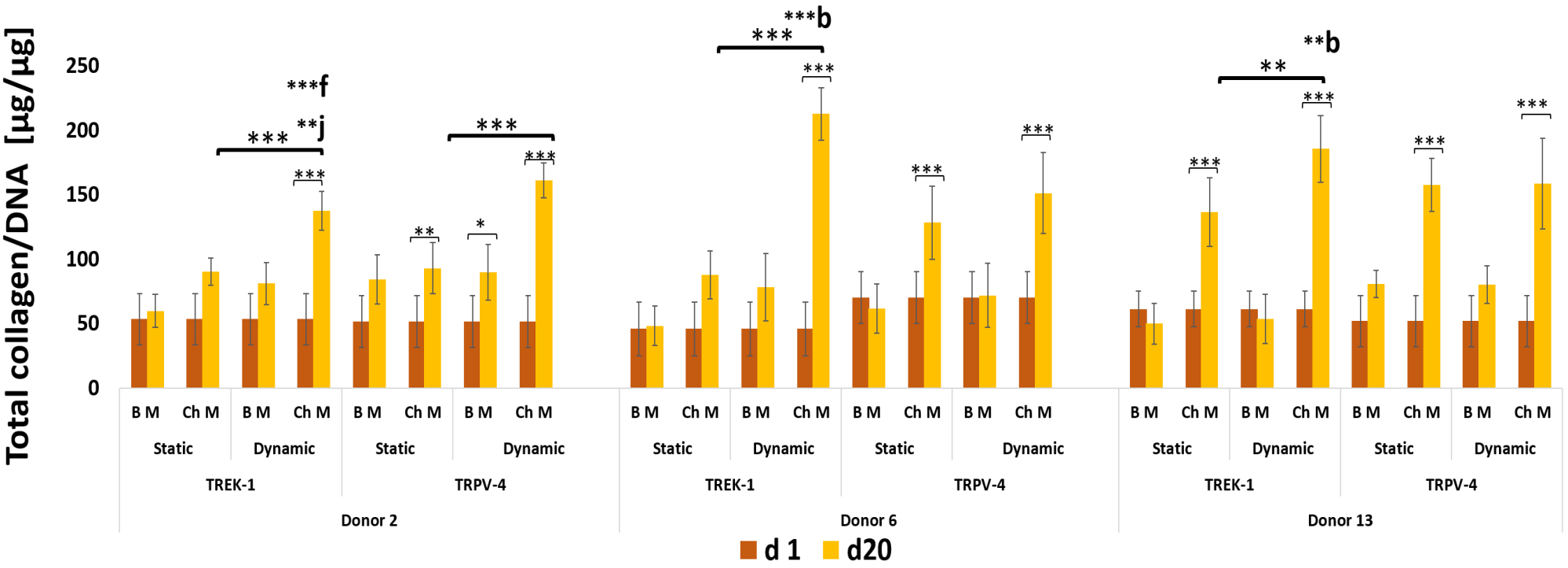

Figure 6. 22: Total collagen content normalised to the DNA. *The results showed increases in the normalised collagen content over 20 days. Significant differences were observed between dynamic and static Ch M groups of donor 2 (both TREK-1 and TRPV4) and for the donor 6 and 13 for TREK-1. The comparison of donor 2, 6 and 13 with each other revealed significant differences between donor 2 (Ch M dynamic TREK -1) and donors 6 and 13 (Ch M dynamic TREK -1). b, f, and j; represent statistically significant difference for: donor 2 dynamic Ch M TREK-1, donor 6 dynamic Ch M of TREK-1 and donor13 dynamic Ch M of TREK- 1. Data are expressed as mean ± standard deviation (n = 3). * p ≤ 0.05, **p ≤ 001, ***p ≤ 0.001.*

6.5.5.8 Collagen content normalised to protein content

The collagen contents of the gel samples were normalised to the total protein content of the same samples (Figure 6.23). Overall, across the experimental time the increases in the normalised total collagen / total protein were not significant. Statistically significant differences were found between the static and dynamic group within TREK-1($P \leq 0.001$) but not TRPV4 ($P \leq 0.01$) group.

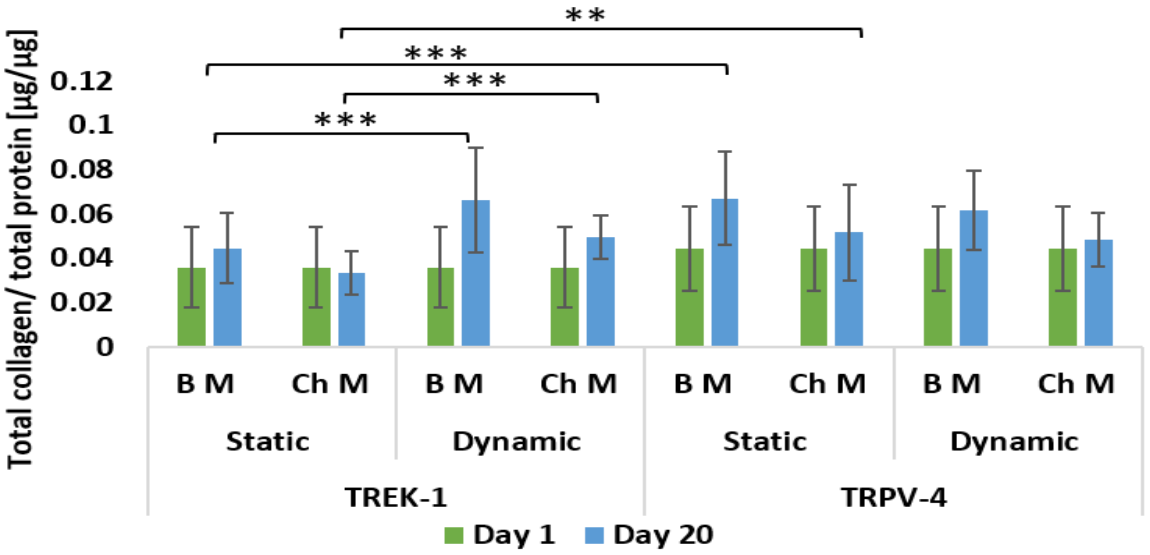

Figure 6. 23: Total collagen content normalised to the total protein content of TREK-1 vs TRPV4 group. *The increases in the normalised total collagen / total protein were not significant across the experimental time. Statistically significant differences were found between the static and dynamic group within TREK-1only.*

Individually for each donor (Figure 6.24) no significant changes in normalised collagen content were observed for donor 2 for all conditions. However, donor 6 revealed statistically significant changes over 20 days for Ch M dynamically cultured gels for both TREK-1 ($P \leq 0.001$) and TRPV4 ($P \leq 0.01$). For donor 13, significant increases were observed over experimental time for the TRPV4 dynamic gels only ($P \leq 0.001$).

Comparing static with dynamic group, significant differences between static and dynamic group were observed for each donor 6 (for TREK-1) ($P \leq 0.001$). donor 13 ($P \leq 0.01$) (for TRPV4).

The comparison of donors with each other showed significant differences in the normalised collagen to total protein content between donor 6 (Ch M, TREK-1) and donor 13 (Ch M, TREK-1) for dynamically cultured gels only ($P \leq 0.01$).

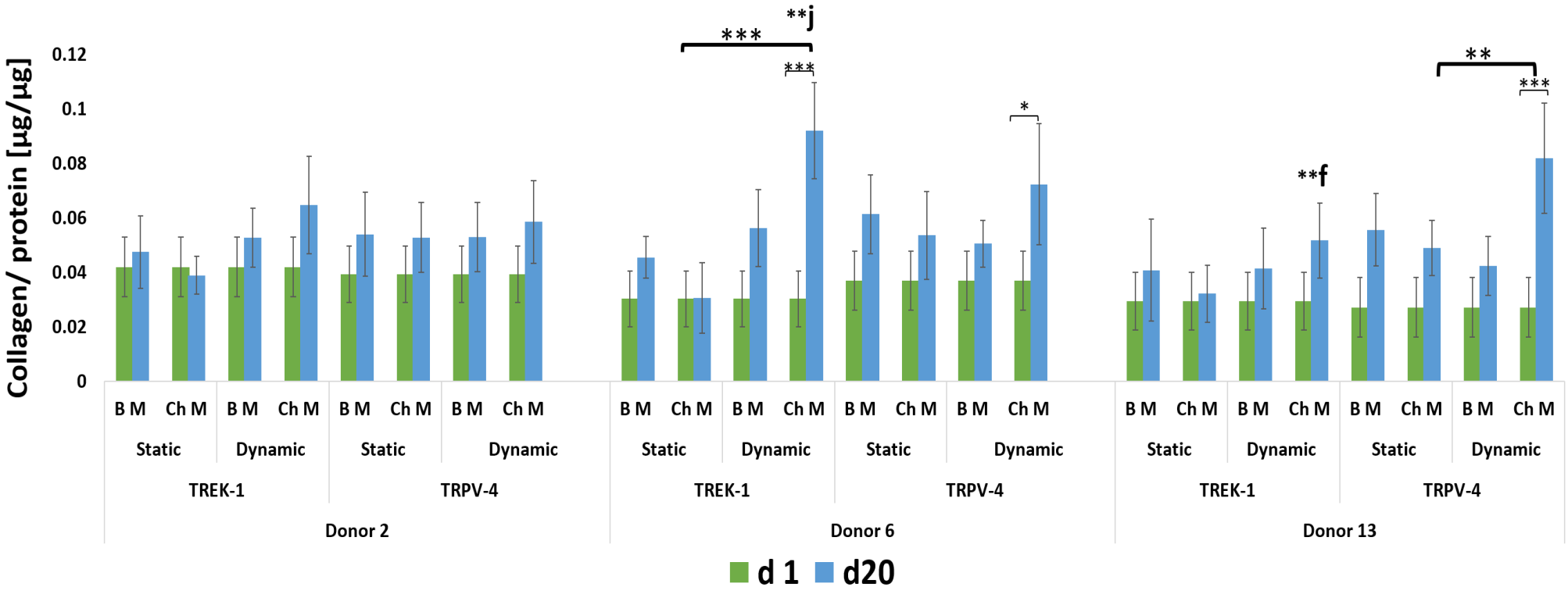

Figure 6. 24: Total collagen content normalised to the total protein content. *No statistically significant differences were observed for donor 2 for all conditions. For donor 6 significant increases in collagen content were observed for Ch M dynamic for both TREK-1 and TRVP4 ($p \leq 0.01$). For donor 13 significant increases were found for dynamic TRPV4 only ($p \leq 0.001$). Donor comparison revealed significant differences between donor 6 and 13 (Ch M, TREK-1, dynamic) at $p \leq 0.01$. f and j; represent statistically significant difference for: 6 dynamic Ch M of TREK-1 and donor13 dynamic Ch M of TREK- 1. Data are expressed as mean ± standard deviation (n = 3). * $p \leq 0.05$, **$p \leq 001$, ***$p \leq 0.001$.*

6.5.6 Histology

6.5.6.1 Haematoxylin and Eosin staining

The bright field micrographs of the H and E stain on day 20 revealed clear differences between B M and Ch M treated gels (Figure 6.25). The B M gels had minimal staining of the extracellular matrix compared to Ch M in both dynamically or statically cultured gels for both TREK-1 and TRPV4 antibodies. However, highest stain intensities were observed for the Ch M dynamic TRPV4 group in all three donors. There were slight differences in dye intensity when comparing Ch M static with Ch M dynamic of the same donor and same antibody.

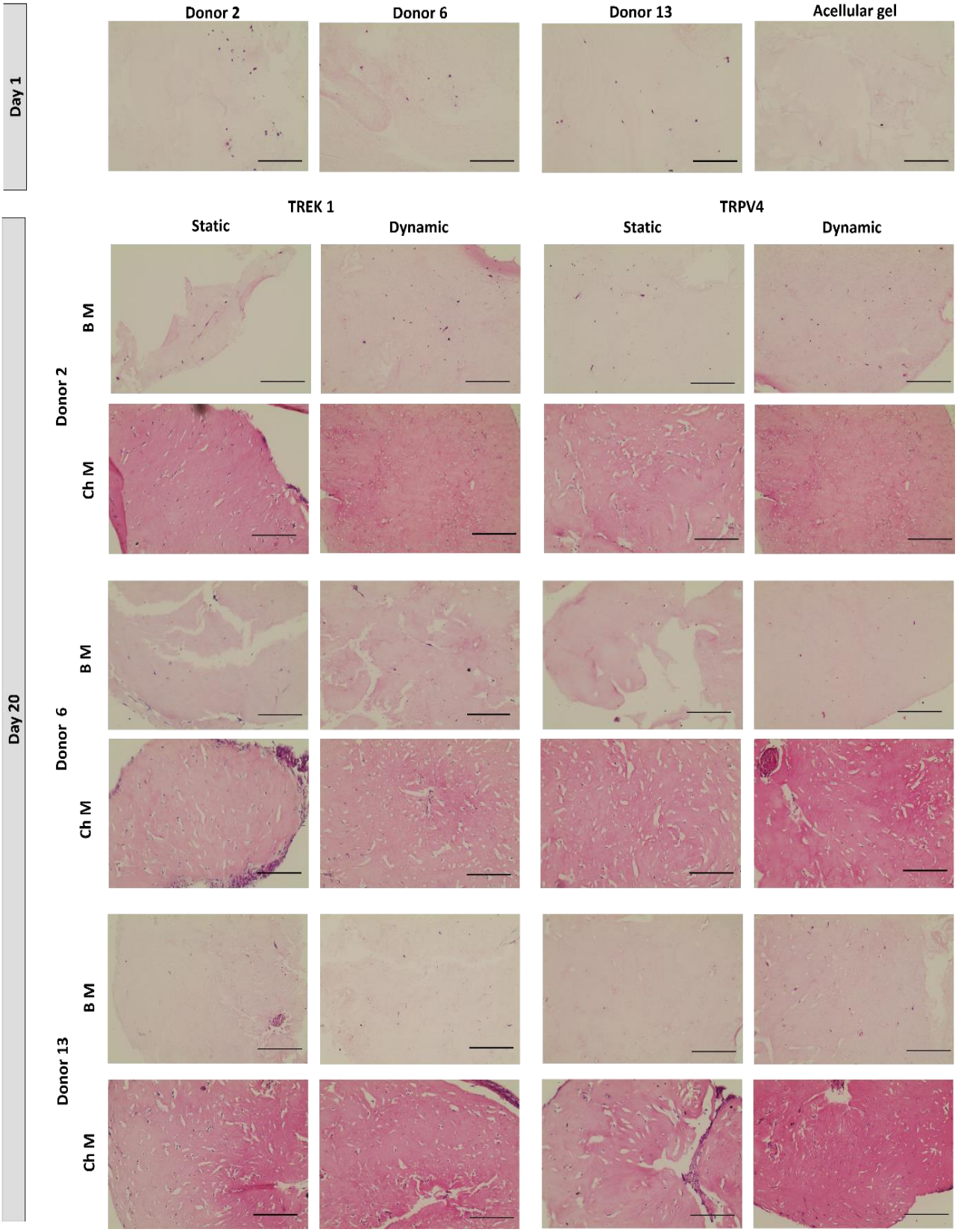

Figure 6. 25: Haematoxylin and Eosin staining. *Bright field micrographs stained 7µm paraffin sections of oMSCs seeded gels were taken (day 1, day 20). Cells were labelled with eitherTREK-1 or TRPV4 coated MNPs. Gels were cultured under dynamic and static conditions and treated with either chondrogenic (Ch M) or basic (B M) media. Differences between B M and Ch M treated gels were observed. In general, stronger stains were observed for Ch M cultured hydrogels for all conditions compared to B M cultured gels. Highest stain intensities were found for Ch M dynamic TRPV4 group for all three donors. Images were taken at 10x magnification. Scale bar = 300 µm.*

6.5.6.2 Picrosirius Red staining for the assessment of total collagen in collagen gels

Picrosirius Red staining was used to stain total collagen in the paraffin section (Figure 6.26). Stains showed clear differences in the dye intensity for the Ch M gels compared to the B M gels for all condition. The highest stain intensity was observed for donor 13 for Ch M gels at culture conditions. No clear differences were observed between dynamic and static gels for both TREK-1 and TRPV4 of the donors, except for donor 2, which revealed differences in stains between dynamically and statically cultured gels in the TRPV4 group.

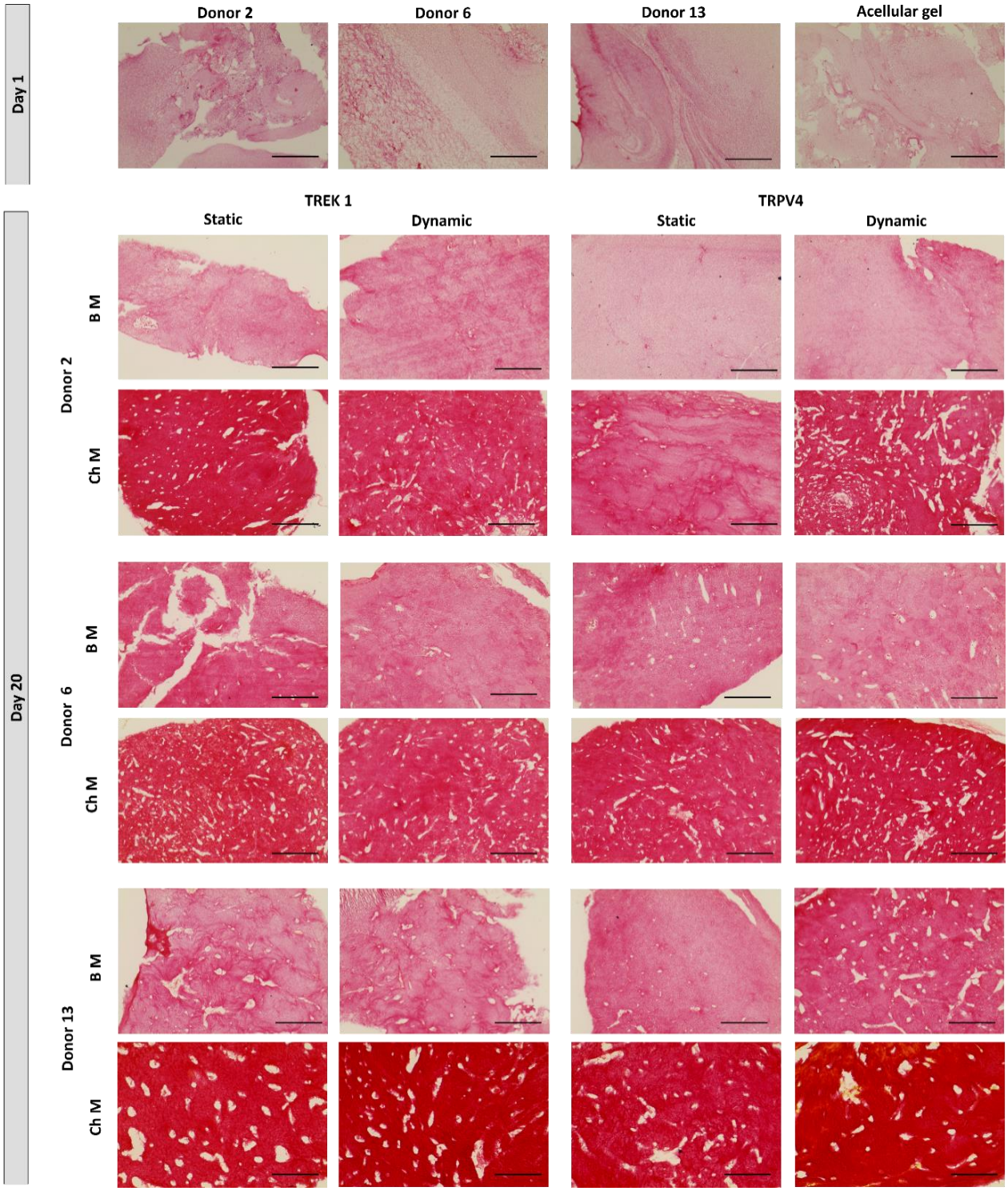

Figure 6. 26: Picrosirius red staining. *Bright field micrographs of Picrosirius red stained 7 µm paraffin sections of oMSCs seeded gels were taken for day1 and day 20. Cells were labelled with either TREK-1 or TRPV4 coated MNPs. Gels were cultured under dynamic and static conditions and treated with either chondrogenic (Ch M) or basic (B M) media. A clear difference between B M and Ch M treated gels was observed. No clear differences between the dynamic and static group for both TREK-1 and TRPV4 of the donors, except donor 2, which showed differences between dynamic and static of the TRPV4 group. Donor 13 (Ch M, TRPV4 dynamic) showed strongest stains for all conditions. Images were taken at 10 x magnification. Scale bar = 300 µm.*

6.5.6.3 Alcian blue staining for the assessment of GAG in collagen gels

Alcan blue stain was performed to identify GAG in the paraffin sections (Figure 6.27). Similar to other two stains, there were noticeable differences between B M and Ch M treated gels for both static and dynamic culture conditions. In general, for the Ch M treated gels higher stain intensity for the dynamic groups were observed for donor 6 and 13. Strongest stains were observed for donor 13 (Ch M, TRPV4 dynamic).

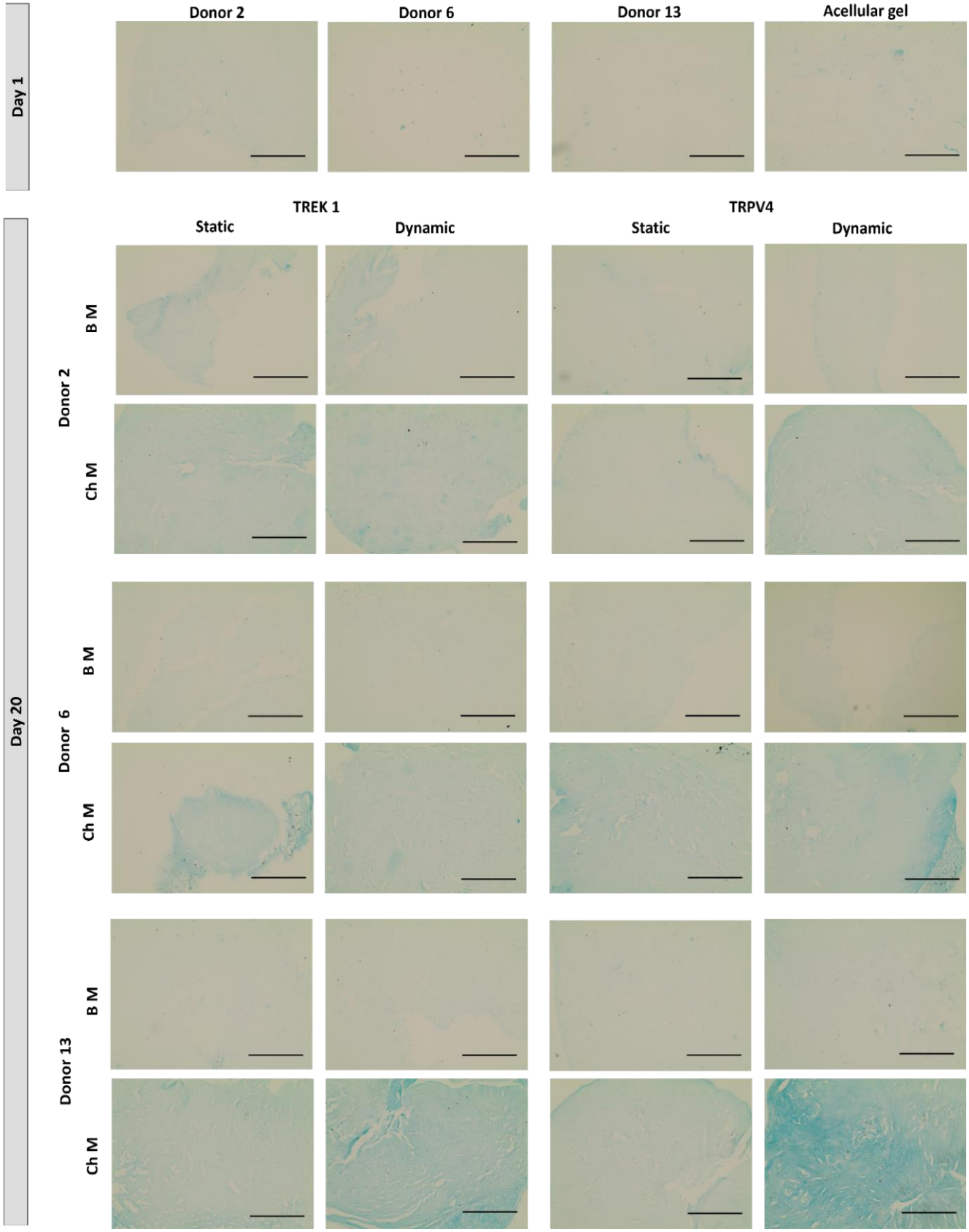

Figure 6. 27: Alcian blue staining. *Bright field micrographs of alcian blue stained 7 µm paraffin sections of oMSCs seeded gels were taken for day1 and day 20. Cells were labelled with either TREK-1 or TRPV4 coated MNPs. Gels were cultured under dynamic and static conditions and treated with either chondrogenic (Ch M) or basic (B M) media. Differences between B M and Ch M treated gels were observed. The B M gels had minimal GAG stains. Donor 13 revealed the strongest stains for Ch M, TRPV4 dynamic. Images were taken at 10 x magnification. Scale bar = 300 µm.*

6.5.7 Immunohistology

An enzymatic method using horseradish peroxidase (HRP) was used to carry out immunohistochemical staining of paraffin embedded samples to detect collagen type II collagen type X and aggrecan expression.

6.5.7.1 Collagen type II immunostaining

The results of the Collagen type II immunostaining (Figure 6.28) showed the presence of the Collagen type II in the samples. In general, the Ch M of the dynamic group of all three donors for both TREK-1 and TRPV4 was higher in the Collagen type II expression than the static group and strongest stains were observed for donor 13, followed by donor 2 and 6.

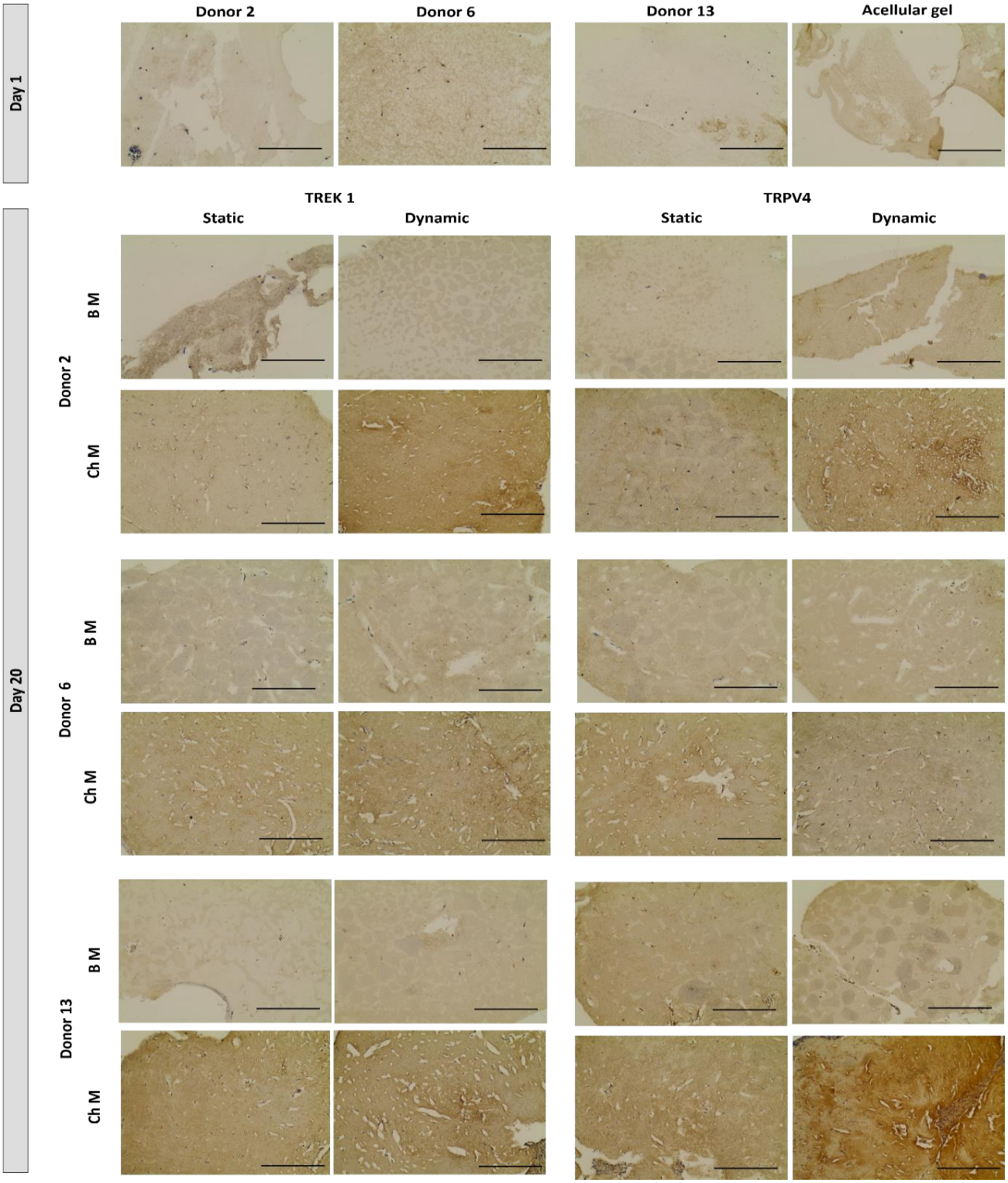

Figure 6. 28: Immuno-peroxidase antibody staining for collagen II*. Bright field micrographs of Collagen II immunostaining of 7 µm paraffin sections of oMSCs seeded gels were prepared for day1 and day 20. Cells were labelled with either TREK-1 or TRPV4 coated MNPs. Gels were cultured under dynamic and static conditions and treated with either chondrogenic (Ch M) or basic (B M) media. Stronger stains were observed for the dynamic Ch M group for both TREK-1 and TRPV4 of all the three donors. Donor 13 Ch M of the TRPV4 dynamic group revealed strongest expression of collagen II. Images were taken at 10 x magnification. Scale bar = 300 µm.*

6.5.7.2 Collagen X immunostaining

The results of the collagen X immunostaining showed that there is no collagen X expression in most of the samples with the exception for donor 13 (Ch M dynamic group) for both TREK-1 and TRPV4 (Figure 6.29).

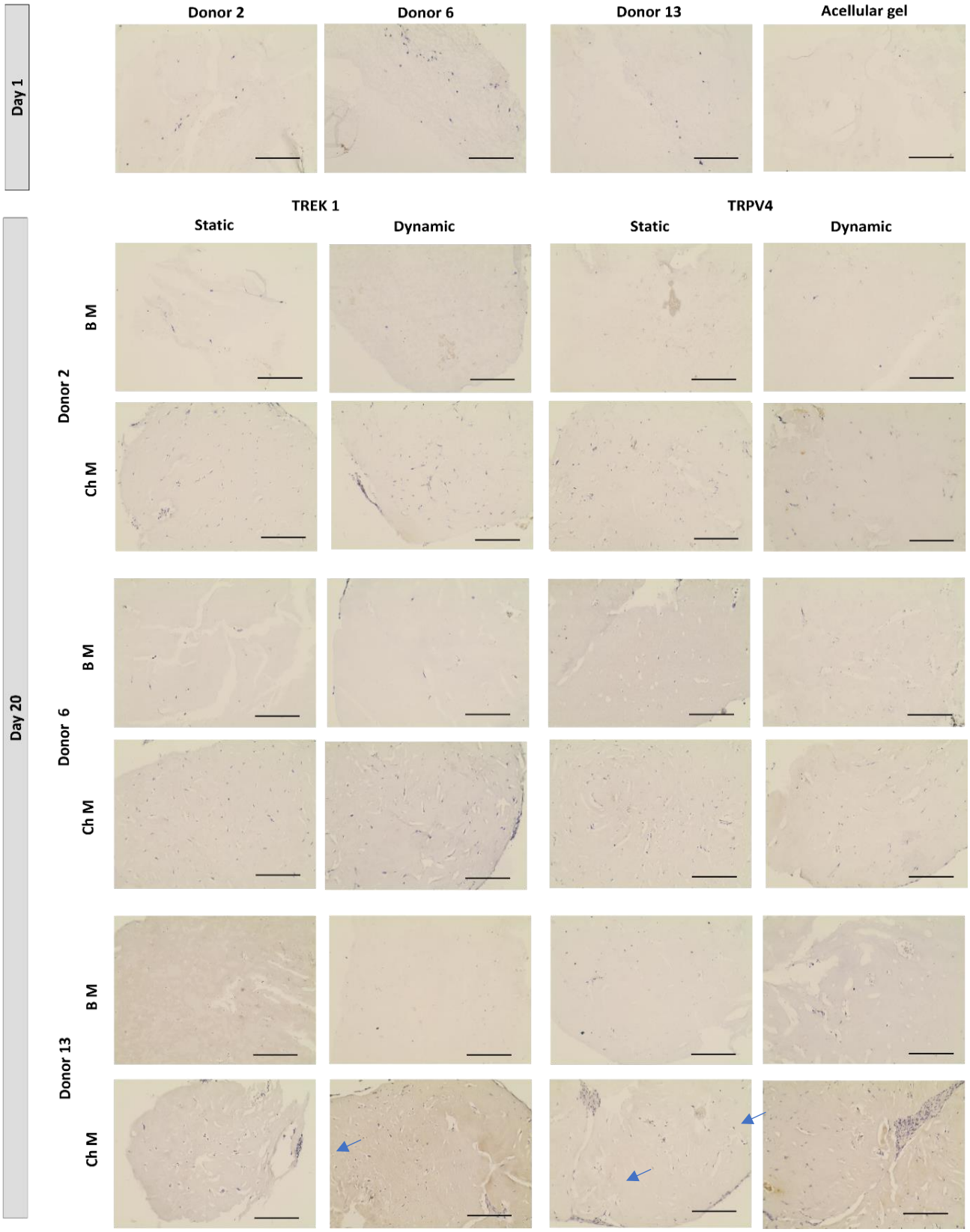

Figure 6. 29: Immuno-peroxidase antibody staining for collagen X. *Bright field micrographs of Collagen X immunostaining of 7 µm paraffin sections of oMSCs seeded gels were taken for day1 and day 20. Cells were labelled with either TREK-1 or TRPV4 coated MNPs. Gels were cultured under dynamic and static conditions and treated with either chondrogenic (Ch M) or basic (B M) media. The results of the collagen X immunostaining showed that there is no collagen X expression in most of the samples with an exception for donor 13 (Ch M dynamic) for both TREK-1 and TRPV4 (blue arrows). Images were taken at 10 x magnification. Scale bar = 300 µm.*

6.5.7.3 Aggrecan immunostaining

Similar to the Collagen type II immunostaining, the results of aggrecan immunostaining (Figure 6.30) showed that the sections expressed the presence of the aggrecan in the samples. In general, Aggrecan staining of gels cultured in Ch M under dynamic conditions for both TREK-1 and TRPV4 was higher for all donors compared to the static group. Overall, strongest stains were obtained for donor 13 followed by donor 2 (TREK-1, dynamic) and donor 6 (TRVP4, dynamic).

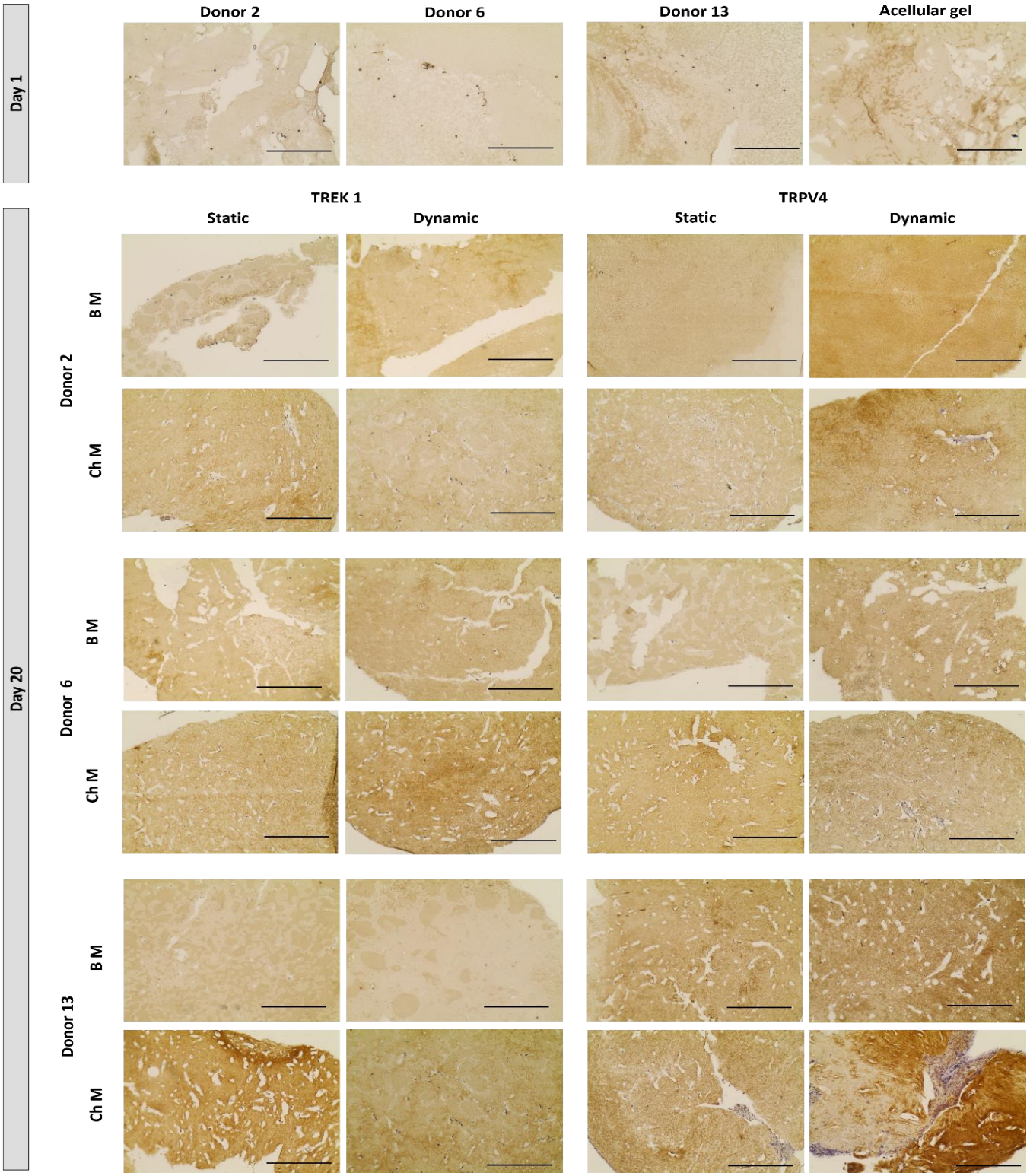

Figure 6. 30: Immuno-peroxidase antibody staining for aggrecan. *Aggrecan immunostaining of 7 µm paraffin sections of oMSCs seeded gels were taken for day1 and day 20. Cells were labelled with eitherTREK-1 or TRPV4 coated MNPs. Gels were cultured under dynamic and static conditions and treated with either chondrogenic (Ch M) or basic (B M) media. Dynamic Ch M group performed better than the static Ch M for both TREK-1 and TRPV4 of all the three donors. Donor 13 Ch M of the TRPV4 dynamic group showed the highest aggrecan expression. Images were taken at 10 x magnification. Scale bar = 300 µm.*

6.6 Discussion

Transient receptor potential vanilloid (TRPV) channels, especially isoforms 1–4 are moderately Ca^{2+} permeable channels (Nilius and Owsianik, 2011; Phan *et al.,* 2009) that play diverse roles in cellular function. TRPV4 seems to have a mechanosensory role and has been shown to be stretch sensitive (Wang *et al.,* 2011). TRPV4 plays an important role in the normal maintenance of the joint and a further role in the differentiation of stem cells into a chondrogenic lineage (Muramatsu *et al.,* 2007; O'conor *et al.,* 2012). In this chapter, the effect of mechanical stimulation on the TRPV4 channel using MICA was investigated and compared with the TREK-1 ion channel. The multimodality of TRPV4 as a Ca^{2+}-preferred membrane ion channel has been shown to transduce external environmental cues into specific metabolic responses via the generation of intracellular Ca^{2+} transients (Everaerts *et al.,* 2010; Liedtke, Wolfgang B, 2006; Moore *et al.,* 2013). The TREK1 channel has also been shown to be mechanosensitive (Hughes *et al.,* 2008) and influences K^{+} transients which influence downstream signal pathways. The MICA technology has been tested for promoting chondrogenesis of oBM-MSCs to differentiate into chondrocytes in a 3D hydrogel cell culture.

Initially, the TRPV4 antibodies have been shown to be cross reactive with the sheep MSCs. This was necessary to demonstrate that the human specific antibody which had been shown to have cross reactivity with rat and mouse was also homologous to the sheep oMSCs TRPV4 channel.

The oMSCs of the three donors chosen for this study have previously been tested for cell viability with culture conditions at passage 1 to 3 in the previous chapter (Chapter 5). Cell viability using the Alamar blue assay was significantly increased across the experimental time at day 10 and day 20 compared to day 0. In general, the results have also showed consistency in the cell viability for each experimental group.

Using the Pico Green assay, we have shown that there is a significant decrease in cell number of the Ch M gels. However, there were no significant differences in the cell activity

assessment by Alamar blue when comparing the three donors for all conditions. The findings imply that the oMSCs cells which have differentiated into chondrocytes in the Ch M have increased their metabolic activity relative to undifferentiated BM gels. (Bonnier *et al.*, 2015). These results could be due to the highly active proliferating chondrocytes in the Ch M gel and the low activity of the over confluent undifferentiated oMSCs in B M gels.

As described in the previous chapter, the engineered cartilage constructs have similar mechanical properties to the native sheep articular cartilage e.g. the curves obtained from stress-strain data were similar to that of native cartilage tissue. A comparison of the computed Young's modulus of the 3D constructs for the three tested donors, between the TRPV4 and the TREK-1 stimulation groups showed that all TRPV4 activated groups were significantly higher than the relevant static groups. In contrast, the TREK-1 group showed a significant difference between the dynamic TREK-1 and their relevant static group in only one of the three donors. Our results confirm that activation of the Ca^{2+} -permeable TRPV4 channel can alter the biochemical and biomechanical properties of tissue engineered articular cartilage as shown previously (Eleswarapu and Athanasiou, 2013). In this study, the computed Young's modulus for the all three donors was about (3.8 MPa) for the TRPV4 dynamic group which is significantly higher than TRPV4 static group (1.89 MPa). The TREK-1 dynamic group was 2.6 MPa which is also significantly higher than their corresponding TREK 1 static group (1.95 MPa). Therefore, we have observed an enhanced mechanical property compared to the computed native sheep cartilage Young's modulus (1.25 MPa) and this may relate to the physical thermotical that the pressure is related to the area (Holman and Gajda, 2001) as explained in the discussion of the previous chapter.

The effectiveness of MICA has been shown previously to promote osteogenesis (Aagaard *et al.*, 2003; Cartmell *et al.*, 2002; Hughes *et al.*, 2007; Markides *et al.*, 2018). In Chapter 5, we have demonstrated the potential of the activation of TREK-1 for chondrogenesis. The potential of the MICA technique was further tested by a comparison of TRPV4 vs TREK-1 in three donors of our study. The chondrogenic capacity was assessed by the production of

ECM (sGAG, total collagen and total protein). As expected, the results demonstrated that the Ch M treated static gel produced a significantly greater amount of the cartilaginous matrix compared with B M treated group. Previous reports have shown accelerated metabolic activity of chondrocytes exposed to mechanical cues. (Grad *et al.,* 2012; Han *et al.,* 2007). Generally, in this study, the total amounts of sGAG, total collagen and total protein produced by the cells during culture were enhanced in all mechanically stimulated gels compared to the static gels. However, there were no significant differences according to the biochemical results for (sGAG, total collagen and total protein) between the TRPV4 vs TREK-1.

According to the histological staining for cartilage ECM specific stain (Alcian blue for GAG and picrosirius for collagen), the stained paraffin sections of the tested groups exhibited chondrogenic differentiation for all Ch M gels for both dynamic and static compared to B M. The cells began to lose their phenotype from fibroblast-like spindle shapes to rounded chondrocytic phenotypes with a surrounding ECM. Generally, the histological stains showed a higher intensity for TRPV4 dynamic gels comparing with TREK-1 dynamic gel but these comparisons were qualitative. Immunocytochemistry confirmed a higher intensity for TRPV4 dynamic gels comparing with TREK-1 dynamic gel.

Recently, TRPV4 has been linked to other mechanotransduction agents such as primary cilia. Corrigan and their colleagues have demonstrated that TRPV4 localises to areas of high strain, specifically the primary cilium. The interplay between the ion channels and the other mechano-transducers need further studies to understand their roles (Corrigan *et al.,* 2018).

CHAPTER 7

Discussion, Conclusion and Future work

7.1 Discussion

Tissue engineering offers potential treatments for orthopaedic conditions such as articular cartilage defect and critical size bone defects. MSCs are a potential cell type which can be utilised to design cell-based repair strategies due to their multi-differentiation capacity and their ability to secrete factors (paracrine activity) (Saldaña *et al.,* 2017).

Autologous MSCs are often the focus of cell base therapies, however little is understood about how variations in the behaviour of each donor will impact the success of the therapy on an individual patient. Animal models such as sheep are in place to enable successful clinical translation of cell-based therapies for bone and cartilage tissue engineering (Black *et al.,* 2015; Kalamegam *et al.,* 2018; Music *et al.,* 2018; Stoddart *et al.,* 2009; Vedicherla and Buckley, 2017; Vega *et al.,* 2017).

There is a considerable variation reported within and between studies (many of these studies are summarised in chapter 1 (Table 1.2 and 1.3). The difficulties observed in oMSC studies, such as donor-to-donor variability and conflicting results, parallel to those observed in hMSC experiments (Music *et al.,* 2018).

Non-specific sheep breeds were used for orthopedic research and oMSCs research (Czernik *et al.,* 2013; Fadel *et al.,* 2011; Jäger *et al.,* 2006; Rentsch *et al.,* 2010). However, most researches were using domestic local sheep breed for their research rather than a specific breed. Hence, in this study English Mule sheep which is an English breed was used.

For most sheep studies the preferred site of bone marrow harvesting is the iliac bone (Adamzyk *et al.,* 2013; Mccarty, Gronthos, *et al.,* 2009; Rentsch *et al.,* 2010). However, for this PhD study, the bone marrow aspirate was successfully collected from the sternum bone and adequate quantities of bone marrow were collected (Delling *et al.,* 2012). Human MSCs can be similarly obtained by taking aspirates of bone marrow from the iliac crest of healthy volunteers (Risbud *et al.,* 2006). In all sheep studies above, ovine MSCs exhibit morphological, immunophenotypical and multipotential characteristics similar to those

observed in human MSC *in vitro* and *in vivo*. (Mccarty, Grothos, *et al.,* 2009). These results were also confirmed by Rentsch and colleagues (Rentsch *et al.,* 2010).

oMSCs were characterised by their ability to undergo osteogenic, adipogenic and chondrogenic differentiation in addition to some CD markers expression. Cells from all thirteen donors were successfully differentiated towards all three lineages with marked donor dependent variations.

The results obtained from both the native sheep characterisation, oMSCs characterisation and the hydrogel experiments, demonstrated variabilities between individual donors in varied degrees. For instance, the trilineage differentiation experiment (chapter 4) exhibited clear donor variation in the all thirteen donors' performance for all the three lineages osteogenic, adipogenic and chondrogenic. For the characterisation of native sheep cartilage, differences between the sheep's left and right legs as well as between individual donors were found for the mechanical, biochemical and histological assessment. This is an indication, that many of the human or animal organs and extremities are not symmetrical (Claes *et al.*, 2015). In previous studies donors with lower osteogenic potential displayed an enhanced osteogenic response after MICA technology application (Markides *et al.,* 2018). In this PhD study, donors, in particular those with lower chondrogenic potential (donors 6 and 8) also displayed an enhanced chondrogenic response after MICA technology application. This proved that MICA Technology may have an effect in the enhancement chondrogenic potential of oMSC.

Also, variations between individual donors were found for the mechanical, biochemical and histological assessments.

The response of five oMSCs donors to MICA activation was assessed in a 3D collagen hydrogel culture model. The results displayed that chondrogenesis was enhanced by the mechanical activation, which resulted in Young's modulus values increasing above the determined Young's modulus of the native sheep cartilage. Whereas, the unstimulated group

was lower than the native sheep cartilage. This may indicate that the dynamic conditioning provided by MICA enhanced chondrogenesis.

The analysis of the ECM matrix composition revealed that the sGAG production was only enhanced upon mechanical conditioning for one out of five donors. Hence sGAG production is not assumed to be affected significantly by dynamic culture conditions. Same trends were observed for the total protein production, where the same donor showed significantly increased protein production compared to the unstimulated gels.

Whereas, for the total collagen production the results differed. Three out of five donors responded to the dynamic stimulation by MICA compared to the static control group. However, the variances between the donors' performance in the ECM production were observed between several donors; between donor 2 and each donor 5, 6, 8 and 13.

Methodologies controlling chondrogenic differentiation of MSCs towards chondrocytes are under attention to improve the outcome of orthopaedic regenerative medicine approaches. During chondrogenic differentiation MSCs proliferate and altered to an extracellular matrix synthesizing chondrocytes which, in the case of endochondral ossification and different cartilage pathologies, ultimately and terminally differentiates into hypertrophic mineralised chondrocytes (Kronenberg, 2003; Mackie *et al.,* 2008). For stem cell-based cartilage regeneration, it is therefore crucial to find optimal strategies to stimulate progenitor cells to differentiate into chondrocytes and preventing them from hypertrophy and mineralisation.

Compression force induced chondrogenic differentiation (Wang *et al.*, 2017). *In vivo*, cells readjust to the physical environment their reside in by translating mechanical stimuli into biochemical signals (mechanotransduction) (Jaalouk and Lammerding, 2009). Ion channels are mechanoreceptors involved in mechanotransduction (Liu *et al.,* 2010). Mechano-sensitive Ca^{2+} channels play a central role in the differentiation of MSCs while sensing the mechanical stimulation and activate mechanotransduction. The important subfamily, TRPV4, is a Ca^{2+} - permeable membrane ion channel widely implicated in transducing external mechanical stimulation into specific intracellular responses in a wide variety of

bone cells (Liedtke, Wolfgang, 2006; Phan *et al.,* 2009). Decreased osteogenic differentiation potential was found in the MSCs from TRPV4 knockout mice (O'conor *et al.,* 2012). However, the role of TRPV4 in transducing and regulating the differentiation of MSCs to chondrocytes in response to mechanical stimulation is unclear. Therefore, based on these findings on the essential role of TRPV4 in skeletal diseases, we investigated whether TRPV4 functions as a mechanoreceptor to mechanical conditioning in oMSCs. We hypothesised, that TRPV4 mediates chondrogenic differentiation of oMSCs under mechanical stimulation using the MICA technology. In this context, the results showed that in addition to the significant differences between the dynamic group compared to the static control, significantly increased Young's modulus in TRPV4 group were observed compared to the TREK-1 group.

For the production of ECM proteins, sGAG, total collagen and total protein, Ch M treated static gels produced a significantly higher amount of the cartilaginous matrix compared with B M treated group. On the other hand, the total amounts of sGAG, total collagen and total protein produced by the cells during culture were enhanced in all mechanically stimulated gels compared to the static gels. These findings are in agreement with literature. Previous reports have shown accelerated metabolic activity of chondrocytes exposed to mechanical cues. (Grad *et al.,* 2012; Han *et al.,* 2007). However, there were no significant differences for sGAG, total collagen and total protein between TRPV4 vs TREK-1-samples, despite TRPV4 values were consistently higher than TREK-1 values for all the three donors.

Alcian blue and Picrosirius red stain were performed to stain cartilage ECM specific proteins, namely sGAG and collagen respectively. Stained paraffin sections of the tested groups exhibited chondrogenic differentiation for all Ch M gels for both dynamic and static culture conditions compared to B M gels.

The cells began to lose their phenotype from fibroblast-like spindle shapes to rounded chondrocyte phenotypes with a surrounding ECM. Generally, the histological stains showed a higher intensity for TRPV4 dynamic gels compared to TREK-1 dynamic gels, but these

comparisons were qualitative. Immunocytochemistry confirmed higher intensity for TRPV4 dynamic gels compared to TREK-1 dynamic gels. These results are in agreement with studies that reported TRPV4 as mechanoreceptor for flow shear stress, mechanical loading and stretch (Hu *et al.,* 2017). In chondrocytes, TRPV4-mediated intracellular Ca^{2+} signaling regulated the metabolic response of chondrocytes to mechanical loading by enhancing matrix accumulation and mechanical properties (O'conor *et al.,* 2014).

For Humans and different animal species practice, the MSCs' donor variation has been studied for *in vitro* expansion, multipotency and tissue engineering applications, Human (Siddappa *et al.,* 2007; Zaim *et al.,* 2012), human and rats (Scuteri *et al.,* 2014), Equine (Colleoni *et al.,* 2009). While, in sheep, neither breed nor cryopreservation appeared to impact proliferative potential, although donor-to-donor variation has been reported as with hMSC (Rhodes *et al.,* 2004).

Large variation among the donors in composition of cells (progenitor to committed, growth, and response to differentiation signals, these variations may due to age, sex, site of the isolation. Another possible explanation is that differential sampling methods by different physicians may result in varying heterogeneity in the final cell composition as reported previously (Jaiswal *et al.,* 1997; Phinney *et al.,* 1999).

7.2 Conclusion

The results obtained from this study showed that MICA have a beneficial effect on the ion channel activation and enhances chondrogenesis of oMSCs in 3d hydrogel culture in vitro. TRPV4 channel activation enhanced chondrogenesis superior to the TREK-1 ion channel activation.

Donor variation was recorded in the 3D hydrogels mechanical stimulation experiments in varied degrees. For trilineage differentiation experiments (adipogenic, osteogenic and chondrogenic) the donor variation was also recorded but according to histological and biochemical assays there was no clear profile for the best performing donor of the thirteen donors for all the three-differentiation lineage.

The expression for the specific epitopes were positive for the MSCs specific epitopes like CD 29 and CD 44. While the expression for the other epitopes like CD 31 and CD 45 were negative. In addition, there is a variation in the potency of the expression to each marker.

In addition, Bone marrow was safely and easily harvested. The other conclusion is that sheep is suitable as animal model for orthopaedic research.

7.3 Future Work

The experiments described in this study has raised some approaches for future work, which could help in the cartilage tissue engineering and pre-clinical animal model.

Use another type of mechanical stimulation like a hydrostatic bioreactor, which provides hydrostatic force, to compare the effects of MICA with other types of mechanical stimulation on *in vitro* chondrogenesis differentiation.

There are indications for the involvement of the WNT signalling pathway in maintaining articular cartilage and its mechanotransduction pathways. Hence, a comparison of our results with other mechano-activated receptors such as RGD and Fz might reveal additional approaches to enhance chondrogenesis.

Furthermore, it would be beneficial to determine the nano-mechanics of the cartilage based on applying atomic force microscopy to determine the mechanical properties of cartilage and /or engineered cartilage at the molecular level.

Using another domestic animal like horses or dogs could be effective for future work for studying the donor variation for BM-MSCs characterisation and cartilage engineering for pre-clinical studies and clinical orthopaedic applications in veterinary medicine.

In addition, different cell density and/or different biomaterial that have been used successfully as an engineered cartilage scaffold can be investigated with the effect of MICA mechanical stimulation. Prolong experiment period could be beneficial to study the effect of the time on the fate of the engineered cartilage.

An *in vivo* study of the MICA technology application for pre-clinical and clinical orthopaedics purview of both veterinary and human practice could be applicable in the next few steps.

References

Aagaard, Henrik, Jørgensen, Uffe & Bojsen-Møller, Finn 2003. Immediate versus delayed meniscal allograft transplantation in sheep. *Clinical orthopaedics and related research,* 406**,** 218-227.

Adamzyk, Carina, Emonds, Tanja, Falkenstein, Julia, Tolba, René, Jahnen-Dechent, Wilhelm, Lethaus, Bernd & Neuss, Sabine 2013. Different culture media affect proliferation, surface epitope expression, and differentiation of ovine MSC. *Stem cells international,* 2013.

Ahern, Benjamin J, Soma, Lawrance R, Boston, Raymond C & Schaer, Thomas P 2009. Comparison of the analgesic properties of transdermally administered fentanyl and intramuscularly administered buprenorphine during and following experimental orthopedic surgery in sheep. *American journal of veterinary research,* 70**,** 418-422.

Aimond, Franck, Rauzier, Jean-Michel, Bony, Claire & Vassort, Guy 2000. Simultaneous activation of p38 MAPK and p42/44 MAPK by ATP stimulates the K+ current ITREK in cardiomyocytes. *Journal of Biological Chemistry,* 275**,** 39110-39116.

Al Faqeh, Hamoud, Hamdan, Bin Mohamad Yahya Nor, Chen, Hui Cheng, Aminuddin, Bin Saim & Ruszymah, Bt Hj Idrus 2012. The potential of intra-articular injection of chondrogenic-induced bone marrow stem cells to retard the progression of osteoarthritis in a sheep model. *Experimental gerontology,* 47**,** 458-464.

Albro, Michael B, Nims, Robert J, Cigan, Alexander D, Yeroushalmi, Kevin J, Alliston, Tamara, Hung, Clark T & Ateshian, Gerard A 2013. Accumulation of exogenous activated TGF-β in the superficial zone of articular cartilage. *Biophysical journal,* 104**,** 1794-1804.

Alford, J Winslow & Cole, Brian J 2005. Cartilage restoration, part 1: basic science, historical perspective, patient evaluation, and treatment options. *The American journal of sports medicine,* 33**,** 295-306.

Amiel, Gilad E, Yoo, James J, Kim, Byung-Soo & Atala, Anthony 2001. Tissue engineered stents created from chondrocytes. *The Journal of urology,* 165**,** 2091-2095.

Andersen, Maria Dahl, Alstrup, Aage Kristian Olsen, Duvald, Christina Søndergaard, Mikkelsen, Emmeli Fredsgaard Ravnkilde, Vendelbo, Mikkel Holm, Ovesen, Per Glud & Pedersen, Michael 2018. Animal Models of Fetal Medicine and Obstetrics.

Andrades, José A, Motaung, Shirley C, Jiménez-Palomo, Pedro, Claros, Silvia, López-Puerta, José M, Becerra, José, Schmid, Thomas M & Reddi, A Hari 2012. Induction of superficial zone protein (SZP)/lubricin/PRG 4 in muscle-derived mesenchymal stem/progenitor cells by transforming growth factor-β1 and bone morphogenetic protein-7. *Arthritis research & therapy,* 14**,** R72.

Angele, P, Yoo, Ju, Smith, C, Mansour, J, Jepsen, Kj, Nerlich, M & Johnstone, Brian 2003. Cyclic hydrostatic pressure enhances the chondrogenic phenotype of human mesenchymal progenitor cells differentiated in vitro. *Journal of orthopaedic research,* 21**,** 451-457.

Aragona, James, Parsons, John R, Alexander, Harold & Weiss, Andrew B 1981. Soft tissue attachment of a filamentous carbon-absorbable polymer tendon and ligament replacement. *Clinical orthopaedics and related research***,** 268-278.

Armstrong, Cg & Mow, Vc 1982. Variations in the intrinsic mechanical properties of human articular cartilage with age, degeneration, and water content. *The Journal of bone and joint surgery. American volume,* 64**,** 88-94.

Arzi, B, Duraine, Gd, Lee, Ca, Huey, Dj, Borjesson, Dl, Murphy, Bg, Hu, Jcy, Baumgarth, N & Athanasiou, Ka 2015. Cartilage immunoprivilege depends on donor source and lesion location. *Acta biomaterialia,* 23**,** 72-81.

Atala, Anthony, Kasper, F Kurtis & Mikos, Antonios G 2012. Engineering complex tissues. *Science translational medicine,* 4**,** 160rv112-160rv112.

Athanasiou, Ka, Zhu, Cf, Wang, X & Agrawal, Cm 2000. Effects of aging and dietary restriction on the structural integrity of rat articular cartilage. *Annals of biomedical engineering,* 28**,** 143-149.

Athanasiou, Kyriacos A, Darling, Eric M & Hu, Jerry C 2009. Articular cartilage tissue engineering. *Synthesis Lectures on Tissue Engineering,* 1**,** 1-182.

Awad, Hani A, Butler, David L, Boivin, Gregory P, Smith, Frost Nl, Malaviya, Prasanna, Huibregtse, Barbara & Caplan, Arnold I 1999. Autologous mesenchymal stem cell-mediated repair of tendon. *Tissue engineering,* 5**,** 267-277.

Babu, Ramesh P, O'connor, Kevin & Seeram, Ramakrishna 2013. Current progress on bio-based polymers and their future trends. *Progress in Biomaterials,* 2**,** 8.

Baksh, Dolores, Yao, Raphael & Tuan, Rocky S 2007. Comparison of proliferative and multilineage differentiation potential of human mesenchymal stem cells derived from umbilical cord and bone marrow. *Stem cells,* 25**,** 1384-1392.

Barker, Mk & Seedhom, Bb 2001. The relationship of the compressive modulus of articular cartilage with its deformation response to cyclic loading: does cartilage optimize its modulus so as to minimize the strains arising in it due to the prevalent loading regime? *Rheumatology,* 40**,** 274-284.

Barlow, Sarah, Brooke, Gary, Chatterjee, Konica, Price, Gareth, Pelekanos, Rebecca, Rossetti, Tony, Doody, Marylou, Venter, Deon, Pain, Scott & Gilshenan, Kristen 2008. Comparison of human placenta-and bone marrow–derived multipotent mesenchymal stem cells. *Stem cells and development,* 17**,** 1095-1108.

Barry, Frank, Boynton, Raymond E, Liu, Beishan & Murphy, J Mary 2001. Chondrogenic differentiation of mesenchymal stem cells from bone marrow: differentiation-dependent gene expression of matrix components. *Experimental cell research,* 268**,** 189-200.

Barry, Frank P & Murphy, J Mary 2004. Mesenchymal stem cells: clinical applications and biological characterization. *The international journal of biochemistry & cell biology,* 36**,** 568-584.

Bartlett, W, Skinner, Ja, Gooding, Cr, Carrington, Rwj, Flanagan, Am, Briggs, Twr & Bentley, G 2005. Autologous chondrocyte implantation versus matrix-induced autologous chondrocyte implantation for osteochondral defects of the knee: a prospective, randomised study. *The Journal of bone and joint surgery. British volume,* 87**,** 640-645.

Battula, Venkata Lokesh, Bareiss, Petra M, Treml, Sabrina, Conrad, Sabine, Albert, Ingrid, Hojak, Sigrid, Abele, Harald, Schewe, Bernhard, Just, Lothar & Skutella, Thomas 2007. Human placenta and bone marrow derived MSC cultured in serum-free, b-FGF-containing medium express cell surface frizzled-9 and SSEA-4 and give rise to multilineage differentiation. *Differentiation,* 75**,** 279-291.

Benders, Kim Em, Van Weeren, P René, Badylak, Stephen F, Saris, Daniël Bf, Dhert, Wouter Ja & Malda, Jos 2013. Extracellular matrix scaffolds for cartilage and bone regeneration. *Trends in biotechnology,* 31**,** 169-176.

Berndt, Albert L & Harty, Michael 1959. Transchondral fractures (osteochondritis dissecans) of the talus. *J Bone Joint Surg Am,* 41**,** 988-1020.

Berry, Catherine C 2005. Possible exploitation of magnetic nanoparticle–cell interaction for biomedical applications. *Journal of Materials Chemistry,* 15**,** 543-547.

Bhosale, Abhijit M & Richardson, James B 2008. Articular cartilage: structure, injuries and review of management. *British medical bulletin,* 87**,** 77-95.

Bieback, Karen, Kinzebach, Sven & Karagianni, Marianna 2010. Translating research into clinical scale manufacturing of mesenchymal stromal cells. *Stem cells international,* 2010.

Black, Cameron Rm, Goriainov, Vitali, Gibbs, David, Kanczler, Janos, Tare, Rahul S & Oreffo, Richard Oc 2015. Bone tissue engineering. *Current molecular biology reports,* 1**,** 132-140.

Bonaventure, J, Kadhom, N, Cohen-Solal, L, Ng, Kh, Bourguignon, J, Lasselin, C & Freisinger, P 1994. Reexpression of cartilage-specific genes by dedifferentiated human articular chondrocytes cultured in alginate beads. *Experimental cell research,* 212**,** 97-104.

Bonnier, Franck, Keating, Me, Wrobel, Tomasz P, Majzner, Katarsyna, Baranska, Malgorzata, Garcia-Munoz, Amaya, Blanco, Alfonso & Byrne, Hugh J 2015. Cell viability assessment using the Alamar blue assay: a comparison of 2D and 3D cell culture models. *Toxicology in vitro,* 29**,** 124-131.

Borenstein, Jeffrey T, Weinberg, Eli J, Orrick, Brian K, Sundback, Cathryn, Kaazempur-Mofrad, Mohammad R & Vacanti, Joseph P 2007. Microfabrication of three-dimensional engineered scaffolds. *Tissue engineering,* 13**,** 1837-1844.

Bornes, Troy D, Adesida, Adetola B & Jomha, Nadr M 2014. Mesenchymal stem cells in the treatment of traumatic articular cartilage defects: a comprehensive review. *Arthritis research & therapy,* 16**,** 432.

Bosnakovski, Darko, Mizuno, Morimichi, Kim, Gonhyung, Takagi, Satoshi, Okumura, Masahiro & Fujinaga, Toru 2006. Chondrogenic differentiation of bovine bone marrow mesenchymal stem cells (MSCs) in different hydrogels: influence of collagen type II extracellular matrix on MSC chondrogenesis. *Biotechnology and bioengineering,* 93**,** 1152-1163.

Boxall, Sally A & Jones, Elena 2012. Markers for characterization of bone marrow multipotential stromal cells. *Stem cells international,* 2012.

Brittberg, Mats, Faxén, Eva & Peterson, Lars 1994. Carbon fiber scaffolds in the treatment of early knee osteoarthritis. A prospective 4-year followup of 37 patients. *Clinical orthopaedics and related research***,** 155-164.

Brown, Thomas D 2000. Techniques for mechanical stimulation of cells in vitro: a review. *Journal of biomechanics,* 33**,** 3-14.

Bruder, Scott P & Fox, Barbara S 1999. Tissue Engineering of Bone: Cell Based Strategies. *Clinical Orthopaedics and Related Research (1976-2007),* 367**,** S68-S83.

Bruder, Scott P, Kurth, Andreas A, Shea, Marie, Hayes, Wilson C, Jaiswal, Neelam & Kadiyala, Sudha 1998. Bone regeneration by implantation of purified, culture-expanded human mesenchymal stem cells. *Journal of orthopaedic research,* 16**,** 155-162.

Buckwalter, Ja 1991. Articular cartilage: composition and structure. *Injury and repair of the musculoskeletal soft tissues*.

Buckwalter, Ja & Mankin, Hj 1998a. Articular cartilage: degeneration and osteoarthritis, repair, regeneration, and transplantation. *Instructional course lectures,* 47**,** 487-504.

Buckwalter, Ja & Mankin, Hj 1998b. Articular cartilage: tissue design and chondrocyte-matrix interactions. *Instructional course lectures,* 47**,** 477-486.

Buckwalter, Joseph A 1992. Mechanical injuries of articular cartilage. *The Iowa orthopaedic journal,* 12**,** 50.

Burdick, Jason A & Prestwich, Glenn D 2011. Hyaluronic acid hydrogels for biomedical applications. *Advanced Materials,* 23**,** H41-H56.

Burger, C, Mueller, M, Wlodarczyk, P, Goost, H, Tolba, Rh, Rangger, C1, Kabir, K & Weber, O 2007. The sheep as a knee osteoarthritis model: early cartilage changes after meniscus injury and repair. *Laboratory animals,* 41**,** 420-431.

Burgin, Leanne V & Aspden, Richard M 2008. Impact testing to determine the mechanical properties of articular cartilage in isolation and on bone. *Journal of Materials Science: Materials in Medicine,* 19**,** 703-711.

Burt, Richard K, Loh, Yvonne, Pearce, William, Beohar, Nirat, Barr, Walter G, Craig, Robert, Wen, Yanting, Rapp, Jonathan A & Kessler, John 2008. Clinical applications of blood-derived and marrow-derived stem cells for nonmalignant diseases. *Jama,* 299**,** 925-936.

Cao, Sheng, Anishkin, Andriy, Zinkevich, Natalya S, Nishijima, Yoshinori, Korishettar, Ankush, Wang, Zhihao, Fang, Juan, Wilcox, David A & Zhang, David X 2018. Transient receptor potential vanilloid 4 (TRPV4) activation by arachidonic acid requires protein kinase A-mediated phosphorylation. *Journal of Biological Chemistry***,** jbc. M117. 811075.

Cartmell, Sh, Dobson, J, Verschueren, S, Hughes, S & El Haj, Aj 2002. Mechanical conditioning of bone cells in vitro using magnetic micro particle technology. *Eur Cells Mater,* 4**,** 130-131.

Chen, Frank S, Frenkel, Sr & Di, Pe Cesare 1997. Chondrocyte transplantation and experimental treatment options for articular cartilage defects. *American journal of orthopedics (Belle Mead, NJ),* 26**,** 396-406.

Chen, Zetao, Klein, Travis, Murray, Rachael Z, Crawford, Ross, Chang, Jiang, Wu, Chengtie & Xiao, Yin 2016. Osteoimmunomodulation for the development of advanced bone biomaterials. *Materials today,* 19**,** 304-321.

Chevrier, Anik, Nelea, Monica, Hurtig, Mark B, Hoemann, Caroline D & Buschmann, Michael D 2009. Meniscus structure in human, sheep, and rabbit for animal models of meniscus repair. *Journal of orthopaedic research,* 27**,** 1197-1203.

Chu, Constance R, Szczodry, Michal & Bruno, Stephen 2010. Animal models for cartilage regeneration and repair. *Tissue Engineering Part B: Reviews,* 16**,** 105-115.

Chung, Cindy & Burdick, Jason A 2008. Engineering cartilage tissue. *Advanced drug delivery reviews,* 60**,** 243-262.

Cibelli, Jose, Emborg, Marina E, Prockop, Darwin J, Roberts, Michael, Schatten, Gerald, Rao, Mahendra, Harding, John & Mirochnitchenko, Oleg 2013. Strategies for improving animal models for regenerative medicine. *Cell stem cell,* 12**,** 271-274.

Claes, Peter, Reijniers, Jonas, Shriver, Mark D, Snyders, Jonatan, Suetens, Paul, Nielandt, Joachim, De Tré, Guy & Vandermeulen, Dirk 2015. An investigation of matching symmetry in the human pinnae with possible implications for 3D ear recognition and sound localization. *Journal of anatomy,* 226**,** 60-72.

Colleoni, Silvia, Bottani, Emanuela, Tessaro, Irene, Mari, Gaetano, Merlo, Barbara, Romagnoli, Noemi, Spadari, Alessandro, Galli, Cesare & Lazzari, Giovanna 2009. Isolation, growth and differentiation of equine mesenchymal stem cells: effect of donor, source, amount of tissue and supplementation with basic fibroblast growth factor. *Veterinary research communications,* 33**,** 811.

Colosimo, Alessia, Russo, Valentina, Mauro, Annunziata, Curini, Valentina, Marchisio, Marco, Bernabò, Nicola, Alfonsi, Melissa, Mattioli, Mauro & Barboni, Barbara 2013. Prolonged in vitro expansion partially affects phenotypic features and osteogenic potential of ovine amniotic fluid-derived mesenchymal stromal cells. *Cytotherapy,* 15**,** 930-950.

Cook, Jl, Hung, Ct, Kuroki, K, Stoker, Am, Cook, Cr, Pfeiffer, Fm, Sherman, Sl & Stannard, Jp 2014. Animal models of cartilage repair. *Bone & joint research,* 3**,** 89-94.

Corpus, Keith T, Bajaj, Sarvottam, Daley, Erika L, Lee, Andrew, Kercher, James S, Salata, Michael J, Verma, Nikhil N & Cole, Brian J 2012. Long-term evaluation of autologous chondrocyte implantation: minimum 7-year follow-up. *Cartilage,* 3**,** 342-350.

Corrigan, Michele A, Johnson, Gillian P, Stavenschi, Elena, Riffault, Mathieu, Labour, Marie-Noelle & Hoey, David A 2018. TRPV4-mediates oscillatory fluid shear mechanotransduction in mesenchymal stem cells in part via the primary cilium. *Scientific reports,* 8**,** 3824.

Crawford, A, Frazer, A, Lippitt, Jm, Buttle, Dj & Smith, T 2006. A case of chondromatosis indicates a synovial stem cell aetiology. *Rheumatology,* 45**,** 1529-1533.

Cremer, Michael A, Rosloniec, Edward F & Kang, Andrew H 1998. The cartilage collagens: a review of their structure, organization, and role in the pathogenesis of

experimental arthritis in animals and in human rheumatic disease. *Journal of molecular medicine,* 76**,** 275-288.

Cruz, Ivana Beatrice Mânica Da, Severo, Antônio Lourenço, Azzolin, Verônica Farina, Garcia, Luiz Filipe Machado, Kuhn, André & Lech, Osvandré 2017. Regenerative potential of the cartilaginous tissue in mesenchymal stem cells: update, limitations, and challenges. *Revista brasileira de ortopedia,* 52**,** 2-10.

Cui, Peng, He, Xiaohong, Pu, Yabin, Zhang, Wenxiu, Zhang, Ping, Li, Changli, Guan, Weijun, Li, Xiangchen & Ma, Yuehui 2014. Biological characterization and pluripotent identification of sheep dermis-derived mesenchymal stem/progenitor cells. *BioMed research international,* 2014.

Czernik, Marta, Fidanza, Antonella, Sardi, Martina, Galli, Cesare, Brunetti, Dario, Malatesta, Daniela, Della Salda, Leonardo, Matsukawa, Kazutsugu, Ptak, Grazyna E & Loi, Pasqualino 2013. Differentiation potential and GFP labeling of sheep bone marrow-derived mesenchymal stem cells. *Journal of cellular biochemistry,* 114**,** 134-143.

Dale, Tina Patricia. 2016. *Investigating the chondrogenic phenotype in clinically relevant cells: the effect of hTERT expression.* Keele University.

Danielson, Keith G, Baribault, Helene, Holmes, David F, Graham, Helen, Kadler, Karl E & Iozzo, Renato V 1997. Targeted disruption of decorin leads to abnormal collagen fibril morphology and skin fragility. *The Journal of cell biology,* 136**,** 729-743.

Darling, Eric M, Wilusz, Rebecca E, Bolognesi, Michael P, Zauscher, Stefan & Guilak, Farshid 2010. Spatial mapping of the biomechanical properties of the pericellular matrix of articular cartilage measured in situ via atomic force microscopy. *Biophysical journal,* 98**,** 2848-2856.

Dawson, Alden B 1925. The age order of epiphyseal union in the long bones of the albino rat. *The Anatomical Record,* 31**,** 1-17.

Delaine-Smith, Robin M & Reilly, Gwendolen C 2012. Mesenchymal stem cell responses to mechanical stimuli. *Muscles, ligaments and tendons journal,* 2**,** 169.

Delling, Uta, Lindner, Katrin, Ribitsch, Iris, Jülke, Henriette & Brehm, Walter 2012. Comparison of bone marrow aspiration at the sternum and the tuber coxae in middle-aged horses. *Canadian Journal of Veterinary Research,* 76**,** 52-56.

Demarteau, O, Wendt, D, Braccini, A, Jakob, M, Schäfer, D, Heberer, M & Martin, I 2003. Dynamic compression of cartilage constructs engineered from expanded human articular chondrocytes. *Biochemical and biophysical research communications,* 310**,** 580-588.

Diekman, Brian O & Guilak, Farshid 2013. Stem cell-based therapies for osteoarthritis: challenges and opportunities. *Current opinion in rheumatology,* 25**,** 119.

Duda, Georg N, Kleemann, Ralf U, Bluecher, Uwe & Weiler, Andreas 2004. A new device to detect early cartilage degeneration. *The American journal of sports medicine,* 32**,** 693-698.

Dy, Peter, Smits, Patrick, Silvester, Amber, Penzo-Méndez, Alfredo, Dumitriu, Bogdan, Han, Yu, Carol, A, Kingsley, David M & Lefebvre, Véronique 2010. Synovial joint morphogenesis requires the chondrogenic action of Sox5 and Sox6 in growth plate and articular cartilage. *Developmental biology,* 341**,** 346-359.

Edwards, Jh & Reilly, Gc 2011. Low magnitude, high frequency vibration modulates mesenchymal progenitor differentiation. *Trans Annu Meet Orthop Res Soc,* 57.

Egermann, Marcus, Goldhahn, Jörg, Holz, R, Schneider, E & Lill, Christoph A 2008. A sheep model for fracture treatment in osteoporosis: benefits of the model versus animal welfare. *Laboratory animals,* 42**,** 453-464.

Eisenberg, Solomon R & Grodzinsky, Alan J 1985. Swelling of articular cartilage and other connective tissues: electromechanochemical forces. *Journal of orthopaedic research,* 3**,** 148-159.

El Haj, Aj & Cartmell, Sh 2010. Bioreactors for bone tissue engineering. *Proceedings of the Institution of Mechanical Engineers, Part H: Journal of Engineering in Medicine,* 224**,** 1523-1532.

El Haj, Alicia J, Glossop, John R, Sura, Harpal S, Lees, Martin R, Hu, Bin, Wolbank, Susanne, Van Griensven, Martijn, Redl, Heinz & Dobson, Jon 2015. An in vitro model of mesenchymal stem cell targeting using magnetic particle labelling. *Journal of tissue engineering and regenerative medicine,* 9**,** 724-733.

Elder, Benjamin D & Athanasiou, Kyriacos A 2009. Hydrostatic pressure in articular cartilage tissue engineering: from chondrocytes to tissue regeneration. *Tissue Engineering Part B: Reviews,* 15**,** 43-53.

Eleswarapu, Sriram V & Athanasiou, Kyriacos A 2013. TRPV4 channel activation improves the tensile properties of self-assembled articular cartilage constructs. *Acta biomaterialia,* 9**,** 5554-5561.

Estes, Bradley T, Gimble, Jeffrey M & Guilak, Farshid 2004. Mechanical signals as regulators of stem cell fate. *Current topics in developmental biology.* Elsevier.

Everaerts, Wouter, Nilius, Bernd & Owsianik, Grzegorz 2010. The vanilloid transient receptor potential channel TRPV4: from structure to disease. *Progress in biophysics and molecular biology,* 103**,** 2-17.

Fadel, Leandro, Viana, Brunno Rosa, Feitosa, Matheus Levi Tajra, Ercolin, Anna Caroline Mazeto, Roballo, Kelly Cristine Santos, Casals, Juliana Barbosa, Pieri, Naira Caroline Godoy, Meirelles, Flávio Vieira, Martins, Daniele Dos Santos & Miglino, Maria Angélica 2011. Protocols for obtainment and isolation of two mesenchymal stem cell sources in sheep. *Acta cirurgica brasileira,* 26**,** 267-273.

Farge, Emmanuel 2003. Mechanical induction of Twist in the Drosophila foregut/stomodeal primordium. *Current biology,* 13**,** 1365-1377.

Farndale, Richard W, Buttle, David J & Barrett, Alan J 1986. Improved quantitation and discrimination of sulphated glycosaminoglycans by use of dimethylmethylene blue. *Biochimica et Biophysica Acta (BBA)-General Subjects,* 883**,** 173-177.

Fayol, D, Frasca, G, Le Visage, C, Gazeau, F, Luciani, N & Wilhelm, C 2013. Use of magnetic forces to promote stem cell aggregation during differentiation, and cartilage tissue modeling. *Advanced Materials,* 25**,** 2611-2616.

Fermor, Hl, Mclure, Swd, Taylor, Sd, Russell, Sl, Williams, S, Fisher, J & Ingham, E 2015. Biological, biochemical and biomechanical characterisation of articular cartilage from the porcine, bovine and ovine hip and knee. *Bio-medical materials and engineering,* 25**,** 381-395.

Ferrari, Giuliana, Angelis, De, Coletta, Marcello, Paolucci, Egle, Stornaiuolo, Anna, Cossu, Giulio & Mavilio, Fulvio 1998. Muscle regeneration by bone marrow-derived myogenic progenitors. *Science,* 279**,** 1528-1530.

Ficklin, Timothy, Thomas, Gregory, Barthel, James C, Asanbaeva, Anna, Thonar, Eugene J, Masuda, Koichi, Chen, Albert C, Sah, Robert L, Davol, Andrew & Klisch, Stephen M 2007. Articular cartilage mechanical and biochemical property relations before and after in vitro growth. *Journal of biomechanics,* 40**,** 3607-3614.

Fiegel, Hc, Lange, Claudia, Kneser, U, Lambrecht, W, Zander, Ar, Rogiers, Xavier & Kluth, D 2006. Fetal and adult liver stem cells for liver regeneration and tissue engineering. *Journal of cellular and molecular medicine,* 10**,** 577-587.

Filardo, Giuseppe, Perdisa, Francesco, Gelinsky, Michael, Despang, Florian, Fini, Milena, Marcacci, Maurilio, Parrilli, Anna Paola, Roffi, Alice, Salamanna, Francesca & Sartori, Maria 2018. Novel alginate biphasic scaffold for osteochondral regeneration: an in vivo evaluation in rabbit and sheep models. *Journal of Materials Science: Materials in Medicine,* 29**,** 74.

Fink, Michel, Duprat, Fabrice, Lesage, Florian, Reyes, Roberto, Romey, Georges, Heurteaux, Catherine & Lazdunski, M 1996. Cloning, functional expression and brain localization of a novel unconventional outward rectifier K+ channel. *The EMBO journal,* 15**,** 6854-6862.

Fortier, Lisa A, Barker, Joseph U, Strauss, Eric J, Mccarrel, Taralyn M & Cole, Brian J 2011. The role of growth factors in cartilage repair. *Clinical Orthopaedics and Related Research®,* 469**,** 2706-2715.

Fragonas, E, Valente, M, Pozzi-Mucelli, M, Toffanin, R, Rizzo, Roberto, Silvestri, F & Vittur, Franco 2000. Articular cartilage repair in rabbits by using suspensions of allogenic chondrocytes in alginate. *Biomaterials,* 21**,** 795-801.

Friedenstein, Alexander Jakovlevich, Petrakova, Klara Vasiljevna, Kurolesova, Alexandra Ivanovna & Frolova, Galina Petrovna 1968. Heterotopic transplants of bone marrow. *Transplantation,* 6**,** 230-247.

Fulcher, Geoffrey R, Hukins, David Wl & Shepherd, Duncan Et 2009. Viscoelastic properties of bovine articular cartilage attached to subchondral bone at high frequencies. *BMC musculoskeletal disorders,* 10**,** 61.

Funayama, Atsushi, Niki, Yasuo, Matsumoto, Hideo, Maeno, Shinichi, Yatabe, Taku, Morioka, Hideo, Yanagimoto, Shigeru, Taguchi, Tetsushi, Tanaka, Junzo & Toyama, Yoshiaki 2008. Repair of full-thickness articular cartilage defects using injectable type II collagen gel embedded with cultured chondrocytes in a rabbit model. *Journal of Orthopaedic Science,* 13**,** 225-232.

Getgood, A, Brooks, R, Fortier, L & Rushton, N 2009. Articular cartilage tissue engineering: today's research, tomorrow's practice? *The Journal of bone and joint surgery. British volume,* 91**,** 565-576.

Glogauer, Michael & Ferrier, J 1997. A new method for application of force to cells via ferric oxide beads. *Pflügers Archiv,* 435**,** 320-327.

Glogauer, Michael, Ferrier, Jack & Mcculloch, Ca 1995. Magnetic fields applied to collagen-coated ferric oxide beads induce stretch-activated Ca2+ flux in fibroblasts. *American Journal of Physiology-Cell Physiology,* 269**,** C1093-C1104.

Go, Nobuhiro, Noguti, Tosiyuki & Nishikawa, Testuo 1983. Dynamics of a small globular protein in terms of low-frequency vibrational modes. *Proceedings of the National Academy of Sciences,* 80**,** 3696-3700.

Godoy, Roberta F, Alves, Ana Liz G, Gibson, Amanda J, Lima, Eduardo Mm & Goodship, Allen E 2014. Do progenitor cells from different tissue have the same phenotype? *Research in veterinary science,* 96**,** 454-459.

Goessler, Ulrich Reinhart, Bugert, Peter, Bieback, Karen, Baisch, Alexander, Sadick, Haneen, Verse, Thomas, Klüter, Harald, Hörmann, Karl & Riedel, Frank 2004. Expression of collagen and fiber-associated proteins in human septal cartilage during in vitro dedifferentiation. *International journal of molecular medicine,* 14**,** 1015-1022.

Goligorsky, Michael S 1988. Mechanical stimulation induces Ca2+ i transients and membrane depolarization in cultured endothelial cells Effects on Ca2+ i in co-perfused smooth muscle cells. *FEBS letters,* 240**,** 59-64.

Grad, Sibylle, Loparic, Marko, Peter, Robert, Stolz, Martin, Aebi, Ueli & Alini, Mauro 2012. Sliding motion modulates stiffness and friction coefficient at the surface of tissue engineered cartilage. *Osteoarthritis and cartilage,* 20**,** 288-295.

Grogan, Shawn P & D D'lima, Darryl 2010. Joint aging and chondrocyte cell death. *International journal of clinical rheumatology,* 5**,** 199.

Gronthos, Stan, Mccarty, Rosa, Mrozik, Krzysztof, Fitter, Stephen, Paton, Sharon, Menicanin, Danijela, Itescu, Silviu, Bartold, P Mark, Xian, Cory & Zannettino, Andrew Cw 2009. Heat shock protein-90 beta is expressed at the surface of multipotential mesenchymal precursor cells: generation of a novel monoclonal antibody, STRO-4, with specificity for mesenchymal precursor cells from human and ovine tissues. *Stem cells and development,* 18**,** 1253-1262.

Gruber, Reinhard, Karreth, Florian, Kandler, Barbara, Fuerst, Gabor, Rot, Antal, Fischer, Michael B & Watzek, Georg 2004. Platelet-released supernatants increase migration and proliferation, and decrease osteogenic differentiation of bone

marrow-derived mesenchymal progenitor cells under in vitro conditions. *Platelets,* 15**,** 29-35.

Guo, Ximin, Wang, Changyong, Zhang, Yufu, Xia, Renyun, Hu, Min, Duan, Cuimi, Zhao, Qiang, Dong, Lingzhi, Lu, Jianxi & Qing Song, Ying 2004. Repair of large articular cartilage defects with implants of autologous mesenchymal stem cells seeded into β-tricalcium phosphate in a sheep model. *Tissue engineering,* 10**,** 1818-1829.

Gupta, A, Bhosale, A, Balbouzis, T, Smith, Hj & Richardson, Jb 2006. Cartilage transplantation. *British Journal of Hospital Medicine (2005),* 67**,** 286-289.

Gupta, Ajay Kumar & Gupta, Mona 2005. Synthesis and surface engineering of iron oxide nanoparticles for biomedical applications. *Biomaterials,* 26**,** 3995-4021.

Gurkan, Umut Atakan & Akkus, Ozan 2008. The mechanical environment of bone marrow: a review. *Annals of biomedical engineering,* 36**,** 1978-1991.

Gurusinghe, Saliya & Strappe, Padraig 2014. Gene modification of mesenchymal stem cells and articular chondrocytes to enhance chondrogenesis. *BioMed research international,* 2014.

Haisch, A, Gröger, A, Radke, C, Ebmeyer, J, Sudhoff, H, Grasnick, G, Jahnke, V, Burmester, Gr & Sittinger, M 2000. Macroencapsulation of human cartilage implants: pilot study with polyelectrolyte complex membrane encapsulation. *Biomaterials,* 21**,** 1561-1566.

Han, S-K, Federico, Salvatore, Grillo, Alfio, Giaquinta, Gaetano & Herzog, Walter 2007. The mechanical behaviour of chondrocytes predicted with a micro-structural model of articular cartilage. *Biomechanics and Modeling in Mechanobiology,* 6**,** 139-150.

Hansmann, Jan, Groeber, Florian, Kahlig, Alexander, Kleinhans, Claudia & Walles, Heike 2013. Bioreactors in tissue engineering—principles, applications and commercial constraints. *Biotechnology journal,* 8**,** 298-307.

Hao, T, Wen, N, Cao, J-K, Wang, H-B, Lü, S-H, Liu, T, Lin, Q-X, Duan, C-M & Wang, C-Y 2010. The support of matrix accumulation and the promotion of sheep articular cartilage defects repair in vivo by chitosan hydrogels. *Osteoarthritis and cartilage,* 18**,** 257-265.

Harrison, Richard, Markides, Hareklea, Morris, Robert H, Richards, Paula, El Haj, Alicia J & Sottile, Virginie 2017. Autonomous magnetic labelling of functional mesenchymal stem cells for improved traceability and spatial control in cell therapy applications. *Journal of tissue engineering and regenerative medicine,* 11**,** 2333-2348.

Hayes, Wc & Mockros, Lf 1971. Viscoelastic properties of human articular cartilage. *Journal of Applied Physiology,* 31**,** 562-568.

Heidari, Banafsheh, Shirazi, Abolfazl, Akhondi, Mohammad Mehdi, Hassanpour, Hossein, Behzadi, Bahareh, Naderi, Mohammad Mehdi, Sarvari, Ali & Borjian, Sara 2013. Comparison of proliferative and multilineage differentiation potential of sheep mesenchymal stem cells derived from bone marrow, liver, and adipose tissue. *Avicenna journal of medical biotechnology,* 5**,** 104.

Henstock, James R, Rotherham, Michael, Rashidi, Hassan, Shakesheff, Kevin M & El Haj, Alicia J 2014. Remotely activated mechanotransduction via magnetic nanoparticles promotes mineralization synergistically with bone morphogenetic protein 2: applications for injectable cell therapy. *Stem cells translational medicine,* 3**,** 1363-1374.

Hickery, Mark S, Bayliss, Michael T, Dudhia, Jayesh, Lewthwaite, Joanne C, Edwards, Jc & Pitsillides, Andrew A 2003. Age-related changes in the response of human articular cartilage to IL-1 [alpha] and TGF-[beta]: Chondrocytes exhibit a diminished sensitivity to TGF-[beta]. *J Biol Chem,* 278**,** 53063-53071.

Hoemann, Caroline, Kandel, Rita, Roberts, Sally, Saris, Daniel Bf, Creemers, Laura, Mainil-Varlet, Pierre, Méthot, Stephane, Hollander, Anthony P & Buschmann, Michael D 2011. International Cartilage Repair Society (ICRS) recommended

guidelines for histological endpoints for cartilage repair studies in animal models and clinical trials. *Cartilage,* 2**,** 153-172.
Hofmann-Amtenbrink, Margarethe, Hofmann, Heinrich & Montet, Xavier 2010. Superparamagnetic nanoparticles–a tool for early diagnostics. *Swiss medical weekly,* 140.
Hogan, Bl 1996. Bone morphogenetic proteins: multifunctional regulators of vertebrate development. *Genes & development,* 10**,** 1580-1594.
Holman, Jack Philip & Gajda, Walter J 2001. *Experimental methods for engineers,* McGraw-Hill New York.
Homicz, Mark R, Mcgowan, Kevin B, Lottman, Lisa M, Beh, Gordon, Sah, Robert L & Watson, Deborah 2003. A compositional analysis of human nasal septal cartilage. *Archives of facial plastic surgery,* 5**,** 53-58.
Hu, Kongzu, Sun, Heyan, Gui, Binjie & Sui, Cong 2017. TRPV4 functions in flow shear stress induced early osteogenic differentiation of human bone marrow mesenchymal stem cells. *Biomedicine & Pharmacotherapy,* 91**,** 841-848.
Huang, Chun-Yuh, Soltz, Michael A, Kopacz, Monika, Mow, Van C & Ateshian, Gerard A 2003. Experimental verification of the roles of intrinsic matrix viscoelasticity and tension-compression nonlinearity in the biphasic response of cartilage. *Journal of biomechanical engineering,* 125**,** 84-93.
Hubbell, Jeffrey A 1995. Biomaterials in tissue engineering. *Nature Biotechnology,* 13**,** 565.
Hughes, Steven, Dobson, Jon & El Haj, Alicia J 2007. Magnetic targeting of mechanosensors in bone cells for tissue engineering applications. *Journal of biomechanics,* 40**,** S96-S104.
Hughes, Steven, El Haj, Alicia J & Dobson, Jon 2005. Magnetic micro-and nanoparticle mediated activation of mechanosensitive ion channels. *Medical engineering & physics,* 27**,** 754-762.
Hughes, Steven, Mcbain, Stuart, Dobson, Jon & El Haj, Alicia J 2008. Selective activation of mechanosensitive ion channels using magnetic particles. *Journal of the Royal Society Interface,* 5**,** 855-863.
Hunziker, Ernst Bruno, Lippuner, Kurt, Keel, Mjb & Shintani, Nahoko 2015. An educational review of cartilage repair: precepts & practice–myths & misconceptions–progress & prospects. *Osteoarthritis and cartilage,* 23**,** 334-350.
Hutmacher, Dietmar W 2006. Scaffolds in tissue engineering bone and cartilage. *The Biomaterials: Silver Jubilee Compendium.* Elsevier.
Ikada, Yoshito 2006. Challenges in tissue engineering. *Journal of the Royal Society Interface,* 3**,** 589-601.
Ilancheran, S, Moodley, Y & Manuelpillai, U 2009. Human fetal membranes: a source of stem cells for tissue regeneration and repair? *Placenta,* 30**,** 2-10.
Ingber, Donald E 2006. Cellular mechanotransduction: putting all the pieces together again. *The FASEB Journal,* 20**,** 811-827.
Iwashina, Toru, Mochida, Joji, Miyazaki, Takeshi, Watanabe, Takuya, Iwabuchi, Sadahiro, Ando, Kiyoshi, Hotta, Tomomitsu & Sakai, Daisuke 2006. Low-intensity pulsed ultrasound stimulates cell proliferation and proteoglycan production in rabbit intervertebral disc cells cultured in alginate. *Biomaterials,* 27**,** 354-361.
Jaalouk, Diana E & Lammerding, Jan 2009. Mechanotransduction gone awry. *Nature reviews Molecular cell biology,* 10**,** 63.
Jackson, L, Jones, Dr, Scotting, P & Sottile, V 2007. Adult mesenchymal stem cells: differentiation potential and therapeutic applications. *Journal of postgraduate medicine,* 53**,** 121.
Jäger, Marcus, Bachmann, Radu, Scharfstädt, Axel & Krauspe, Rüdiger 2006. Ovine cord blood accommodates multipotent mesenchymal progenitor cells. *in vivo,* 20**,** 205-214.

Jaiswal, Neelam, Haynesworth, Stephen E, Caplan, Arnold I & Bruder, Scott P 1997. Osteogenic differentiation of purified, culture-expanded human mesenchymal stem cells in vitro. *Journal of cellular biochemistry,* 64**,** 295-312.

Jansen, Idc, Hollander, Ap, Buttle, Dj & Everts, V 2010. Type II and VI collagen in nasal and articular cartilage and the effect of IL-1α on the distribution of these collagens. *Journal of molecular histology,* 41**,** 9-17.

Jerosch, Jörg 2011. Effects of glucosamine and chondroitin sulfate on cartilage metabolism in OA: outlook on other nutrient partners especially omega-3 fatty acids. *International journal of rheumatology,* 2011.

Jessop, Helen L, Noble, Brendon S & Cryer, Anthony 1994. The differentiation of a potential mesenchymal stem cell population within ovine bone marrow. Portland Press Limited.

Jin, Moonsoo, Frank, Eliot H, Quinn, Thomas M, Hunziker, Ernst B & Grodzinsky, Alan J 2001. Tissue shear deformation stimulates proteoglycan and protein biosynthesis in bovine cartilage explants. *Archives of biochemistry and biophysics,* 395**,** 41-48.

Johnson-Nurse, C & Dandy, Dj 1985. Fracture-separation of articular cartilage in the adult knee. *The Journal of bone and joint surgery. British volume,* 67**,** 42-43.

Johnson, Kristen, Zhu, Shoutian, Tremblay, Matthew S, Payette, Joshua N, Wang, Jianing, Bouchez, Laure C, Meeusen, Shelly, Althage, Alana, Cho, Charles Y & Wu, Xu 2012. A stem cell–based approach to cartilage repair. *Science***,** 1215157.

Jurvelin, Js, Buschmann, Md & Hunziker, Eb 1997. Optical and mechanical determination of Poisson's ratio of adult bovine humeral articular cartilage. *Journal of biomechanics,* 30**,** 235-241.

Jurvelin, Js, Buschmann, Md & Hunziker, Eb 2003. Mechanical anisotropy of the human knee articular cartilage in compression. *Proceedings of the Institution of Mechanical Engineers, Part H: Journal of Engineering in Medicine,* 217**,** 215-219.

Kadiyala, S, Young, Rg, Thiede, Ma & Bruder, Sp 1997. Culture expanded canine mesenchymal stem cells possess osteochondrogenic potential in vivo and in vitro. *Cell transplantation,* 6**,** 125-134.

Kalamegam, Gauthaman, Memic, Adnan, Budd, Emma, Abbas, Mohammed & Mobasheri, Ali 2018. A Comprehensive Review of Stem Cells for Cartilage Regeneration in Osteoarthritis.

Kalaszczynska, Ilona, Ruminski, Slawomir, Platek, Anna E, Bissenik, Igor, Zakrzewski, Piotr, Noszczyk, Maria & Lewandowska-Szumiel, Malgorzata 2013. Substantial differences between human and ovine mesenchymal stem cells in response to osteogenic media: how to explain and how to manage? *BioResearch open access,* 2**,** 356-363.

Kandel, Ra, Grynpas, M, Pilliar, R, Lee, J, Wang, J, Waldman, S, Zalzal, P & Hurtig, M 2006. Repair of osteochondral defects with biphasic cartilage-calcium polyphosphate constructs in a sheep model. *Biomaterials,* 27**,** 4120-4131.

Kern, Susanne, Eichler, Hermann, Stoeve, Johannes, Klüter, Harald & Bieback, Karen 2006. Comparative analysis of mesenchymal stem cells from bone marrow, umbilical cord blood, or adipose tissue. *Stem cells,* 24**,** 1294-1301.

Kiyotake, Emi A, Beck, Emily C & Detamore, Michael S 2016. Cartilage extracellular matrix as a biomaterial for cartilage regeneration. *Annals of the New York Academy of Sciences,* 1383**,** 139-159.

Kleemann, Ralf U, Schell, Hanna, Thompson, Mark, Epari, Devakara R, Duda, Georg N & Weiler, Andreas 2007. Mechanical behavior of articular cartilage after osteochondral autograft transfer in an ovine model. *The American journal of sports medicine,* 35**,** 555-563.

Klein, Travis J, Malda, Jos, Sah, Robert L & Hutmacher, Dietmar W 2009. Tissue engineering of articular cartilage with biomimetic zones. *Tissue Engineering Part B: Reviews,* 15**,** 143-157.

Knecht, Sven. 2006. *Biomechanical assessment of native and tissue engineered articular cartilage.* ETH Zurich.
Kobayashi, Takeshi 2011. Cancer hyperthermia using magnetic nanoparticles. *Biotechnology journal,* 6**,** 1342-1347.
Kobayashi, Yuka, Sakai, Daisuke, Iwashina, Toru, Iwabuchi, Sadahiro & Mochida, Joji 2009. Low-intensity pulsed ultrasound stimulates cell proliferation, proteoglycan synthesis and expression of growth factor-related genes in human nucleus pulposus cell line. *Eur Cell Mater,* 17**,** 15-22.
Kock, Linda, Van Donkelaar, Corrinus C & Ito, Keita 2012. Tissue engineering of functional articular cartilage: the current status. *Cell and tissue research,* 347**,** 613-627.
Koh, Sang D, Monaghan, Kevin, Sergeant, Gerard P, Ro, Seungil, Walker, Rebecca L, Sanders, Kenton M & Horowitz, Burton 2001. TREK-1 regulation by nitric oxide and CGMP dependent protein kinase: An essential role in smooth muscle inhibitory neurotransmission. *Journal of Biological Chemistry*.
Kontturi, Leena-Stiina, Järvinen, Elina, Muhonen, Virpi, Collin, Estelle C, Pandit, Abhay S, Kiviranta, Ilkka, Yliperttula, Marjo & Urtti, Arto 2014. An injectable, in situ forming type II collagen/hyaluronic acid hydrogel vehicle for chondrocyte delivery in cartilage tissue engineering. *Drug delivery and translational research,* 4**,** 149-158.
Koobatian, Maxwell T, Liang, Mao-Shih, Swartz, Daniel D & Andreadis, Stelios T 2015. Differential effects of culture senescence and mechanical stimulation on the proliferation and leiomyogenic differentiation of MSC from different sources: implications for engineering vascular grafts. *Tissue engineering Part A,* 21**,** 1364-1375.
Kratchmarova, Irina, Blagoev, Blagoy, Haack-Sorensen, Mandana, Kassem, Moustapha & Mann, Matthias 2005. Mechanism of divergent growth factor effects in mesenchymal stem cell differentiation. *Science,* 308**,** 1472-1477.
Kronenberg, Henry M 2003. Developmental regulation of the growth plate. *Nature,* 423**,** 332.
Kumar, Sachin, Raj, Shammy, Kolanthai, Elayaraja, Sood, Ak, Sampath, S & Chatterjee, Kaushik 2015. Chemical functionalization of graphene to augment stem cell osteogenesis and inhibit biofilm formation on polymer composites for orthopedic applications. *ACS applied materials & interfaces,* 7**,** 3237-3252.
Kunisaki, Shaun M, Fuchs, Julie R, Steigman, Shaun A & Fauza, Dario O 2007. A comparative analysis of cartilage engineered from different perinatal mesenchymal progenitor cells. *Tissue engineering,* 13**,** 2633-2644.
Kuroda, R, Ishida, K, Matsumoto, T, Akisue, T, Fujioka, H, Mizuno, K, Ohgushi, H, Wakitani, S & Kurosaka, M 2007. Treatment of a full-thickness articular cartilage defect in the femoral condyle of an athlete with autologous bone-marrow stromal cells. *Osteoarthritis and cartilage,* 15**,** 226-231.
Kuyinu, Emmanuel L, Narayanan, Ganesh, Nair, Lakshmi S & Laurencin, Cato T 2016. Animal models of osteoarthritis: classification, update, and measurement of outcomes. *Journal of orthopaedic surgery and research,* 11**,** 19.
Lai, W Michael, Hou, Js & Mow, Van C 1991. A triphasic theory for the swelling and deformation behaviors of articular cartilage. *Journal of biomechanical engineering,* 113**,** 245-258.
Lammi, Pirkko E, Lammi, Mikko J, Tammi, Raija H, Helminen, Heikki J & Espanha, M Margarida 2001. Strong hyaluronan expression in the full-thickness rat articular cartilage repair tissue. *Histochemistry and cell biology,* 115**,** 301-308.
Las Heras, Facundo, Gahunia, Harpal K & Pritzker, Kenneth Ph 2012. Articular cartilage development: a molecular perspective. *Orthopedic Clinics,* 43**,** 155-171.

Lau, Esther, Al-Dujaili, Saja, Guenther, Axel, Liu, Dawei, Wang, Liyun & You, Lidan 2010. Effect of low-magnitude, high-frequency vibration on osteocytes in the regulation of osteoclasts. *Bone,* 46**,** 1508-1515.

Laurencin, Cato T, Ambrosio, Ama, Borden, Md & Cooper Jr, Ja 1999. Tissue engineering: orthopedic applications. *Annual review of biomedical engineering,* 1**,** 19-46.

Lawless, Bernard M, Sadeghi, Hamid, Temple, Duncan K, Dhaliwal, Hemeth, Espino, Daniel M & Hukins, David Wl 2017. Viscoelasticity of articular cartilage: Analysing the effect of induced stress and the restraint of bone in a dynamic environment. *Journal of the mechanical behavior of biomedical materials,* 75**,** 293-301.

Lawrence, Reva C, Felson, David T, Helmick, Charles G, Arnold, Lesley M, Choi, Hyon, Deyo, Richard A, Gabriel, Sherine, Hirsch, Rosemarie, Hochberg, Marc C & Hunder, Gene G 2008. Estimates of the prevalence of arthritis and other rheumatic conditions in the United States: Part II. *Arthritis & Rheumatism,* 58**,** 26-35.

Lee, Wayne Yuk-Wai & Wang, Bin 2017. Cartilage repair by mesenchymal stem cells: clinical trial update and perspectives. *Journal of orthopaedic translation,* 9**,** 76-88.

Lesage, Florian & Lazdunski, Michel 2000. Molecular and functional properties of two-pore-domain potassium channels. *American Journal of Physiology-Renal Physiology,* 279**,** F793-F801.

Letouzey, Vincent, Tan, Ker Sin, Deane, James A, Ulrich, Daniela, Gurung, Shanti, Ong, Y Rue & Gargett, Caroline E 2015. Isolation and characterisation of mesenchymal stem/stromal cells in the ovine endometrium. *PloS one,* 10**,** e0127531.

Leung, Kwok Sui, Shi, Hong Fei, Cheung, Wing Hoi, Qin, Ling, Ng, Wai Kin, Tam, Kam Fai & Tang, Ning 2009. Low-magnitude high-frequency vibration accelerates callus formation, mineralization, and fracture healing in rats. *Journal of orthopaedic research,* 27**,** 458-465.

Li, Zhiqiang, Tian, Xiaojun, Yuan, Yan, Song, Zhixiu, Zhang, Lili, Wang, Xia & Li, Tong 2013. Effect of cell culture using chitosan membranes on stemness marker genes in mesenchymal stem cells. *Molecular medicine reports,* 7**,** 1945-1949.

Liedtke, Wolfgang 2006. 22 TRPV Channels' Function in Osmo-and Mechanotransduction. *TRP Ion Channel Function in Sensory Transduction and Cellular Signaling Cascades***,** 303.

Liedtke, Wolfgang B 2006. *TRP ion channel function in sensory transduction and cellular signaling cascades*, CRC Press.

Liu, Guizhong, Vijayakumar, Sapna, Grumolato, Luca, Arroyave, Randy, Qiao, Huifang, Akiri, Gal & Aaronson, Stuart A 2009. Canonical Wnts function as potent regulators of osteogenesis by human mesenchymal stem cells. *The Journal of cell biology,* 185**,** 67-75.

Liu, Liyue, Yuan, Wenji & Wang, Jinfu 2010. Mechanisms for osteogenic differentiation of human mesenchymal stem cells induced by fluid shear stress. *Biomechanics and Modeling in Mechanobiology,* 9**,** 659-670.

Liu, Yu, Zhou, Guangdong & Cao, Yilin 2017. Recent Progress in Cartilage Tissue Engineering—Our Experience and Future Directions. *Engineering,* 3**,** 28-35.

Lo Monaco, Melissa, Merckx, Greet, Ratajczak, Jessica, Gervois, Pascal, Hilkens, Petra, Clegg, Peter, Bronckaers, Annelies, Vandeweerd, Jean-Michel & Lambrichts, Ivo 2018. Stem Cells for Cartilage Repair: Preclinical Studies and Insights in Translational Animal Models and Outcome Measures. *Stem cells international,* 2018.

Lodi, Daniele, Iannitti, Tommaso & Palmieri, Beniamino 2011. Stem cells in clinical practice: applications and warnings. *Journal of Experimental & Clinical Cancer Research,* 30**,** 9.

Loeser, Richard F, Shanker, Gouri, Carlson, Cathy S, Gardin, Jean F, Shelton, Brent J & Sonntag, William E 2000. Reduction in the chondrocyte response to insulin-like

growth factor 1 in aging and osteoarthritis: studies in a non-human primate model of naturally occurring disease. *Arthritis & Rheumatism: Official Journal of the American College of Rheumatology,* 43**,** 2110-2120.
Loparic, Marko. 2012. *Biomechanical assessment of extracellular matrix in native and tissue engineered cartilage across lenght scales.* University_of_Basel.
Loparic, Marko, Wirz, Dieter, Daniels, Au, Raiteri, Roberto, Vanlandingham, Mark R, Guex, Geraldine, Martin, Ivan, Aebi, Ueli & Stolz, Martin 2010. Micro-and nanomechanical analysis of articular cartilage by indentation-type atomic force microscopy: validation with a gel-microfiber composite. *Biophysical journal,* 98**,** 2731-2740.
Lu, Pengfei, Takai, Ken, Weaver, Valerie M & Werb, Zena 2011. Extracellular matrix degradation and remodeling in development and disease. *Cold Spring Harbor perspectives in biology***,** a005058.
Lu, Xin L & Mow, Van C 2008. Biomechanics of articular cartilage and determination of material properties. *Medicine & Science in Sports & Exercise,* 40**,** 193-199.
Lui, Pauline Po Yee 2015. Stem cell technology for tendon regeneration: current status, challenges, and future research directions. *Stem cells and cloning: advances and applications,* 8**,** 163.
Lv, Feng-Juan, Tuan, Rocky S, Cheung, Kenneth Mc & Leung, Victor Yl 2014. Concise review: the surface markers and identity of human mesenchymal stem cells. *Stem cells,* 32**,** 1408-1419.
Lyahyai, Jaber, Mediano, Diego R, Ranera, Beatriz, Sanz, Arianne, Remacha, Ana Rosa, Bolea, Rosa, Zaragoza, Pilar, Rodellar, Clementina & Martín-Burriel, Inmaculada 2012. Isolation and characterization of ovine mesenchymal stem cells derived from peripheral blood. *BMC veterinary research,* 8**,** 169.
Ma, Jinling. 2013. *Cell-based strategies in bone tissue engineering. Effects of mesenchymal stem cell origin and cocultures with angiogenic cells.* [Sl: sn].
Machado, Joana, Viriato, Nuno, Marta, Miguel & Vaz, Mário 2017. Experimental characterization of the mechanical properties of knee articular cartilages in compression: first approach with swine tissues. *Rheumatology and Orthopedic Medicine,* 2**,** 1-4.
Mackie, Ej1, Ahmed, Ya, Tatarczuch, L, Chen, K-S & Mirams, M 2008. Endochondral ossification: how cartilage is converted into bone in the developing skeleton. *The international journal of biochemistry & cell biology,* 40**,** 46-62.
Malloy, Kelly M & Hilibrand, Alan S 2002. Autograft versus allograft in degenerative cervical disease. *Clinical Orthopaedics and Related Research (1976-2007),* 394**,** 27-38.
Mammoto, Akiko, Mammoto, Tadanori & Ingber, Donald E 2012. Mechanosensitive mechanisms in transcriptional regulation. *J Cell Sci***,** jcs. 093005.
Mankin, Henry J 1982. The response of articular cartilage to mechanical injury. *JBJS,* 64**,** 460-466.
Marcos-Campos, I, Asin, L, Torres, Te, Marquina, C, Tres, A, Ibarra, Mr & Goya, Gf 2011. Cell death induced by the application of alternating magnetic fields to nanoparticle-loaded dendritic cells. *Nanotechnology,* 22**,** 205101.
Markides, H, Rotherham, M & El Haj, Aj 2012. Biocompatibility and toxicity of magnetic nanoparticles in regenerative medicine. *Journal of Nanomaterials,* 2012**,** 13.
Markides, Hareklea, Kehoe, Oksana, Morris, Robert H & El Haj, Alicia J 2013. Whole body tracking of superparamagnetic iron oxide nanoparticle-labelled cells–a rheumatoid arthritis mouse model. *Stem cell research & therapy,* 4**,** 126.
Markides, Hareklea, Mclaren, Jane S, Telling, Neil D, Alom, Noura, E'atelaf, A, Oreffo, Richard Oc, Zannettino, Andrew, Scammell, Brigitte E, White, Lisa J & El Haj, Alicia J 2018. Translation of remote control regenerative technologies for bone repair. *NPJ Regenerative medicine,* 3**,** 9.

Marks, Ray 2017. Articular Cartilage Regeneration: An Update of Possible Treatment Approaches. *International Journal of Orthopaedics,* 4**,** 770-778.
Marlovits, Stefan, Zeller, Philip, Singer, Philipp, Resinger, Christoph & Vécsei, Vilmos 2006. Cartilage repair: generations of autologous chondrocyte transplantation. *European journal of radiology,* 57**,** 24-31.
Maroudas, A, Wachtel, E, Grushko, G, Katz, Ep & Weinberg, P 1991. The effect of osmotic and mechanical pressures on water partitioning in articular cartilage. *Biochimica et Biophysica Acta (BBA)-General Subjects,* 1073**,** 285-294.
Martin, Ivan, Muraglia, Anita, Campanile, Giuliano, Cancedda, Ranieri & Quarto, Rodolfo 1997. Fibroblast growth factor-2 supports ex vivo expansion and maintenance of osteogenic precursors from human bone marrow. *Endocrinology,* 138**,** 4456-4462.
Martini, Lucia, Fini, Milena, Giavaresi, Gianluca & Giardino, Roberto 2001. Sheep model in orthopedic research: a literature review. *Comparative medicine,* 51**,** 292-299.
Matricali, Giovanni A, Dereymaeker, Gp & Luyten, Frank P 2010. Donor site morbidity after articular cartilage repair procedures: a review. *Acta orthopaedica Belgica,* 76**,** 669.
Matsumoto, Tomoyuki, Kubo, Seiji, Meszaros, Laura B, Corsi, Karin A, Cooper, Gregory M, Li, Guangheng, Usas, Arvydas, Osawa, Aki, Fu, Freddie H & Huard, Johnny 2008. The influence of sex on the chondrogenic potential of muscle-derived stem cells: Implications for cartilage regeneration and repair. *Arthritis & Rheumatism: Official Journal of the American College of Rheumatology,* 58**,** 3809-3819.
Mccarty, Rosa C, Gronthos, Stan, Zannettino, Andrew C, Foster, Bruce K & Xian, Cory J 2009. Characterisation and developmental potential of ovine bone marrow derived mesenchymal stem cells. *Journal of cellular physiology,* 219**,** 324-333.
Mccarty, Rosa C, Grothos, Stan, Andrew , Zannettino C, Foster, Bruce K & Xian, Cory J 2009. Characterisation and Developmental Potential of Ovine Bone Marrow Derived Mesenchymal Stem Cells. *Journal of Cellular Physiology,* 219**,** 324–333.
Mccredie, Alexandra Jane. 2010. *Ultrasound elastography for the characterisation of cartilage.* UCL (University College London).
Mcgovern, Jacqui Anne, Griffin, Michelle & Hutmacher, Dietmar Werner 2018. Animal models for bone tissue engineering and modelling disease. *Disease models & mechanisms,* 11**,** dmm033084.
Mckay, Rd 2004. Stem cell biology and neurodegenerative disease. *Philosophical Transactions of the Royal Society of London B: Biological Sciences,* 359**,** 851-856.
Medhurst, Andrew D, Rennie, Gillian, Chapman, Conrad G, Meadows, Helen, Duckworth, Malcolm D, Kelsell, Rosemary E, Gloger, Israel I & Pangalos, Menelas N 2001. Distribution analysis of human two pore domain potassium channels in tissues of the central nervous system and periphery. *Molecular brain research,* 86**,** 101-114.
Meinert, Christoph, Schrobback, Karsten, Hutmacher, Dietmar W & Klein, Travis J 2017. A novel bioreactor system for biaxial mechanical loading enhances the properties of tissue-engineered human cartilage. *Scientific reports,* 7**,** 16997.
Mikos, Antonios G, Herring, Susan W, Ochareon, Pannee, Elisseeff, Jennifer, Lu, Helen H, Kandel, Rita, Schoen, Frederick J, Toner, Mehmet, Mooney, David & Atala, Anthony 2006. Engineering complex tissues. *Tissue engineering,* 12**,** 3307-3339.
Moeinzadeh, Seyedsina, Shariati, Seyed Ramin Pajoum & Jabbari, Esmaiel 2016. Comparative effect of physicomechanical and biomolecular cues on zone-specific chondrogenic differentiation of mesenchymal stem cells. *Biomaterials,* 92**,** 57-70.
Moore, Carlene, Cevikbas, Ferda, Pasolli, H Amalia, Chen, Yong, Kong, Wei, Kempkes, Cordula, Parekh, Puja, Lee, Suk Hee, Kontchou, Nelly-Ange & Yeh, Iwei 2013. UVB radiation generates sunburn pain and affects skin by activating epidermal TRPV4 ion channels and triggering endothelin-1 signaling. *Proceedings of the National Academy of Sciences,* 110**,** E3225-E3234.

Mow, Van C, Kuei, Sc, Lai, W Michael & Armstrong, Cecil G 1980. Biphasic creep and stress relaxation of articular cartilage in compression: theory and experiments. *Journal of biomechanical engineering,* 102**,** 73-84.

Mow, Vc, Lai, Wm & Holmes, Mh 1982. Advanced theoretical and experimental techniques in cartilage research. *Biomechanics: Principles and applications.* Springer.

Mow, Vc, Proctor, Cs & Kelly, Ma 1989. Basic biomechanics of the musculoskeletal system. *Philadelphia Lea, and Febiger***,** 31.

Moyad, Thomas F 2011. Cartilage injuries in the adult knee: evaluation and management. *Cartilage,* 2**,** 226-236.

Mrozik, Krzysztof M, Zilm, Peter S, Bagley, Christopher J, Hack, Sandra, Hoffmann, Peter, Gronthos, Stan & Bartold, P Mark 2010. Proteomic characterization of mesenchymal stem cell-like populations derived from ovine periodontal ligament, dental pulp, and bone marrow: analysis of differentially expressed proteins. *Stem cells and development,* 19**,** 1485-1499.

Mrugala, D, Bony, C, Neves, N, Caillot, L, Fabre, S, Moukoko, D, Jorgensen, C & Noël, D 2007. Phenotypic and functional characterization of ovine mesenchymal stem cells: application to a cartilage defect model. *Annals of the rheumatic diseases*.

Muramatsu, Shuji, Wakabayashi, Makoto, Ohno, Takeshi, Amano, Katsuhiko, Ooishi, Rika, Sugahara, Toshinori, Shiojiri, Satoshi, Tashiro, Kosuke, Suzuki, Yutaka & Nishimura, Riko 2007. Functional gene screening system identified TRPV4 as a regulator of chondrogenic differentiation. *Journal of Biological Chemistry,* 282**,** 32158-32167.

Music, Ena, Futrega, Kathryn & Doran, Michael R 2018. Sheep as a model for evaluating mesenchymal stem/stromal cell (MSC)-based chondral defect repair. *Osteoarthritis and cartilage*.

Nehrer, S, Breinan, Ha, Ramappa, A, Hsu, Hp, Minas, T, Shortkroff, S, Sledge, Cb, Yannas, Iv & Spector, M 1998. Chondrocyte-seeded collagen matrices implanted in a chondral defect in a canine model. *Biomaterials,* 19**,** 2313-2328.

Nejadnik, Hossein, Hui, James H, Feng Choong, Erica Pei, Tai, Bee-Choo & Lee, Eng Hin 2010. Autologous bone marrow–derived mesenchymal stem cells versus autologous chondrocyte implantation: an observational cohort study. *The American journal of sports medicine,* 38**,** 1110-1116.

Newman, E, Turner, As & Wark, Jd 1995. The potential of sheep for the study of osteopenia: current status and comparison with other animal models. *Bone,* 16**,** S277-S284.

Nguyen, Lonnissa H, Kudva, Abhijit K, Guckert, Nicole L, Linse, Klaus D & Roy, Krishnendu 2011. Unique biomaterial compositions direct bone marrow stem cells into specific chondrocytic phenotypes corresponding to the various zones of articular cartilage. *Biomaterials,* 32**,** 1327-1338.

Nicoll, Steven B, Wedrychowska, Anna, Smith, Nancy R & Bhatnagar, Rajendra S 2001. Modulation of proteoglycan and collagen profiles in human dermal fibroblasts by high density micromass culture and treatment with lactic acid suggests change to a chondrogenic phenotype. *Connective tissue research,* 42**,** 59-69.

Nilius, Bernd & Owsianik, Grzegorz 2011. The transient receptor potential family of ion channels. *Genome biology,* 12**,** 218.

Nilius, Bernd, Watanabe, Hiroyuki & Vriens, Joris 2003. The TRPV4 channel: structure-function relationship and promiscuous gating behaviour. *Pflügers Archiv,* 446**,** 298-303.

Niwa, Hitoshi 2013. Mechanisms of stem cell self-renewal. *Handbook of Stem Cells (Second Edition).* Elsevier.

Nöth, Ulrich, Rackwitz, Lars, Heymer, Andrea, Weber, Meike, Baumann, Bernd, Steinert, Andre, Schütze, Norbert, Jakob, Franz & Eulert, Jochen 2007. Chondrogenic differentiation of human mesenchymal stem cells in collagen type I hydrogels.

Journal of Biomedical Materials Research Part A: An Official Journal of The Society for Biomaterials, The Japanese Society for Biomaterials, and The Australian Society for Biomaterials and the Korean Society for Biomaterials, 83**,** 626-635.

Nuernberger, Sylvia, Cyran, Norbert, Albrecht, Christian, Redl, Heinz, Vécsei, Vilmos & Marlovits, Stefan 2011. The influence of scaffold architecture on chondrocyte distribution and behavior in matrix-associated chondrocyte transplantation grafts. *Biomaterials,* 32**,** 1032-1040.

O'conor, Christopher J, Griffin, Timothy M, Liedtke, Wolfgang & Guilak, Farshid 2012. Increased susceptibility of Trpv4-deficient mice to obesity and obesity-induced osteoarthritis with very high-fat diet. *Annals of the rheumatic diseases***,** annrheumdis-2012-202272.

O'Neil, Roger G & Heller, Stefan 2005. The mechanosensitive nature of TRPV channels. *Pflügers Archiv,* 451**,** 193-203.

O'conor, Christopher J, Leddy, Holly A, Benefield, Halei C, Liedtke, Wolfgang B & Guilak, Farshid 2014. TRPV4-mediated mechanotransduction regulates the metabolic response of chondrocytes to dynamic loading. *Proceedings of the National Academy of Sciences,* 111**,** 1316-1321.

Oldershaw, Rachel A 2012. Cell sources for the regeneration of articular cartilage: the past, the horizon and the future. *International journal of experimental pathology,* 93**,** 389-400.

Orciani, Monia, Fini, Milena, Di Primio, Roberto & Mattioli-Belmonte, Monica 2017. Biofabrication and bone tissue regeneration: cell source, approaches, and challenges. *Frontiers in bioengineering and biotechnology,* 5**,** 17.

Orozco, Lluis, Munar, Anna, Soler, Robert, Alberca, Mercedes, Soler, Francesc, Huguet, Marina, Sentís, Joan, Sánchez, Ana & García-Sancho, Javier 2013. Treatment of knee osteoarthritis with autologous mesenchymal stem cells: a pilot study. *Transplantation,* 95**,** 1535-1541.

Oshima, Yasushi, Watanabe, Nobuyoshi, Matsuda, Ken-Ichi, Takai, Shinro, Kawata, Mitsuhiro & Kubo, Toshikazu 2005. Behavior of transplanted bone marrow-derived GFP mesenchymal cells in osteochondral defect as a simulation of autologous transplantation. *Journal of Histochemistry & Cytochemistry,* 53**,** 207-216.

Pagnotto, Mr, Wang, Z, Karpie, Jc, Ferretti, M, Xiao, X & Chu, Cr 2007. Adeno-associated viral gene transfer of transforming growth factor-β1 to human mesenchymal stem cells improves cartilage repair. *Gene therapy,* 14**,** 804.

Pankhurst, Quentin A, Connolly, J, Jones, Sk & Dobson, Jj 2003. Applications of magnetic nanoparticles in biomedicine. *Journal of physics D: Applied physics,* 36**,** R167.

Parsons, Jr 2016. Chapter B1 Cartilage. *Handbook of Biomaterial Properties.* Springer.

Parsons, Jr & Black, J 1977. The viscoelastic shear behavior of normal rabbit articular cartilage. *Journal of biomechanics,* 10**,** 21-29.

Patel, Amanda J & Honoré, Eric 2001. Properties and modulation of mammalian 2P domain K+ channels. *Trends in neurosciences,* 24**,** 339-346.

Patel, Amanda J, Honoré, Eric, Maingret, François, Lesage, Florian, Fink, Michel, Duprat, Fabrice & Lazdunski, Michel 1998. A mammalian two pore domain mechano-gated S-like K+ channel. *The EMBO journal,* 17**,** 4283-4290.

Patel, Purvi Sd, Shepherd, Duncan Et & Hukins, David Wl 2008. Compressive properties of commercially available polyurethane foams as mechanical models for osteoporotic human cancellous bone. *BMC musculoskeletal disorders,* 9**,** 137.

Pazhoumand-Dar, Hossein, Lam, Chiou-Peng & Masek, Martin 2015. Joint movement similarities for robust 3D action recognition using skeletal data. *Journal of Visual Communication and Image Representation,* 30**,** 10-21.

Pearce, Ai, Richards, Rg, Milz, S, Schneider, E & Pearce, Sg 2007. Animal models for implant biomaterial research in bone: a review. *Eur Cell Mater,* 13**,** 1-10.

Pearle, Andrew D, Warren, Russell F & Rodeo, Scott A 2005. Basic science of articular cartilage and osteoarthritis. *Clinics in sports medicine,* 24**,** 1-12.

Peters, Abby E, Comerford, Eithne J, Macaulay, Sophie, Bates, Karl T & Akhtar, Riaz 2017. Micromechanical properties of canine femoral articular cartilage following multiple freeze-thaw cycles. *Journal of the mechanical behavior of biomedical materials,* 71**,** 114-121.

Phan, Mimi N, Leddy, Holly A, Votta, Bartholomew J, Kumar, Sanjay, Levy, Dana S, Lipshutz, David B, Lee, Suk Hee, Liedtke, Wolfgang & Guilak, Farshid 2009. Functional characterization of TRPV4 as an osmotically sensitive ion channel in porcine articular chondrocytes. *Arthritis & Rheumatism: Official Journal of the American College of Rheumatology,* 60**,** 3028-3037.

Phinney, Donald G, Kopen, Gene, Righter, William, Webster, Stephen, Tremain, Nicola & Prockop, Darwin J 1999. Donor variation in the growth properties and osteogenic potential of human marrow stromal cells. *Journal of cellular biochemistry,* 75**,** 424-436.

Pickard, Mark R, Barraud, Perrine & Chari, Divya M 2011. The transfection of multipotent neural precursor/stem cell transplant populations with magnetic nanoparticles. *Biomaterials,* 32**,** 2274-2284.

Piek, Ester, Heldin, Carl-Henrik & Ten Dijke, Peter 1999. Specificity, diversity, and regulation in TGF-β superfamily signaling. *The FASEB Journal,* 13**,** 2105-2124.

Pittenger, Mf, Mackay, Am, Beck, Sc, Jaiswal, Rk, Douglas, R, Mosca, Jd, Moorman, Ma, Simonetti, Dw, Craig, S & Marshak, Dr 1999. Multilineage potential of adult human mesenchymal stem cells. science. 1999; 284 (5411): 143–7. *Transfus Med Hemother,* 43**,** 120-132.

Pommerenke, H, Schreiber, E, Dürr, F, Nebe, B, Hahnel, C, Möller, W & Rychly, J 1996. Stimulation of integrin receptors using a magnetic drag force device induces an intracellular free calcium response. *European journal of cell biology,* 70**,** 157-164.

Potes, José Caeiro, Reis, J, Capela E Silva, Fernando, Relvas, Carlos, Cabrita, António Silvério & Simões, José António 2008. The sheep as an animal model in orthopaedic research.

Puelacher, Wc, Kim, Sw, Vacanti, Jp, Schloo, B, Mooney, D & Vacanti, Ca 1994. Tissue-engineered growth of cartilage: the effect of varying the concentration of chondrocytes seeded onto synthetic polymer matrices. *International journal of oral and maxillofacial surgery,* 23**,** 49-53.

Quirici, Nadia, Scavullo, Cinzia, De Girolamo, Laura, Lopa, Silvia, Arrigoni, Elena, Deliliers, Giorgio Lambertenghi & Brini, Anna T 2009. Anti-L-NGFR and-CD34 monoclonal antibodies identify multipotent mesenchymal stem cells in human adipose tissue. *Stem cells and development,* 19**,** 915-925.

Rahfoth, B, Weisser, J, Sternkopf, F, Aigner, T, Von Der Mark, K & Bräuer, R 1998. Transplantation of allograft chondrocytes embedded in agarose gel into cartilage defects of rabbits. *Osteoarthritis and cartilage,* 6**,** 50-65.

Redman, Sn, Oldfield, Sf & Archer, Cw 2005. Current strategies for articular cartilage repair. *Eur Cell Mater,* 9**,** 23-32.

Reinwald, Yvonne, Bratt, Jessica & El Haj, Aj 2016. Pluripotent stem cells and their dynamic niche.

Reinwald, Yvonne & El Haj, Alicia J 2018. Hydrostatic pressure in combination with topographical cues affects the fate of bone marrow-derived human mesenchymal stem cells for bone tissue regeneration. *Journal of Biomedical Materials Research part A,* 106**,** 629-640.

Rentsch, C, Hess, R, Rentsch, B, Hofmann, A, Manthey, S, Scharnweber, D, Biewener, A & Zwipp, H 2010. Ovine bone marrow mesenchymal stem cells: isolation and characterization of the cells and their osteogenic differentiation potential on embroidered and surface-modified polycaprolactone-co-lactide scaffolds. *In Vitro Cellular & Developmental Biology-Animal,* 46**,** 624-634.

Rentsch , C, Hess , R, Rentsch , B, Hofmann , A, Manthey , S, Scharnweber , D, Biewener , A & Zwipp, H 2010. Ovine bone marrow mesenchymal stem cells: isolationand characterization of the cells and their osteogenic differentiation potential on embroidered and surface-modifie dpolycaprolactone-co-lactide scaffolds. *In Vitro Cell.Dev.Biol.Animal* 46**,** 624-634.

Rhodes, Np, Srivastava, Jk, Smith, Rf & Longinotti, C 2004. Heterogeneity in proliferative potential of ovine mesenchymal stem cell colonies. *Journal of Materials Science: Materials in Medicine,* 15**,** 397-402.

Rickard, Dj, Sullivan, Ta, Shenker, Bj, Leboy, Ps And & Kazhdan, I 1994. Induction of rapid osteoblast differentiation in rat bone marrow stromal cell cultures by dexamethasone and BMP-2. *Developmental biology,* 161**,** 218-228.

Risbud, M V, Shapiro, I M, Guttapalli, A, Di Martino, A, Danielson, K G, Beiner, J M, Hillibrand, A, Albert, T J, Anderson, D G & Vaccaro, A R 2006. Osteogenic potential of adult human stem cells of the lumbar vertebral body and the iliac crest. *Spine,* 31**,** 83-89.

Rotherham, Michael & El Haj, Alicia J 2015. Remote activation of the Wnt/β-catenin signalling pathway using functionalised magnetic particles. *PloS one,* 10**,** e0121761.

Roundy, Shad, Wright, Paul K & Rabaey, Jan 2003. A study of low level vibrations as a power source for wireless sensor nodes. *Computer communications,* 26**,** 1131-1144.

Saladin, K 2010. Anatomy and physiology: The unity of form and function. 2007. *Ohio: McGraw-Hill*.

Saldaña, Laura, Vallés, Gema, Bensiamar, Fátima, Mancebo, Francisco José, García-Rey, Eduardo & Vilaboa, Nuria 2017. Paracrine interactions between mesenchymal stem cells and macrophages are regulated by 1, 25-dihydroxyvitamin D3. *Scientific reports,* 7**,** 14618.

Sarugaser, Rahul, Lickorish, David, Baksh, Dolores, Hosseini, M Morris & Davies, John E 2005. Human umbilical cord perivascular (HUCPV) cells: a source of mesenchymal progenitors. *Stem cells,* 23**,** 220-229.

Schulz, Ronny Maik & Bader, Augustinus 2007. Cartilage tissue engineering and bioreactor systems for the cultivation and stimulation of chondrocytes. *European Biophysics Journal,* 36**,** 539-568.

Schumacher, Barbara L, Hughes, Clare E, Kuettner, Klaus E, Caterson, Bruce & Aydelotte, Margaret B 1999. Immunodetection and partial cDNA sequence of the proteoglycan, superficial zone protein, synthesized by cells lining synovial joints. *Journal of orthopaedic research,* 17**,** 110-120.

Schwarz, Silke, Koerber, Ludwig, Elsaesser, Alexander F, Goldberg-Bockhorn, Eva, Seitz, Andreas M, Dürselen, Lutz, Ignatius, Anita, Walther, Paul, Breiter, Roman & Rotter, Nicole 2012. Decellularized cartilage matrix as a novel biomatrix for cartilage tissue-engineering applications. *Tissue engineering Part A,* 18**,** 2195-2209.

Scott, Alexander, Khan, Karim M, Duronio, Vincent & Hart, David A 2008. Mechanotransduction in human bone. *Sports Medicine,* 38**,** 139-160.

Scuteri, Arianna, Donzelli, Elisabetta, Foudah, Dana, Caldara, Cristina, Redondo, Juliana, D'amico, Giovanna, Tredici, Giovanni & Miloso, Mariarosaria 2014. Mesengenic differentiation: comparison of human and rat bone marrow mesenchymal stem cells. *International journal of stem cells,* 7**,** 127.

Sell, Scott A, Wolfe, Patricia S, Garg, Koyal, Mccool, Jennifer M, Rodriguez, Isaac A & Bowlin, Gary L 2010. The use of natural polymers in tissue engineering: a focus on electrospun extracellular matrix analogues. *Polymers,* 2**,** 522-553.

Septiadi, Dedy, Crippa, Federica, Moore, Thomas Lee, Rothen-Rutishauser, Barbara & Petri-Fink, Alke 2018. Nanoparticle–cell interaction: a cell mechanics perspective. *Advanced Materials,* 30**,** 1704463.

Siddappa, Ramakrishnaiah, Licht, Ruud, Van Blitterswijk, Clemens & De Boer, Jan 2007. Donor variation and loss of multipotency during in vitro expansion of human mesenchymal stem cells for bone tissue engineering. *Journal of orthopaedic research,* 25**,** 1029-1041.

Sidhaye, Venkataramana K, Schweitzer, Kelly S, Caterina, Michael J, Shimoda, Larissa & King, Landon S 2008. Shear stress regulates aquaporin-5 and airway epithelial barrier function. *Proceedings of the National Academy of Sciences,* 105**,** 3345-3350.

Sigal, Ian R, Grande, Daniel A, Dines, David M, Dines, Joshua & Drakos, Mark 2016. Biologic and Tissue Engineering Strategies for Tendon Repair. *Regenerative Engineering and Translational Medicine,* 2**,** 107-125.

Slomianka, L 2009. Blue histology-skeletal tissues-cartilage. *Available:[Accessed 05/03/2012 2012] http://www. lab. anhb. uwa. edu. au/mb140/CorePages/Cartilage/Cartil. htm.*

Smith, Roger Kw & Goodship, Allen E 2008. Tendon and ligament physiology: responses to exercise and training. *Hinchcliff, KW, Geor, RJ, Kanep AJ: Equine Exercise Physiology, the Science of Exercise in the Athletic Horse. Elsevier Ltd, London***,** 106-131.

Solchaga, Luis A, Gao, Jizong, Dennis, James E, Awadallah, Amad, Lundberg, Magnus, Caplan, Arnold I & Goldberg, Victor M 2002. Treatment of osteochondral defects with autologous bone marrow in a hyaluronan-based delivery vehicle. *Tissue engineering,* 8**,** 333-347.

Solchaga, Luis A, Goldberg, Victor M & Caplan, Arnold I 2001. Cartilage regeneration using principles of tissue engineering. *Clinical Orthopaedics and Related Research®,* 391**,** S161-S170.

Solheim, Eirik, Hegna, Janne, Inderhaug, Eivind, Øyen, Jannike, Harlem, Thomas & Strand, Torbjørn 2016. Results at 10–14 years after microfracture treatment of articular cartilage defects in the knee. *Knee Surgery, Sports Traumatology, Arthroscopy,* 24**,** 1587-1593.

Soltz, Michael A & Ateshian, Gerard A 2000. A conewise linear elasticity mixture model for the analysis of tension-compression nonlinearity in articular cartilage. *Journal of biomechanical engineering,* 122**,** 576-586.

Somoza, Rodrigo A, Welter, Jean F, Correa, Diego & Caplan, Arnold I 2014. Chondrogenic differentiation of mesenchymal stem cells: challenges and unfulfilled expectations. *Tissue Engineering Part B: Reviews,* 20**,** 596-608.

Sophia Fox, Alice J, Bedi, Asheesh & Rodeo, Scott A 2009. The basic science of articular cartilage: structure, composition, and function. *Sports health,* 1**,** 461-468.

Spakova, Timea, Plsikova, Jana, Harvanova, Denisa, Lacko, Marek, Stolfa, Stefan & Rosocha, Jan 2018. Influence of Kartogenin on Chondrogenic Differentiation of Human Bone Marrow-Derived MSCs in 2D Culture and in Co-Cultivation with OA Osteochondral Explant. *Molecules,* 23**,** 181.

Steadman, J Richard, Briggs, Karen K, Rodrigo, Juan J, Kocher, Mininder S, Gill, Thomas J & Rodkey, William G 2003. Outcomes of microfracture for traumatic chondral defects of the knee: average 11-year follow-up. *Arthroscopy: The Journal of Arthroscopic & Related Surgery,* 19**,** 477-484.

Stewart, Matthew C, Saunders, Kathryn M, Burton-Wurster, Nancy & Macleod, James N 2000. Phenotypic stability of articular chondrocytes in vitro: the effects of culture models, bone morphogenetic protein 2, and serum supplementation. *Journal of bone and mineral research,* 15**,** 166-174.

Stoddart, Martin J, Grad, Sibylle, Eglin, David & Alini, Mauro 2009. Cells and biomaterials in cartilage tissue engineering.

Story, Gina M 2006. The emerging role of TRP channels in mechanisms of temperature and pain sensation. *Current neuropharmacology,* 4**,** 183-196.

Takada, Ichiro, Kouzmenko, Alexander P & Kato, Shigeaki 2009. Wnt and PPARγ signaling in osteoblastogenesis and adipogenesis. *Nature Reviews Rheumatology,* 5**,** 442.

Terzic, Andre & Nelson, Timothy J. Regenerative medicine primer. Mayo Clinic Proceedings, 2013. Elsevier, 766-775.

Toai, Tran Cong, Thao, Huynh Duy, Thao, Nguyen Phuong, Gargiulo, Ciro, Ngoc, Phan Kim, Van, Pham Hung & Strong, D Michael 2010. In vitro culture and differentiation of osteoblasts from human umbilical cord blood. *Cell and tissue banking,* 11**,** 269-280.

Torzilli, Pa 1985. Influence of cartilage conformation on its equilibrium water partition. *Journal of orthopaedic research,* 3**,** 473-483.

Tran, Scott C, Cooley, Avery J & Elder, Steven H 2011. Effect of a mechanical stimulation bioreactor on tissue engineered, scaffold-free cartilage. *Biotechnology and bioengineering,* 108**,** 1421-1429.

Tuan, Rocky S, Boland, Genevieve & Tuli, Richard 2002. Adult mesenchymal stem cells and cell-based tissue engineering. *Arthritis Res Ther,* 5**,** 32.

Turner, A Simon 2007. Experiences with sheep as an animal model for shoulder surgery: strengths and shortcomings. *Journal of shoulder and elbow surgery,* 16**,** S158-S163.

Turner, A Simon, Athanasiou, Kyriacos A, Zhu, Chong-Fang, Alvis, Mark R & Bryant, Henry U 1997. Biochemical effects of estrogen on articular cartilage in ovariectomized sheep. *Osteoarthritis and cartilage,* 5**,** 63-69.

Turner, As 2002. The sheep as a model for osteoporosis in humans. *The Veterinary Journal,* 163**,** 232-239.

Van De Graaff, K 2001. Van de Graaff: Human Anatomy. Boston: MacGraw-Hill.

Van Der Kraan, Pm & Van Den Berg, Wb 2012. Chondrocyte hypertrophy and osteoarthritis: role in initiation and progression of cartilage degeneration? *Osteoarthritis and cartilage,* 20**,** 223-232.

Vedicherla, Srujana & Buckley, Conor T 2017. Cell-based therapies for intervertebral disc and cartilage regeneration—Current concepts, parallels, and perspectives. *Journal of orthopaedic research,* 35**,** 8-22.

Vega, Sebastián L, Kwon, Mi Y & Burdick, Jason A 2017. Recent advances in hydrogels for cartilage tissue engineering. *European cells & materials,* 33**,** 59.

Von Der Mark, Klaus, Gauss, Verena, Von Der Mark, Helga & Müller, Peter 1977. Relationship between cell shape and type of collagen synthesised as chondrocytes lose their cartilage phenotype in culture. *Nature,* 267**,** 531.

Wakitani, Shigeyuki, Mitsuoka, Tomoki, Nakamura, Norimasa, Toritsuka, Yukiyoshi, Nakamura, Yukio & Horibe, Shuji 2004. Autologous bone marrow stromal cell transplantation for repair of full-thickness articular cartilage defects in human patellae: two case reports. *Cell transplantation,* 13**,** 595-600.

Wakitani, Shigeyuki, Nawata, Masashi, Tensho, Keiji, Okabe, Takahiro, Machida, Hiroko & Ohgushi, Hajime 2007. Repair of articular cartilage defects in the patello-femoral joint with autologous bone marrow mesenchymal cell transplantation: three case reports involving nine defects in five knees. *Journal of tissue engineering and regenerative medicine,* 1**,** 74-79.

Waldman, Stephen D, Spiteri, Caroline G, Grynpas, Marc D, Pilliar, Robert M & Kandel, Rita A 2003. Long-term intermittent shear deformation improves the quality of cartilaginous tissue formed in vitro. *Journal of orthopaedic research,* 21**,** 590-596.

Wang, Hangjun & Kandel, Rita A 2004. Chondrocytes attach to hyaline or calcified cartilage and bone1. *Osteoarthritis and cartilage,* 12**,** 56-64.

Wang, I-Chun, Ueng, Steve Wn, Lin, Song-Shu, Niu, Chi-Chien, Yuan, Li-Jen, Su, Chun-I, Chen, Chih-Hwa & Chen, Wen-Jer 2011. Effect of hyperbaric oxygenation on intervertebral disc degeneration: an in vitro study with human lumbar nucleus pulposus. *Spine,* 36**,** 1925-1931.

Wang, J, Wang, Cd, Zhang, N, Tong, Wx, Zhang, Yf, Shan, Sz, Zhang, Xl & Li, Qf 2017. Mechanical stimulation orchestrates the osteogenic differentiation of human bone marrow stromal cells by regulating HDAC1. *Cell death & disease,* 7**,** e2221.

Wang, Wen, He, Na, Feng, Chenchen, Liu, Victor, Zhang, Luyi, Wang, Fei, He, Jiaping, Zhu, Tengfang, Wang, Shuyang & Qiao, Weiwei 2015. Human adipose-derived mesenchymal progenitor cells engraft into rabbit articular cartilage. *International journal of molecular sciences,* 16**,** 12076-12091.

Wang, Ye-Fu, Zhang, Ye-Qin & Jiang, Xiao-Di 2008. The application of nanoparticles in biochips. *Recent patents on biotechnology,* 2**,** 55-59.

Wang, Yongzhong, Kim, Hyeon-Joo, Vunjak-Novakovic, Gordana & Kaplan, David L 2006. Stem cell-based tissue engineering with silk biomaterials. *Biomaterials,* 27**,** 6064-6082.

Watt, Fiona M 1988. Effect of seeding density on stability of the differentiated phenotype of pig articular chondrocytes in culture. *Journal of cell science,* 89**,** 373-378.

Wegmeyer, Heike, Bröske, Ann-Marie, Leddin, Mathias, Kuentzer, Karin, Nisslbeck, Anna Katharina, Hupfeld, Julia, Wiechmann, Kornelius, Kuhlen, Jennifer, Von Schwerin, Christoffer & Stein, Carsten 2013. Mesenchymal stromal cell characteristics vary depending on their origin. *Stem cells and development,* 22**,** 2606-2618.

Weiler, Andreas, Hoffmann, Reinhard Fg, Bail, Hermann J, Rehm, Oliver & Südkamp, Norbert P 2002. Tendon healing in a bone tunnel. Part II: Histologic analysis after biodegradable interference fit fixation in a model of anterior cruciate ligament reconstruction in sheep. *Arthroscopy: The Journal of Arthroscopic & Related Surgery,* 18**,** 124-135.

Weiss, Leon & Sakai, Hidetaka 1984. The hematopoietic stroma. *American journal of anatomy,* 170**,** 447-463.

Wilke, Hans-Joachim, Kettler, Annette, Wenger, Karl Howard & Claes, Lutz Eberhardt 1997. Anatomy of the sheep spine and its comparison to the human spine. *The Anatomical Record: An Official Publication of the American Association of Anatomists,* 247**,** 542-555.

Williams, Emma L, White, Kate & Oreffo, Richard Oc 2013. Isolation and enrichment of Stro-1 immunoselected mesenchymal stem cells from adult human bone marrow. *Stem Cell Niche.* Springer.

Williams, Riley J, Peterson, L & Cole, B 2007. *Cartilage repair strategies,* Springer.

Wong, M, Wuethrich, P, Eggli, P & Hunziker, E 1996. Zone-specific cell biosynthetic activity in mature bovine articular cartilage: a new method using confocal microscopic stereology and quantitative autoradiography. *Journal of orthopaedic research,* 14**,** 424-432.

Wong, Melissa Hirose. Regulation of intestinal stem cells. Journal of Investigative Dermatology Symposium Proceedings, 2004. Elsevier, 224-228.

Woodruff, Maria Ann & Hutmacher, Dietmar Werner 2010. The return of a forgotten polymer—polycaprolactone in the 21st century. *Progress in polymer science,* 35**,** 1217-1256.

Yang, Guang, Rothrauff, Benjamin B & Tuan, Rocky S 2013. Tendon and ligament regeneration and repair: clinical relevance and developmental paradigm. *Birth Defects Research Part C: Embryo Today: Reviews,* 99**,** 203-222.

Yang, Shoufeng, Leong, Kah-Fai, Du, Zhaohui & Chua, Chee-Kai 2001. The design of scaffolds for use in tissue engineering. Part I. Traditional factors. *Tissue engineering,* 7**,** 679-689.

Yoshiya, Shinichi & Dhawan, Aman 2015. Cartilage repair techniques in the knee: stem cell therapies. *Current reviews in musculoskeletal medicine,* 8**,** 457-466.

Young, Randell G, Butler, David L, Weber, Wade, Caplan, Arnold I, Gordon, Stephen L & Fink, David J 1998. Use of mesenchymal stem cells in a collagen matrix for Achilles tendon repair. *Journal of orthopaedic research,* 16**,** 406-413.

Yu, Feng, Cao, Xiaodong, Li, Yuli, Zeng, Lei, Yuan, Bo & Chen, Xiaofeng 2013. An injectable hyaluronic acid/PEG hydrogel for cartilage tissue engineering formed by integrating enzymatic crosslinking and Diels–Alder "click chemistry". *Polymer Chemistry*, 5**,** 1082-1090.

Yuan, Tun, Zhang, Li, Li, Kuifeng, Fan, Hongsong, Fan, Yujiang, Liang, Jie & Zhang, Xingdong 2014. Collagen hydrogel as an immunomodulatory scaffold in cartilage tissue engineering. *Journal of Biomedical Materials Research Part B: Applied Biomaterials*, 102**,** 337-344.

Zaim, Merve, Karaman, Serap, Cetin, Guven & Isik, Sevim 2012. Donor age and long-term culture affect differentiation and proliferation of human bone marrow mesenchymal stem cells. *Annals of hematology*, 91**,** 1175-1186.

Zhang, Lijie, Hu, Jerry & Athanasiou, Kyriacos A 2009. The role of tissue engineering in articular cartilage repair and regeneration. *Critical Reviews™ in Biomedical Engineering*, 37.

Zhang, Wei, Ouyang, Hongwei, Dass, Crispin R & Xu, Jiake 2016. Current research on pharmacologic and regenerative therapies for osteoarthritis. *Bone research*, 4**,** 15040.

Zhao, Qinjun, Ren, Hongying & Han, Zhongchao 2016. Mesenchymal stem cells: Immunomodulatory capability and clinical potential in immune diseases. *Journal of Cellular Immunotherapy*, 2**,** 3-20.

Zuk, Patricia A, Zhu, Min, Ashjian, Peter, De Ugarte, Daniel A, Huang, Jerry I, Mizuno, Hiroshi, Alfonso, Zeni C, Fraser, John K, Benhaim, Prosper & Hedrick, Marc H 2002. Human adipose tissue is a source of multipotent stem cells. *Molecular biology of the cell*, 13**,** 4279-4295.

Appendix

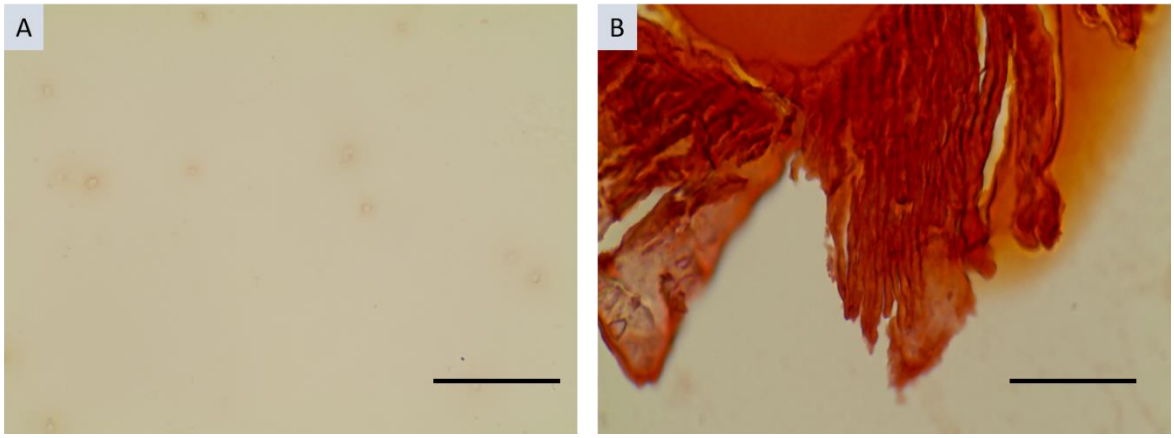

***Figure A. 1* Calcium deposition investigation by alizarin red of some sellected gel samples.** Alizarin red staining of 7 µm paraffin sections section of A) day 20 dynamic Ch M group hydrogel sample. B) a positive chontrol (subchondral bone of native sheep cartilage). This indicated that MICA stimulation did not promote osteogenic differentiation. Immages were taken at x10 magnification, scale bar = 300µm.

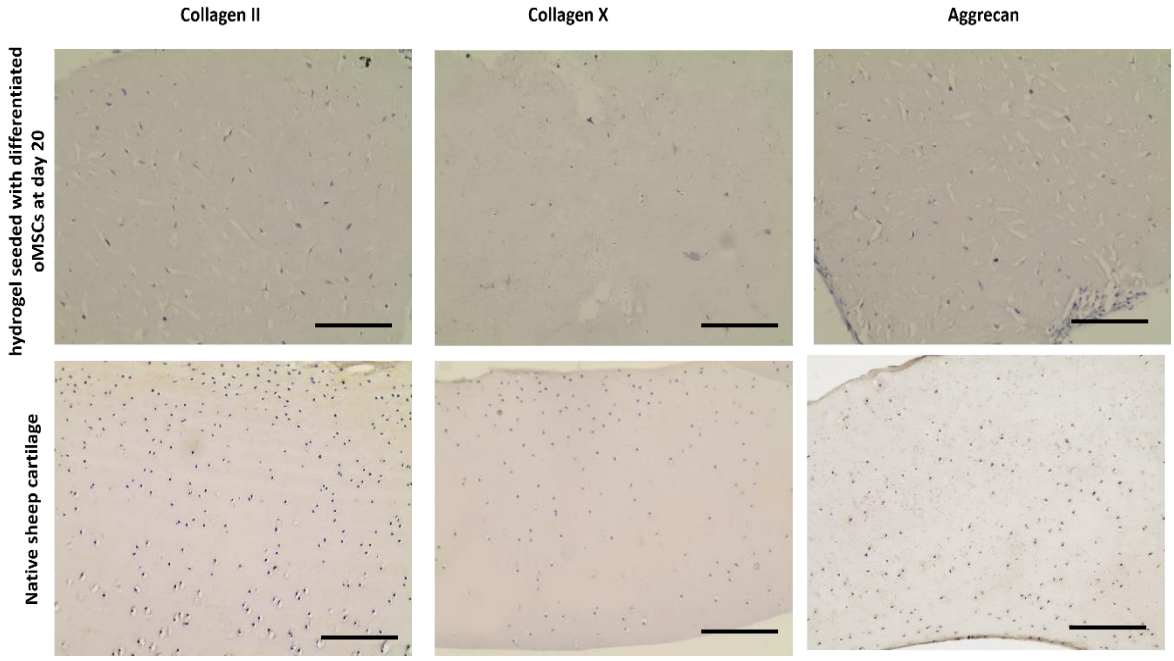

***Figure A. 2*: Negative control for immunostain.** Bright field micrographs of immunohistology stains negative control for collagen-type II, collagen type-X and aggrecan of 7 µm paraffin sections of day 20 dynamic Ch M group hydrogel sample. and native sheep cartilage. Immages were taken at x10 magnification, scale bar = 300µm.